The use of charged aerosol detection for the analysis of excipients and active pharmaceutical ingredients

Dissertation zur Erlangung des
naturwissenschaftlichen Doktorgrades
der Julius-Maximilians-Universität Würzburg

vorgelegt von

David Ilko

aus Bad Nauheim

Würzburg 2015

The use of charged aerosol detection for the analysis of excipients and active pharmaceutical ingredients

Dissertation zur Erlangung des
naturwissenschaftlichen Doktorgrades
der Julius-Maximilians-Universität Würzburg

vorgelegt von

David Ilko

aus Bad Nauheim

Würzburg 2015

Eingereicht bei der Fakultät für Chemie und Pharmazie am

_____

Gutachter der schriftlichen Arbeit

1. Gutachter: _____

2. Gutachter: _____

Prüfer des öffentlichen Promotionskolloquiums

1. Prüfer: _____

2. Prüfer: _____

3. Prüfer: _____

Datum des öffentlichen Promotionskolloquiums

_____

Doktorurkunde ausgehändigt am

_____

Danksagung

Die vorliegende Arbeit entstand am Institut für Pharmazie und Lebensmittelchemie der Bayerischen Julius-Maximilians-Universität Würzburg auf Anregung und unter Anleitung von

Frau Prof. Dr. Ulrike Holzgrabe

Ich möchte ihr hiermit für die freundliche Aufnahme in ihren Arbeitskreis, das in mich gesetzte Vertrauen und Ihre Unterstützung und Hilfe in jeder Phase der Erstellung dieser Dissertationsarbeit danken.

Weiterhin danken möchte ich Dr. Stefan Almeling, der sich während meines Aufenthalts beim EDQM in Straßburg stets Zeit für mich genommen hat und von dem ich viel lernen durfte. Ebenso danke ich Cees-Jan Nap, der mir durch seine Erfahrung und sein Wissen oft weitergeholfen hat. Dem gesamten DLab danke ich für die freundliche Aufnahme in ihr Team und die schöne Zeit.

Bedanken möchte ich mich auch bei Prof. Dr. Dr. Lorenz Meinel sowie Dr. Oliver Germershaus für die zahlreichen erfolgreichen Kooperationen, sowie bei Alexandra Braun, Sebastian Puhl und Christoph Steiger für die unkomplizierte und gute Zusammenarbeit.

Dem gesamten AK Holzgrabe danke ich für die schöne Zeit – sowohl auf, als auch abseits der Arbeit.

Table of Contents

List of abbreviations

AAA	amino acid analyzer
Ala	alanine
API	active pharmaceutical ingredient
Asp	aspartic acid
CAD	charged aerosol detector
CF	correction factor
CMC	critical micelle concentration
CNLSD	condensation nucleation light-scattering detector
CoA	certificate of analysis
DSC	differential scanning calorimetry
EAA	electrical aerosol analyzer
EC	electrochemical
EDQM	European Directorate for the Quality of Medicines & HealthCare
EIC	extracted ion chromatogram
ELSD	evaporative light-scattering detector
EO	ethylene oxide
EP	European Pharmacopoeia
ESI	electro-spray ionization
FA	fatty acid
FA	formic acid
FDA	food and drug administration
FRC	functionality related characteristics
GC	gas chromatography
Gln	glutamine
Glu	glutamic acid
HFBA	heptaflurobutyric acid

HILIC	hydrophilic interaction chromatography
HLB	hydrophilic-lipophilic balance
HPLC	high performance liquid chromatography
HPMC	hydroxypropoylmethylcellulose
HPTLC	high performance thin layer chromatography
ICH	International Conference on Harmonisation of Technical Requirements for Registration of Pharmaceuticals for Human Use
Imp.	impurity
IS	internal standard
JP	Japanese Pharmacopoeia
LC	liquid chromatography
LED	light-emitting diode
LoD	limit of detection
LoQ	limit of quantification
m/z	mass-to-charge ratio
MALDI	matrix assisted laser desorption ionization
MM_W	micelle molecular weight
MR	Maillard reaction
MS	mass spectrometry
MTBE	methyl-*tert.*-butyl ether
NMR	nuclear magnetic resonance
NQAD®	nano quantity analyte detector
O/W emulsion	oil-in-water emulsion
ODS	octadecylsilyl
PAD	pulsed amperometric detection
PBS	phosphate buffered saline
PCL	poly-ε-caprolactone
PD	polidocanol
PEG	poly(ethylene glycol)

PFHA	perfluoroheptanoic acid
PFP	pentafluorophenyl
PFPA	perfluoropentanoic acid
Ph. Eur.	European Pharmacopoeia
PLGA	poly(lactic-*co*-glycolic acid)
PLL	poly(L-lysine)
PS	polysorbate
PVDF	polyvinylidene fluoride
QC	quality control
R^2	coefficient of determination
RHLB	required HLB
RI	refractive index
RP	reversed phase
rpm	rounds per minute
RRF	relative response factors
R_S	resolution
rsd	relative standard deviation
S/N-ratio	signal-to-noise ratio
SD	standard deviation
SEC	size exclusion chromatography
SEM	scanning electron microscope
SLM	standard liter per minute
SPE	solid phase extraction
TFA	trifluoroacetic acid
TIC	total ion current
TLC	thin layer chromatography
T_n	nebulizer temperature
TOF/MS	time-of-flight mass spectrometry

Tris	Tris(hydroxymethyl)-aminomethane
UHPLC	ultra high performance liquid chromatography
USP	United States Pharmacopeia
UV	ultra violet
UV/Vis	ultra violet/visible

1 Introduction

Quality control (QC) in the pharmaceutical industry is of utmost importance and a necessary step for the patients' safety. It includes the testing of active pharmaceutical ingredients (API) and excipients as well as the analysis and the stability monitoring of the finished drug products. Pharmacopoeias provide the pharmaceutical analyst with a set of methods for identification, content determination and assessment of impurities with respective specifications in the API's monograph. The three major pharmacopoeias are the European Pharmacopoeia (Ph. Eur.) [1], the United Stated Pharmacopeia (USP) [2], and the Japanese Pharmacopoeia (JP) [3].

In most cases, the determination of related substances is carried out with high performance liquid chromatography (HPLC) as it is a powerful and versatile separation technique. HPLC is often combined with a UV/Vis detector. It is easy to use, provides a linear detector signal over a large concentration range with good sensitivity.

Other detectors have to be used if the analyte does not provide a suitable UV/Vis chromophore, e.g. refractive index, fluorescence, mass-selective, conductivity, electrochemical, or aerosol-based detectors. The latter are subject of this doctoral thesis and are therefore described in detail in the next sections.

1.1 Aerosol-based detectors

When searching for a universal detector for (HPLC), the evaporative light scattering detector (ELSD) was developed in the 1970s [4]. The ELSD as well as other aerosol-based detectors provide a signal independent from the physico-chemical properties of the analyte. Their application is therefore interesting when it comes to the analysis of substances lacking a UV/Vis-chromophore.

With the development of the „Corona® Charged Aerosol Detector" (CAD) and the „Nano Quantity Analyte Detector" (NQAD™), two additional instruments became commercially available. The working principle and some characteristics are different in the respective detectors and are pointed out in detail in the further sections.

The initial steps of the detection process are similar in all aerosol-based detectors and the theoretical principles of particle formation discussed in this section also apply to the other detectors. After nebulization and evaporation of the mobile phase, the

analyte is present as dried, solid particles. The mechanism of measuring these particles is different in all detectors.

In a first step, the mobile phase is nebulized by the inlet gas (nitrogen) to an aerosol. The diameter of the resulting droplets d_d is determined by various parameters.

The Nukiyama-Tanasawa equation [5] describes the droplet diameter d_d as:

$$d_d = \frac{585 \times \sqrt{\sigma}}{(v_g - v_l) \times \sqrt{\rho}} + 597 \times \left(\frac{\mu}{\sqrt{\rho \times \sigma}}\right)^{0,45} \times \left(\frac{1000 \times Q_l}{Q_g}\right)^{1,5} \qquad (1\text{-}1)$$

where:

v_g, v_l: velocity of the gas and liquid streams in the nebulizer

Q_g, Q_l: volume flow rate of the mobile phase and the scavenger gas

σ: surface tension

μ: viscosity

ρ: density of the mobile phase.

The droplet size is therefore given by the properties of the mobile phase (flow rate, composition) as well as the gas flow rate. The composition of the mobile phase is determined by the compounds to be separated and can only be changed slightly without affecting the separation. Thus, an optimization of the detection has to be done by the parameters of the detector, e.g. nebulizer pressure and gas flow rate.

After nebulization, the aerosol is evaporated in a heated evaporation tube. The size of the resulting particles d_p is given by [6]:

$$d_p = d_d \left(\frac{C}{\rho_p}\right)^{1/3} \qquad (1\text{-}2)$$

where:

d_d: droplet diameter

C: concentration of the analyte

ρ_p: density of the analyte.

The largest droplets are removed before the drying step in order to prevent an incomplete evaporation, which could impair the detection process. That means that the actual droplet size is smaller than the diameter given by equation (1-1). Further-

more, a certain amount of the analyte is lost in this process, thus lowering the detector signal. This effect is mostly pronounced when eluents having a large portion of water or aqueous buffer, hence high viscosity μ and low volatility, are used. This explains the dependence of the detector signal on the amount of organic phase in the eluent [7].

Using aerosol-based detectors, the detection of the analyte takes place after nebulization and evaporation of the mobile phase. Hence, as the only prerequisite, the analyte must have a considerably lower volatility than the mobile phase. Volatility of a substance is determined by its vapor pressure. Detector response in aerosol-based detectors and vapor pressure correlate inversely [4].

Universal detection comes along with some limitations. Considering the mobile phase, the user is restricted to volatile buffer salts and mobile phase additives. On the other hand, a method designed for aerosol-based detectors can readily be applied to an LC-MS system without any modification.

Another drawback is that the analyte mass and the detector response do not follow a linear relationship. The response curve is described by following equation:

$$y = Ax^b \qquad (1\text{-}3)$$

where:

x: analyte mass

y: area response

A, b: values depending on experimental conditions.

The equation can be transformed into a linear form:

$$\log y = b \times \log x + \log A \qquad (1\text{-}4)$$

Using this equation, a linear log-log calibration curve can be established. However, this model does not provide satisfactory results, when quantification over a range of more than two orders of magnitude is desired [8].

Furthermore, the detector response is dependent on the composition of the mobile phase. A higher content of organic solvent leads to a higher response. This has to be considered when applying gradients, as the mobile phase composition changes over the run time. The response factor of peaks eluting in the beginning and at the end of

the chromatogram can differ considerably. Quantification of all peaks in a chromatogram with a single-point-calibration using a single reference substance, as it is common practice in the determination of related substances by HPLC-UV in the Ph. Eur. [9], is often not feasible [8, 10].

This can be compensated by using a second pump which delivers an inverse gradient that is mixed with the mobile phase after the column [11]. The solvent reaching the detector has the same composition over the entire chromatographic run.

1.1.1 Evaporative Light Scattering Detector (ELSD)

The detection principle of an ELSD is shown in Figure 1-1. After nebulization and evaporation, the dried, solid particles pass a light beam. The scattered light is measured by a photomultiplier. It is often positioned in an angle of 120° to the light source to gather as much scattered light as possible without acquiring non-scattered light from the light source. An LED (light-emitting diode), providing polychromatic light is often used. There is no need for a monochromatic light source. This could even lead to a vastly decreased response, if e.g. the analyte has a high absorptivity at the particular wavelength.

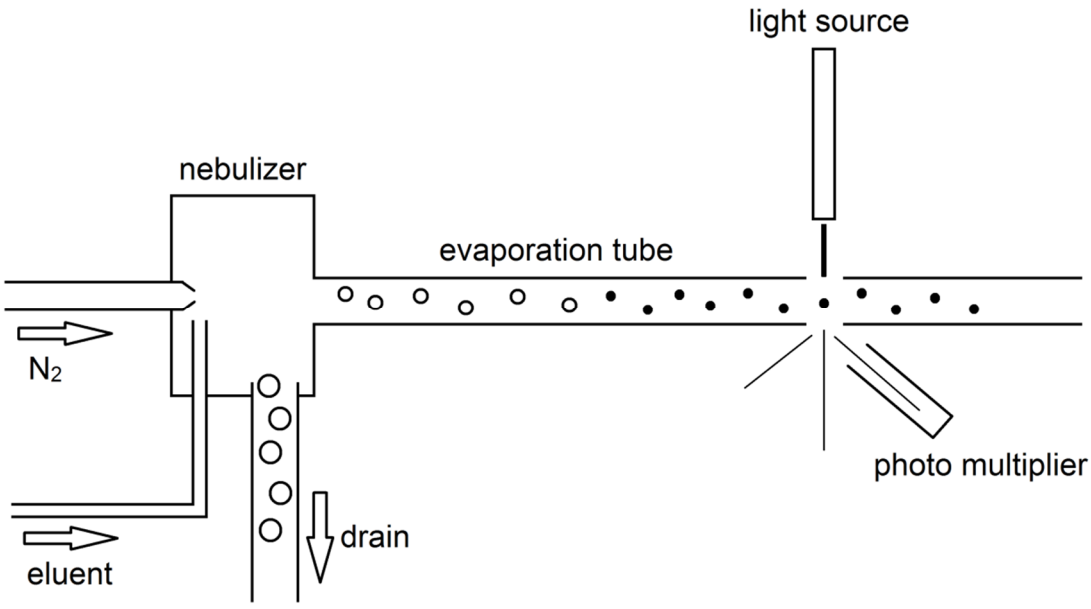

Figure 1-1. Working principle of an ELSD.

There are four mechanisms how light can interact with solid particles: Rayleigh-scattering, Mie-scattering, refraction and reflection. It is depending on the ratio of particle radius r and wavelength λ of the incident light which mechanism prevails [4]. If

r/*λ* is less than 0.1 Rayleigh-scattering can be observed; Mie-scattering for values between 0.1 and 2. If the ratio is more than 2, reflection and refraction can be observed [8]. For maximum sensitivity, Rayleigh-scattering should be avoided, as the other mechanisms are more effective [12].

When using the ELSD for impurity control, the occurrence of non-reproducible spike peaks eluting after the principle peak of a highly concentrated test solution was observed [13] making impurity determination impossible.

1.1.2 Nano Quantity Analyte Detector

The Nano Quantity Analyte Detector (NQAD™) is working with the condensation nucleation light scattering detection (CNLSD) principle that was introduced as a detector for HPLC by Allen and Koropchak et al. [14, 15].

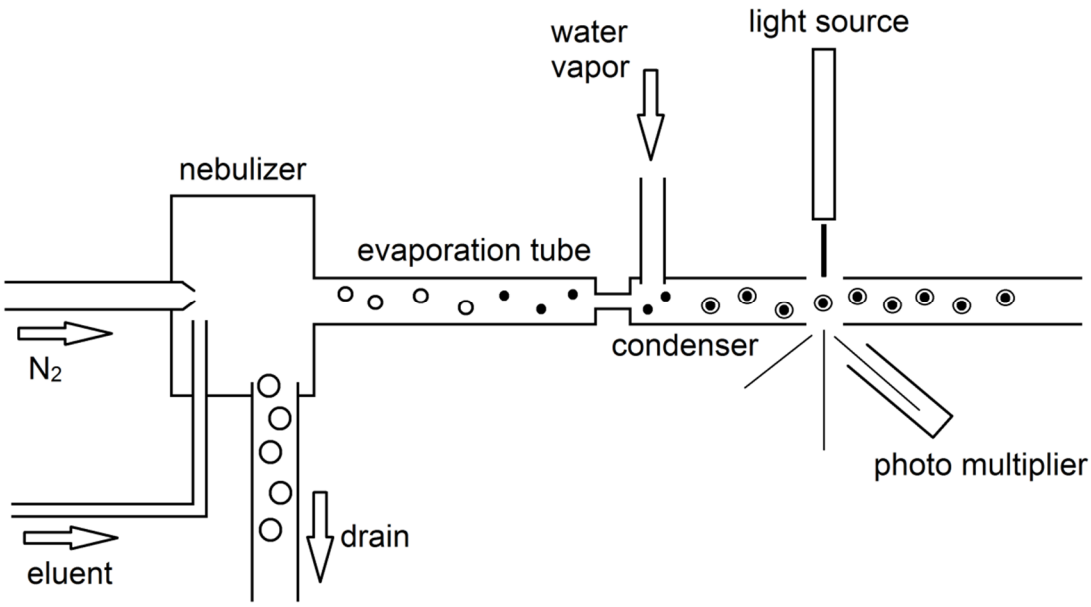

Figure 1-2. Principle of condensation nucleation light scattering detection in the Nano Quantity Analyte Detector.

Similar to an ELSD, the scattered light caused by analyte particles formed after nebulization and drying of the mobile phase is measured. However, before the detection of the particles takes place, they are further grown through condensation of water vapor (Figure 1-2). This technique is routinely used in the determination of the size distribution of particles (condensation particle counter, CPC). This allows for the detection of particles of much smaller size than an ELSD is capable of. For that reason, the NQAD™ provides a considerably higher sensitivity than an ELSD [15, 16].

1.1.3 Corona® Charged Aerosol Detector

The Corona® Charged Aerosol Detector (CAD) was introduced by Dixon and Peterson in 2002 [17]. As with the ELSD, the initial step is the formation of dried particles after nebulization and evaporation of the mobile phase. A second stream of nitrogen is charged by passing a corona needle. This charge is transferred to the particle stream in the mixing chamber. An ion trap is used to remove excessive charge, i.e. positive charged gas molecules, before the particles are detected by an electrometer (Figure 1-3).

As all other aerosol-based detectors, the CAD provides a non-linear response over its dynamic range [17]. However, it is reported to be linear when a small concentration range of about two orders of magnitude is investigated [18-21]. In low concentrations, i.e. from the limit of quantification (LOQ) of a substance to about 250 – 500 ng on column, a linear response curve is observed [22]. A recent model of the CAD, the CAD ultra RS, provides an additional option for linearization. With a mathematical transformation (“power function”) of the raw data, calibration curves can be linearized, the resolution of two peaks and the sensitivity can be increased [23, 24].

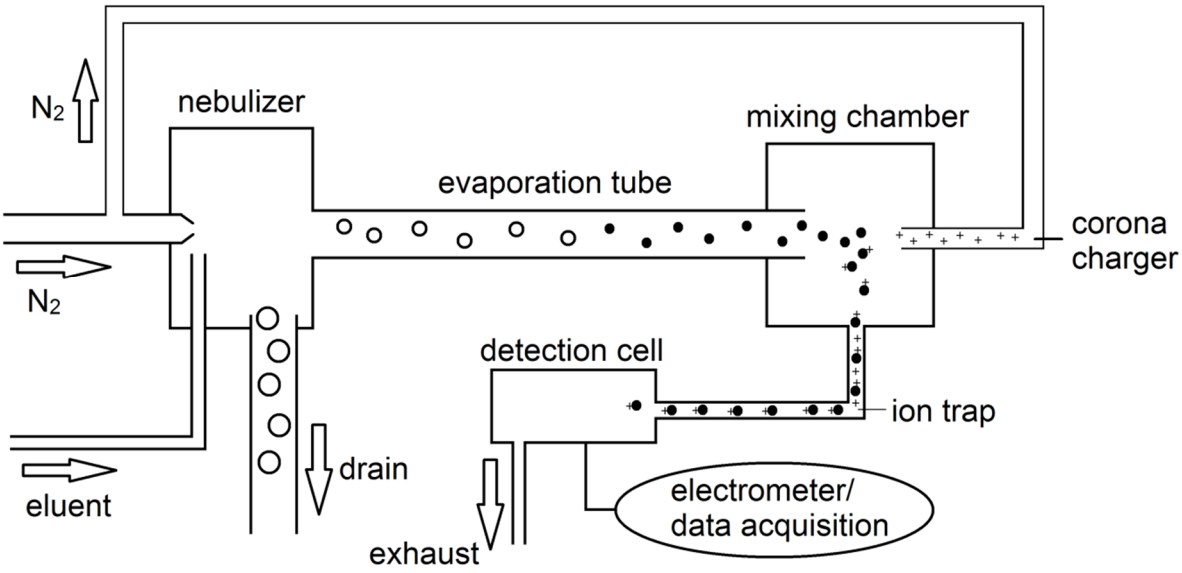

Figure 1-3. Working principle of the Corona® CAD.

The CAD shows better performance compared to the ELSD in many characteristics. Higher sensitivity [12, 25-32], higher precision [12, 25-30, 32], an increased linear range [12, 25, 26, 29-31] and uniform response for different chemical substances [26, 28] is reported. Compared to the NQAD™, the CAD is also superior in terms of re-

peatability [25], whereas it seems to be depending on the compounds analyzed, if the CAD provides a higher [25, 33], lower [16] or comparable sensitivity [34].

1.2 Application of aerosol-based detectors in pharmaceutical analysis

The ELSD is the only aerosol-based detector that is currently used in pharmacopoeias. Eight monographs in the European Pharmacopoeia (8th Edition (8.5), [1]) and only two monographs in the United Stated Pharmacopeia (USP 38 NF 33, [2]) make use of evaporative light scattering detection (see Table 1-1). Neither of the other aerosol-based detectors has found their way into compendial testing yet, but in some monographs under development, the CAD is considered for evaluation of related substances.

Table 1-1. The use of ELS detection in the European Pharmacopoeia (8th Edition (8.5)) and the United States Pharmacopeia (USP 38 NF 33).

Monograph	Type of analytical procedure	Pharmacopoeia
Astragalus mongholicus root	Assay (content of astragaloside IV)[a]	Ph. Eur. 8.5
Black cohosh	Assay (content of monoammonium glycyrrhizate)[a]	Ph. Eur. 8.5
Coix seed	Assay (content of triolein)[a]	Ph. Eur. 8.5
Ginkgo	Assay (content of terpene lactones)[a]	USP 38 NF 33
Hydroxypropylbetadex	Test for related substances (free β-cyclodextrin)[a]	Ph. Eur. 8.5
Isatis root	Assay (content of arginine)[a]	Ph. Eur. 8.5
Lecithin	Assay (content of phospholipids)[a]	USP 38 NF 33
Sesame oil refined	Composition of triglycerides[b]	Ph. Eur. 8.5
Sucrose monopalmitate	Test for related substances (free sucrose)[c]	Ph. Eur. 8.5
Sucrose stearate	Test for related substances (free sucrose)[c]	Ph. Eur. 8.5

[a] quantification via log-log-calibration curve; [b] quantification via area normalization; [c] quantification via linear calibration curve

The analytes mentioned in Table 1-1 belong to the compound classes fats, amino acids, sugars, and triterpene glycosides, all of which do not provide sufficient UV absorption. In most cases, quantification is performed via log-log calibration.

A brief description of substances or substance classes which are interesting analytes for the CAD caused by their lacking UV-absorption is given in the following sections.

1.2.1 Excipients

The CAD has widely been used for the analysis of excipients, such as polysorbates, hydroxypropylmethylcellulose (HPMC), fatty acids and oils, carbohydrates, polyethylene glycols, preservatives, and pharmaceutical plant extracts [35]

Usually, excipients do not consist of one defined chemical entity. They are rather complex and heterogeneous mixtures of a variety of substances. Determination of every single compound is often not achievable. Besides the specific control of highly toxic impurities such as e.g. ethylene oxide, dioxan, or heavy metals, excipients are often characterized via general, unspecific methods such as the determination of the acid, ester, hydroxyl, iodine, peroxide, or saponification value.

None of these tests, however, address the functionality of excipient. To the user of excipients, i.e. for the development and manufacturing of drug products, this information would be more helpful.

Table 1-2. Examples for functionality-related characteristics of excipients FRCs in the Ph. Eur. (8th Edition).

physical grades
particle-size distribution
specific surface area
bulk density
flowability
wettability
water sorption
polymorphism, pseudopolymorphism
crystallinity
density of solids
chemical grades
structure of homopolymers, blockpolymers and copolymers
degree of polymerization (molecular mass/mass distribution)
degree of substitution
different substituents on the polymer backbone

In 2013, the general text “5.15 Functionality-related characteristics of excipients” (FRCs) was included in the Ph. Eur. [36]. It names physical and chemical properties that can be used to describe performance characteristics of excipients. Examples are given in Table 1-2. The FRCs mentioned in monographs are no specifications but rather a tool for the excipient users in order to monitor properties that are crucial to the manufacturing process. The manufacturer is encouraged to evaluate the impact of these critical FRCs on the quality of his medicinal product and define them as critical quality attributes (CQA) if necessary.

Similarly to the Ph. Eur., there is the general chapter <1059> “excipient performance” in the USP [37]. It categorizes excipients into different classes and provides physical, chemical, biological, or microbiological properties that are not assessed in the respective monograph. Similarly to CQAs in the Ph. Eur., they are defined as critical material attributes (CMA) in the USP if the quality of the drug products may be adversely affected. Although not part of the respective monograph, the user should carefully monitor CMAs.

Polysorbate 80

Polysorbate 80 (PS80) is used as emulsifying agent for O/W-emulsions, solubilizing agent for poorly soluble drug substances or wetting agent [38]. It is composed of mixed esters of mainly oleic acid with “sorbitol and its anhydrides ethoxylated with about 20 moles of ethylene oxide for each mole sorbitol and sorbitol anhydrides” [39, 40]. The preparation of PS80 is not a strictly stoichiometric reaction; it rather yields a mixture of various PS80 species. The reaction scheme is depicted in Figure 1-4 [41]. In a first step, an aqueous solution of sorbitol, mixed with the methyl ester of oleic acid is heated under reduced pressure in a nitrogen atmosphere. This dehydration step yields different sorbitans (cf. Figure 1-5), which build the backbone of PS80. The transesterification of the fatty acid (FA) ester with sorbitol and/or sorbitan is induced by adding an alkali catalyst. Formally, one FA is bound to the backbone. However, up to four hydroxyl groups of sorbitol/sorbitan were found to be esterified [42]. In the last step, one mole of sorbitol/sorbitan FA ester reacts with about 20 moles ethylene oxide (EO). The distribution of the EO chains was found to be heterogeneous (approximately 9 – 36 EO units per sorbitol/sorbitan, [42]).

CAD and other aerosol-based detectors have often been proven as suitable detection techniques for polysorbates [42-53]. The complex chemical composition is well

demonstrated using these methods. However, the influence of the chemical composition on FRCs was never investigated.

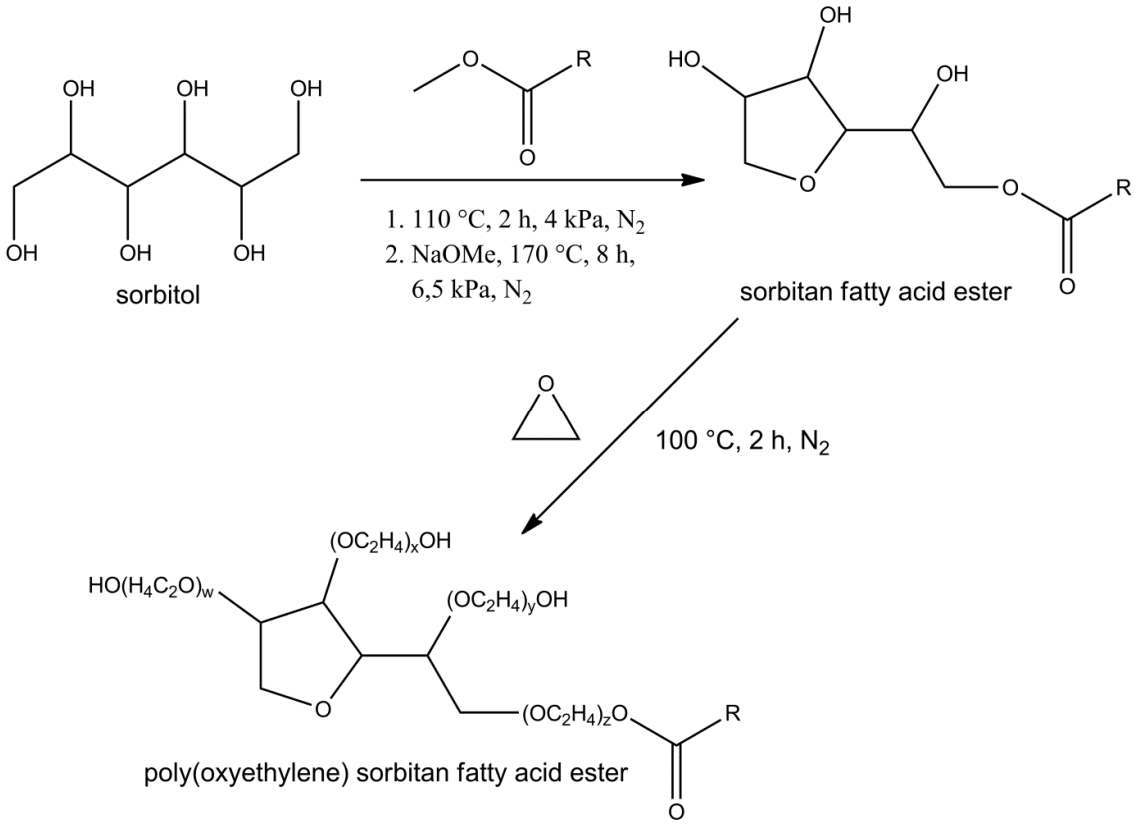

Figure 1-4. Synthetic route for the preparation of polysorbate 80 according to [41]. The fatty acid moiety of the methyl ester is oleic acid.

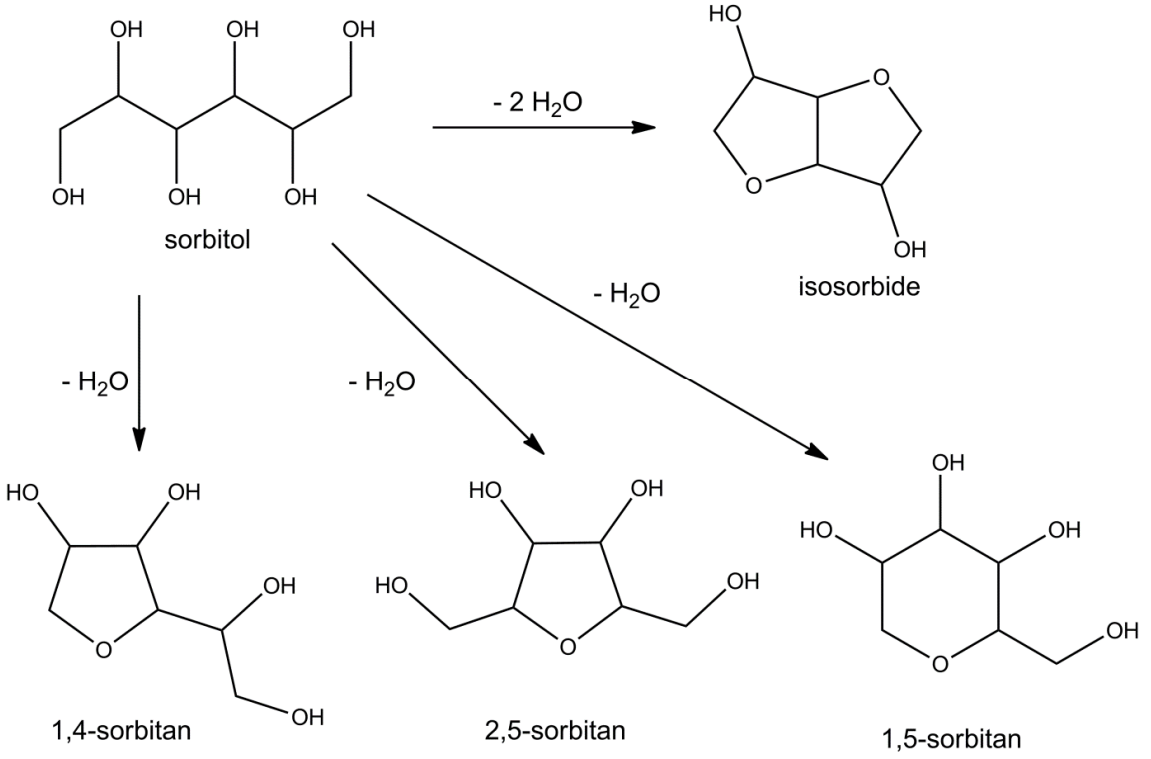

Figure 1-5. Possible products formed through dehydration of sorbitol in the first step of the PS80 synthesis.

Our aim was to show how chemical properties assessed with CAD can be linked to FRCs. According to USP <1059>, PS80 belongs to the group of “wetting and/or solubilizing agents”. As physical properties, it is suggested to determine the hydrophilic-lipophilic-balance (HLB value) and the critical micelle concentration (CMC). Furthermore, the cloud point, the micelle molecular weight and the second virial coefficient (<851> Spectrophotometry and Light-Scattering) can be determined to characterize surfactants.

Polidocanol

Polidocanol (PD) is an alcohol (dodecanol) ethoxylated with approximately 9 moles EO per mole dodecanol (Figure 1-6). It is applied as O/W emulsifier in drug products and cosmetic preparations [38]. PD is also in use as sclerosant, local anesthetic, and antipruritic drug. Different specifications are demanded when a substance is used as API compared to its employment as excipient. For that reason, there are two different monographs for PD in the Ph. Eur.:

- Lauromacrogol 400 (API monograph, [54])
- Macrogoli aether laurilicus (excipient monograph, [55]).

No method for the content determination is described in any of these monographs. Showing no UV absorption, PD is an eligible analyte for the detection with CAD. We therefore intended to develop an HPLC-CAD assay method.

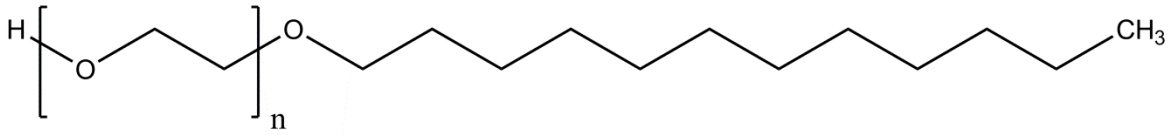

Figure 1-6. Structure of polidocanol. The average number of ethylene oxide monomers n is 7 – 11 for lauromacrogol 400 and 3 – 23 for macrogoli aether laurilicus.

1.2.2 Counterions

A great number of APIs are used as salts in order to modify physico-chemical properties. Characteristics such as solubility, bioavailability, polymorphism, stability, and dissolution rate can be influenced by selecting an appropriate counterion [56-58].

Frequently used ions are inorganic acids, sulfonic acids, organic acids, amino acids, fatty acids, organic amines, or metallic ions [59], all of which are known to show poor or no UV-absorption. For that reason, CAD seems to be a promising approach for the

determination of different counterions with one analytical technique. Furthermore, it delivers nearly uniform response for substances of different compound classes.

In recent years, hydrophilic interaction chromatography (HILIC) and mixed-mode chromatography became more and more popular for the separation of polar compounds [60]. The application of HILIC or mixed-mode chromatography in combination with the CAD to the analysis of counterions has been demonstrated [61-63].

1.2.3 Topiramate

Topiramate (2,3;4,5-di-*O*-isopropylidene-β-D-fructopyranose sulfamate, Figure 1-7) is an anticonvulsant drug substance that is also used against obesity, trigeminus neuralgia, substance-related diseases, and for migraine prevention [64-68].

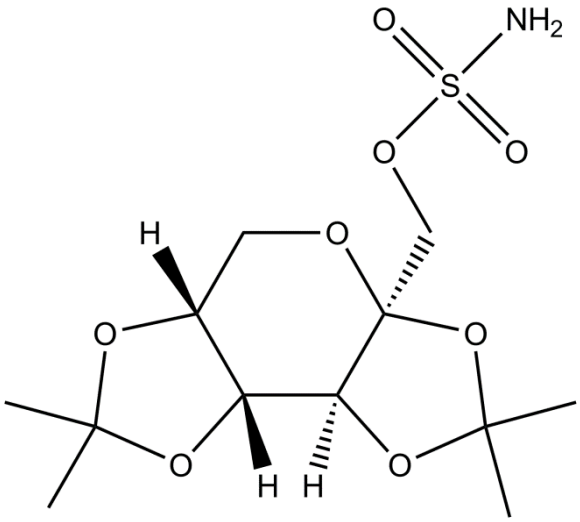

Figure 1-7. Structural formula of topiramate.

It is a carbohydrate derivative and therefore not a suitable analyte for UV/Vis spectroscopic detection. The use of aerosol-based detectors might represent a promising alternative for assay and impurity control to current methods using UV/Vis at very high analyte concentration or refractive index (RI) detectors [69, 70].

1.3 References

[1] *European Pharmacopoeia*. 8th Edition. 2014, Strasbourg, France: European Directorate for the Quality of Medicines & HealthCare (EDQM).

[2] *United States Pharmacopeia*. USP 38 NF 33. United States Pharmacopoeia, ed. The United States Pharmacopeial Convention. 2015, Rockville, MD, USA.

[3] *Japanese Pharmacopoeia*. 16th Edition. 2014, Tokio, Japan: Society of Japanese Pharmacopoeia.

[4] Charlesworth, J.M., *Evaporative analyzer as a mass detector for liquid chromatography.* Anal. Chem., 1978. **50**(11): p. 1414-1420.

[5] Nukiyama, S., Tanasawa, Y., *Experiment on atomization of liquid by means of air stream.* Trans. Soc. Mech. Eng., 1938. **4**: p. 86-93.

[6] Koropchak, J.A., Magnusson, L.-E., Heybroek, M., Sadain, S., Yang, X., Anisimov, M.P., *Fundamental aspects of aerosol-based light-scattering detectors for separations.* Adv. Chromatogr., 2000. **40**: p. 275-314.

[7] Megoulas, N.C., Koupparis, M.A., *Enhancement of evaporative light scattering detection in high-performance liquid chromatographic determination of neomycin based on highly volatile mobile phase, high-molecular-mass ion-pairing reagents and controlled peak shape.* J. Chromatogr. A, 2004. **1057**(1–2): p. 125-131.

[8] Kohler, M., Haerdi, W., Christen, P., Veuthey, J.-L., *The evaporative light scattering detector: some applications in pharmaceutical analysis.* TrAC, Trends Anal. Chem., 1997. **16**(8): p. 475-484.

[9] *Technical Guide for the Elaboration of Monographs,* 6th Edition, European Directorate for the Quality of Medicinces & HealthCare (EDQM), 2011, Strasbourg, France.

[10] Lane, S., Boughtflower, B., Mutton, I., Paterson, C., Farrant, D., Taylor, N., Blaxill, Z., Carmody, C., Borman, P., *Toward Single-Calibrant Quantification in HPLC. A Comparison of Three Detection Strategies: Evaporative Light Scattering, Chemiluminescent Nitrogen, and Proton NMR.* Anal. Chem., 2005. **77**(14): p. 4354-4365.

[11] Gorecki, T., Lynen, F., Szucs, R., Sandra, P., *Universal response in liquid chromatography using charged aerosol detection.* Anal. Chem., 2006. **78**(9): p. 3186-92.

[12] Ramos, R.G., Libong, D., Rakotomanga, M., Gaudin, K., Loiseau, P.M., Chaminade, P., *Comparison between charged aerosol detection and light scattering detection for the analysis of Leishmania membrane phospholipids.* J. Chromatogr. A, 2008. **1209**(1-2): p. 88-94.

[13] Almeling, S., Holzgrabe, U., *Use of evaporative light scattering detection for the quality control of drug substances: influence of different liquid chromatographic and evaporative light scattering detector parameters on the appearance of spike peaks.* J. Chromatogr. A, 2010. **1217**(14): p. 2163-70.

[14] Allen, L.B., Koropchak, J.A., Szostek, B., *Condensation Nucleation Light Scattering Detection for Conventional Reversed-Phase Liquid Chromatography.* Anal. Chem., 1995. **67**(3): p. 659-666.

[15] Koropchak, J.A., Heenan, C.L., Allen, L.B., *Direct comparison of evaporative light-scattering and condensation nucleation light-scattering detection for liquid chromatography.* J. Chromatogr. A, 1996. **736**(1–2): p. 11-19.

[16] Hutchinson, J.P., Li, J., Farrell, W., Groeber, E., Szucs, R., Dicinoski, G., Haddad, P.R., *Comparison of the response of four aerosol detectors used with ultra high pressure liquid chromatography.* J. Chromatogr. A, 2011. **1218**(12): p. 1646-1655.

[17] Dixon, R.W., Peterson, D.S., *Development and testing of a detection method for liquid chromatography based on aerosol charging.* Anal. Chem., 2002. **74**(13): p. 2930-2937.

[18] Holzgrabe, U., Nap, C.-J., Almeling, S., *Control of impurities in l-aspartic acid and l-alanine by high-performance liquid chromatography coupled with a corona charged aerosol detector.* J. Chromatogr. A, 2010. **1217**(3): p. 294-301.

[19] Holzgrabe, U., Nap, C.J., Kunz, N., Almeling, S., *Identification and control of impurities in streptomycin sulfate by high-performance liquid chromatography coupled with mass detection and corona charged-aerosol detection.* J. Pharm. Biomed. Anal., 2011. **56**(2): p. 271-9.

[20] Nováková, L., Solichová, D., Solich, P., *Hydrophilic interaction liquid chromatography – charged aerosol detection as a straightforward solution for simultaneous analysis of ascorbic acid and dehydroascorbic acid.* J. Chromatogr. A, 2009. **1216**(21): p. 4574-4581.

[21] Forsatz, B., Snow, N.H., *HPLC with charged aerosol detection for pharmaceutical cleaning validation.* LCGC North Am., 2007. **25**(9): p. 960, 962, 964, 966, 968.

[22] Crafts, C., Bailey, B., Plante, M., Acworth, I., *Validating analytical methods with charged aerosol detection*. http://www.dionex.com/en-us/webdocs/110512-PO-HPLC-ValidateAnalyticalMethods-CAD-31Oct2011-LPN2949-01.pdf *(Accessed: 10.07.2014)*

[23] Shalliker, R.A., Stevenson, P.G., Shock, D., Mnatsakanyan, M., Dasgupta, P.K., Guiochon, G., *Application of power functions to chromatographic data for the enhancement of signal to noise ratios and separation resolution.* J. Chromatogr. A, 2010. **1217**(36): p. 5693-5699.

[24] Dasgupta, P.K., Chen, Y., Serrano, C.A., Guiochon, G., Liu, H., Fairchild, J.N., Shalliker, R.A., *Black Box Linearization for Greater Linear Dynamic Range: The Effect of Power Transforms on the Representation of Data.* Anal. Chem., 2010. **82**(24): p. 10143-10150.

[25] Holzgrabe, U., Nap, C.-J., Beyer, T., Almeling, S., *Alternatives to amino acid analysis for the purity control of pharmaceutical grade L-alanine.* J. Sep. Sci., 2010. **33**(16): p. 2402-2410.

[26] Vervoort, N., Daemen, D., Török, G., *Performance evaluation of evaporative light scattering detection and charged aerosol detection in reversed phase liquid chromatography.* J. Chromatogr. A, 2008. **1189**(1–2): p. 92-100.

[27] Jia, S., Park, J.H., Lee, J., Kwon, S.W., *Comparison of two aerosol-based detectors for the analysis of gabapentin in pharmaceutical formulations by hydrophilic interaction chromatography.* Talanta, 2011. **85**(5): p. 2301-2306.

[28] Jia, S., Lee, W.J., Ee, J.W., Park, J.H., Kwon, S.W., Lee, J., *Comparison of ultraviolet detection, evaporative light scattering detection and charged aerosol detection methods for liquid-chromatographic determination of anti-diabetic drugs.* J. Pharm. Biomed. Anal., 2010. **51**(4): p. 973-978.

[29] Wang, L., He, W.-S., Yan, H.-X., Jiang, Y., Bi, K.-S., Tu, P.-F., *Performance Evaluation of Charged Aerosol and Evaporative Light Scattering Detection for the Determination of Ginsenosides by LC.* Chromatographia, 2009. **70**(3/4): p. 603-608.

[30] Nair, L.M., Werling, J.O., *Aerosol based detectors for the investigation of phospholipid hydrolysis in a pharmaceutical suspension formulation.* J. Pharm. Biomed. Anal., 2009. **49**(1): p. 95-99.

[31] Hazotte, A., Libong, D., Matoga, M., Chaminade, P., *Comparison of universal detectors for high-temperature micro liquid chromatography.* J. Chromatogr. A, 2007. **1170**(1-2): p. 52-61.

[32] Gamache, P., McCarthy, R.S., Freeto, S.M., Asa, D.J., Woodcock, M.J., Laws, K., Cole, R.O., *HPLC Analysis of Nonvolatile Analytes Using Charged Aerosol Detection.* LCGC North Am., 2005. **23**(2): p. 105-161.

[33] Cohen, R.D., Liu, Y., Gong, X., *Analysis of volatile bases by high performance liquid chromatography with aerosol-based detection.* J. Chromatogr. A, 2012. **1229**: p. 172-9.

[34] Cintrón, J.M., Risley, D.S., *Hydrophilic interaction chromatography with aerosol-based detectors (ELSD, CAD, NQAD) for polar compounds lacking a UV chromophore in an intravenous formulation.* J. Pharm. Biomed. Anal., 2013. **78–79**(0): p. 14-18.

[35] Almeling, S., Ilko, D., Holzgrabe, U., *Charged aerosol detection in pharmaceutical analysis.* J. Pharm. Biomed. Anal., 2012. **69**: p. 50-63.

[36] *5.15 Functionality-related characteristics of excipients*, *European Pharmacopoeia 8th Edition*, European Directorate for the Quality of Medicines & HealthCare (EDQM), 2014, European Directorate for the Quality of Medicines & HealthCare (EDQM), Strasbourg, France.

[37] performance, e., *Topiramate*, *United States Pharmacopoeia*, USP 38 NF 33, The United States Pharmacopeial Convention, 2015, Rockville, MD, USA.

[38] Kibbe, A.H., *Handbook of Pharmaceutical Excipients*. third. 2000, Washington, DC: American Pharmaceutical Association.

[39] *Polysorbate 80 Monograph 01/2011:0428*, *European Pharmacopoeia*, 8th Edition, European Directorate for the Quality of Medicines & HealthCare (EDQM), 2014, European Directorate for the Quality of Medicines & HealthCare (EDQM), Strasbourg, France.

[40] *Polysorbate 80 Monograph*, *United States Pharmacopoeia*, USP 37 NF 32, 2014, The United States Pharmacopeial Convention, Rockville, MD, USA.

[41] Wakita, K., Tanaka, S., Maruyama, K., *Process for producing polyoxyethylene sorbitan fatty acid ester*, Patent No. 8,334,397, issued 18.12.2012.

[42] Zhang, R., Wang, Y., Tan, L., Zhang, H.Y., Yang, M., *Analysis of polysorbate 80 and its related compounds by RP-HPLC with ELSD and MS detection.* J. Chromatogr. Sci., 2012. **50**(7): p. 598-607.

[43] Li, Y., Hewitt, D., Lentz, Y.K., Ji, J.A., Zhang, T.Y., Zhang, K., *Characterization and Stability Study of Polysorbate 20 in Therapeutic Monoclonal Antibody Formulation by Multidimensional UHPLC-CAD-MS.* Anal. Chem., 2014.

[44] Kishore, R.S., Pappenberger, A., Dauphin, I.B., Ross, A., Buergi, B., Staempfli, A., Mahler, H.C., *Degradation of polysorbates 20 and 80: studies on thermal autoxidation and hydrolysis.* J. Pharm. Sci., 2011. **100**(2): p. 721-31.

[45] Nair, L.M., Stephens, N.V., Vincent, S., Raghavan, N., Sand, P.J., *Determination of polysorbate 80 in parenteral formulations by high-performance liquid chromatography and evaporative light scattering detection.* J. Chromatogr. A, 2003. **1012**(1): p. 81-86.

[46] Nayak, V.S., Tan, Z., Ihnat, P.M., Russell, R.J., Grace, M.J., *Evaporative light scattering detection based HPLC method for the determination of polysorbate 80 in therapeutic protein formulations.* J. Chromatogr. Sci., 2012. **50**(1): p. 21-5.

[47] Fekete, S., Ganzler, K., Fekete, J., *Fast and sensitive determination of Polysorbate 80 in solutions containing proteins.* J. Pharm. Biomed. Anal., 2010. **52**(5): p. 672-9.

[48] Hewitt, D., Alvarez, M., Robinson, K., Ji, J., Wang, Y.J., Kao, Y.H., Zhang, T., *Mixed-mode and reversed-phase liquid chromatography-tandem mass spectrometry methodologies to study composition and base hydrolysis of polysorbate 20 and 80.* J. Chromatogr. A, 2011. **1218**(15): p. 2138-45.

[49] Hewitt, D., Zhang, T., Kao, Y.H., *Quantitation of polysorbate 20 in protein solutions using mixed-mode chromatography and evaporative light scattering detection.* J. Chromatogr. A, 2008. **1215**(1-2): p. 156-60.

[50] Abrar, S., Trathnigg, B., *Separation of nonionic surfactants according to functionality by hydrophilic interaction chromatography and comprehensive two-dimensional liquid chromatography.* J. Chromatogr. A, 2010. **1217**(52): p. 8222-9.

[51] Adamo, M., Dick, L.W., Jr., Qiu, D., Lee, A.H., Devincentis, J., Cheng, K.C., *A simple reversed phase high-performance liquid chromatography method for polysorbate 80 quantitation in monoclonal antibody drug products.* J Chromatogr B Analyt Technol Biomed Life Sci, 2010. **878**(21): p. 1865-70.

[52] Fekete, S., Ganzler, K., Fekete, J., *Simultaneous determination of polysorbate 20 and unbound polyethylene-glycol in protein solutions using new core-shell reversed phase column and condensation nucleation light scattering detection.* J. Chromatogr. A, 2010. **1217**(40): p. 6258-66.

[53] Christiansen, A., Backensfeld, T., Kuhn, S., Weitschies, W., *Stability of the non-ionic surfactant polysorbate 80 investigated by HPLC-MS and charged aerosol detector.* Pharmazie, 2011. **66**(9): p. 666-71.

[54] *Lauromacrogolum 400 Monograph 01/2009:2046*, *European Pharmacopoeia*, 8th Edition, European Directorate for the Quality of Medicines & HealthCare (EDQM), 2014, European Directorate for the Quality of Medicines & HealthCare (EDQM), Strasbourg, France.

[55] *Macrogoli aether laurilicus Monograph 01/2008:1124*, *European Pharmacopoeia*, 8th Edition, European Directorate for the Quality of Medicines & HealthCare (EDQM), 2014, European Directorate for the Quality of Medicines & HealthCare (EDQM), Strasbourg, France.

[56] Elder, D.P., Holm, R., Diego, H.L.d., *Use of pharmaceutical salts and cocrystals to address the issue of poor solubility.* Int. J. Pharm., 2013. **453**(1): p. 88-100.

[57] Morissette, S.L., Almarsson, Ö., Peterson, M.L., Remenar, J.F., Read, M.J., Lemmo, A.V., Ellis, S., Cima, M.J., Gardner, C.R., *High-throughput crystallization: polymorphs, salts, co-crystals and solvates of pharmaceutical solids.* Advanced Drug Delivery Reviews, 2004. **56**(3): p. 275-300.

[58] Rodríguez-Spong, B., Price, C.P., Jayasankar, A., Matzger, A.J., Rodríguez-Hornedo, N.r., *General principles of pharmaceutical solid polymorphism: A supramolecular perspective.* Advanced Drug Delivery Reviews, 2004. **56**(3): p. 241-274.

[59] Bastin, R.J., Bowker, M.J., Slater, B.J., *Salt Selection and Optimisation Procedures for Pharmaceutical New Chemical Entities.* Organic Process Research & Development, 2000. **4**(5): p. 427-435.

[60] Jandera, P., *Stationary and mobile phases in hydrophilic interaction chromatography: a review.* Anal. Chim. Acta, 2011. **692**(1–2): p. 1-25.

[61] Zhang, K., Dai, L., Chetwyn, N.P., *Simultaneous determination of positive and negative pharmaceutical counterions using mixed-mode chromatography coupled with charged aerosol detector.* J. Chromatogr. A, 2010. **1217**(37): p. 5776-84.

[62] Kanedai, Y., Hashiguti, K., Fukushima, K., Senda, M., Crafts, C., Gray, J., Plante, M., Acworth, I., *Simultaneous analysis of cations and anions using charged aerosol detection method.* Chromatography, 2009. **30**(Suppl. 1): p. 113-116.

[63] Huang, Z., Richards, M.A., Zha, Y., Francis, R., Lozano, R., Ruan, J., *Determination of inorganic pharmaceutical counterions using hydrophilic interaction chromatography coupled with a Corona® CAD detector.* J. Pharm. Biomed. Anal., 2009. **50**(5): p. 809-814.

[64] Ferrari, A., Tiraferri, I., Neri, L., Sternieri, E., *Clinical pharmacology of topiramate in migraine prevention.* Expert Opin Drug Metab Toxicol, 2011. **7**(9): p. 1169-81.

[65] Allison, D.B., Gadde, K.M., Garvey, W.T., Peterson, C.A., Schwiers, M.L., Najarian, T., Tam, P.Y., Troupin, B., Day, W.W., *Controlled-Release Phentermine/Topiramate in Severely Obese Adults: A Randomized Controlled Trial (EQUIP).* Obesity, 2012. **20**(2): p. 330-342.

[66] Wang, Q.-P., Bai, M., *Topiramate versus carbamazepine for the treatment of classical trigeminal neuralgia: a meta-analysis.* CNS Drugs, 2011. **25**(10): p. 847-857.

[67] Johnson, B.A., Ait-Daoud, N., Bowden, C.L., DiClemente, C.C., Roache, J.D., Lawson, K., Javors, M.A., Ma, J.Z., *Oral topiramate for treatment of alcohol dependence: a randomised controlled trial.* Lancet, 2003. **361**(9370): p. 1677-1685.

[68] Shinn, A.K., Greenfield, S.F., *Topiramate in the treatment of substance-related disorders: a critical review of the literature.* J. Clin. Psychiatry (Memphis, TN, U. S.), 2010. **71**(5): p. 634-648.

[69] Biro, A., Pergel, E., Arvai, G., Ilisz, I., Szepesi, G., Peter, A., Lukacs, F., *High-performance liquid chromatographic study of Topiramate and its impurities.* Chromatographia, 2006. **63**(Suppl.): p. S137-S141.

[70] *Topiramate Monograph*, *United States Pharmacopoeia*, USP 38 NF 33, 2015, The United States Pharmacopeial Convention, Rockville, MD, USA.

2 Aim of the thesis

The use of the Corona® charged aerosol detector in the analysis of pharmaceutical substances is the subject of this doctoral thesis. Its suitability as a potential detection technique for high performance liquid chromatogratic methods in the European Pharmacopoeia (Ph. Eur.) was investigated.

For this purpose, various substances from different compound classes lacking a suitable UV chromophore were chosen. HPLC methods for either content determination or impurity control were developed and validated. The conformity of the method performance with the Ph. Eur. given by the “Technical Guide for the Elaboration of Monographs” is a key requirement for the acceptance as a compendial method. The nonlinearity of the detector signal and its negative impact on accuracy is often crucial when it comes to the validation of CAD methods. It should be investigated if accurate quantification in assay as well as in impurity control can still be achieved.

In particular, following projects were investigated:

- Establishment and validation of a screening method for pharmaceutical counterions
- Comparison of the performance characteristics of ELSD with CAD for the impurity control in topiramate
- Verification of the suitability of the CAD for the content determination of topiramate
- Exploring the means of sensitivity enhancement for a semi-volatile impurity of topiramate
- Development and validation of an assay for polidocanol as bulk product and in a pharmaceutical polymer matrix
- Development and validation of a method for the determination of the free fatty acids and the fatty acid composition in polysorbates
- Characterization of the overall composition of polysorbate 80

3 Pharmaceutical applications of the CAD

Charged aerosol detection in pharmaceutical analysis

Stefan Almeling, David Ilko, Ulrike Holzgrabe

Reprinted with permission from J Pharm Biomed Anal **2012**, 69, 50-63.

Abstract

Due to its wide field of application, sensitivity, wide range of linearity and the applicability to gradient elution, the most common detection technique for HPLC nowadays is UV/Vis spectrophotometry. However, UV/Vis detection comes to its limits when the analytes are lacking suitable chromophors or exhibit very different UV responses. In the past years, different types of evaporation/aerosol based HPLC detectors have been developed to fill this gap in HPLC detection. Amongst those, the corona-charged aerosol detector (CAD) is one of the most powerful and versatile representatives. In the recent past a variety of papers have been published, demonstrating the potential of the CAD in different fields of analytical chemistry. This paper is intended to provide an overview of the key performance characteristics and manifold applications for HPLC-CAD in the field of pharmaceutical analysis.

1. Introduction

From its discovery by M.S. Tswett [1] in 1903 until today, liquid chromatography has taken an impressive development. High performance liquid chromatography (HPLC) is nowadays one of the most widespread techniques in analytical laboratories, and modern pharmaceutical analysis and quality control would not be thinkable without. Due to its wide field of applications, its sensitivity, the wide range of linearity and the compatibility with gradient elution, the most common detection technique for HPLC is UV/Vis spectrophotometry. However, UV/Vis and also fluorescence detection come to their limits when the analyte molecules are lacking a suitable chromophor or fluorophor [2]. In these cases refractive index (RI) and electrochemical (EC) detection or post-column derivatization UV detection are often employed instead. However, all these alternatives have their limitations [3]: refractometry is not sufficiently sensitive and is not suitable for gradient elution. Amperometric detection is technically difficult to apply and requires a skilled operator. Derivatization is difficult to validate as different compounds in a mixture may interact differently with the derivatization agent.

In the past years, several evaporation/aerosol based detectors have been developed with the evaporative light scattering detector (ELSD), first mentioned in 1978 by Charlesworth [4], being one of the early representatives. However, the relatively low sensitivity, the non-linear detector response and the occurrence of non-reproducible spike peaks at high analyte concentrations [5] are clear limitations of the ELSD. Therefore, this detector is not necessarily the most suitable choice for pharmaceutical applications like the control of impurities, where usually high analyte concentrations are employed and high sensitivity is a key requirement for detection and quantification of the related impurities often present below 0.1% concentration of the sample. Fortunately, further evaporation/aerosol based detection systems have been developed in the recent past. One example is the corona-charged aerosol detector (CAD) which was introduced by Dixon and Peterson [6] about 10 years ago. Another one is the nano quantity analyte detector (NQAD) which is partly based on the condensation nucleation light scattering detector (CNLSD) developed by Allen et al. [7,8]. Amongst these detectors, the authors consider the CAD being the most versatile one. Moreover, although this analysis was not necessarily comprehensive, a comparative study of the different evaporation based detectors revealed that the performance of the CAD is clearly superior to the ELSD and to some extent also to the NQAD [9]. This

review article is intended to give an overview to what extent the CAD is currently used to solve analytical problems in pharmaceutical analysis.

2. Characteristics of the charged aerosol detector

2.1. General principles

After having passed the separation column, the HPLC eluent is transferred to the CAD where it is nebulized by means of the Venturi effect produced by a carrier gas, typically nitrogen, which flows coaxially to the mobile phase eluting from the chromatographic column. This step transforms the liquid phase into small droplets. After nebulization, the droplets are carried by the nebulizer gas into a heated drift tube. In the drift tube the eluent is evaporated and a cloud of the non-volatile material contained in the eluent is formed. The detection of the resultant aerosol takes place through electrical charging of the aerosol and detection of the charged particles using an electrical aerosol analyser (EAA) (Fig. 1).

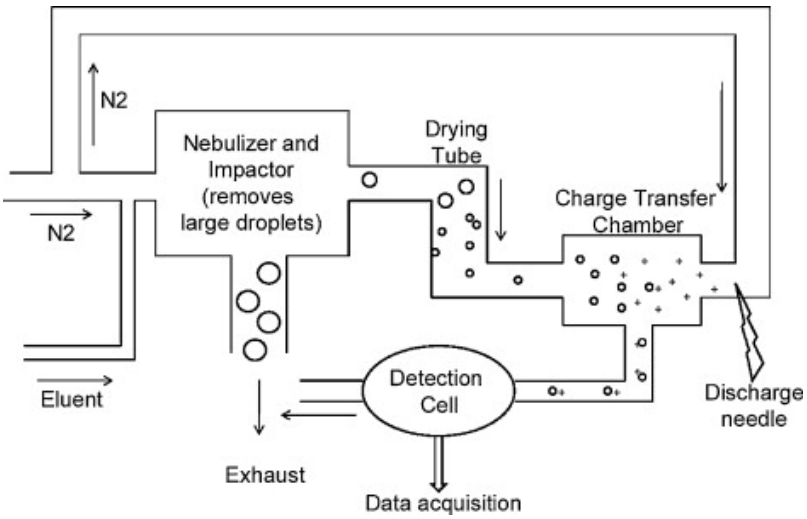

Fig. 1. Principles of the CAD (taken from [10] with permission of the author).

The EAA is a commercial instrument built in the 1970s for sizing aerosols and is described in detail by Liu and Pui [11]. The EAA operates by charging particles as they pass near a region of positive corona discharge. Subsequently small particles, having a larger mobility are removed through attraction to a rod of negative charge. Eventually the remaining charged particles are detected with a filter/electrometer. Compared with the ELSD, aerosol charging is more sensitive to small particles (diameter of less than 100 nm), which explains why CAD offers inherent advantages over ELSD [6]. When the CAD is operated under normal conditions, the charge imparted to particles

in the corona discharge region depends primarily on the particle size whilst the particle composition does not seem to have a significant impact on the signal [11,12]. According to Dixon and Peterson [6] the maximum sensitivity per particle mass occurs at particle diameters of about 10 nm. It is theoretically possible to use equations to predict the instrument sensitivity along with the size distribution of droplets generated by a pneumatic nebulizer. However, in practise this is complicated by a number of facts, such as the loss of droplets striking the walls of the spray chamber or the possible charging of droplets from the spray electrification. Thus, the determination of the response is usually done by an empirical approach. Fortunately, operating the CAD is rather simple and just requires setting a few controllable parameters like the gas inlet pressure and the signal output range [13]. Compared with the ELSD, the CAD detector was reported to have an about 10-fold increased sensitivity [5,6,14-17]. A detailed review of the operating principles of the CAD is given by Vehovec and Obreza [13].

It is however important to notice that, like for all other evaporation based detectors, a prerequisite for detection by CAD is that the solute is considerably less volatile than the mobile phase. In practise this means that the choice of mobile phase additives is limited and that volatile mobile phases must be used. Concerning the selection of the stationary phase it is important to ensure that the columns show little to no bleeding since all non-volatile particles will be detected by the CAD.

On the other hand it is worth mentioning that the choice of organic modifiers for the preparation of the mobile phase is larger than for HPLC with UV detection. For example acetone is not normally used in HPLC–UV as it has a UV cut-off of 330 nm. However, this is not an issue when HPLC is coupled with CAD. In contrast, in this case the relatively high volatility of acetone can even be advantageous.

2.2. Detector response, sensitivity and gradient compatibility

Compared with other detection method like UV/Vis spectrophotometry, fluorescence detection or pulsed amperometric detection, the detector response of the CAD does not depend on certain functional groups or moieties within the molecules. Therefore a similar detector response can be expected for different compounds [6,14,18-20]. This is a considerable advantage when screening for impurities where no structural information is available or where the detector response is unknown. In this respect, the CAD can even be used for the estimation of the UV relative response factors of impurities that have not been isolated but are only available in unknown amounts in a mix-

ture with the drug substance. In these cases, a comparison of the CAD and UV/Vis detector responses of the impurity and the drug substance can give a good estimation of the UV relative response factor of the impurity in question. However some caution as regards the assumption of a unique detector response in CAD is advisable as differences in the volatility and of the chargeability of different compound may lead to different relative response factors even when detection is performed by CAD [21].

The CAD detector response depends very much on the amount of organic modifier present in the mobile phase. Based on our experience, an increase of the detector signal of a factor of 5–10 can be achieved when changing from a 100% aqueous HPLC eluent to an eluent containing 100% of organic modifier. Unfortunately, the strong dependence of the detector response on the eluent composition results in some limitations as regards the compatibility of the CAD with gradient elutions. In these cases it would not be possible to use a single external standard for the quantification of different analytes in a mixture as it is often the case in pharmaceutical analysis. To overcome this constraint, post column compensation of the gradient by a corresponding counter gradient represents a viable option. A corresponding dual pump HPLC system has recently become commercially available. We [22] found that this system is easy to use and is prone to deliver a unique detector response over an HPLC gradient. Moreover, it could be shown that post column addition of organic modifier to isocratic methods with highly aqueous mobile phase can also contribute to reduce the baseline noise and to increase the detector sensitivity by a factor of 3–4 (cf. Fig. 2).

Compared with widely used ESLD, the CAD is reported to show a significantly higher detector response [6,14,16,17,23]. Typical limits of quantification (LoQs) found for the CAD range between 1 and 240 ng on column [9,15,19,21,24].

2.3. Linearity of range

Similar to the ELSD, the response of CAD is not directly linear over a broad concentration range [6,14,18]. However, the response of the CAD was reported to be linear over a limited range of about 2 orders of magnitude in different studies [19,21,25,26]. This is in many cases sufficient for an assay determination or for the determination of impurities when an external standard is used in an appropriate concentration (cf. Fig. 3).

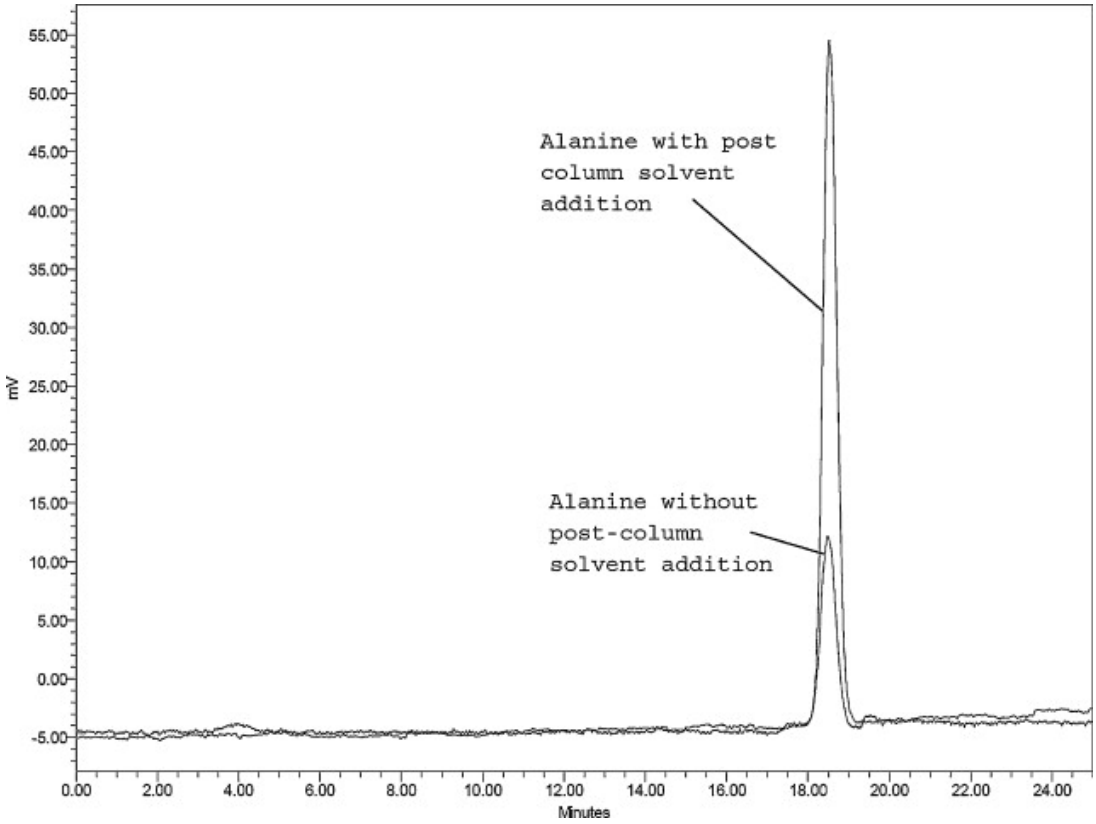

Fig. 2. Overlay of the detector response of a 0.05 mg/mL aqueous L-alanine test solution recorded with and without post column addition of 1 mL/min of acetonitrile to a highly aqueous mobile phase. Chromatographic conditions: Inertsil ODS 3 column (150 mm x 4.6 mm; particle size 5 µm), column temperature of 30 °C. Mobile phase: 96 vol. of 1.5 mmol/L PFHA in water and 4 vol. of 150 mmol/L PFHA in methanol, flow-rate: 1 mL/min, detection by CAD.

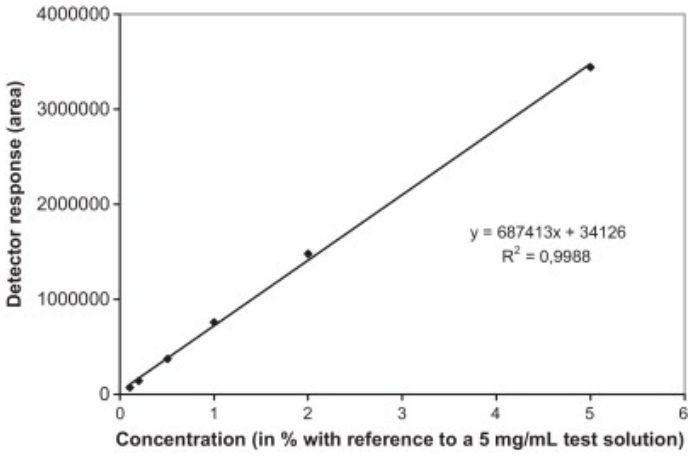

Fig. 3. LC-CAD calibration curve of streptomycin sulfate from 5 µg/mL to 250 µg/mL (6 concentration levels). Chromatographic conditions: YMC-Pack Pro column (250 mm x 4.6 mm; particle size 3 µm); Column temperature: 40 °C; Mobile phase: 20 mmol/L of PFPA in a mixture of water/acetone 99/1 (v/v). Flow rate: 0.8 mL/min. Injection of 10 µL of a 5 mg/mL solution of streptomycin sulfate in water. Modified from [19].

3. Case studies

In 2009 Nováková et al. [25] concluded that, although an increasing number of papers about CAD are being published in literature, pharmaceutical applications of the CAD would still be rare. However, for the last two years the CAD is more frequently

used also in the pharmaceutical world which is demonstrated in the following chapters.

3.1. Impurities control

A key objective in the quality control of active pharmaceutical ingredients (API) and excipients used for the production of drug products is an appropriate control of impurities. In guideline Q3A(R) on the control of impurities in new drug substances [27], the International Conference on Harmonisation of Technical Requirements for Registration of Pharmaceuticals for Human Use (ICH) has set a reporting threshold of 0.05% for impurities in new drug substances with an average daily dose below 2 g and 0.03% for drugs of a daily dose higher than 2 g. Impurities exceeding this threshold must be quantified and reported. In the European Pharmacopoeia (Ph. Eur.) [28] the above concept is not limited to new drug substances, but was extended to all substances for pharmaceutical use. As a consequence, methods used for the control of impurities must exhibit a LoQ which corresponds at least to the *reporting threshold*. Hence, the method employed for the control of impurities in “substances for pharmaceutical use” need to be sufficiently sensitive to comply with the above requirement. Moreover, the question of a unique relative response of the impurities is often an issue when it comes to the quantification with a dilution of the active pharmaceutical ingredient (API) as an external standard.

3.1.1. Aminoglycosides

Numerous papers describing LC methods for the identification and control of impurities in aminoglycoside antibiotics using detection by UV-spectrophotometry [29,30], mass spectrometry [31], and pulsed amperometric detection (PAD) [32-39] have been published. Unfortunately, each of these methods has major disadvantages. Due to a lack of a suitable chromophor, the analysis by UV/Vis-spectrophotometry requires high analyte concentrations and a low detection wavelength (about 200 nm). In addition, impurities lacking a UV/Vis-absorbing chromophor will not be detected. The application of mass spectrometry requires suitable specific reference materials for the quantification of the impurities. However, these are often not available. The application of PAD is technically very difficult and requires a skilled operator. Another disadvantage is that non-oxidizable compounds are not detected. Recently, four papers have been published describing methods for the determination of gentamicin

[40,41], streptomycin [19] and netilmicin sulphate [42] and their related substances using the CAD. For the determination of netilmicin sulphate and its impurities a step-gradient method using pentafluoropropionic acid (PFPA)/water/acetonitrile (0.1/96/4, v/v/v) as mobile phase A and trifluoroacetic acid (TFA)/water/acetonitrile (1/96/4, v/v/v) as mobile phase B on a Restek Allure pentafluorophenyl (PFP) propyl column (100 mm × 4.6 mm, 5 µm particle size) was employed.

A slightly modified approach was developed by the same working group to determine gentamicin and impurities. Here, a Restek Allure PFP propyl column (50 mm × 4.6 mm, 3 µm particle size) was used with heptafluorobutyric acid (HFBA)/water/acetonitrile (0.025/95/5, v/v/v) as mobile phase A and TFA/water/acetonitrile (1/95/5, v/v/v) as mobile phase B. After extraction, 20 µL of a sample solution containing approximately 0.5 mg/mL of gentamicin were injected.

Stypulkowska et al. achieved the quantification of all gentamicin components on a common C18 column (150 mm × 4.6 mm, 3 µm particle size) in isocratic mode [41] utilizing TFA (55 mmol/L)/methanol/acetonitrile (98/1/1, v/v/v) as mobile phase. This method was successfully applied to analyse gentamicin in different pharmaceutical preparations.

The separation of streptomycin and impurities was carried out in isocratic mode using a YMC-Pack Pro C18 column (250 mm × 4.6 mm, 3 µm particle size) and a mobile phase composed of 20 mmol/L of PFPA in water/acetone (99/1, v/v). 10 µL of 5 mg/mL sample solutions were injected at a HPLC flow-rate of 0.8 mL/min.

The methods allowed the separation and sensitive quantification of numerous impurities with LoQs between 4 ng on column [19] and 100 ng on column [42] for streptomycin and netilmicin, respectively (Fig. 4).

Since mobile phases compatible with HPLC-CAD methods must be volatile, the methods developed for the separation of the impurities from streptomycin and gentamicin could be coupled to MS detection without any further modification and thus, could be used for the structural elucidation of unknown impurities.

All four methods represent viable alternatives for the purity control of aminoglycoside antibiotics and demonstrate the potential of HPLC coupled with CAD for this class of pharmaceutical substances.

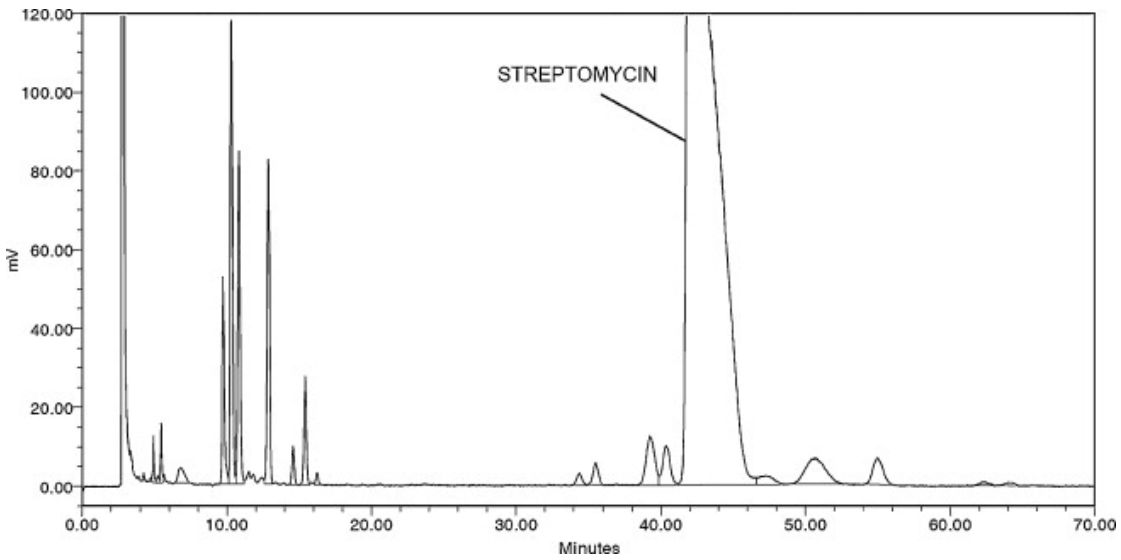

Fig. 4. Separation of streptomycin from its impurities. Column: YMC-Pack Pro column (250 mm x 4.6 mm; particle size 3 µm); Column temperature: 40 °C; Mobile phase: 20 mmol/L of PFPA in a mixture of water/acetone 99/1 (v/v). Flow rate: 0.8 mL/min. Injection of 10 µL of a 5 mg/mL solution of streptomycin sulfate sample 4 in water. Modified from [19].

3.1.2. Paclitaxel

Paclitaxel, a complex tetracyclic substance with a heptacarbon skeleton and 11 stereocenters, was first isolated from the bark of the Pacific yew tree. It is widely used in anticancer therapy and has been demonstrated to be effective against different tumor types [43,44].

In a study conducted by Wang and co-workers [18], the relative response factors (RRFs) of paclitaxel-related impurities were determined by HPLC-CAD and compared to those obtained by HPLC–UV analysis. Using a Curosil-PFP column (150 mm × 4.6 mm, 3 µm particle size) and a mobile phase composed of water/acetonitrile (52/48, v/v) at a flow rate of 1.2 mL/min, 9 impurities were separated from paclitaxel. The RRFs were determined employing calibration curves of the peak areas and analyte concentrations in a range of 0.1–2.0 µg/mL by linear regression analysis. CAD provided almost constant RRFs for the 9 analysed impurities and paclitaxel with a relative standard deviation (rsd) of the slope of the different calibration curves of 5.6%, whilst the UV detector response was found to differ significantly from one compound to another with individual RRFs between 0.5 and 1.0 (rsd: 25%; $n = 9$). This study demonstrated that significant mistakes in the quantification may occur when the UV-response factor of unknown compounds is assumed to be one. In contrast, the HPLC-CAD is a fast, convenient, and accurate method to determine UV RRFs of known and unknown impurities.

3.1.3. Maillard reaction impurities in memantine tablets

Memantine (3,5-dimethyladamantan-1-amine) is approved for treatment of moderate to severe Alzheimer's disease [45]. As a primary amine, memantine reacts with reducing sugars in a complex pathway known as Maillard reaction (MR) [46]. Such degradation products from the MR have been reported to occur in pharmaceutical products containing drug substances with primary amino groups and lactose, a standard excipient used for the production of tablets [47]. Therefore, Rystov et al. [48] have carried out work to determine MR impurities in memantine tablets using HPLC-CAD. The gradient method employing a Hydro-RP column (100 mm × 3.0 mm, 2.5 µm particle size) and mobile phases consisting of 0.6% (v/v) of heptafluorobutyric acid (HFBA) in two acetonitrile/isopropyl-alcohol/water mixtures, was capable of separating 4 MR impurities from memantine. Detection by CAD allowed the quantification of the impurities without a chromophor at levels of 0.02–0.03% (20–30 ng on column) referred to the labelled content of the drug substance. The method, which was fully validated, was found to be robust and easy to apply for the routine quality control of MR impurities in memantine tablets.

3.1.4. Amino acids

Amino acids, are widely used biological compounds e.g. in the fields of nutrition, cosmetics and agriculture [49]. Moreover, they are widely used in medicinal applications including the parenteral nutrition or the use of certain amino acids like tryptophan because of specific pharmacological effects [50,52].

Based on their widespread use, a proper control of the quality of the amino acids is of crucial importance for the consumer or patient. Unfortunately, due to their physicochemical properties, i.e. the lack of a chromophor in most of the amino acids, their analysis and especially the purity control of low level impurities is a particular analytical challenge and no analytical method has yet been found which is superior to all the others [53]. Although classical amino acid analysis (AAA) using HPLC–UV with derivatization of the amino acids prior to quantification is one of the most widely used methods, it is interesting to note that an application using UHPLC-CAD for the separation and quantification of 22 amino acids has just been developed [54]. Furthermore, a fully validated C18 reversed phase ion-pair HPLC method using 1 mmol/L of perfluoroheptanoic acid (PFHA) as an ion-pair reagent and a CAD for the purity con-

trol of aspartic acid (Asp) was published [21]. The method was capable of separating the major organic and amino acids known to occur as process related impurities. With a slight increase of the PFHA concentration from 1.0 mmol/L to 1.5 mmol/L, it was also found to be suitable for the purity control of alanine (Ala) (Fig. 5).

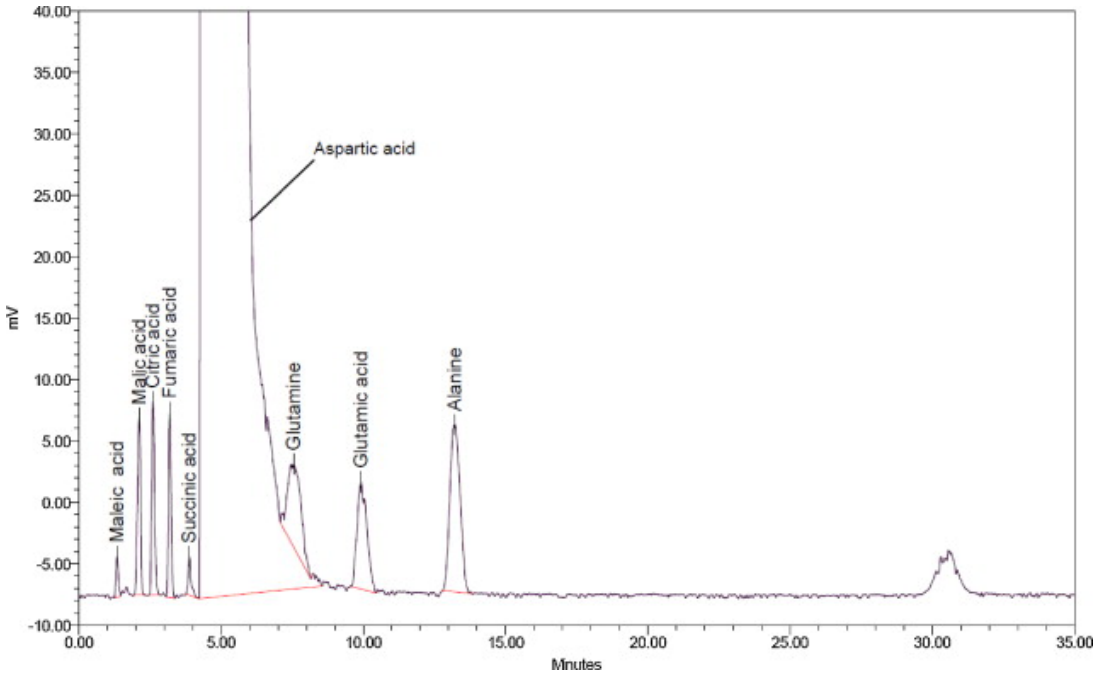

Fig. 5. Injection of a 10 mg/ml solution of Asp spiked with about 0.1% with maleic acid, malic acid, citric acid, fumaric acid, succinic acid, Gln, Glu and Ala. Chromatographic conditions: Inertsil ODS 3 column (150 mm x 4.6 mm, 5 µm), column temperature 30 °C, flow rate 1.0 mL/min, injection volume 40 µL, mobile phase 10 mmol/L PFHA in water/methanol 96/4 v/v. Detection by CAD. Elution order: maleic acid, malic acid, citric acid, fumaric acid, succinic acid, Asp, Gln, Glu, Ala. Modified from [21].

The LoQs for the potential impurities were found between 0.006% and 0.03% (24–120 ng on column) referred to the concentration of the API in the test solution. In this study the detector response of the CAD was found to be linear in a range from 2.5 µg/mL to 20 µg/mL. The LC method described in [21] represents an easy to use alternative to amino acid analysis for the control of impurities in Asp and Ala. Additionally, it has the benefit of controlling not only related amino acids but also other process impurities like organic acids. The method was also used in a study comparing the performance characteristics of different evaporation based detection systems; i.e. ELSD, NQAD and CAD [9]. The study concluded that for the selected application CAD was clearly superior to ELSD and appeared also slightly superior to NQAD in terms of repeatability and sensitivity.

3.1.5. Neuromuscular blocking drugs

Blazewicz et al. [55] have published a paper dealing with the determination of atracurium, cisatracurium and mivacurium and their impurities in pharmaceutical preparations. All three substances are non-depolarizing neuromuscular blocking drugs of different potency and duration of action [56,57]. Atracurium and its 1R-cis, 1R′-cis isomer, cisatracurium undergo Hofmann elimination, resulting in the formation of laudanosine and quarternary monoacrylate [58,59]. Below pH 3, atracurium also degrades by ester hydrolysis. Mivacurium, a mixture of 3 isomers, degrades by hydrolysis forming a monoquarternary alcohol and acid. The purpose of the work performed by Blazewicz et al. [55] was to develop a fast and sensitive HPLC-CAD method for the simultaneous determination of the three isomers of atracurium, cisatracurium, three isomers of mivacurium, and their degradants applicable to corresponding pharmaceutical preparations. Best analytical results were obtained using a Thermo C18 column (150 mm × 4.0 mm, 3 µm particle size) and a mobile phase containing 0.1% formic acid (FA) in water (solvent A) and 0.1% FA in methanol (solvent B) with the following gradient: 0–2 min 30% B, 2–10 min 30–50% B, 10–15 min 50% B and a flow rate of 0.5 mL/min. Linear detector response was found for atracurium in the concentration range from 5 to 150 µg/mL. The lowest LoQs were obtained for the impurity laudanosine with 16 ng on column. Accuracy and precision of the method were found appropriate with mean recoveries for all samples in the range from 96.5 to 101.6% and repeatability standard deviations (n = 3) between 0.1 and 1.6%.

3.2. Assay determinations

The determination of the content is an integral part of pharmacopoeial monographs and specifications for drug substance and also for many excipients. Also for finished products, the determination of the API content is a key parameter for the evaluation of the compliance with the approved specifications and for its suitability for use. As the following examples may demonstrate, CAD appears to become a more and more versatile detector also in this field of application.

3.2.1. Statin drugs

Statin drugs play a major role in the treatment of hypercholesterolemia. The class of statins consist of natural (lovastatin), semi-synthetic (simvastatin, and pravastatin) as

well as synthetic compounds (fluvastatin, atorvastatin, cerivastatin, rosuvastatin, and pitavastatin). Nováková et al. [24] have carried out a study to develop and validate a HPLC-CAD method for the assay determination of atorvastatin, lovastatin and simvastatin in tablets. For the separation a Zorbax Eclipse XDB C18 column (75 mm × 4.6 mm, 3.5 µm particle size) was used. The LC analysis was carried out in isocratic mode employing a mobile phase composed of acetonitrile and 0.1% formic acid (70/30, v/v) at a flow rate of 1.0 mL/min. The separation was completed in 4.5 min. In the validated concentration range of 0.1–50 µg/mL, the CAD delivered a linear response. In terms of sensitivity and precision, the CAD was found to be superior to a UV detector. A LoQ of 1 ng on column was determined for simvastatin, which was 2.5 times more sensitive than for the detection by UV 238 nm.

3.2.2. Antidiabetic drugs

In a study on 4 antidiabetic drugs (glipicide, gliclacide, glibenclamide and glimepiride) Kwon, Lee et al. [60] compared the performance of 3 different HPLC detectors: UV detection, ELSD and CAD. The LC separation was carried out using a GraceSmart RP-18 column (250 mm × 4.6 mm, 5 µm) and an isocratic eluent consisting of 35% mobile phase A (water/formic acid/acetonitrile, 90/0.1/10 v/v/v) and 65% mobile phase B (acetonitrile/water 90/10 v/v) at a HPLC flow rate of 1 mL/min. In terms of accuracy all three detectors delivered acceptable results. With regards to recovery, CAD was clearly better than ELSD and also slightly superior to detection by UV at 210 nm. In terms of precision, both UV detection and CAD were found more precise than ELSD. As a measure for the sensitivity, the LoD of the different antidiabetic drug substances were determined. CAD was found to be 5 fold more sensitive than ELSD and also up to three times more sensitive than detection by UV at 210 nm. The lowest LoQ for gliclacide was found to amount to 16 ng on column.

3.2.3. Vitamins

Simultaneous determination of ascorbic acid (vitamin C) and dehydroascorbic acid is a particular analytical challenge and no simple analytical method for the determination of both compounds was available. As these molecules are difficult to retain on conventional reversed phase HPLC columns and the differences in their properties do not allow simultaneous detection by UV absorption, fluorescence or electrochemical detection, Nováková et al. [25] developed a new HPLC method with detection by

CAD based on hydrophilic interaction chromatography (HILIC). A Sielc Obelisk R column (100 mm × 3.2 mm, 5 µm particle size) in isocratic elution mode employing a mobile phase consisting of acetonitrile and 75 mmol/L ammonium acetate (15/85, v/v) at a flow-rate of 1.0 mL/min resulted in a good separation of the two molecules. Linearity of the CAD response was confirmed in the range from 1 to 250 µg/mL for ascorbic acid and from 1 to 100 µg/mL for dihydroascorbic acid. Accuracy and precision of the method were acceptable and CAD resulted in a LoQ of 10 µg/mL for ascorbic acid and 1 µg/mL for dehydroascorbic acid. Using a UV detector at 268 nm for ascorbic acid and at 210 nm for dehydroascorbic acid instead of CAD, the method was twice more sensitive for ascorbic acid whilst dehydroascorbic acid could not be detected at all.

3.2.4. Gabapentin

Analysis of the anti-epileptic drug gabapentin is challenging because it possesses no suitable UV chromophor. Jia et al. developed an HPLC method for the determination of gabapentin in pharmaceutical preparations without derivatization prior to analysis [61]. In their study, the performance of an ELSD and the CAD were compared on four different HILIC columns (Luna HILIC (100 mm × 2.0 mm, 3 µm particle size), Atlantis HILIC Silica (100 mm × 2.0 mm particle size), ZIC HILIC (100 mm × 2.1 mm, 3 µm particle size), and ZIC pHILIC (150 mm × 2.1 mm, 5 µm particle size). It was found that the sensitivity achieved by ELS detection was comparable to that with CAD and both superior to UV detection in HILIC mode. LoDs were found to be 5–30 ng on column and 7.5–10 ng on column for ELSD and CAD, respectively, compared to 300–425 ng on column for UV detection depending on the column applied. However, employing a RP-C18 column, CAD was about 25-times more sensitive than ELSD. The application of this method on gabapentin tablets and capsules showed good recovery and precision (Fig. 6).

3.3. Further applications in pharmaceutical and related areas

3.3.1. Determination of pharmaceutical counterions

In order to obtain desired physicochemical properties or pharmacokinetic effects, drug substances are in many cases produced in the form of a salt. Moreover, salts can be formed during the synthesis and can remain in the product as impurities.

Therefore, the identification and quantification of counterions is an analytical task that plays an important role; i.e. in the verification of the completeness of the salt forming process, the control of the mass balance or in the limitation of undesirable counterions. A method for the simultaneous determination of the 25 most commonly used pharmaceutical counterions using mix-mode HPLC coupled with CAD has been developed by Zhang et al. [62]. The method used a 25 min ternary gradient at a flow rate of 0.5 mL/min, employing 200 mmol/L ammonium formate, pH 4, water and acetonitrile as mobile phases. The separation was carried out on an Acclaim Trinity P1 column (50 mm × 3.0 mm, 3 µm particle size), which consists of porous silica particles coated with charged nanopolymer beads. Separation of the following ions was achieved: anions; besilate, bromide, chloride, citrate, fumarate, gluconate, lactate, malate, maleate, mesilate, nitrate, phosphate, succinate, sulphate, tartrate, tosylate, and cations; calcium, cholin, magnesium, meglumine, potassium, sodium, tromethamine, procaine and zinc. Limits of detection between 5 ng on column for sodium and 400 ng on column for lactate were reached. Moreover, the method was capable of accurately determining the content of sodium, chloride and fumarate in different drug substances.

Huang et al. developed a method to determine several counterions in presence of an API as well [63]. Their method is carried out in HILIC mode. Two different chromatographic conditions were applied to quantify either monovalent ions (nitrate, chloride, bromide, sodium, potassium) or divalent ions (calcium, magnesium, sulphate, phosphate): isocratic separation with acetonitrile/0.1 M ammonium acetate (75/25, v/v) on a SeQuant ZIC-pHILIC (150 mm × 4.6 mm, 5 µm particle size) column for monovalent ions and acetonitrile/0.1 M ammonium formate (70/30, v/v) on a SeQuant ZIC-pHILIC (50 mm × 4.6 mm, 5 µm particle size). The authors showed that their method was superior to ion chromatography. HILIC columns allow the mobile phase to contain a higher amount of organic solvent, compared to ion chromatography, providing better solubility of drug substances.

However, the drawback of universal detection is also well demonstrated. The utilisation of certain silica based HILIC columns is not suitable, because of the high background noise due to column bleeding. These findings are in good agreement with the study performed by Jia et al. who applied the same HILIC columns for the determination of gabapentin [61].

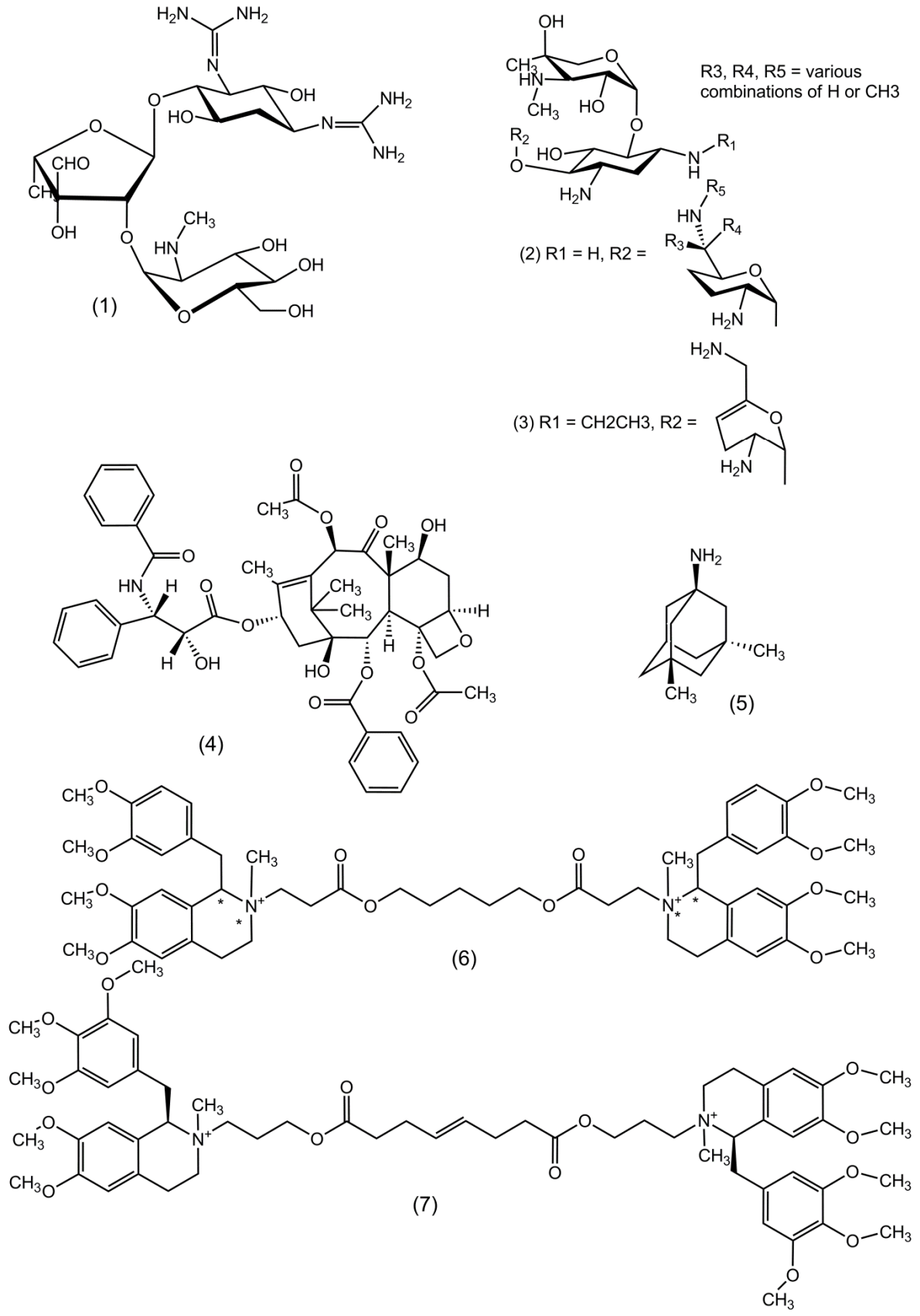

Fig. 6. Structural formulae of the drugs discussed here, (1) streptomycin, (2) gentamicin coumpounds, (3) netilmicin, (4) paclitaxel, (5) memantin, (6) atracurium, (7) mivacurium, (8) atorvastatin, (9) simvastatin, (10) lovastatin, (11) glibenclamid, (12) glimepiride, (13) glipizide, (14) gliclazide, (15) gabapentin.

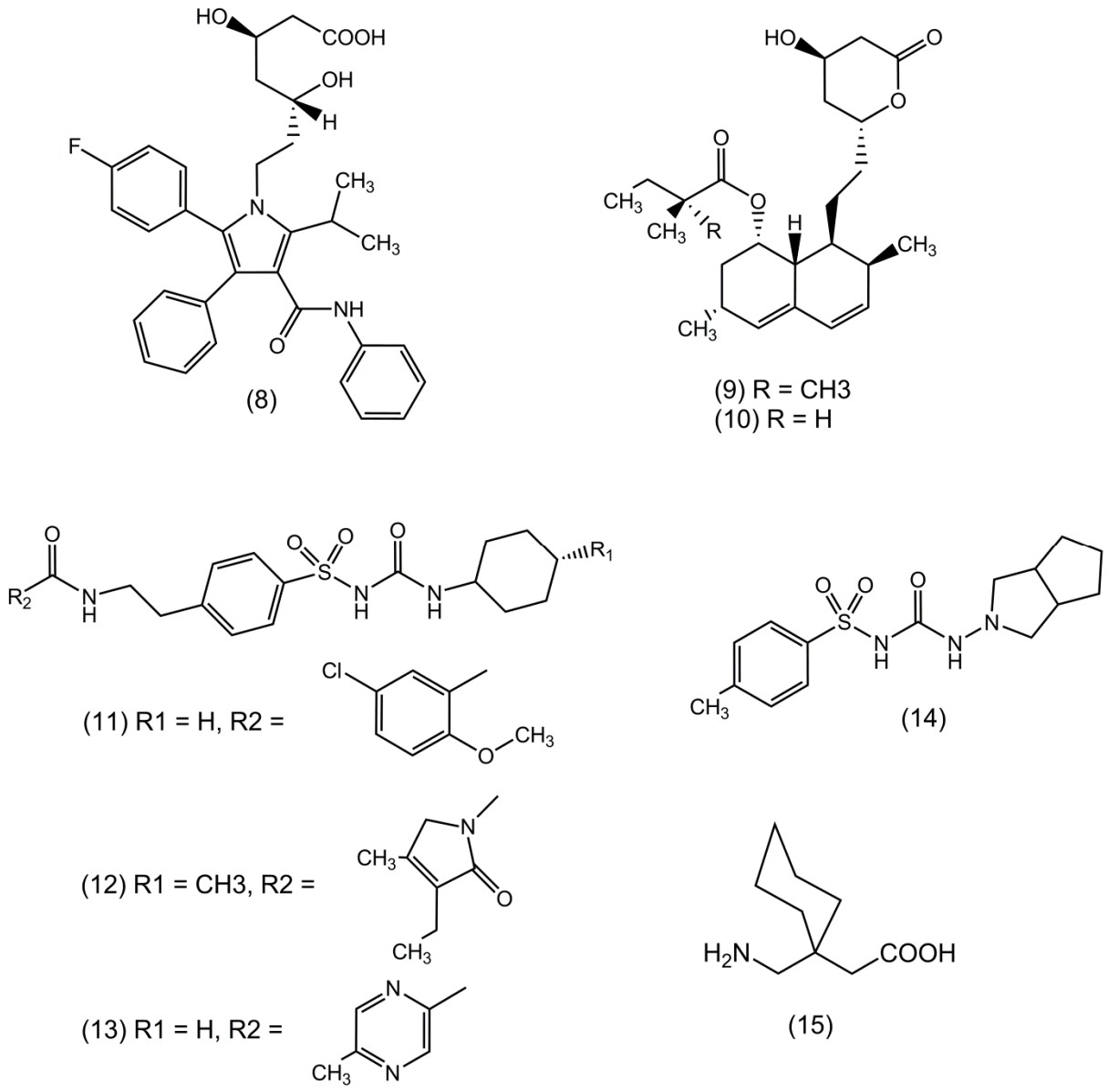

Fig. 6. *(Continued).*

Further methods for the determination of counter-ions in pharmaceutical salts using charged aerosol detection are published [64,65]. In both studies a HILIC column with a zwitterionic stationary phase was employed. The method developed by Fukushima et al. [65] was additionally capable of determining several organic ions (i.e. maleate, succinate, fumarate, tartrate, choline, Tris, lysine).

3.3.2. CAD in the assessment of excipients

3.3.2.1. Polysorbate 80

Polysorbate 80 is a non-ionic surfactant. It is a heterogeneous compound, consisting of oleic acid esters of sorbitol and its anhydrides copolymerised with about 20 mole ethylene oxide for each mole sorbitol and its anhydrides [28]. Current methods for the

quantitative determination of polysorbate 80 use a spectrophotometric determination after derivatization [66], HPLC–UV determination of oleic acid after alkalimetric hydrolysis at 195 nm [67] or size exclusion chromatography [68]. Fekete et al. developed a fast HPLC-CAD method for determining polysorbate 80 in drug solutions containing proteins using a Poroshell 300SB-C18 column (75 mm × 2.1 mm, 5 µm particle size) without any sample preparation [69]. This column material has a solid core with a porous shell, which provides high efficiency and fast analysis on a conventional HPLC system. A gradient elution was applied with acetonitrile/methanol/water–TFA (80/20/900/1, v/v/v/v) as mobile phase A and acetonitrile/methanol/water/TFA (720/180/100/1, v/v/v/v) as mobile phase B at a flow rate of 0.65 mL/min. The first main peak of polysorbate 80 was used for its quantification, as it showed no interference with protein peaks even after oxidation, reduction or deamidation of the protein. This allows quantification in about 10 min.

Lobback et al. compared the performance of an ELS detector and a CAD in quantifying polysorbate 80. Charged aerosol detection was shown to be 10 times more sensitive [70].

Another application investigating the stability of polysorbate 80 was developed by Christiansen et al. [71]. Separation was achieved on a Zorbax SB-Aq C18 (100 mm × 2.1 mm, 3.5 µm particle size) with gradient elution using acetonitrile and water as mobile phases. However, due to the non-uniform response of the CAD in gradient mode, authors choose to apply a single quadrupole mass selective detector for quantification.

3.3.2.2. Hydroxypropylmethylcellulose

Hydroxypropylmethylcellulose (HPMC) is widely used as a tablet binder, film-coating, extended-release tablet matrix, capsule shell and thickening agent in ophthalmic preparations [72]. It is a polymer, whose cellulose hydroxyl groups are partly methylated and 2-hydroxypropylated. Several types of HPMC are available differing in the degree of substitution and molecular weight distribution (approximately 10–1500 kDa). This heterogeneity makes it difficult to develop a simple method that covers all these parameters. The Ph. Eur. makes use of gas chromatography (GC) after ether cleavage with hydroiodic acid [28] in order to determine the degree of substitution. However, sample pre-treatment is time-consuming and only averaged data can be provided.

Greiderer et al. developed a method to illustrate the distribution in molecular weight and degree of substitution [73]. Two-dimensional liquid chromatography was used to characterize HPMC batches from different manufacturers. In the first dimension, reversed phase liquid chromatography (RP-HPLC) was applied to analyse the degree of substitution, as methoxy and hydroxypropoxy substituents influence hydrophobicity. Molecular weight was assessed by size-exclusion chromatography (SEC) in the second dimension. In particular, a linear gradient elution was carried out on a Zorbax 300SB-C8 column (150 mm × 2.1 mm, 3.5 µm particle size) with water/TFA (99.95/0.05, v/v) as mobile phase A and 1-propanol/TFA (99.95/0.05, v/v) as mobile phase B. The column used in SEC was a HSPgel AQ column (150 mm × 6.0 mm, 4.0 µm particle size, 10–400 kDa molecular-weight range) in isocratic mode with mobile phase A. Moreover, the method was capable of estimating the cloud point temperature by applying appropriate column temperatures—an additional criterion to distinguish different HPMC samples.

3.3.3. CAD in pharmaceutical cleaning validation

Cleaning of the production equipment is a critical step in the pharmaceutical production process. For this reason competent authorities have set up strict requirements for the validation of equipment cleaning [74,75]. Analytical methods used for the cleaning validation are often similar to the method used for the impurities control or content determination of drug substances. A technique commonly applied for this purpose is HPLC with UV/Vis detection. However, residual material not possessing a suitable chromophor, like in the case of many active ingredients and excipients, will be difficult to detect. A study was carried out by Forsatz and Snow [26], to demonstrate how HPLC coupled with CAD can successfully be used for cleaning validation. Several common cleaning solvents (water, methanol, ethanol, tetrahydrofuran, acetone) for manufacturing equipment spiked with typical APIs and excipients, i.e. albuterol, mometasone furoate and loratadine, and lactose, were analysed and the results compared to those obtained by a HPLC–UV method. The separation was carried out on a YMC Pack Pro C18 column (50 mm × 4.6 mm, 3 µm particle size) with a mobile phase consisting of methanol/water (75/25, v/v) at a flow-rate of 1 mL/min. For all analysed substances, the CAD showed a linear detector response over the full concentration range from about 10 ng to 400 ng on column. For the three analysed APIs LoQs were found between 2 ng on column and 5 ng on column when using CAD and

between 3 ng on column and 6 ng on column with UV-detection. Compared with UV-detection at 205 nm, the interference with the cleaning solvents was less pronounced when CAD was employed. In terms of recovery, both CAD and UV provided acceptable results with the CAD giving slightly better recoveries. For the analysis of lactose as an example for a compound with poor or no chromophors, CAD clearly demonstrated its superiority to UV detection. Taken together, the study indicates that CAD can be a very useful detector for cleaning validation, especially when it comes to the analysis of substances with low UV-response.

3.3.4. Further application of the CAD

The above detailed examples underline in an impressing manner the potential and usefulness of the CAD in different areas of pharmaceutical analysis. However, in literature several more fields of application in the pharmaceutical sector and related areas are described. These papers which are listed in Table 1 demonstrate that CAD is a versatile detector with a large variety of applications that is especially useful when analysing substances with a suitable chromophor or samples of unknown composition.

Table 1. Further publications dealing with the use of CAD in pharmaceutical and related analysis.

Title	Area	Analytical method information	Key performance characteristics / Conclusion	Corresponding Author
Evaluation of charged aerosol detection as a complementary technique for high-throughput LC-MS-UV-ELSD analysis of drug discovery screening libraries	Drug discover, high throughput screening	Flow injection analysis using a mixture of acetonitrile/water (with 0.01% TFA) (50/50 v/v) as carrier phase with a 0.55 mL flow rate	CAD shows potential for generalized application as a complementary detection technique in high-throughput screening. Data obtained using a generalized CAD calibration curve are sufficiently accurate to confirm that samples are present in both quantities and purities	John Loughlin [76]
Aerosol based detectors for the investigation of phospholipid hydrolysis in pharmaceutical suspension formulation	Fatty acid analysis	Column: Zorbax SB C18 (150 mm x 4.6 mm; 3.5 µm particle size) Mobile phase: water/acetonitrile (20/80 v/v) at a flow rate of 1.0 mL/min	Recovery of different fatty acids between 90.8% and 108.6% (concentration range: 150 to 2250 ng on column) Limits of quantification [ng on column]: linolenic acid: 3.9, linoleic acid: 4.5, palmitic acid: 5.7, Oleic acid: 6.2, Stearic acid: 11.3	Lakshmy M. Nair [77]
Lipid analysis via HPLC with a charged aerosol detector	Fatty acid analysis	Normal phase HPLC-CAD gradient elution method for quantification of the major non-polar lipid class components in vegetable oils and hexane extracts (Details not reported)	Minimum limit of detection: 1 ng on column Signal linear in the range from 1 ng to 20 ng	Robert A. Moreau [78]
Quantitation of triglycerols from plant oils using charged aerosol detection with gradient compensation	Fatty acid analysis, plant extracts	Column: Hypersil ODS (250 mm x 4.6 mm; 5 µm particle size) Mobile phase: Linear gradient from 20% eluent A to 75% eluent A in 80 min withel-uent A: 2-propanol /hexane (1/1 v/v) and eluent B: acetonitrile; inverse gradient was applied resulting in a total flow at the detector inlet of 2.0 mL/min	The response factors of triglycerides containing saturated and unsaturated fatty acids from 12 to 19 carbon atoms showed only 5% variation, which is sufficient for simple quantitative analysis without the need of response factors	Pat Sandra [79]
Direct determination method of oligosaccharides by high-performance liq-	Carbohydrate analysis	Column: Kaseisorb LC ODS 2000 (150 mm x 4.6 mm; 5 µm particle size) and TSK gel Amido-80 (150 mm x 2.0 mm)	Method was 5 times more sensitive than that using a UV detector. It was 10 times less sensitive when compared with fluores-	Toshimasa Toyóok [15]

Title	Area	Analytical method information	Key performance characteristics / Conclusion	Corresponding Author
uid chromatography with charged aerosol detection		Mobile phase: Linear gradient using 0.1% TFA in water (solvent A) and 0.1% TFA in acetonitrile (solvent B) at a flow rate of 1.0 mL/min and 0.4 m/min, respectively	cence detection. Detection limits for different oligosaccharides ranged between 0.35 and 0.63 pmol. Linear detector response between 5.0 and 1000 pmol.	
Quantitative comparison of a corona-charged aerosol detector and evaporative light-scattering detector for the analysis of a synthetic polymer by supercritical fluid chromatography	Polyethylene glycols	Column: SFCpak SIL 5 silica gel column (250 mm x 4.6 mm, 5 µm particle size). Mobile phase: Carbon dioxide with methanol/water (90/10 v/v) as a modifier solvent run at gradient conditions at a constant temp of 50 ºC. Carbon dioxide flow rate: 2.0 mL/min; Flow-rate gradients of the modifier solvent was 0.00667 mL/min^2 from initial flow rates of 0.6 mL/min.	Performance characteristics: Uniform PEGs of various degree of polymerization and the certified reference material of PEG 1000 were analysed. The repeatability of the CAD is greater than ELSD. The limit of detection is about 10 times lower (Limit of detection of the CAD: 50 ng on column).	Kayori Takahashi [16]
Comparison between evaporative light scattering detection and charged aerosol detection for the analysis of saikosaponins	Saponin analysis, plant extracts	Column: Supelco Ascentis Express C18 (100 mm x 4.6 mm, 2.7 µm particle size) and Phenomenex Security Guard C18 column (4.0 mm x 3.0 mm) Mobile phase: Gradient elution of eluent A (acetonitrile/water 90/10 v/v) and eluent B (water/ acetonitrile 90/10 v/v); 0-5 min isocratic at 20% A, 5-35 min linear gradient to 50% A, 35-36 min to 90% A, 36-46 min isocratic at 90% A. Flow rate of 1.0 mL/min (post column split ELSD / CAD 50/50).	Linear range: between 10-1000 ng on column and 30-3000 ng on column. Limit of quantification: between 10-30 ng on column.	Sang Beom Han [80]
Comparison between charged aerosol detection and light scattering detection for the analysis of Leishmania membrane phospholipids	Phospholipids, biological material	Column: YMC PVA-SIL (150 mm x 2.0 mm, 5 µm particle size) and YMC PVA-SIL Guard column (10 mm x 2.0 mm) Mobile phase: Gradient elution over 68 min with: eluent A (n-Heptane/2-propanol 98/2 v/v), eluent B	The limits of quantification and limits of detection are, on average, three times lower with CAD than with ELSD. Linear range CAD: between 30-2000 ng on column and 1280-20000 ng on column depending on the phospholipid.	Pierre Chaminade [81]

Title	Area	Analytical method information	Key performance characteristics / Conclusion	Corresponding Author
		(chloroform/2-propanol 65/35 v/v) and eluent C (methanol/water 95/5 v/v); all mobile phases containing 0.08% triethylamine and 1% acetic acid (v/v). Flow rate of 0.4 mL/min.	Limit of detection CAD: between 15-249 ng on column depending on the phospholipid. Limit of quantification CAD: between 45-756 ng on column depending on the phospholipid.	
Determination of parabens in cosmetic products using multi-walled carbon nanotubes as solid phase extraction sorbent and corona-charged aerosol detection system	Preservatives in cosmetic products	Column: RP-C18 (250 mm x 4.6 mm) Mobile phase: Isocratic elution with acetonitrile:water (50:50, v/v)	Limit of detection: between 10-42 ng on column Limit of quantification: between 40-106 ng on column	Miguel Valcárcel [82]
Analysis of terpene lactones in a ginkgo leaf extract by high-performance liquid chromatography using charged aerosol detection	Active ingredients of plant extracts	Column: Mightysil RP-18 (150 mm x 4.6 mm, 5 µm particle size) Mobile phase: Gradient elution with water as mobile phase A and methanol as mobile phase B, 0-20 min isocratic with 30% B, 20-25 min to 70% B, 25-30 min isocratic at 70% B, 30-40 min decrease to 30% B and re-equilibration, flow rate of 1.0 ml/min	Limit of detection: between 0.87-2 ng on column Limit of quantification: between 2.9-15 ng on column	Yasuhiro Kakigi [83]
Polyketide analysis using mass spectrometry, evaporative light scattering, and charged aerosol detector systems	Fermentation products	Direct introduction of the sample into the detector	Comparison of CAD, ELSD an MS detection. CAD was shown to be even more sensitive than mass detection providing a similar dynamic range Limit of detection: 0.12 ng introduced directly into the detector (0.19 ng for MS detection)	Michael Pistorino, Blaine A. Pfeifer [84]
Direct stability-indicating method development and validation for analy-	Assay determination, stability analysis	Column: Primesep SB (50 mm x 3.2 mm, 5 µm particle size)	Limit of detection: 50 ng for the API and impurities	Jiang B. Fang [85]

Title	Area	Analytical method information	Key performance characteristics / Conclusion	Corresponding Author
sis of etidronate disodium using a mixed-mode column and charged aerosol detector		Mobile phase: Gradient elution with water-acetonitrile (95/5, v/v) containing 0.03% TFA as mobile phase A and water-acetonitrile (95/5, v/v) containing 0.2% TFA as mobile phase B. 0-5 min linear gradient from 0-100% B, 5-8 min isocratic with 100% B. Flow rate of 0.5 ml/min	Limit of quantification: 144 ng and 75 ng for the API and its impurities, respectively	

Title	Area	Analytical method information	Key performance characteristics / Conclusion	Corresponding Author
The analysis of lipids via HPLC with a charged aerosol detector	Lipid analysis	Column: LiChrosorb Diol (100 mm x 3.0 mm, 7 µm particle size) and Prevail RP18 (150 mm x 2.1 mm, 3 µm particle size) Mobile phase: Different gradient methods using hexane and isopropanol with various modifiers as mobile phases depending on the lipid class to be analysed in normal phase HPLC, and gradient elution with methanol-acetonitrile-dichlormethane-acetic acid (49.3:47:3:0.2, v/v/v/v) as mobile phase A and isopropanol as mobile phase B in reversed phase HPLC	CAD might become a powerful tool for lipid analysis. However, it was less sensitive than fluorescence detection for the determination of tocopherols. Limit of detection: between 1-25 ng depending on the lipid and the method used	Robert A. Moreau [86]
Simple and precise detection of lipid compounds present within liposomal formulations using a charged aerosol detector	Lipid analysis	Column: XBridge C18 (150 mm x 3.0 mm, 3.5 µm particle size) Mobile phase: Gradient elution with acetonitrile-water (90:10, v/v) as mobile phase A and methanol as mobile phase B, both containing 0.05% trifluoroacetic acid. 0-25 min 40% of mobile phase B, 25-35 min 100% of mobile phase B	CAD is superior to UV detection in terms of precision, sensitivity and peak shape	Giancarlo Francese [87]

4. Conclusion

HPLC coupled with a UV/Vis-spectrophotometric detector is the most commonly used analytical technique in pharmaceutical analysis. However, detection by UV/Vis absorbance shows its limitations for molecules lacking a suitable chromophor. In the past years, several evaporation based detector were developed, amongst which the corona charged aerosol detector currently appears to be the most powerful and versatile representative.

Numerous papers have been published demonstrating the potential and advantages of HPLC coupled to detection by CAD in a wide range of pharmaceutical applications. A prerequisite for the use of the CAD is, similar to MS detection, the use of volatile mobile phases. However, if this is given, its ease of use, high sensitivity with limits of quantification down to 1 ng of substance on column and good linearity over a limited range of concentration make the CAD a powerful detector for research purposes, method development and routine analysis. The limited suitability for gradient methods can be overcome by post-column gradient compensation and corresponding dual-pump solutions are now commercially available. Taken together, the CAD appears to fill a gap in the range of HPLC detectors and an even more growing number of applications in pharmaceutical analysis is expected in the coming years.

References

[1] L.S. Ettre, M.S. Tswett and the invention of chromatography, LC–GC N. Am. 21 (2003) 458–467.

[2] C.F. Poole, The Essence of Chromatography, 1st ed., Elsevier Science, Amsterdam, 2003.

[3] V. Douville, A. Lodi, J. Miller, A. Nicolas, I. Clarot, B. Prilleux, N. Megoulas, M. Koupparis, Evaporative light scattering detection (ELSD): a tool for improved quality control of drug substances, Pharmeuropa Scientific Notes 1 (2006) 9–15.

[4] J.M. Charlesworth, Evaporative analyzer as a mass detector for liquid chromatography, Anal. Chem. 50 (1978) 1414–1420.

[5] S. Almeling, U. Holzgrabe, Use of evaporative light scattering detection for the quality control of drug substances: influence of different liquid chromato-graphic and evaporative light scattering detector parameters on the appearance of spike peaks, J. Chromatogr. A 1217 (2010) 2163–2170.

[6] R.W. Dixon, D.S. Peterson, Development and testing of a new detector for liquid chromatography based on aerosol charging, Anal. Chem. 74 (2002) 2930–2937.

[7] L.B. Allen, J.A. Koropchak, Condensation nucleation light scattering: a new approach to development of high sensitivity, universal detectors for separa-tions, Anal. Chem. 65 (1993) 841–844.

[8] L.B. Allen, J.A. Koropchak, B. Szostek, Condensation nucleation light scattering detection for conventional reversed-phase liquid chromatography, Anal. Chem. 67 (1995) 659–666.

[9] U. Holzgrabe, C.J. Nap, T. Beyer, S. Almeling, Alternatives to amino acid analysis for the purity control of pharmaceutical grade l-alanine, J. Sep. Sci. 33 (2010) 2402–2410.

[10] S. Almeling, The use of aerosol-based detection systems in the quality control of drug substances, Dissertation, 2011, University of Wuerzburg, http://opus.bibliothek.uni-wuerzburg.de/volltexte/2011/6472/.

[11] B.Y.H. Liu, D.Y.H. Pui, On the performance of the electrical aerosol analyzer, J. Aerosol Sci. 6 (1975) 249–264.

[12] M. Adachi, Y. Kousaka, K. Okuyama, Unipolar and bipolar diffusion charging of ultrafine aerosol particles, J. Aerosol Sci. 16 (1985) 109.

[13] T. Vehovec, A. Obreza, Review of operating principle and application of the charged aerosol detector, J. Chromatogr. A 1217 (2010) 1549–1556.

[14] T. Gorecki, F. Lynen, R. Szucs, P. Sandra, Universal response in liquid chromatog-raphy using charged aerosol detection, Anal. Chem. 78 (2006) 3186–3193.

[15] N. Vervoort, D. Daemen, G. Török, Performance evaluation of evaporative light scattering detection and charged aerosol detection in reversed phase liquid chromatography, J. Chromatogr. A 1189 (2008) 92–100.

[16] S. Inagaki, J.Z. Min, T. Toyóoka, Direct detection method of oligosaccharides by high-performance liquid chromatography with charged aerosol detection, Biomed. Chromatogr. 21 (2007) 338–342.

[17] K. Takahashi, S. Kinugasa, M. Senda, K. Kimizuka, K. Fukushima, Y. Shibata, J. Christensen, Quantitative comparison of a corona-charged aerosol detec-tor and an evaporative light-sacttering detector for the analysis of a synthetic polymer by supercritical fluid chromatography, J. Chromatogr. A 1193 (2008) 151–155.

[18] P. Sun, X. Wang, L. Alquier, C.A. Maryanoff, Determination of relative response factors of impurities in paclitaxel with high performance liquid chromatogra-phy equipped with ultraviolet and charged aerosol detectors, J. Chromatogr. A 1177 (2008) 87–91.

[19] U. Holzgrabe, C.J. Nap, N. Kunz, S. Almeling, Identification and control of impurities in streptomycin sulfate by high-performance liquid chromatography coupled with mass detection and corona charged-aerosol detection, J. Pharm. Biomed. Anal. 56 (2011) 271–279.

[20] P.H. Gamache, R.S. McCarthy, S.M. Freeto, D.J. Asa, M.J. Woodcock, K. Laws, R.O. Cole, HPLC analysis of non-volatile analytes using charged aerosol detection, LC–GC Europe 18 (2005) 345–354.

[21] U. Holzgrabe, C.J. Nap, S. Almeling, Control of impurities in l-aspartic acid and l-alanine by high-performance liquid chromatography coupled with a corona charged aerosol detector, J. Chromatogr. A 1217 (2010) 294–301.

[22] Unpublished data of the Author.

[23] N. Vervoort, D. Daemen, G. Török, Performance evaluation of evaporative light scattering detection and charged aerosol detection in reversed phase liquid chromatography, J. Chromatogr. A. 1189 (2008) 92–100.

[24] L. Nováková, S.A. Lopez, D. Solichova, D. Satinsky, B. Kulichova, A. Horna, P. Solich, Comparison of UV and charged aerosol detection approach in pharmaceutical analysis of statins, Talanta 78 (2009) 834–839.

[25] L. Nováková, D. Solichová, P. Solich, Hydrophilic interaction liquid chromatography—charged aerosol detection as a straightforward solu-tion for simultaneous analysis of ascorbic acid and dehydroascorbic acid, J. Chromatogr. A 1216 (2009) 4574–4581.

[26] B. Forsatz, H.N. Snow, HPLC with charged aerosol detection for pharmaceutical cleaning validation, LC–GC N. Am. 25 (2007) 960–968.

[27] Guideline Q3A(R2), Impurities in New Drug Substances, International Conference on Harmonisation 2006, http://www.ich.org.

[28] European Pharmacopoeia, 7th ed., European Directorate for the Quality of Medicines and HealthCare, Strasbourg, 2010.

[29] E. Adams, M. Rafiee, E. Roets, J. Hoogmartens, Liquid chromatographic analysis of streptomycin sulfate, J. Pharm. Biomed. Anal. 24 (2000) 219–226.

[30] M. Pendela, J. Hoogmartens, A. Van Schepdael, E. Adams, LC–MS of streptomycin following desalting of a nonvolatile mobile phase and pH gradient, J. Sep. Sci. 32 (2009) 3418–3424.

[31] S.I. Kawano, Analysis of impurities in streptomycin and dihydrostrepto-mycin by hydrophilic interaction chromatography/electrospray ionization quadrupole ion trap/time-of-flight mass spectrometry, Rapid Commun. Mass Spectrom. 23 (2009) 907–914.

[32] E. Adams, R. Schepers, E. Roets, J. Hoogmartens, Determination of neomycin sulfate by liquid chromatography with pulsed electrochemical detection, J. Chromatogr. A 741 (1996) 233–240.

[33] E. Adams, J. Dalle, E. De Bie, I. De Smedt, E. Roets, J. Hoogmartens, Analysis of kanamycin sulfate by liquid chromatography with pulsed electrochemical detection, J. Chromatogr. A 766 (1997) 133–139.

[34] E. Adams, G. van Vaerenbergh, E. Roets, J. Hoogmartens, Analysis of amikacin by liquid chromatography with pulsed electrochemical detection, J. Chromatogr. A 819 (1998) 93–97.

[35] J. Szunyog, E. Adams, E. Roets, J. Hoogmartens, Analysis of tobramycin by liquid chromatography with pulsed electrochemical detection, J. Pharm. Biomed. Anal. 23 (2000) 891–896.

[36] E. Adams, W. Roetlants, R. de Paepe, E. Roets, J. Hoogmartnes, Analysis of gen-tamicin by liquid chromatography with pulsed electrochemical detection, J. Pharm. Biomed. Anal. 18 (1998) 689–698.

[37] E. Adams, D. Puelings, M. Rafiee, E. Roets, J. Hoogmartens, Determination of netilmicin sulfate by liquid chromatography with pulsed electrochemical detection, J. Chromatogr. A 812 (1998) 151–157.

[38] D. Debremaeker, E. Adams, E. Nadal, B. van Hove, E. Roets, J. Hoogmartens, Anal-ysis of spectinomycin by liquid chromatography with pulsed electrochemical detection, J. Chromatogr. A 953 (2002) 123–132.

[39] Dionex Application Note 181, http://www.dionex.com/en-us/webdocs/62476-AN181 IC Streptomycin HPAE-PAD 28Nov07 LPN1887.pdf.

[40] A. Joseph, A. Rustum, Development and validation of a RP-HPLC method for the determination of gentamicin sulfate and its related substances in a pharmaceutical cream using a short pentafluorophenyl column and a charged aerosol detector, J. Pharm. Biomed. Anal. 51 (2010) 521–531.

[41] K. Stypulkowska, A. Blazewicz, Z. Fijalek, K. Sarna, Determination of gentamicin sulphate composition and related substances in pharmaceutical preparations by LC with charged aerosol detection, Chromatographia 72 (2010) 1225–1229.

[42] A. Joseph, S. Patel, A. Rustum, Development and validation of a RP-HPLC method for the estimation of netilmicin sulfate and its related substances using charged aerosol detection, J. Chromatogr. Sci. 48 (2010) 607–612.

[43] W.P. MeGuire, E.K. Rowinsky, N.B. Rosenheim, F.C. Grumbine, D.S. Ettinger, D.K. Armstrong, R.C. Donehower, Taxol: a unique antineoplastic agent with significant activity in advanced ovarian neoplasma, Ann. Intern. Med. 111 (1989) 273–279.

[44] A. Sparreboom, O. van Tellingen, W.J. Nooijen, J.H. Beijnen, Tissue distribution, metabolism and excretion of paclitaxel in mice, Anti-Cancer Drugs 7 (1996) 78–86.
[45] C. Mount, C. Downton, Alzheimer disease: progress or profit? Nat. Med. 12 (2006) 780–784.

[46] W. Grosch, H.D. Belitz, Lehrbuch der Lebensmittelchemie, 3. Auflage, Springer-Verlag, Berlin, 1987.

[47] S.S. Bharate, S.B. Bharate, A.N. Bajaj, Interactions and incompatibilities of pharmaceutical excipients with active pharmaceutical ingredients: a compre-hensive review, J. Excipients Food Chem. 1 (2010) 3–26.

[48] L. Rystov, R. Chadwick, K. Krock, T. Wang, Simultaneous determination of Maillard reaction impurities in memantine tablets using HPLC with charged aerosol detector, J. Pharm. Biomed. Anal. 56 (2011) 887–894.

[49] A. Kleemann, W. Leuchtenberger, B. Hoppe, H. Tanner, in: W. Gerhartz (Hrsg.), Ullmann's Encyclopedia of Industrial Chemistry, 5th ed., vol. A2, VCH Verlagsgesellschaft mbh, Weinheim, 1985.

[50] E. Körner, G. Bertha, E. Flooh, B. Reinhart, R. Wolf, H. Lechner, Sleep-inducing effect of l-tryptophan, Eur. Neurol. 25 (1986) 75–81.

[51] G. Hajak, G. Huether, J. Blanke, M. Blömer, C. Freyer, B. Poeggeler, A. Reimer, A. Rodenbeck, M. Schulz-Varszegi, E. Rüther, The influence of intravenous l-tryptophan on plasma melatonin and sleep in men, Pharmacopsychiatry 24 (1991) 17–20.

[52] Rote Liste, Hrsg. Rote Liste Verlagsservice GmbH, Edition 2000, 71/149 and 71/169, Editio Cantor Verlag Aulendorf, 2000.

[53] K. Petritis, C. Elfakir, M. Dreux, A comparative study of commercial liquid chromatographic detectors for the analysis of underivatized amino acids, J. Chromatogr. A 961 (2002) 9–21.

[54] C. Crafts, B. Bailey, I. Acworth, UHPLC analysis of underivatized amino acids, LC–GC-Chromatogr. Online 01.09.2011; <http://chromatographyonline. findanaly tichem.com/lcgc/Articles/UHPLC-Analysis-of-Underivatized-Amino- Acids/Article Standard/Article/detail/739811>.

[55] A. Blazewicz, Z. Fijalek, M. Warowna-Grzeskiewicz, M. Jadach, Determina-tion of atracurium, cisatracurium and mivacurium with their impurities in pharmaceutical preparations by liquid chromatography with charged aerosol detection, J. Chromatogr. A 1217 (2010) 1266–1272.

[56] D.F. Kisor, V.D. Schmith, Clinical pharmacokinetics of cisatracurium besilate, Clin. Pharmacokinet. 36 (1999) 27–40.

[57] D.P. Atherton, J.M. Hunter, Clinical pharmacokinetics of the newer neuromus-cular blocking drugs, Clin. Pharmacokinet. 36 (1999) 169–189.

[58] M. Weindlmayr-Goettel, H.G. Kress, F. Hammerschmidt, V. Nigrovic, In vitro degradation of atracurium and cisatracurium at pH 7.4 and 37 °C depends on the composition of the incubation solution, Br. J. Anaesth. 81 (1998) 409–414.

[59] M. Weindlmayr-Goettel, H. Gilly, H.G. Kress, Does ester hydrolysis change the in vitro degradation rate of cisatracurium and atracurium, Br. J. Anaesth. 88 (2002) 555–562.

[60] J. Shaodong, W.J. Lee, J.W. Ee, J.H. Park, S.W. Kwon, J. Lee, Comparison of ultra-violet detection, evaporative light scattering detection and charged aerosol detection methods for liquid-chromatographic determination of anti-diabetic drugs, J. Pharm. Biomed. Anal. 51 (2010) 973–978.

[61] S. Jia, J.H. Park, J. Lee, S.W. Kwon, Comparison of two aerosol-based detectors for the analysis of gabapentin in pharmaceutical formulations by hydrophilic interaction chromatography, Talanta 85 (2011) 2301–2306.

[62] K. Zhang, L. Dai, N.P. Chetwyn, Simultaneous determination of positive and neg-ative pharmaceutical counterions using mixed-mode chromatography coupled with charged aerosol detector, J. Chromatogr. A 1217 (2010) 5776–5784.

[63] Z. Huang, M.A. Richards, Y. Zha, R. Francis, R. Lozano, J. Ruan, Determination of inorganic pharmaceutical counterions using hydrophilic interaction chromatography coupled with Corona® CAD detector, J. Pharm. Biomed. Anal. 50 (2009) 809–814.

[64] Y. Kanedai, K. Hashiguti, K. Fukushima, M. Senda, C. Crafts, J. Gray, M. Plante, I. Acworth, Simultaneous analysis of cations and anions using charged aerosol detection method, Chromatography 30 (Suppl. 1) (2009) 113–116.

[65] K. Fukushima, Y. Kanedai, K. Hashiguchi, M. Senda, I.N. Acworth, Generic approach to analysis of pharmaceutical salts including inorganic and organic counterions, Chromatography 30 (Suppl. 1) (2009) 105–108.

[66] N.H. Anderson, J. Girling, Determination of polyoxyethylene non-ionic surfactants at trace levels, Analyst 107 (1982) 836–838.

[67] M. Adamo, L.W. Dick Jr., D. Qiu, A.-H. Lee, J. Devincentis, K.-C. Cheng, A simple reversed phase high-performance liquid chromatography method for polysorbate 80 quantitation in monoclonal antibody drug products, J. Chromatogr. B 878 (2010) 1865–1870.

[68] T.H. Tani, J.M. Moore, T.W. Patapoff, Single step method for the accurate concentration determination of polysorbate 80, J. Chromatogr. A 786 (1997) 99–106.

[69] S. Fekete, K. Ganzler, J. Fekete, Fast and sensitive determination of polysorbate 80 in solutions containg proteins, J. Pharm. Biomed. Anal. 52 (2010) 672–679.

[70] C. Lobback, T. Backensfeld, A. Funke, W. Weitschies, Analysis of polysorbate 80 using fast HPLC and charged aerosol detection, Pharm. Technol. 34 (2010) 48–54.

[71] A. Christiansen, T. Backensfeld, S. Kuehn, W. Weitschies, Stability of the non-ionic surfactant polysorbate 80 investigated by HPLC–MS and charged aerosol detector, Pharmazie 66 (2011) 666–671.

[72] A.H. Kibbe, Handbook of Pharmaceutical Excipients, 3rd ed., American Pharmaceutical Association, Washington, DC, 2000.

[73] A. Greiderer, L. Steeneken, T. Aalbers, G. Vivó-Truyols, P. Schoenmakers, Characterization of hydroxypropylmethylcellulose (HPMC) using comprehen-sive two-dimensional liquid chromatography, J. Chromatogr. A 1218 (2011) 5787–5793.

[74] EMA, Note for guidance on good manufacturing practice for active pharmaceu-tical ingredients, CPMP/ICH/4106/00, 2000.

[75] FDA, Guide to inspections: validation of cleaning process, 1993.

[76] J. Loughlin, H. Phan, M. Wan, S. Guo, K. May, B. Lin, Evaluation of charged aerosol detection as a complementary technique for high-throughput LC–MS–UV–ELSD analysis of drug discovery screening libraries, Am. Lab. 39 (2007) 24–27.

[77] L.M. Nair, J.O. Werling, Aerosol based detectors for the investigation of phospholipid hydrolysis in pharmaceutical suspension formulation, J. Pharm. Biomed. Anal. 49 (2009) 95–99.

[78] R.A. Moreau, Lipid analysis via HPLC with a charged aerosol detector, Lipid Technol. 21 (2009) 191–194.

[79] M. Lisa, F. Lynen, M. Holcapek, P. Sandra, Quantitation of triacyglycerols from plant oils using charged aerosol detection with gradient compensation, J. Chro-matogr. A 1176 (2007) 135–142.

[80] H.Y. Eom, S.-Y. Park, M.K. Kim, J.H. Suh, H. Yeom, J.W. Min, U. Kim, J. Lee, J.-R. Youm, S.B. Han, Comparison between evaporative light scattering detection and charged aerosol detection for the analysis of saikosaponins, J. Chromatogr. A 1217 (2010) 4347–4354.

[81] R. Godoy Ramos, D. Libong, M. Rakotomanga, K. Gaudin, P.M. Loiseau, P. Cham-inade, Comparison between charged aerosol detection and light scattering detection for the analysis of Leishmania membrane phospholipide, J. Chro-matogr. A 1209 (2008) 88–94.

[82] I. Márquez-Sillero, E. Aguilera-Herrador, S. Cárdenas, M. Valcárcel, Determina-tion of parabens in cosmetic products using multi-walled carbon nanotubes as solid phase extraction sorbent and corona-charged aerosol detection system, J. Chromatogr. A 1217 (2010) 1–6.

[83] Y. Kakigi, N. Mochizuki, T. Icho, T. Hakamatsuka, Y. Goda, Analysis of terpene lactones in a ginkgo leaf extract by high-performance liquid chromatogra-phy using charged aerosol detection, Biosci. Biotechnol. Biochem. 74 (2010) 590–594.

[84] M. Pistorino, B.A. Pfeifer, Polyketide analysis using mass spectrometry, evap-orative light scattering, and charged aerosol detector systems, Anal. Bioanal. Chem. 390 (2008) 1189–1193.

[85] X.-K. Liu, J.B. Fang, N. Cauchon, P. Zhou, Direct stability-indicating method development and validation for analysis of etidronate disodium using a mixed-mode column and charged aerosol detector, J. Pharm. Biomed. Anal. 46 (2008) 639–644.

[86] R.A. Moreau, The analysis of lipids via HPLC with a charged aerosol detector, Lipids 41 (2006) 727–734.

[87] C. Schoenherr, S. Touchene, G. Wilser, R. Peschka-Suess, G. Francese, Simple and precise detection of lipid compounds present within liposomal formulations using a charged aerosol detector, J. Chromatogr. A 1216 (2009) 781–786.

4 Results

4.1 Validation and application of an HPLC-CAD-TOF/MS method for identification and quantification of pharmaceutical counterions

D. Ilko, C.J. Nap, U. Holzgrabe, S. Almeling

Reprinted with permission[1] from Pharmeuropa Bio & SN **2014**, 2014, 81-91.

Abstract

A generic approach for the analysis of counterions of pharmaceutical reference substances, which are established by the laboratory department of the European Pharmacopoeia (Ph. Eur.), was developed. A mixed-mode chromatography method using charged aerosol detection (CAD) published by Zhang et al. separating 25 commonly used pharmaceutical counterions was selected for this purpose. The method was validated in terms of specificity, repeatability, limits of quantification (LOQs), linearity and range according to ICH guideline Q2(R1) and the Technical Guide for the Elaboration of Monographs of the Ph. Eur. Moreover, the applicability of the method for the purpose of counterion identification and quantification in drug substances as well as for the control of inorganic ions as impurities was demonstrated using selected examples of Ph. Eur. reference standards and other samples of substances for pharmaceutical use (e.g. cloxacillin sodium, somatostatin). It was shown that for identification purposes of the parent substance as well as organic ions the chromatographic system can easily be coupled to a mass selective detector without any modification.

[1] The reprint permission granted by the EDQM is gratefully acknowledged. The article can be consulted free of charge at http://pharmeuropa.edqm.eu/.

1. Introduction

The Laboratory Department of the European Directorate for the Quality of Medicines & HealthCare (EDQM) is responsible for the establishment of reference standards described in the general methods and the individual monographs of the European Pharmacopoeia (Ph. Eur.). As these standards are often established as primary standards, a thorough characterisation of the corresponding candidate material is of utmost importance. Besides unambiguous structure elucidation and characterisation using the tests and methods described in the corresponding Ph. Eur. monographs, additional analytical methods, such as mass spectrometry and NMR, are usually applied to complement the establishment work.

Impurities dedicated as reference standards for quantification in an HPLC or GC method for related substances are not necessarily available in the same salt form as the corresponding substance for pharmaceutical use which is subject to a test prescribed in a monograph. Since differences in the counterions of the impurity reference standard and the substance to be tested may lead to an under- or overestimation of the impurity content in a substance, identification of the counterions or salt form and consideration of a corresponding stoichiometric conversion factor for the calculation of the impurity content is of particular importance. In the same context, verification of the stoichiometric composition of a reference standard present as a salt may be an important element for the characterisation of the standard.

The aim of this work was to verify the suitability of a generic HPLC method for the identification and quantification of counterions and to perform corresponding method validation. An aerosol-based detector, like an evaporative light scattering detector (ELSD), a charged aerosol detector (CAD) or a nano quantity analyte detector (NQAD) were considered to be best suited for this analytical task. Using these detectors, all non-volatile and some semi-volatile analytes are detected providing consistent response independent of the chemical nature of the substances [1]. Thus, they cover a wide range of typical pharmaceutical counterions and overcome the obstacle that they mostly lack a suitable UV/Vis-chromophore.

Several methods dealing with the analysis of counterions using CAD [2-5] or ELSD [6,7] were recently published. Separations were carried out either with mixed-mode HPLC [2], hydrophilic interaction liquid chromatography (HILIC) [3-5] or ion chromatography [6,7].

The HPLC-CAD method proposed by Zhang *et al.* [2] was finally chosen for our study, because it covered the widest range of ions to be analysed and CAD seems to provide better sensitivity and repeatability than other aerosol-based detectors [8]. The method is capable of separating 25 of the most common pharmaceutical counterions in a single chromatographic run. An Acclaim Trinity P1 analytical column was employed for this purpose. This mixed-mode column contains reversed phase and weak anion exchange properties in the inner-pore area of the spherical silica particles. They are additionally coated with nanopolymer beads on the outer surface providing strong cation exchange properties. The steric separation of anion and cation exchange functionalities allows the simultaneous operation of both mechanisms [9,10].

Zhang and co-workers [2] investigated the quite complex retention behaviour for this mixed mode column. It is influenced by mobile phase pH, salt type, ionic strength, content of organic modifier and it depends on the nature of the analyte itself. In our study, we focus on the validation and application of this method demonstrating its added values for the reference standard establishment based on selected examples.

2. Material and Method

2.1. Reagents and material

All chemicals were of analytical grade or better unless otherwise stated. Ammonium formate, citric acid monohydrate, magnesium chloride hexahydrate, maleic acid and procaine hydrochloride were purchased from Fisher Scientific (Illkirch, France); formic acid, magnesium sulfate, potassium bromide, potassium dihydrogenphosphate, sodium sulfate and sodium sulfite from Merck Chemicals (Molsheim, France); ammonium acetate (HPLC-grade) and sodium nitrate from Fluka (St-Quentin-Fallavier, France). Further substances were from Sigma-Aldrich (St‑Quentin Fallavier, France).

All other samples analysed in this study were provided by the EDQM (Strasbourg, France).

Ultra-pure water (>18.2 MΩ) was delivered by an ELGA PureLab Ultra system (Elga Antony, France). Gradient grade acetonitrile (Chromasolv®) was purchased from Sigma-Aldrich (St‑Quentin-Fallavier, France). A pH-meter 780 (Metrohm, Villebon-sur-Yvette, France) was used for pH adjustment. Mobile phases were filtered through a 0.2 µm filter (Sartorius stedim, Lyon, France) prior to use.

2.2. Apparatus and chromatographic conditions

Measurements were carried out on a Dionex UltiMate® 3000 x2 chromatographic system (Dionex, Courtaboeuf, France) equipped with a ternary pump, an online degasser, a thermostated autosampler, a thermostated column compartment and a single wavelength UV/Vis detector. An Acclaim Trinity P1 (50 x 3 mm; 3.0 µm particle size) (Thermo Scientific, Courtaboeuf, France) analytical column was used in this study. Detection was performed with a Corona® CAD or a Corona® CAD ultra RS, respectively (Thermo Fisher, Courtaboeuf, France). Gas inlet pressure (nitrogen) was 35.0 psi for both detectors. The detection range was set to 100 pA and filter to “none”. Nebulizer temperature is adjustable for CAD ultra RS. It was set to 35 °C.

For MS-detection a Bruker microTOF (Bruker Daltonik GmbH, Bremen, Germany) was connected to the above mentioned LC-system by installing a flow-splitter (split ratio 1:10) after the UV detector outlet.

The column compartment was maintained at 35 °C, the autosampler was operated at ambient temperature. Flow rate was 0.5 mL/min and the injection volume 10 µL. A ternary gradient was applied with 0.2 M ammonium formate (pH 4.0, adjusted with formic acid) as mobile phase A, water as mobile phase B and acetonitrile as mobile phase C. The gradient profile is shown in Table 1.

Table 1. Gradient profile. Mobile phase A: 0.2 M ammonium formate, pH 4.0. Mobile phase B: water. Mobile phase C: acetonitrile. Flow rate: 0.5 mL/min.

time (min)	% A	% B	% C
0	2	38	60
7	5	35	60
15	90	5	5
20	90	5	5
20.1	2	38	60
25	2	38	60

2.3. Sample preparation

All samples were dissolved in acetonitrile/water (25/75; v/v). Although glassware of Ph. Eur. Type I was used, the sample solvent was found capable of dissolving ions

from the glassware. Instead, polypropylene equipment was used throughout the preparation of samples.

3. Results and discussion

3.1. Method validation

The optimised method which is characterised by a mixed-mode column and a ternary gradient (see chapter 2.2) was validated according to the Technical Guide for the Elaboration of Monographs [11] and ICH guideline Q2(R1) [12] in terms of specificity, repeatability, limits of quantification (LOQ), linearity and range. Furthermore, the stability of the sample solution was investigated.

Concerning validation of method accuracy, it was considered that validation is not possible without knowledge of the sample matrix / substance to be examined since co-elution of some counterions with the analyte or other compounds in the sample solution may occur. Moreover, analytes may interfere with some counterions (e.g. cloxacillin might cover the presence of e.g. polyvalent cations in the sample due to the formation of a poorly soluble salt). As this method was intended to provide a generic approach, accuracy had to be validated for a particular application on a case-by-case basis, if quantification was desired. This could easily be achieved by applying the standard addition method, which allowed at the same time to re-verify linearity of range and application of an appropriate calibration function. An example following this approach is given in chapter 3.2.2.

3.1.1. Specificity

Method specificity was confirmed by injecting a sample containing 23 ions that can be separated (benzenesulfonate (=besilate), bromide, calcium, chloride, choline, citrate, fumarate, potassium, procaine, sodium, succinate, sulfate, tartrate, p-toluenesulfonate (=tosylate), tromethamine (=tris), zinc) in concentrations of about 0.05 to 0.20 mg/mL. Peak identification was achieved by single injection of a salt of each ion. A typical chromatogram is shown in Fig. 1.

Some of the ions were not baseline separated (e.g. potassium/meglumine or chloride/bromide) in this example. Here, due to the fact that several cations were only available as chloride salts, the rather high concentration of chloride when preparing a solution containing all substances caused the poor separation. At lower concentra-

tions of both ions, i.e. about 25 µg/mL of chloride and 35 µg/mL of bromide, a baseline separation was achieved (data not shown). For the unambiguous distinction of 2 close-eluting peaks, test solutions should be spiked with the respective ions in addition to the comparison of the retention times.

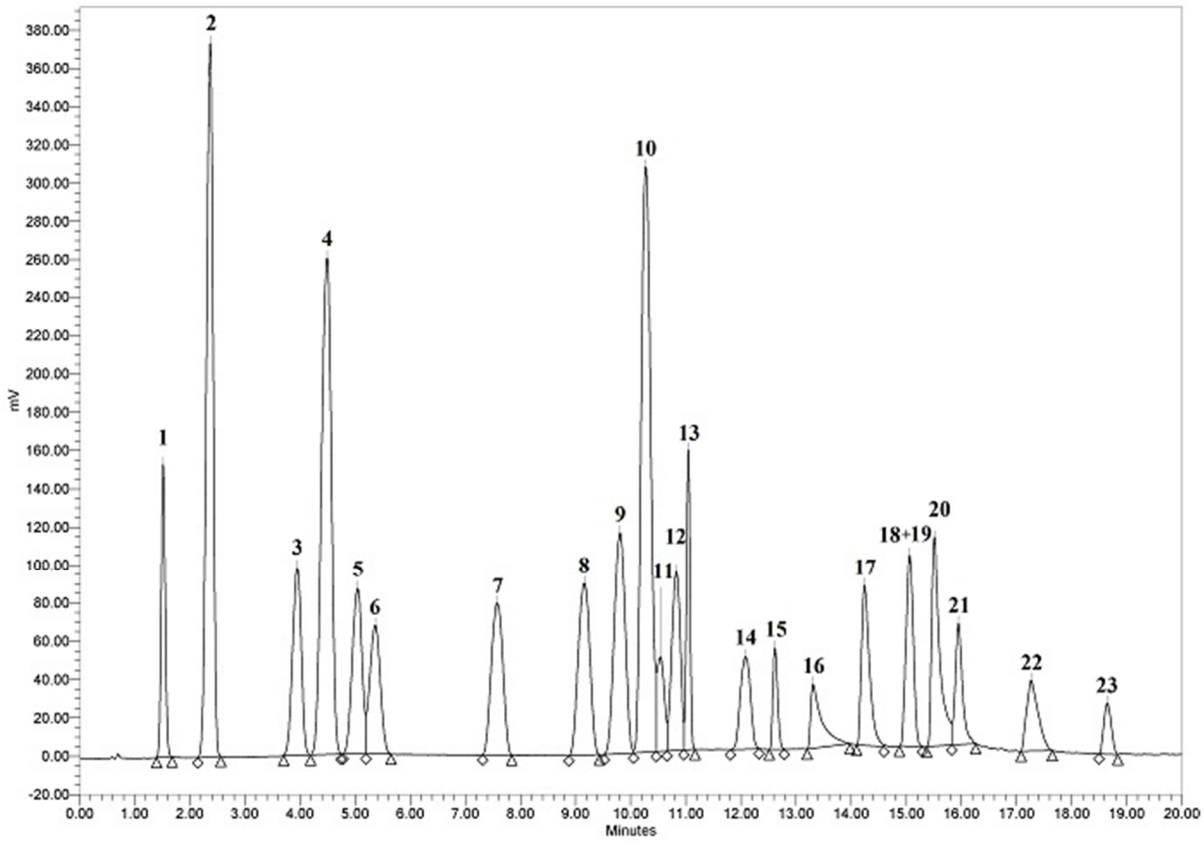

Fig. 1. Typical chromatogram of the separation of 23 pharmaceutically relevant counterions. Chromatographic conditions as described in section 2.2. Peak assignment: 1 – procaine, 2 – choline, 3 – TRIS, 4 – sodium, 5 – potassium, 6 – meglumine, 7 – mesylate, 8 – maleate, 9 – nitrate, 10 – chloride, 11 – bromide, 12 – besylate, 13 – succinate, 14 – tosylate, 15 phosphate, 16 – malate, 17 – zinc, 18 – magnesium, 19 - fumarate, 20 – tartrate, 21 – citrate, 22 – calcium, 23 – sulphate. Gluconate and lactate were not included in this separation due to the sensitivity issues mentioned in section 3.1.2.

It is noted that the elution order reported by Zhang et al. could not be fully confirmed in this study. The peak due to lactate – reported to be the first peak – was found to elute between meglumine and mesilate at about 6.6 min. Peak identity was verified via TOF/MS analysis of magnesium lactate and lactic acid. This is in good agreement with the fact that singly charged cations were found to elute before other ions. All anions and polyvalent cations appeared after meglumine which represents the last monovalent cation.

Specificity aspects concerning the separation of the corresponding substance for pharmaceutical use and its counterion are discussed in chapter 3.2.1.

3.1.2. Sensitivity

Sensitivity is of particular importance when it comes to the quantification of ionic impurities. LOQs, based on a signal-to-noise ratio (S/N-ratio) of 10:1, were determined employing solutions of the counterions in concentrations resulting in an S/N-ratio between 10 and 50 and extrapolating to 10. In the case of magnesium, calcium and sulfate, as they are present in the blank, the LOQ was considered to be the concentration that raises the S/N-ratio of the corresponding peaks in the blank by 10. All measurements were carried out in triplicate.

For most of the ions quantification was found possible in the range of 2 to 40 ng on column (cf. Table 2). Ions as impurities can then be quantified at less than 0.1% assuming a concentration of 10 mg/mL for the test solution. As a result of the good solubility of pharmaceutical substances in salt form, far lower limits of quantification may be achieved for many substances.

Because of their relatively high vapour pressure, the CAD lacks sensitivity for some organic acids. This is most pronounced for lactate, where the CAD is about 100 times less sensitive than for other analytes investigated such as e.g. sodium or nitrate. To overcome this sensitivity problem, a mass selective detector operating in ESI-negative mode can be used instead for the quantification of these compounds at impurity levels.

Moreover, it was not possible to precisely determine the LOQ for gluconate as the substance eluted as a very broad peak over a time of about 4 min. When lowering its concentration, gluconate appears as a simple rise of the baseline making proper integration impossible. Because of the above mentioned difficulties, lactate and gluconate were not considered in the further validation process.

3.1.3. Repeatability

To evaluate repeatability, 6 replicate injections of a solution containing all ions in a concentration of about 0.1 mg/mL were analysed. The relative standard deviation (RSD) values found were < 2.5 % for all ions except for citrate (cf. Table 2).

It is however noted that the 1st injection for malate and the 1st 2 injections for citrate were disregarded as they gave a lower response than the following injections. Adsorption of those 2 substances to surfaces of the chromatographic system used (Di-

onex UltiMate® 3000 x2 chromatographic system) is assumed to be responsible for this observation. Using an instrument from a different manufacturer (LC 1100, Agilent, Waldbronn, Germany), the extent of adsorption was found to be less pronounced. However, if quantification of 1 of these substances is desired, the application of an orthogonal analytical technique such as titration could also be considered. This would additionally overcome possible integration issues due to their poor peak shape.

3.1.4. Linearity and range

Linearity was determined for the most common pharmaceutical ions in the range from the LOQ of the analyte to 0.1 mg/mL. For each counterion a minimum of at least 6 concentration levels was measured in triplicate. The results were analysed by linear regression. Like other evaporation-based detectors, response in CAD is not linear over the full detector range [1]. A log-log transformation is then needed to obtain a linear calibration curve. However, over a small concentration range of about 2 orders of magnitude, it is reported to be linear [7,13,14]. This is in particular the case when operating at low concentrations (i.e. from LoD to about 250 to 500 ng on column, corresponding to 25 to 50 µg/mL having an injection volume of 10 µL [15]) and is also in good agreement with the findings of this study. Except for sodium, all correlation coefficients (R^2) obtained with a linear regression were > 0.995. The linearity for sodium was investigated over 3 orders of magnitude. Only after log-log transformation, the correlation coefficient was found to be satisfactory (> 0.995). Regarding a smaller range however, a linear relationship without log-log transformation could be achieved. Hence, quantification using single-point-calibration with an external standard, which is common practice in pharmaceutical analysis, is possible provided that the concentrations of reference and test solutions are sufficiently similar.

3.1.5. Stability of the sample solution

In order to evaluate stability, solutions containing all the ions were prepared and stored protected from light at ambient temperature for 30h. The peak areas were determined at different points in time and compared to the initial peak areas. Apart from malate where a 10 % decrease of the peak area was found after 12h, all other ions were found to be stable for 30h. However, in a solution containing all analytes, a slight decrease of the peak area of some ions, i.e. bromide and citrate was found. As

this may be due to incompatibility of the different compounds in the solution (e.g. formation of poorly soluble salts), external standards for quantification should be prepared as individual solutions.

Table 2. Limits of quantification (LOQs) and repeatability (n=6) of all investigated ions (at concentrations between approximately 100 and 200 µg/mL). * Because of the difficulties discussed in section 3.1.2, lactate was left out of the repeatability studies.

Counterion	LOQ (ng on column)	LOQ (% of a 10 mg/mL) solution	% RSD of six replicate injections
Besylate	14	0.014	1.4
Bromide	11	0.011	1.7
Calcium	17	0.018	2.0
Chloride	8	0.008	0.6
Choline	2	0.002	0.6
Citrate	$1.2*10^3$	1.2	2.9
Fumaric acid	51	0.051	0.5
Lactate	$8.6*10^3$	8.6	-*
Magnesium	2	0.003	0.5
Malate	$8.0*10^2$	0.80	2.3
Maleate	14	0.015	1.2
Meglumine	7	0.007	0.8
Mesylate	12	0.012	0.7
Nitrate	10	0.010	1.0
Phosphate	38	0.038	1.7
Potassium	2	0.003	1.4
Procaine	9	0.009	1.9
Sodium	2	0.002	0.8
Succinate	9	0.010	2.3
Sulphate	34	0.035	1.0
Tartaric acid	82	0.082	1.2
Tosylate	19	0.019	2.2
TRIS	5	0.005	1.1
Zinc	20	0.020	1.2

It has to be taken into account, that the active pharmaceutical ingredient (API) can have an effect on the stability of the counterion. Its degradation might be accelerated or reactions between drug and ion are possible.

3.2. Applications

3.2.1. Identification of counterions

Twelve Ph. Eur. drug and impurity reference substances (acesulfame potassium, amlodipine besilate, amobarbital sodium, codergocrine mesilate, flunixin meglumine, ipratropium bromide impurity A, kanamycin monosulfate, mepyramine impurity A,

mepyramine maleate, oseltamivir impurity C, oseltamivir phosphate and xylometazoline impurity A) were investigated. Corresponding counterions, as far as present, were identified. Peak identification was done via retention times / relative retentions compared with authentic samples of the corresponding ions. In all cases, unambiguous identification of the counterion, if present, was found to be feasible.

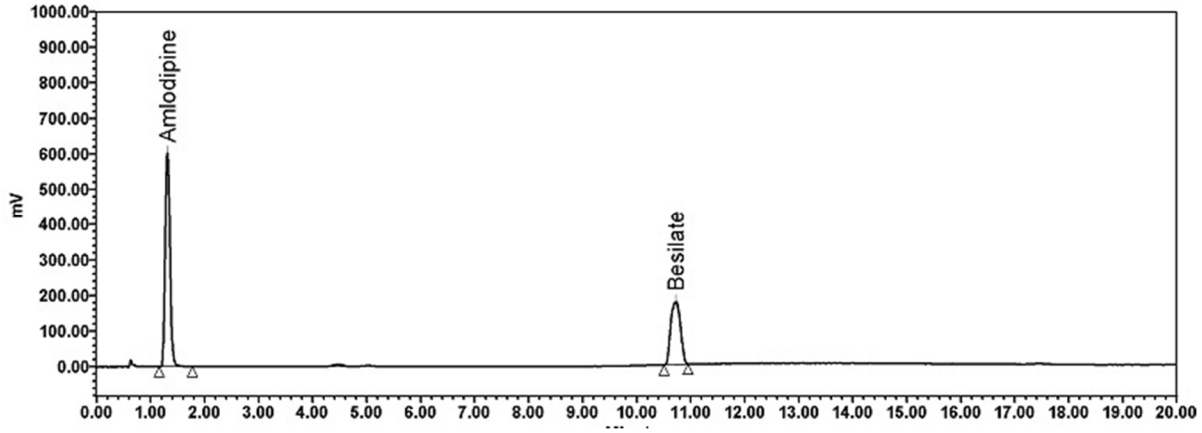

Fig. 2. The chromatogram shows the separation of amlodipine besylate. As for most of the reference substances we analysed, the API shows a retention time of less than 2 min. This allows the assignment of the besylate-peak without coupling to a mass selective detector.

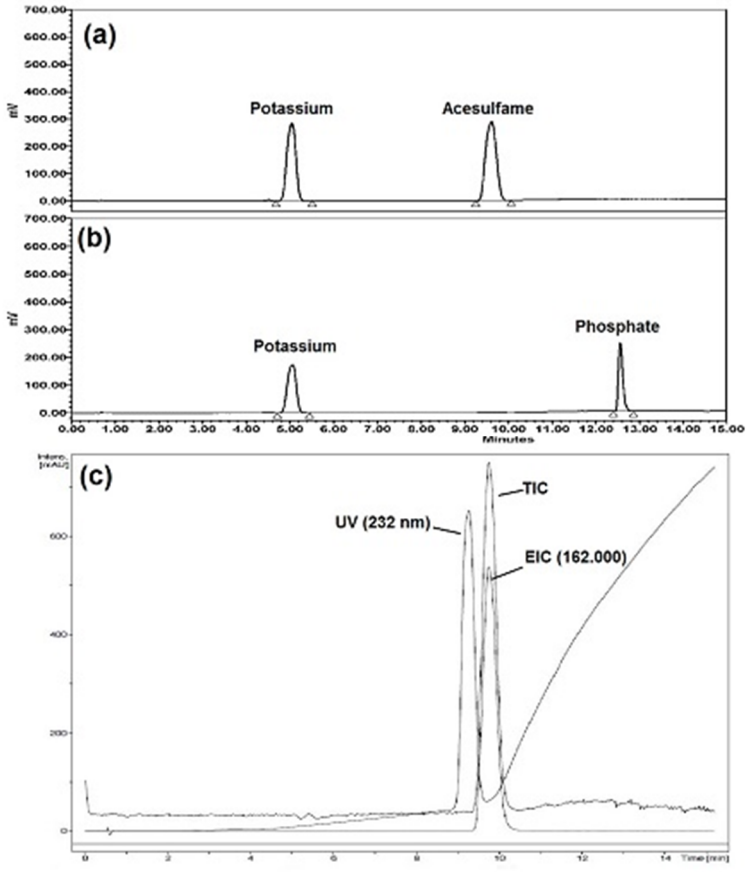

Fig. 3. CAD signal of (a) acesulfame potassium (c = 0.2 mg/mL) and (b) potassium phosphate (c = 0.36 mg/mL). (c) shows the UV (at 232 nm), the total ion current (TIC) and the extracted ion chromatogram (EIC) at an m/z of 162.000 signals of (a) in ESI-neg mode. Chromatographic conditions are described in section 2.2.

Whilst the counterions eluted as shown in Fig. 1, most of the active ingredients tested showed a retention time of less than 2 minutes. This prevents the ion peak from being confounded with the drug compound, which is representatively shown for amlodipine besylate (Fig. 2).

However, in some cases confirmation of peak identity may be required. Since the method is mass-compatible, identification of ions with suitable mass-to-charge ratios can be carried out by TOF/MS installing a flow-splitter (split ratio 10:1) after the UV/Vis detector. Suitability of this approach was demonstrated analysing acesulfame potassium in ESI-negative mode. The exact mass of acesulfame found confirmed its identity (cf. Fig. 3).

3.2.2. Quantification of ions

To demonstrate the methods capability for quantification purpose, the counterion content in amlodipine besilate was determined and the stoichiometric composition of a commercially available sample of amikacin sulfate was explored. Reference solutions containing the respective ions were measured at a minimum of 5 concentration levels, in triplicate. Calibration curves were established after log-log transformation of the data.

The amount of besilate in amlodipine besilate was found to be 28.1 %. This was in good agreement with the theoretical value (recovery: 100.8 %). Furthermore, we quantified sulfate in amikacin sulfate. 20.5 % sulfate was found, resulting in a stoichiometric ratio for amikacin to sulfate of 1:1.8 referred to the dried substance.

Table 3. Results of the quantitative counterion and ionic impurity determination of selected Ph. Eur. reference substances.

Substance	Ion investigated	Content found (% m/m)	% RSD (n=3)
Amlodipine besylate	Besylate	28.1	1.1
Amikacin sulphate	Sulphate	20.5	1.1
Mesalazin Imp. A	Sulphite	2.74	1.7
Somatostatin batch 1	Chloride	1.26	0.47
Somatostatin batch 2	Chloride	< 0.005	-
Cloxacillin sodium batch 1	Chloride	0.06	4.2
Cloxacillin sodium batch 2	Chloride	0.38	1.1
Cloxacillin sodium batch 3	Chloride	0.47	1.6

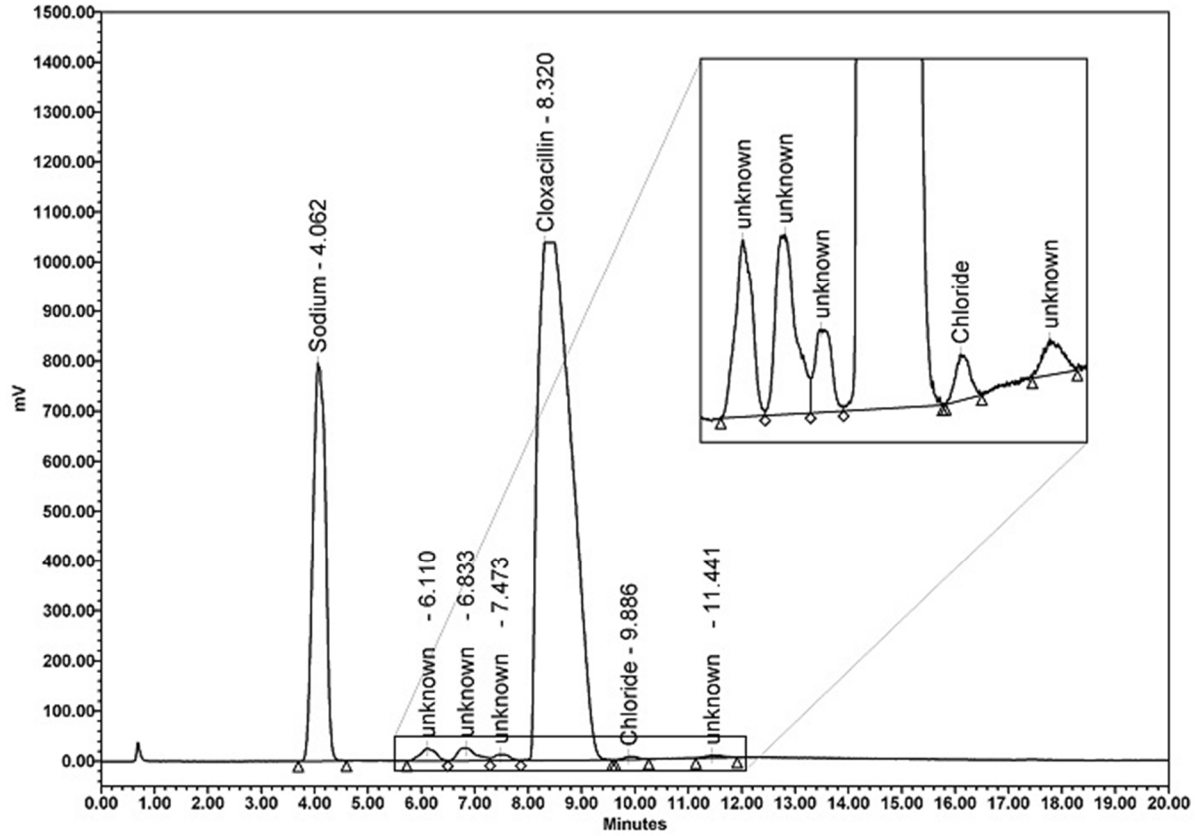

Fig. 4. 0.38 % chloride as impurity was found in a batch of cloxacillin sodium. Chromatographic conditions are described in section 2.2. The concentration of cloxacillin sodium was about 4 mg/mL.

The high sensitivity of the CAD allows determination of ions as potential impurities at trace levels, provided that the concentration of the sample solution is sufficiently high (up to 15 mg/mL for somatostatin). On selected examples from beta-lactam antibiotics and from peptides it could be shown that the method is also suitable for the identification and quantification of ionic impurities. For this purpose, several batches of cloxacillin sodium and somatostatin were analysed. A considerable amount of chloride (1.26 %) was found as an “impurity” in 1 batch of somatostatin. Chloride (about 0.4 % to 0.5 %) could also be found in 2 samples of cloxacillin sodium (cf. Fig. 4). A summary of the results is presented in Table 3.

4. Conclusion

In this study an HPLC-CAD method for the separation of 23 pharmaceutically relevant counterions could be successfully validated with regard to specificity, sensitivity, linearity and range. The method was found suitable for the intended purpose of counterion screening in pharmaceutically used salts. This was demonstrated on numerous examples using Ph. Eur. reference substances. Furthermore, ions can be determined quantitatively to verify the stoichiometric composition or in trace levels, e.g. as ionic

impurities in substances for pharmaceutical use. In order to achieve satisfactory analytical performance, the concentration of the respective ion should be in the range of about 10 to 200 µg/mL in both cases. Coupling to a mass selective detector in order to gain additional structural information on the analytes or for selective quantification can easily be done by installing a flow-splitter.

Taken together, this work confirms that the method examined can provide a very useful contribution to a thorough characterisation of Ph. Eur. reference standards. Moreover, it can be used as a universal method for the identification and control of the most pharmaceutically relevant ions in Ph. Eur. monographs.

5. References

[1] Dixon RW, Peterson DS. Development and testing of a detector for liquid chromatography based on aerosol charging. *Anal Chem* 2002;**74**(13):2930-7.

[2] Zhang K, Dai L, Chetwyn NP. Simultaneous determination of positive and negative pharmaceutical counterions using mixed-mode chromatography coupled with charged aerosol detector. *J Chromatogr A* 2010;**1217**(37):5776-84.

[3] Huang Z, Richards MA, Zha Y et al. Determination of inorganic pharmaceutical counterions using hydrophilic interaction chromatography coupled with Corona® CAD detector. *J Pharm Biomed Anal* 2009;**50**(5):809-14.

[4] Kanedai Y, Hashiguti K, Fukushima K *et al.* Simultaneous analysis of cations and anions using charged aerosol detection method. *Chromatography* 2009;**30**(Suppl 1):113-6.

[5] Fukushima K, Kanedai Y, Hashiguchi K *et al.* Generic approach to analysis ofpharmaceutical salts including inorganic and organic counter-ions. *Chromatography* 2009;**30**(Suppl 1):105-8.

[6] Mouchère F, El Haddad M, Elfakir C *et al.* Determination of inorganic cations and anions by ion-exchange chromatography with evapoorative light-scattering detection. *J Chromatogr A* 2001;**914**(1-2):167-73.

[7] El Haddad M, Mouchère F, Elfakir C *et al.* Conditions for rapid determination of inorganic cations in water by ion-exchange chromatography and evaporative light scattering detection. *J Sep Sci* 2001;**24**(8):669-73.

[8] Holzgrabe U, Nap CJ, Beyer T *et al.* Alternatives to amino acid analysis for the purity control of pharmaceutical grade l-alanine. *J Sep Sci* 2010;**33**(16):2402-10.

[9] Liu X, Pohl CA. HILIC behaviour of a reversed-phase/cation-exchange/anion-exchange trimode column. *J Sep Sci* 2010;**33**(6-7):779-86.

[10] Liu X, Pohl C, Woodruff A *et al.* Chromatographic evaluation of reversed-phase/anionexchange/cation-exchange trimodal stationary phases prepared by electrostatistically driven self-assembly process. *J Chromatogr A* 2011;**1218**(22):3407-12.

[11] Technical guide for the elaboration of monographs, 6th Edition, Strasbourg, France:Council of Europe; 2011.

[12] Validation of analytical procedures: text and methodology [guideline]. Ref: Q2(R1). ICH; 2005 Nov.

[13] Holzgrabe U, Nap CJ, Kunz N et al. Identification and control of impurities in streptomycin sulfate by high-performance liquid chromatography coupled with mass detection and corona charged-aerosol detection. *J Pharm Biomed Anal* 2011;**56**(2):271-9.

[14] Holzgrabe U, Nap CJ, Almeling S. Control of impurities in l-aspartic acid and l-alanine by high-performance liquid chromatography coupled with a corona charged aerosol detector. J *Chromatogr A* 2010;**1217**(3):294-301.

[15] Crafts C, Bailey B, Plante M *et al.* Validating analytical methods with charged aerosol detection. *Thermo Scientific Application Note* 2011.

4.2 Impurity control in Topiramate with high performance liquid chromatography: Validation and comparison of the performance of evaporative light scattering detection and charged aerosol detection

David Ilko, Robert C. Neugebauer, Sophie Brossard, Stefan Almeling, Michael Türck, Ulrike Holzgrabe

Unpublished manuscript.

Abstract

An HPLC method using a pentafluorophenyl column for the impurity control in Topiramate is presented. The performance of an ELSD and a Corona® CAD for the detection of the substances lacking a suitable UV chromophor was investigated. The method was validated according to ICH guideline Q2(R1) and the “Technical Guide for the Elaboration of Monographs” of the Ph. Eur. for both detectors. Although CAD appeared to be superior in terms of repeatability, sensitivity and linearity, both detectors gave satisfactory results in the accuracy studies. However, the use of an ELSD was considered not feasible due to the appearance of ghost peaks when injecting the high concentrated test solution of topiramate. Due to its relatively high vapor pressure, one of the impurities (impurity A) gave no or little response in ELSD and CAD, respectively. We were able to achieve a nine-fold increase in sensitivity by means of post-column addition of acetonitrile and a lower nebulizer temperature with the CAD ultra RS. As the sensitivity for all other impurities was still about a factor 10^3 better, simultaneous detection of all impurities was still not feasible. Thus, an HPTLC limit test modified from the USP was applied.

1 Introduction

Topiramate was developed as an anticonvulsant drug substance. Moreover, its use for the prophylaxis of migraine [1] and the treatment of obesity [2], trigeminus neuralgia [3] and substance-related diseases [4, 5] are discussed.

Numerous studies dealing with the determination of topiramate in plasma for therapeutic drug monitoring and pharmacokinetic and bioequivalence investigations are reported [6-13]. However, almost no method for the control of impurities can be found. One method controlling topiramate and impurity C in liquid oral solutions was presented [14]. However, neither of the other impurities was detected. All impurities could be determined by Biro et al., but a total of four different HPLC methods were necessary [15].

The aim of this study was to develop and validate a high performance liquid chromatographic method for the determination of impurities in topiramate. The possible impurities derive from the given synthetic route [16] (Figure 1): Impurity A: 2,3:4,5-bis-O-(1-methylethylidene)-β-D-fructopyranose; Impurity B: N-[(diethylamino) carbonyl]-2,3:4,5-bis-O-(1-methylethylidene)-β–D-fructopyranose sulfamic acid; Impurity C: 2,3-O-(1-methylethylidene)-β–D-fructopyranose sulfamic acid; Impurity D: N-{[2,3:4,5-bis-O-(1-methylethylidene)-β–D-fructopyranosyl] oxycarbonyl}-2,3:4,5-bis-O-(1-methylethylidene)- β -D-fructopyranose sulfamic acid, and Impurity E: D-Fructose.

Impurity control of this pharmaceutical substance is challenging. Due to the lack of a suitable UV chromophor of the substituted monosaccharides, the analytes show poor or even no UV absorption. Furthermore, the great difference in polarity makes it difficult to separate all substances in a single HPLC run.

To overcome the detection problem, we decided to evaluate the suitability of aerosolbased detectors, i.e. an evaporative light scattering detector (ELSD) and a charged aerosol detector (CAD), because all non-volatile substances are detected regardless of their chemical properties.

Preliminary experiments revealed that, due to its relatively high vapour pressure, one of the impurities (impurity A) gave little or no response in CAD and ELSD, respectively. Therefore, the second aim was to enhance the sensitivity for impurity A using the CAD ultra RS, where the temperature of the nebulizer can be varied. Furthermore, it

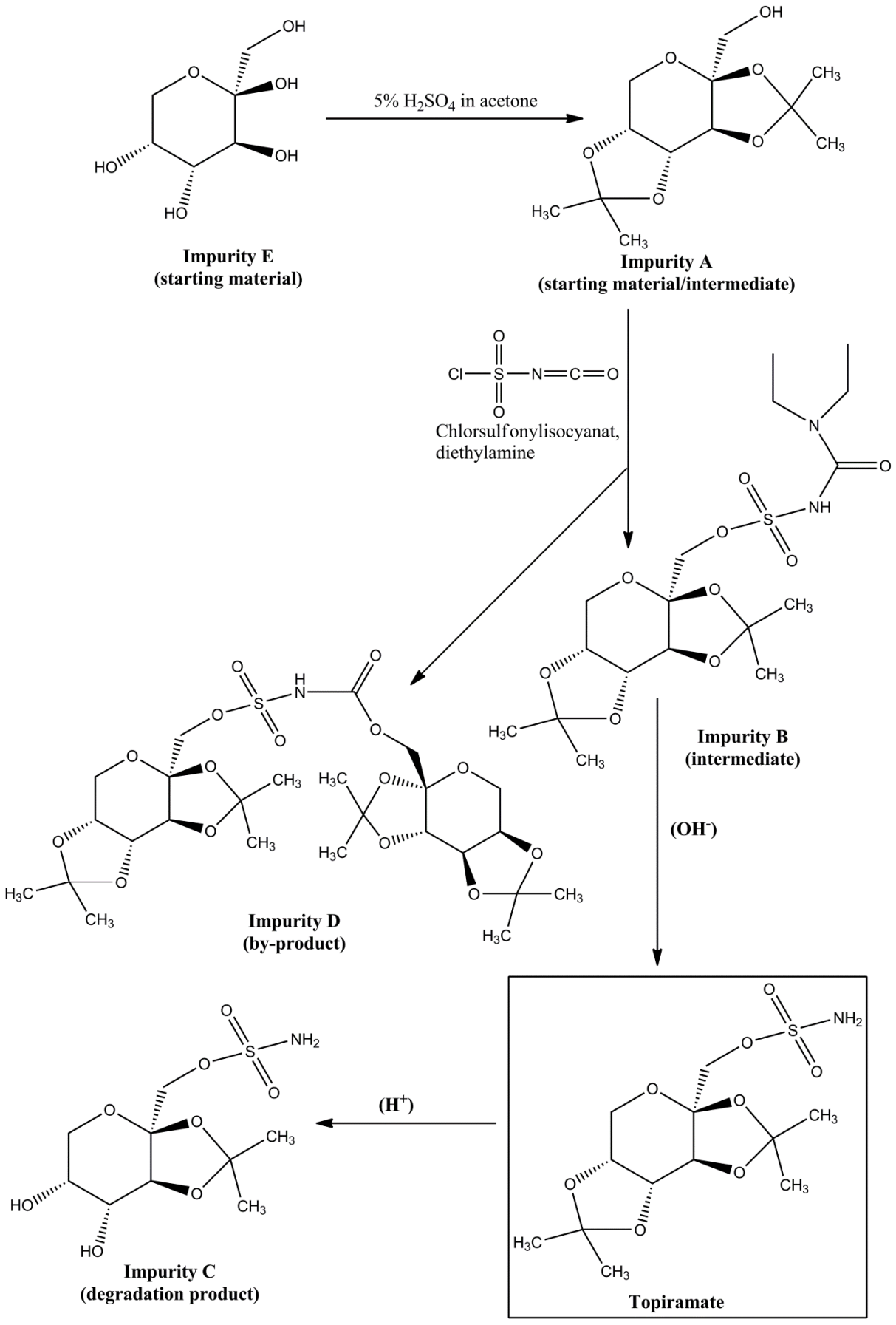

Figure 1. Structural formulae of Topiramate and its impurities derived from the synthetic route [16]. Impurity A is commercially available and can thus be either starting material or intermediate.

is known, that high amounts of organic modifier in the mobile phase result in an increased response in evaporation based detectors [17]. Post-column addition of an organic solvent is the only means of exerting influence on the composition of the eluent reaching the detector without modifying the HPLC parameters. Chromatographic systems possessing two individual pumps are commercially available and were successfully applied for gradient compensation in order to provide consistent response over the entire chromatographic run [18].

2 Material and methods

2.1 Reagents and material

Topiramate and its impurities A, B, C and D were provided by the European Directorate for the Quality of Medicines & HealthCare (EDQM). Ammonium acetate for HPLC, fructose (impurity E), glacial acetic acid and sodium chloride were purchased from Sigma-Aldrich (St-Quentin Fallavier, France).

Ultra-pure water (>18.2 MΩ) was delivered by an ELGA PureLab Ultra system (Elga Antony, France) or a Milli-Q Synthesis system (Billerica; MA, USA). Gradient grade acetonitrile was purchased from Sigma-Aldrich (Chromasolv®) (St-Quentin Fallavier, France) and VWR International (HiPerSolv Chromanorm®) (Darmstadt, Germany).

2.2 HPLC-ELSD/CAD

The optimized method makes use of a Kinetex PFP (100 x 4.6 mm, 2.6 µm particle size) analytical column from Phenomenex (Aschaffenburg, Germany). The column compartment was maintained at 40.0 °C. Flow rate was 1.0 mL/min and the injection volume 20 µL. A gradient was applied with 25 mM ammonium acetate (pH 3.5, adjusted with glacial acetic acid) as mobile phase A and acetonitrile as mobile phase B. The proportion of mobile phase B was 20% for the initial 5 minutes and then increased to 50% within further 10 minutes.

A PL-ELS 2100 ELS detector (Polymer Laboratories, Marseille, France) and a CAD ultra RS (Thermo Fisher, Courtaboeuf, France) were operated with a Dionex UltiMate® 3000 x2 chromatographic system (Dionex, Courtaboeuf, France) equipped with two ternary pumps, an online degasser, a thermostated autosampler, a thermostated column compartment and a single wavelength UV/Vis detector. The first pump delivered the gradient as described above and the second pump the organic modifier

(acetonitrile) for the experiments with post-column addition at a flow rate of 1.0 mL/min. Mixing of the two eluents took place in a peek tee before introducing into the detector.

The evaporation temperature of the ELSD was set to 80 °C, the nebulizer temperature to 50 °C and the flow rate of the nebulization gas (nitrogen) to 1.0 standard liter per minute (SLM). The gas inlet pressure (nitrogen) for the CAD ultra RS was 35 psi, the range to 100 pA, the filter to “0” and the nebulizer temperature was varied between 18 and 35 °C.

The method validation using the Corona® CAD (Thermo Scientific, Idstein, Germany) was conducted on an Agilent 1100 LC system (Waldbronn, Germany) equipped with a binary pump, an online degasser, a thermostated column compartment and a diode array detector. The settings for the Corona® CAD were as follows: gas inlet pressure (nitrogen): 35 psi, filter: “none”, range: 100 pA.

A pH-meter 780 (Metrohm, Villebon-sur-Yvette, France) and a PHM220 Lab pH-Meter (Radiometer Analytical SAS, Lyon, France) were used for pH adjustment. For measurements using the ELSD, the test solution was prepared by dissolving 20 mg topiramate in 1.0 mL of a mixture of mobile phase A and mobile phase B (80:20, v/v). The concentration of the test solution when using the CAD was 5 mg/mL. For the content determination with the CAD, the concentration of topiramate was 25 µg/mL.

Impurities A, B, C and D were stored as 1 mg/mL stock solutions in acetonitrile at -20 °C. Impurity E was dissolved and stored in water. Spiked solutions were then prepared by dilution of the stock solutions.

2.3 TLC and HPTLC limit test for impurity A

The TLC and HPTLC test is based on the USP monograph for topiramate [19] with modifications from Cilag AG [personal communication, 2011]. The preconditioning, the development of the plates, and the detection were performed according to [19]. Ethylsilyl TLC (Silica Gel RP-2 TLC plates, Merck, Molsheim, France) and HPTLC (Silica Gel RP-2 HPTLC plates, Merck, Molsheim, France) plates were used. The test and reference solutions differred from those of the USP monograph and were prepared as follows. The *test solution* was prepared by dissolving 40 mg of the substance to be examined in 1.0 mL methanol. *Reference solution (a)* was prepared by

dissolving 10 mg impurity A in 50.0 mL methanol and diluting 1.0 mL of this solution to 5.0 mL with methanol. The resulting concentration of impurity A in *reference solution (a)* was 0.04 mg/mL, accordingly 0.1% of the concentration of topiramate in the test solution. *Reference solution (b)* was obtained by dissolving 40 mg of the substance to be examined in 1.0 mL of *reference solution (a)*.

The system suitability is given when the spots due to topiramate and impurity A in *reference solution (b)* are separated. The substance to be examined complies with the specification, when the spot due to impurity A in the *test solution* is not more intense than the corresponding spot in *reference solution (a)*.

3 Results and discussion

3.1 Method validation: impurity control

The LC method makes use of a pentafluorophenyl column. Mobile phase A consisted of 25 mM ammonium acetate (pH 3.5), and mobile phase B was acetonitrile. A gradient was applied starting with 20% mobile phase B for 5 minutes and increasing the proportion of mobile phase B from 20 to 50% within further 10 minutes. For the detection of the substances lacking a suitable UV chromophore, an ELSD and a CAD were employed.

Specificity. A solution of topiramate (20 mg/mL for the ELSD and 5 mg/mL for the CAD) spiked with each impurity at concentrations of 0.1% was analyzed to show specificity. All impurities were separated from topiramate and each other (Figure 2). Impurity E eluted before the void volume. Usually, retention times less than the hold up time indicate the exclusion of an analyte from the pores of the column material, usually by reason of the analyte size. Here, we assume that the intrusion of impurity E (fructose) into the particles is cumbered by the repulsion of the highly polar nature of the analyte, which is opposite to the non-polar surfaces of the column. Due to the partial overlap with the system peak, impurity E was quantified using the peak height.

Repeatability was investigated on three levels (0.05%, 0.10% and 0.15% referred to the concentration of the test solution, n=3). The values found for the relative standard deviation (% RSD) were between 0.24 and 2.43% for the CAD and 1.22 and 18.3% for the ELSD, respectively. These exceptionally high % RSD values for the ELSD were observed at the lowest concentration only. Regarding the mid and high concen-

tration level, % RSD was not more than 6%. Still, the CAD was found to provide a more consistent response than the ELSD.

Sensitivity. The limits of quantification (LOQ) of topiramate and impurities B, C, D and E were 20 – 48 ng on column for the ELSD and 4.5 and 10 ng on column for the CAD. Thus, the sensitivity of the CAD was about 3 to 9 times higher compared to the ELSD.

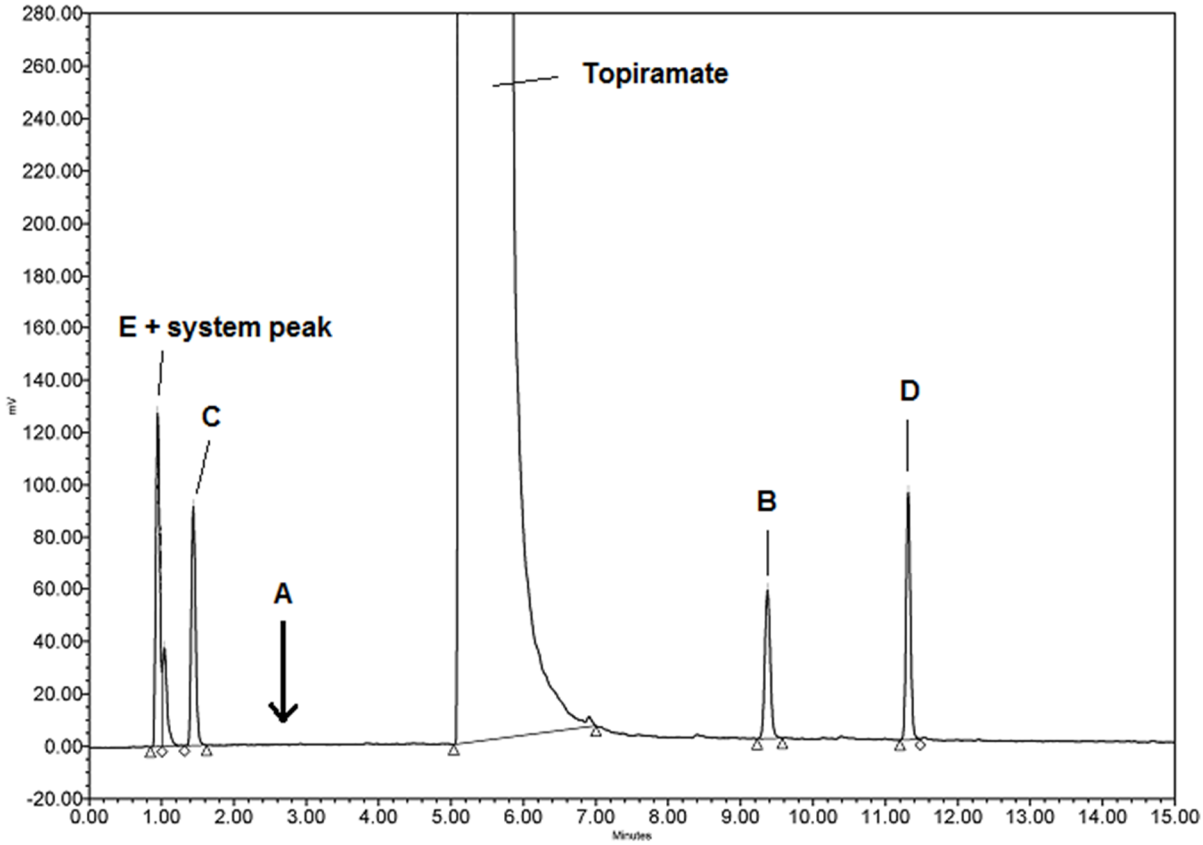

Figure 2. Example chromatogram of the test solution of Topiramate (c = 5 mg/mL) spiked with each impurity at concentrations of 0.1%. Chromatographic conditions are described in section 2.2.; Detection: CAD ultra RS (nebulizer temperature: 35 °C); Impurity A was not detectable at this concentration. The retention time derived from the experiments for sensitivity enhancement with the CAD ultra RS, cf. Figure 3.

Impurity A (diacetonide) gave no signal in the ELSD due to its relatively high vapour pressure. It is entirely vaporized along with the mobile phase in the evaporation tube at the set temperature of 80 °C. It was not possible to detect impurity A by lowering the temperature of the nebulizer (T_n) or the evaporation tube.

Using the CAD ultra RS, impurity A can be detected at a concentration of 12 µg on column. The LOQ is 38 µg on column. By post-column addition of acetonitrile at a flow rate of 1.0 mL/min, a gain in sensitivity by a factor of about five was achieved (LOQ = 7.8 µg on column).

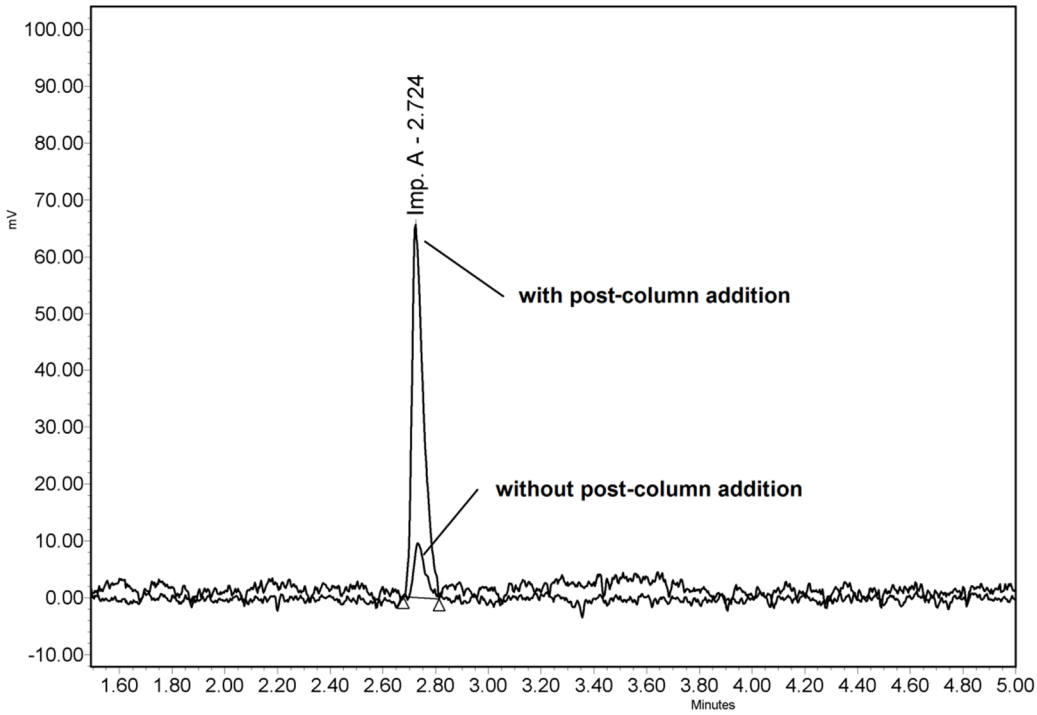

Figure 3. Influence of post-column addition of acetonitrile on the response of impurity A (c = 2.6 mg/mL). Detection: CAD ultra RS (nebulizer temperature: 35 °C). The chromatographic conditions are described in section 2.2.

Furthermore, the influence of T_n on the response was investigated. It can be varied between 5 and 35 °C in the CAD ultra RS. However, according to the instrument manual, the minimum T_n that can actually be reached is depending on several factors such as the temperature of the mobile phase, the mobile phase flow rate, and the ambient temperature. Thus, it was impossible to set a T_n of less than 18 °C in the experimental setup. A decreased T_n correlates with a decreasing LOQ, thus increased sensitivity. A maximum gain in sensitivity of about a factor 2 was observed (data not shown). In combination with the post-column addition of acetonitrile, a ninefold increase in sensitivity could be achieved (LOQ of 4.2 µg on column with post-column addition of acetonitrile at 18 °C vs. 38 µg on column without addition of acetonitrile at 35 °C).

However, the detector is still about 10^3 times more sensitive for other impurities than for impurity A. Proper impurity control of all impurities within a single HPLC-CAD run was not feasible. Therefore, impurity A was controlled by an HPTLC test (cf. chapter 3.3).

Linearity. We investigated linearity in the range from the LOQ of the respective substance to 0.15% (0.50% for impurity E) referred to the concentration of topiramate in the test solution.

All evaporation-based detectors show a non-linear response, which is described by following equation:

(Eq. 1) $$A = a \times m^b$$

where *A* is the peak area, *m* is the analyte mass and *a* and *b* are numerical coefficients. Log-log-transformation gives a linear relation expressed by:

(Eq. 2) $$\log A = b \times \log m + \log a$$

A coefficient of *b* = 1 will result in a linear response curve. Regarding a small concentration range of about two orders of magnitude, the response curve is reported to be sufficiently linear without log-log-transformation [20].

The results of the linearity studies are summarized in Table 1. As can be seen from the coefficients of determination (R^2) of the linear regression and the values for the coefficient b of the logarithmic calibration curves, the signal provided by the CAD showed better linearity than the ELSD. After log-log transformation however, the differences were negligible.

Table 1. Parameters of the linear regression before and after log-log transformation of analyte concentration and peak area for both ELSD and CAD are shown. As impurity E is intended to be quantified via peak height, we additionally investigated its linearity.

	linear			logarithmic		
	R^2	**slope**	**y-intercept**	**R^2**	**b**	**log a**
ELSD						
Topiramate	0.9860	34869781	-381799	0.9981	1.5375	7.9551
Imp. B	0.9854	30520686	-199509	0.9992	1.5174	8.0115
Imp. C	0.9981	23431043	-91228	0.9982	1.3822	7.8052
Imp. D	0.9845	41574416	-407210	0.9966	1.4310	7.9952
Imp. E	0.9965	45985745	-171743	0.9974	1.3650	8.0251
CAD						
Topiramate	0.9982	4481	5.4067	0.9998	0.9338	3.5794
Imp. B	0.9991	3984	4.9791	0.9992	0.9275	3.5199
Imp. C	0.9956	4511	5.8785	0.9974	0.9603	3.6316
Imp. D	0.9924	5126	11.6463	0.9972	0.9041	3.6201
Imp. E	0.9890	3276	10.1519	0.9966	0.8620	3.3762
Imp. E*	0.9880	1108	4.0472	0.9966	0.8330	2.8698

Correction factors and accuracy. As it is common practice in the impurity control of drug substances in pharmacopoeias, a dilution of the test solution serves as external standard for the calculation of the impurity content [21]. In order to adjust possible differences in response, correction factors were determined for each impurity. Cor-

rection factors were calculated based on the peak areas of each impurity compared to that of topiramate. Correction factors were not constant over the entire concentration range. Decreasing correction factors with higher concentrations for all impurities were observed. The factors applied for the calculations were the mean values of all determinations.

Accuracy was expressed as the recovery of each impurity in spiked test solutions. Three concentration levels were investigated covering the range from the reporting threshold to 150% of the specification limit. Results are shown in Table 2. Impurity contents found with the CAD showed a better closeness to the true value. In accordance to the trend in correction factors, we observed a decreasing recovery with increasing concentrations of the impurities. This trend seemed to be more pronounced for the ELSD than for the CAD. Still, both detectors gave satisfactory recovery rates with averaged correction factors.

Table 2. Correction factors (CFs) and accuracy expressed as % recovery of the spiked impurities. * for the calculation of the correction factor and the impurity content of impurity E, the peak height was used instead of the peak area. Measurements were carried out in triplicate. ND = not determined

	correction factor	**% recovery**			
		0.05%	**0.10%**	**0.15%**	**0.30%**
ELSD					
Imp. B	0.6	93.2	90.3	88.5	ND
Imp. C	0.6	119.7	103.8	99.0	ND
Imp. D	0.5	109.1	98.0	97.8	ND
Imp. E*	0.4	101.0	95.0	95.0	ND
CAD					
Imp. B	0.8	99.3	104.9	101.1	ND
Imp. C	0.9	112.6	108.5	104.4	ND
Imp. D	0.6	99.8	101.6	99.1	ND
Imp. E*	0.4	104.8	ND	101.5	94.5

When the ELSD was used, we observed peaks eluting after the principle peak due to topiramate in the test solution (see Figure 4). These peaks were not reproducible and added up to a content of more than 0.3% in total, which exceeds the limit for total impurities and would result in the refusal of an actually conform batch.

Such ghost or “spike peaks” have previously been reported and investigated [22]. Their occurrence can be minimized or even avoided by adjusting ELSD and HPLC parameters, but results in a loss in sensitivity. As the method presented here is intended to be part of a Ph. Eur. monograph, it has to be applicable to ELS detectors different from the model used in this study. For that reason, we cannot state generally

valid detector settings that ensure the avoidance of ghost peaks and provide a sufficiently sensitive detection at the same time. Therefore, we considered the evaporation light scattering detection to be not feasible in this particular case. In contrast, when using the CAD, no ghost peaks occurred (cf. Figure 2).

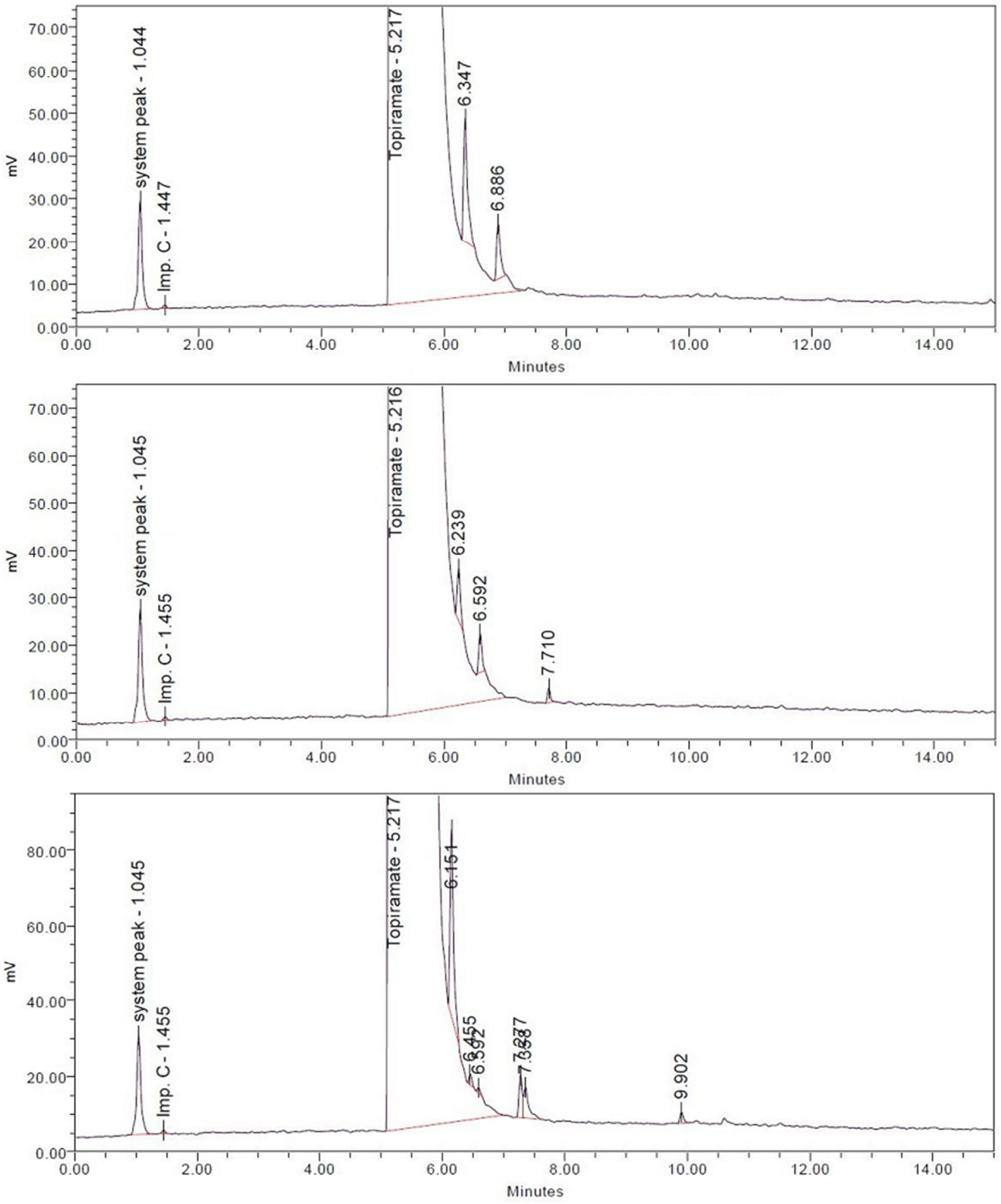

Figure 4. Three consecutive injections of a solution of Topiramate (c = 20 mg/mL) from the same vial are shown. The content of impurity C, as the only impurity found in this batch, was below the LOQ. All other peaks are non-reproducible ghost peaks. The chromatographic conditions are described in section 2.2. Detection: ELSD.

3.2 Method validation: assay

The HPLC-CAD method for the impurity control was also used for the content determination of topiramate. Some of the validation parameters had to be reassessed for this purpose, i.e. linearity and range, repeatability, and accuracy.

Linearity and range. It is reported, that the CAD delivers a linear signal up to a concentration of approximately 250-500 ng on column [23]. Accordingly, the concentration of the test solution was set to 25 µg/mL (equivalent to 500 ng on column with an injection volume of 20 µL). Linearity was therefore investigated from 20 to 30 µg/mL, which is equivalent to 80 to 120% of the concentration of the test solution. Coefficient of determination (R^2) of the linear regression was 0.9983, indicating satisfactory linearity.

Repeatability was assessed at 80, 100 and 120% of the concentration of the test solution in triplicate. The % RSD values found were 0.22, 0.51 and 0.18%, respectively, which is highly satisfactory for aerosol-based detectors [23].

Accuracy. Recovery was determined at three levels (80, 100 and 120% of the concentration of the test solution) against the reference solution at 100% of the concentration of the test solution. All solutions were prepared in triplicate. Recoveries ranged from 98.89 to 102.05% (mean: 100.27%, 1.04% RSD).

3.3 TLC and HPTLC limit test for impurity A

As the above described HPLC-CAD method is not sensitive enough for the detection of impurity A, we applied an HPTLC limit test for its control. The test is based on the USP monograph for topiramate [19], where TLC is employed to limit any impurity other than impurity A. For our purpose, the method was changed using an ethylsilylated silica stationary phase instead of bare silica [personal communication, Cilag AG, 2011]. We evaluated the performance of TLC and HPTLC plates.

The *test solution* contained 40 mg/mL topiramate, *reference solution (a)* impurity A at a concentration of 0.1%, i.e. 0.04 mg/mL. *Reference solution (b)* was prepared by dissolving 40 mg of topiramate in 1.0 mL of *reference solution (a)*. 20 µL of each solution was applied to the TLC plates and 5 µL to the HPTLC plates. The preconditioning, the development of the plates, and the detection were performed according to [19].

According to ICH guideline Q2(R1) [24] and the “Technical Guide for the Elaboration of Monographs” [21], specificity and sensitivity need to be evaluated for the validation of a limit test.

Specificity. Solutions of impurities A, B, C, D, and E at a concentration of 0.04 mg/mL, corresponding to 0.1%, were applied to the TLC and the HPTLC plates. Additionally, a solution containing topiramate (40 mg/mL) spiked with all impurities at 0.1% was applied. Using the TLC plates, impurity A was fully separated from topiramate and impurities C, D, and E, but co-eluted with impurity B. When the HPTLC plates were applied, impurity A was separated from topiramate and from all other detectable impurities. The HPTLC test was found to be sufficiently specific, while the application of TLC was not feasible.

Sensitivity. In order to ensure sufficient sensitivity, a series of dilutions of impurity A was prepared with following concentrations: 0.04%, 0.08%, 0.10%, 0.15% and 0.20% corresponding to the concentration of the test solution (40 mg/mL). For both, the TLC as well as the HPTLC plates, the spot due to impurity A in the 0.04% solution was still detectable. Additionally, the spot in the 0.15% solution could visually be distinguished from the spot of the 0.10% solution, proving sufficient discriminating power.

In summary, the HPTLC limit test was found suitable to control impurity A, whereas the use of TLC plates did not allow its complete separation from another impurity.

4 Concluding remarks

We were able to develop and validate an HPLC method with either evaporation light scattering and charged aerosol detection that separates all possible impurities from topiramate in a single run. The highly polar impurity E was not retained under these conditions and eluted before the system peak. Nevertheless, accurate and precise quantification is achievable using the peak height for the calculation of the impurity content. In addition, the HPLC method was successfully applied to the content determination of topiramate.

Because of its relatively high vapour pressure, impurity A was not detectable with the ELSD, but gave a signal in the CAD, that was significantly lower compared to all other impurities. By means of post-column addition of acetonitrile and a decreased nebulizer temperature of the CAD ultra RS, a nine-fold increase in response was achieved. Still, the LOQ of impurity A is about a factor of 10^3 higher compared to all

other impurities. Therefore, an HPTLC limit test was applied for the control of impurity A.

It was found that the CAD was superior to ELSD in terms of repeatability, sensitivity and linearity. Still, both detectors gave satisfactory recoveries for all impurities. The lack of sensitivity in ELSD could easily be compensated by increasing the concentration of the test solution. However, the occurrence of non-reproducible peaks eluting on the tail of the principle peak when using the ELSD impeded its use in our study.

5 Acknowledgement

The authors gratefully thank the European Directorate for the Quality of Medicines & HealthCare (EDQM) for the provision of analytical equipment, consumables and samples. Furthermore, thanks are due to the Federal Institute of Drugs and Medical Devices (BfArM, Bonn, Germany) for financial support.

6 References

[1] Ferrari, A., Tiraferri, I., Neri, L., Sternieri, E., *Clinical pharmacology of topiramate in migraine prevention.* Expert Opin Drug Metab Toxicol, 2011. **7**(9): p. 1169-81.

[2] Allison, D.B., Gadde, K.M., Garvey, W.T., Peterson, C.A., Schwiers, M.L., Najarian, T., Tam, P.Y., Troupin, B., Day, W.W., *Controlled-Release Phentermine/Topiramate in Severely Obese Adults: A Randomized Controlled Trial (EQUIP).* Obesity, 2012. **20**(2): p. 330-342.

[3] Wang, Q.-P., Bai, M., Topiramate versus carbamazepine for the treatment of classical trigeminal neuralgia: a meta-analysis. CNS Drugs, 2011. **25**(10): p. 847-857.

[4] Johnson, B.A., Recent advances in the development of treatments for alcohol and cocaine dependence: focus on topiramate and other modulators of GABA or glutamate function. CNS Drugs, 2005. **19**(10): p. 873-96.

[5] Shinn, A.K., Greenfield, S.F., *Topiramate in the treatment of substance-related disorders: a critical review of the literature.* J. Clin. Psychiatry (Memphis, TN, U. S.), 2010. **71**(5): p. 634-648.

[6] Popov, T.V., Maricic, L.C., Prosen, H., Voncina, D.B., *Determination of topiramate in human plasma using liquid chromatography tandem mass spectrometry.* Acta Chim Slov, 2013. **60**(1): p. 144-50.

[7] Shibata, M., Hashi, S., Nakanishi, H., Masuda, S., Katsura, T., Yano, I., Detection of 22 antiepileptic drugs by ultra-performance liquid chromatography coupled with tandem mass spectrometry applicable to routine therapeutic drug monitoring. Biomed. Chromatogr., 2012. **26**(12): p. 1519-1528.

[8] La, M.G., Malvagia, S., Filippi, L., Fiorini, P., Innocenti, M., Luceri, F., Pieraccini, G., Moneti, G., Francese, S., Dani, F.R., Guerrini, R., *Rapid assay of topiramate in dried blood spots by a new liquid chromatography-tandem mass spectrometric method.* J. Pharm. Biomed. Anal., 2008. **48**(5): p. 1392-1396.

[9] Contin, M., Riva, R., Albani, F., Baruzzi, A., Simple and rapid liquid chromatographic-turbo ion spray mass spectrometric determination of topiramate in human plasma. J Chromatogr B Biomed Sci Appl, 2001. **761**(1): p. 133-7.

[10] Vnučec Popov, T., Maričič, L.C., Prosen, H., Vončina, D.B., Development and validation of dried blood spots technique for quantitative determination of topiramate using liquid chromatography–tandem mass spectrometry. Biomed. Chromatogr., 2013. **27**(8): p. 1054-1061.

[11] Bahrami, G., Mohammadi, B., A novel high sensitivity HPLC assay for topiramate, using 4-chloro-7-nitrobenzofurazan as pre-column fluorescence derivatizing agent. J. Chromatogr. B, 2007. **850**(1–2): p. 400-404.

[12] Bahrami, G., Mirzaeei, S., Mohammadi, B., Kiani, A., *High performance liquid chromatographic determination of topiramate in human serum using UV detection.* J. Chromatogr. B, 2005. **822**(1–2): p. 322-325.

[13] Britzi, M., Soback, S., Isoherranen, N., Levy, R.H., Perucca, E., Doose, D.R., Maryanoff, B.E., Bialer, M., Analysis of Topiramate and Its Metabolites in Plasma and Urine of Healthy Subjects and Patients With Epilepsy by Use of a Novel Liquid Chromatography–Mass Spectrometry Assay. Therapeutic Drug Monitoring, 2003. **25**(3): p. 314-322.

[14] Styslo-Zalasik, M., Li, W., Determination of topiramate and its degradation product in liquid oral solutions by high performance liquid chromatography with a chemiluminescent nitrogen detector. J. Pharm. Biomed. Anal., 2005. **37**(3): p. 529-534.

[15] Biro, A., Pergel, E., Arvai, G., Ilisz, I., Szepesi, G., Peter, A., Lukacs, F., *Highperformance liquid chromatographic study of Topiramate and its impurities.* Chromatographia, 2006. **63**(Suppl.): p. S137-S141.

[16] Arvai, G., Garaczi, S., Mate, A.G., Lukacs, F., Viski, Z., Schneider, G., Process for the preparation of topiramate derivatives from 2,3:4,5-bis-O-(1-methylylidene)-β-D-fructofuranose, Patent No. US20060040874A1.

[17] Cobb, Z., Shaw, P.N., Lloyd, L.L., Wrench, N., Barrett, D.A., Evaporative light-scattering detection coupled to microcolumn liquid chromatography for the analysis of underivatized amino acids: Sensitivity, linearity of response and comparisons with UV absorbance detection. J. Microcolumn Sep., 2001. **13**(4): p. 169-175.

[18] Gorecki, T., Lynen, F., Szucs, R., Sandra, P., *Universal response in liquid chromatography using charged aerosol detection.* Anal. Chem., 2006. **78**(9): p. 3186-92.

[19] *Topiramate*, *United States Pharmacopoeia*, USP 38 NF 33, The United States Pharmacopeial Convention, 2015, Rockville, MD, USA.

[20] Almeling, S., Ilko, D., Holzgrabe, U., *Charged aerosol detection in pharmaceutical analysis.* J. Pharm. Biomed. Anal., 2012. **69**: p. 50-63.

[21] *Technical Guide for the Elaboration of Monographs,* 6th Edition, European Directorate for the Quality of Medicinces & HealthCare (EDQM), 2011, Strasbourg, France.

[22] Almeling, S., Holzgrabe, U., Use of evaporative light scattering detection for the quality control of drug substances: influence of different liquid chromatographic and evaporative light scattering detector parameters on the appearance of spike peaks. J. Chromatogr. A, 2010. **1217**(14): p. 2163-70.

[23] Crafts, C., Bailey, B., Plante, M., Acworth, I., *Validating analytical methods with charged aerosol detection*. http://www.dionex.com/en-us/webdocs/110512-PO-HPLC-ValidateAnalyticalMethods-CAD-31Oct2011-LPN2949-01.pdf *(Accessed: 10.07.2014).*

[24] *ICH Guideline Q2(R1), Validation of Analytical Procedures: Text and Methodology,* International Conference on Harmonisation of Technical Requirements for Registration of Pharmaceuticals for Human Use, 2005, Geneva, Switzerland.

4.3 Simple and rapid high performance liquid chromatography method for the determination of polidocanol as bulk product and in pharmaceutical polymer matrices using charged aerosol detection

David Ilko, Sebastian Puhl, Lorenz Meinel, Oliver Germershaus, Ulrike Holzgrabe

Reprinted with permission from J Pharm Biomed Anal **2015**, 104, 17-20.

Abstract

Currently, neither the European nor the United States Pharmacopoeia provide a method for the determination of polidocanol (PD) content despite the fact that PD, besides being an excipient, is also used as an active pharmaceutical ingredient. We therefore developed a method where the PD content was determined using a Kinetex C_{18} column operated at 40 °C with water–acetonitrile (15:85, v/v) as mobile phase. A Corona® charged aerosol detector was employed for the detection of PD that is lacking a suitable UV chromophore. The method was fully validated. Additionally, the method was applied for the determination of PD release from a pharmaceutical polymer matrix consisting of poly-ε-caprolactone and poly(lactic-*co*-glycolic acid) and PD.

1. Introduction

Polidocanol (PD) is a heterogeneous compound consisting of ethers of mainly lauryl alcohol with polyethylene glycols of variable chain length with an average of nine ethylene oxide monomers (Fig. 1). It is widely used as an O/W emulsifier in pharmaceutical and cosmetic products [1]. PD also serves as an active pharmaceutical ingredient (API) as local anesthetic and antipruritic substance, and in sclerotherapy [2]. Furthermore, ethoxylated alcohols are extensively used in household cleaning products [3]. In addition, PD was recently employed to increase the protein release from polymer matrices [4].

Only a few procedures for the determination of PD in pharmaceutical formulations are reported. Quantitative thin layer chromatographic methods were described [5,6], but such methods are no longer considered to be state of the art. Numerous HPLC methods for the determination of ethoxylated alcohols using UV detection after derivatization [7], evaporative light scattering detection [8–13] or mass spectrometry [14–17] are reported, as their determination in waste water is of great importance in environmental analysis.

The European Pharmacopoeia (Ph. Eur.) addresses the dual use as excipient and as API in two separate monographs (macrogol lauryl ether as excipient [18] and lauromacrogol 400 as API [19]). In the API monograph, the specifications for impurities are tighter, e.g., the amounts of free lauryl alcohol and free polyethylene glycol as well as alcohols of differing chain length are restricted. No limits for these impurities are given in the excipient monograph as well as the USP monograph (polyoxyl lauryl ether, [20]).

Because the major pharmacopoeias do not provide an assay method, the aim of this study was to develop and validate a potential compendial method suitable for routine analysis of PD content. Here, a Corona® charged aerosol detector (CAD) was used. Like an ELSD, the CAD is an aerosol-based detector. The mobile phase is nebulized with nitrogen and the resulting droplets are dried in a heated tube. The remaining analyte particles are charged through adsorption of second stream of nitrogen that was charged by passing a corona needle. The electric charge is measured with an electrometer. The resulting signal is proportional to the analyte mass. The CAD is capable of detecting all non-volatile and some semi-volatile substances giving a re-

sponse regardless of the chemical properties of the analyte [21] and is therefore well suited for PD detection, which lacks a UV chromophore.

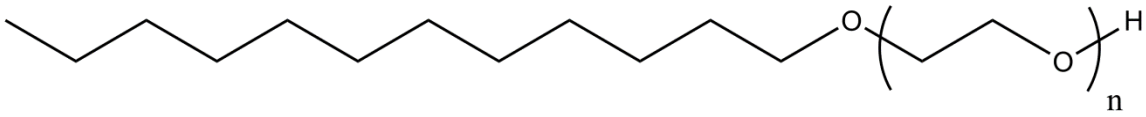

Fig. 1. Structural formula of polidocanol (PD). The number of ethylene oxide n = 3 – 23 for PD used as excipient and n = 9 for PD used as API.

2. Materials and methods

2.1. Reagents and material

Ultra-pure water (>18.2 MΩ) was delivered by a Milli-Q Synthesis water purification system (Millipore, Billerica; MA, USA). Gradient grade acetonitrile and lauryl alcohol were purchased from VWR International (HiPerSolv Chromanorm®) (Darmstadt, Germany), and polidocanol (Macrogoli aether laurilicum 9, Ph. Eur. 6.0) and polyethylene glycol 1500 from Fagron (Barsbüttel, Germany).

2.2. Instrumentation

Measurements were carried out on an Agilent 1100 LC system (Waldbronn, Germany) equipped with a binary pump, an online degasser and a thermostated column compartment. A Corona® CAD (Thermo Scientific, Idstein, Germany) was used for the detection. The gas inlet pressure (nitrogen) was 35 psi, the filter was set to “none” and the range to 100 pA.

2.3. Chromatographic conditions

The optimized method makes use of a Kinetex C18 (100 × 3.0 mm, 2.6 µm particle size) analytical column (Phenomenex, Aschaffenburg, Germany). The column compartmentwas maintained at 40.0 °C. The mobile phase consisted of water–acetonitrile (15:85, v/v) at a flow rate of 0.6 mL/min. The injection volume was 10 µL. The sample solution was prepared by dissolving PD in the mobile phase and diluting with mobile phase to a concentration of 50.0 µg/mL. The PD content was calculated using a reference solution prepared in the same way as the sample solution.

3. Results and discussion

3.1. Method development

The aim of the study was to develop a rapid HPLC method for the content determination of PD. The different PD homologues should be eluted as one single peak, which is separated from potential impurities present in the sample, i.e., lauryl alcohol, polyethyleneglycol. Reversed phase chromatography is optimally suited as it suppresses the separation according to the number of ethoxylate units [22].

Initially, the retention behavior of PD at various contents of acetonitrile in the mobile phase (70/75/80/85/90%) was investigated (Fig. 2). Utilizing acetonitrile contents of 75% and below, the different PD species were partly separated and eluted over a broad span of time, thus aggravating its proper integration. A narrow PD peak was observed when using 90% acetonitrile as mobile phase. However, the PD peak was not sufficiently separated from the injection peak, indicated by a retention factor $k < 1$ ($k = 0.94$). A mobile phase composition of water–acetonitrile (15:85, v/v) was considered to be best suited. The different PD species appeared as one single peak with sufficient retention (k = 1.20, retention time 1.7 min). The influence of the column temperature on the peak shape was studied. A reduction of 30% of the peak width at half height was achieved at 40 °C compared to 25 °C.Thus, the separation was therefore carried out at 40 °C with a mobile phase consisting of water–acetonitrile (15:85, v/v).

3.2. Validation for the determination of PD as bulk product

The method's suitability was evaluated as a potential assay procedure for the compendial testing of PD as bulk product. It was validated in terms of specificity, sensitivity, repeatability, accuracy, linearity and range according to ICH guideline Q2(R1) [23].

3.2.1. Specificity

It was shown that potential impurities, polyethylene glycol and lauryl alcohol, do not interfere with the peak of the main substance. Polyethylene glycol eluted with the injection peak (Fig. 3) with an LOQ of 0.9 µg/mL. Due to its high vapour pressure, lauryl alcohol gave no response in the CAD.

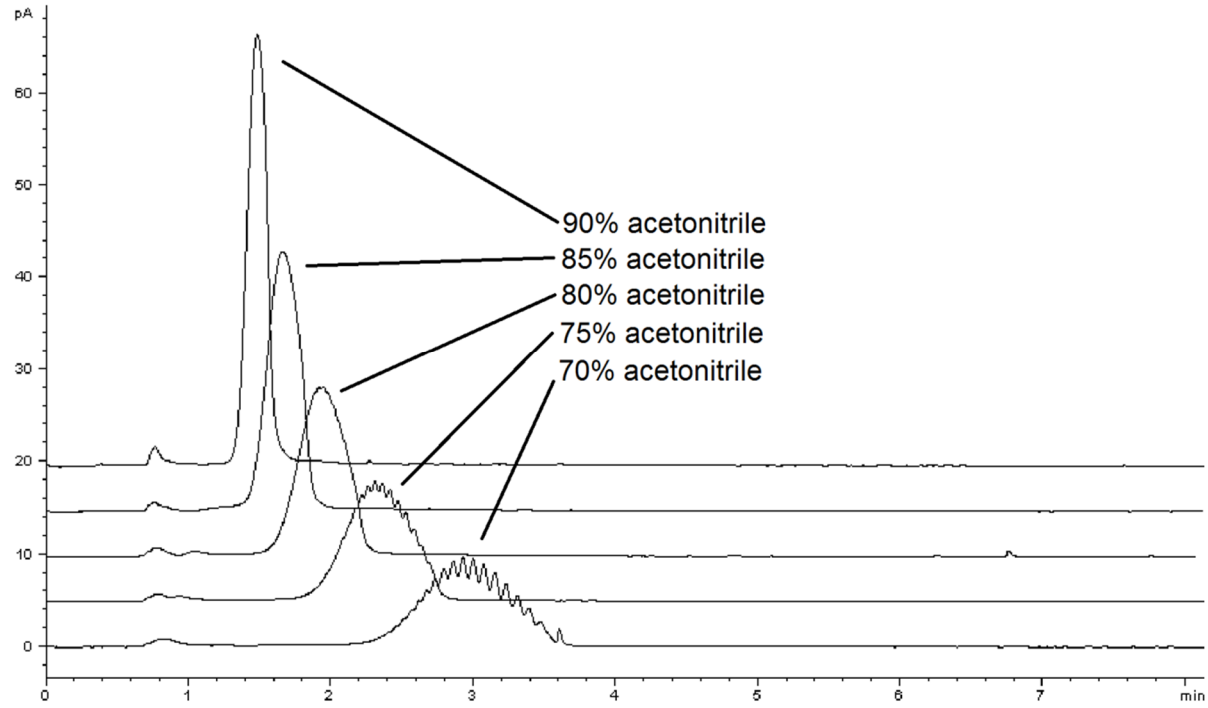

Fig. 2. Influence of the content of acetonitrile in the mobile phase on peak shape and retention time of the polidocanol peak (50 µg/mL). Mobile phase flow rate 0.6 mL/min; column temperature 40 °C; detection CAD.

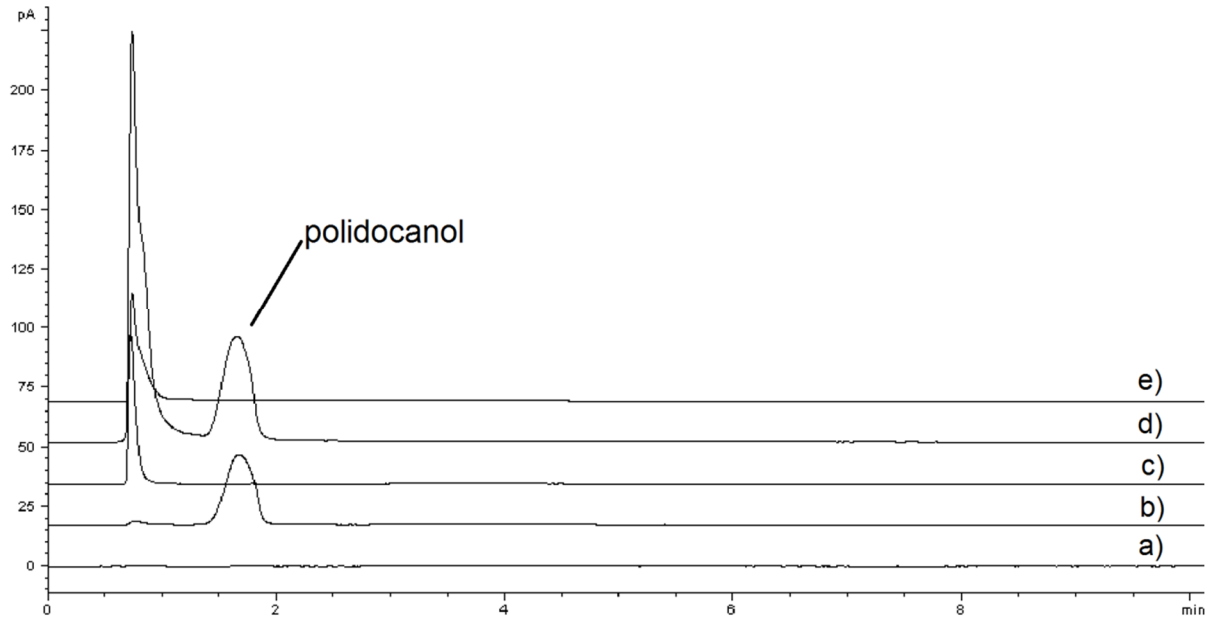

Fig. 3. a) blank (H_2O); b) polidocanol (50 µg/mL); c) polyethylene glycol 1500 (35 µg/mL); d) polidocanol in the dissolution medium in the presence of lysozym; e) nonwoven scaffold without polidocanol after 7 weeks of incubation in the dissolution medium. Chromatographic conditions are stated in chapter 2.3.

3.2.2. Sensitivity

The limit of quantification (LOQ), corresponding to a signal-to-noise ratio of 10, was found to be 0.9 µg/mL for PD.

3.2.3. Linearity and range

Linearity was determined in the range from 80% to 120% referred to a solution of PD at 50 µg/mL, which was chosen as the concentration of the test and reference solution, respectively. The coefficient of determination (R^2) after linear regression was 0.9973 (Fig. 4a).

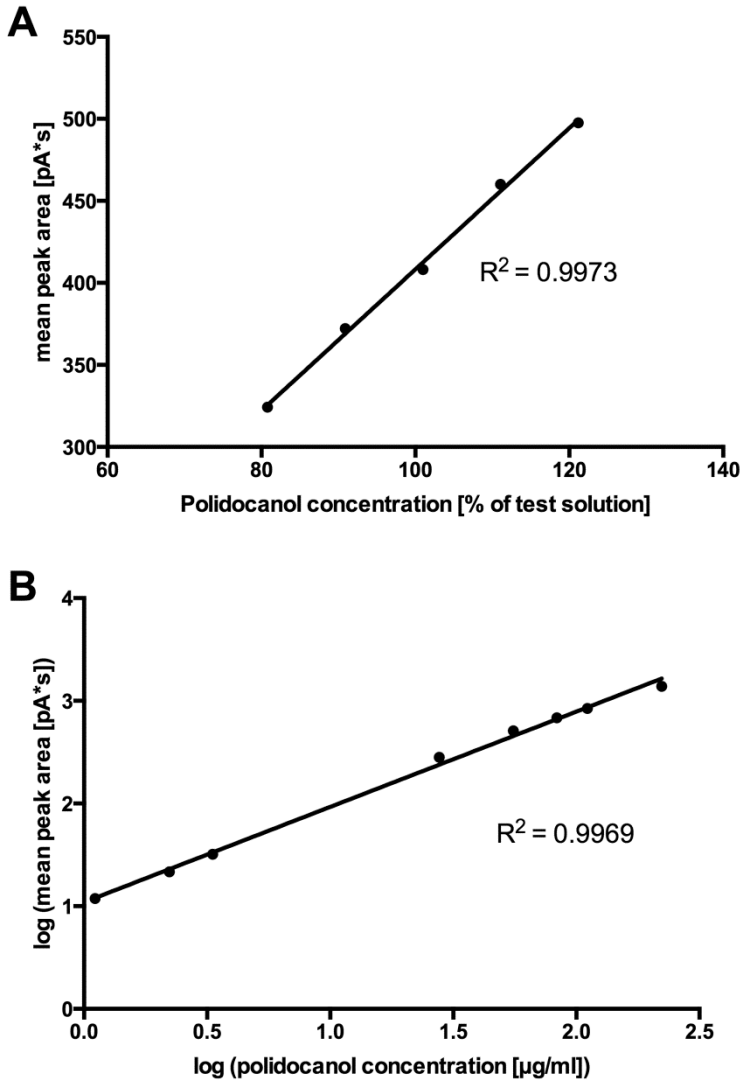

Fig. 4. Linearity plots of polidocanol: a) from 80 to 120% of the concentration of the test solution (i.e. from 40 to 60 µg/mL), y = 4.3054x – 22.313; b) from 1 to 200 µg/mL (after log-log transformation), y = 0.9281x + 1.0386.

3.2.4. Repeatability

Repeatability was assessed at 100% of the concentration of the test solution (50 µg/mL, n = 6). The value for the relative standard deviation (% RSD) was 0.87%, indicating a precise method.

3.2.5. Accuracy

Accuracy was investigated at three levels (80–100–120%) against a reference solution at 100% of the test concentration. Every solution was prepared in triplicate. The recoveries found were between 98.3% and 101.1% (0.13–0.45% RSD), which is a satisfactory result for evaporation-based detectors [24].

3.3. Validation for the determination of PD in pharmaceutical polymer matrices and analysis of the samples

Beside the application as an assay for PD as bulk product, the method can be used for the determination of the PD release from pharmaceutical formulations. Here, the PD release from electrospun nonwoven scaffolds that were developed and manufactured in-house was investigated. These nonwovens consisted of PD, poly-ε-caprolactone and poly(lactic-*co*-glycolic acid) and were designed for the controlled release of a protein (lysozyme) [4]. For the release study of PD, pieces of the nonwovens were incubated in a dissolution medium consisting of PBS, pH 7.4 with 0.1% sodium azide. The above described method had to be revalidated for this purpose. Except from PD, all other compounds present in the sample eluted with the void volume (Fig. 3). Buffer salts and lysozyme did not show any retention on the C_{18}-column. The dissolution analysis of a nonwoven that did not contain PD incubated for 7 weeks showed no interfering peaks caused by potential degradation products of the matrix. Most probably, they are eluted with the void volume due to their hydrophilic character or cannot be detected with the CAD due to their high vapour pressure. Similarly, the diminished response of two of the monomers in the CAD was shown in previous work (lactic acid [25] and caproic acid [26]).The concentration of PD in the investigated samples ranged from 10 µg/mL to 50 mg/mL. The measuring range was set to 5–150 µg/mL. All samples exceeding this range were diluted adequately with mobile phase. Sufficient linearity was only achieved after log–log transformation of concentration and peak area with an R^2 of 0.9969 after log–log transformation (Fig. 4b). Therefore, quantification had to be performed by establishing a calibration curve instead of single point calibration. Accuracy was assessed at three concentration levels (5, 50 and 150 µg/mL). Recoveries found were between 92.7% and 102.7% with RSD value of 0.73% to 1.46%. This was considered to be sufficiently accurate for our purpose. The better accuracy of the assay for bulk product can be attributed to the considerably smaller range improving the linearity of the CAD

[21]. Repeatability was satisfactory with %RSD values between 0.04%and 0.28% at the three different concentration levels (5, 50 and 150 µg/mL).The analysis of different nonwovens revealed that the maximum PD release was reached after 1 h of incubation. It was also shown that PD is adsorbed to the nonwovens. This was indicated by the decreased PD concentration of dissolution medium that contained PD prior to incubation. A complete presentation and discussion of the results obtained for the electrospun nonwoven scaffolds are given in [4].

4. Conclusions

A simple and rapid reversed phase HPLC method using a charged aerosol detector for the determination of PD was developed and validated. This method can be applied as assay for bulk product using single point calibration. By establishing a calibration curve, PD can be quantified over a wide concentration range with good precision and sufficient accuracy. This was demonstrated with the determination of the PD release from a pharmaceutical polymer matrix for controlled protein release.

References

[1] A.H. Kibbe, Handbook of Pharmaceutical Excipients, 3rd Edition, American Pharmaceutical Association, Washington, DC, 2000.

[2] D.M. Eckmann, Polidocanol for endovenous microfoam sclerosant therapy, Expert Opin. Invest. Drugs 18 (2009) 1919–1927.

[3] HERA, Human & Environmental Risk Assessment on Ingredients of EuropeanHousehold Cleaning Products: Alcohol Ethoxylates, http://www.heraproject.com/files/34-F-09%20HERA%20AE%20Report%20Version%202%20-%203%20Sept%2009.pdf (Accessed: 15.07.2014).

[4] S. Puhl, D. Ilko, L. Li, U. Holzgrabe, L. Meinel, O. Germershaus, Protein release from electrospun nonwovens: improving the release characteristics through rational combination of polyester blend matrices with polidocanol, Int. J.Pharm. 477 (2014) 273–281.

[5] R. Brahm, W. Ziegenblag, B. Renger, TLC-spectrodensitometric determination of polidocanol (Thesit) in different pharmaceutical preparations, J. Planar Chromatogr. Mod. TLC 3 (1990) 77–78.

[6] B. Krumholz, K. Wenz, Identification and determination of polidocanol in a suppository formulation, J. Planar Chromatogr. Mod. TLC 4 (1991) 370–372.

[7] L. Nitschke, L. Huber, Analysis for ethoxylated alcohol surfactants in water by HPLC, Fresenius' J. Anal. Chem. 345 (1993) 585–588.

[8] W. Miszkiewicz, J. Szymanowski, Analysis of nonionic surfactants with poly-oxyethylene chains by high-performance liquid chromatography, Crit. Rev.Anal. Chem. 25 (1996) 203–246.

[9] S. Brossard, M. Lafosse, M. Dreux, Comparison of ethoxylated alcohols and polyethylene glycols by high-performance liquid chromatography and supercritical fluid chromatography using evaporative light-scattering detection, J.Chromatogr. 591 (1992) 149–157.

[10] T.C.G. Kibbey, T.P. Yavaraski, K.F. Hayes, High-performance liquid chromato-graphic analysis of polydisperse ethoxylated non-ionic surfactants in aqueous samples, J. Chromatogr. A 752 (1996) 155–165.

[11] W. Miszkiewicz, J. Szymanowski, Operational characteristics of the evaporative light scattering detector used in analysis of ethoxylated alcohols, J. Liquid Chromatogr. Relat. Technol. 19 (1996) 1013–1032.

[12] H.S. Park, C.K. Rhee, Simultaneous determination of nonionic and anionic industrial surfactants by liquid chromatography combined with evaporative light-scattering detection, J. Chromatogr. A 1046 (2004) 289–291.

[13] T. Kamiusuki, T. Monde, K. Omae, K. Morioka, T. Konakahara, Simultaneous separation of nonionic surfactants and polyethylene glycols by reversed phase high performance liquid chromatography, Chromatographia 51 (2000) 390–396.

[14] P.A. Lara-Martin, E. Gonzalez-Mazo, B.J. Brownawell, Environmental analysis of alcohol ethoxylates and nonylphenol ethoxylate metabolites by ultra-performance liquid chromatography-tandem mass spectrometry, Anal.Bioanal. Chem. 402 (2012) 2359–2368.

[15] P.D. DeArmond, A.L. DiGoregorio, Rapid liquid chromatography-tandem mass spectrometry-based method for the analysis of alcohol ethoxylates and alkylphenol ethoxylates in environmental samples, J. Chromatogr. A 1305(2013) 154–163.

[16] L.H. Levine, J.L. Garland, J.V. Johnson, Simultaneous quantification of poly-dispersed anionic, amphoteric and nonionic surfactants in simulated waste water samples using C18 high-performance liquid chromatography-quadrupole ion-trap mass spectrometry, J. Chromatogr. A 1062 (2005) 217–225.

[17] A. Zgola-Grzeskowiak, T. Grzeskowiak, Solid-phase extraction combined with dispersive liquid-liquid microextraction, fast derivatisation and high performance liquid chromatography-tandem mass spectrometry analysis for trace determination of short-chained dodecyl alcohol ethoxylates and dodecyl alcohol in environmental water samples, J. Chromatogr. A 1251 (2012) 40–47.

[18] Macrogoli aether laurilicus Monograph 01/2008:1124, in: European Pharmacopoeia, 8th ed., European Directorate for the Quality of Medicines &HealthCare (EDQM), Strasbourg, France, 2014.

[19] Lauromacrogolum 400 Monograph 01/2009:2046, in: European Pharmacopoeia, 8th ed., European Directorate for the Quality of Medicines &HealthCare (EDQM), Strasbourg, France, 2014.

[20] Polyoxyl Lauryl Ether Monograph, in: United States Pharmacopoeia, USP 37 NF32, 8th ed., The United States Pharmacopeial Convention, Rockville, MD, USA,2014.

[21] R.W. Dixon, D.S. Peterson, Development and testing of a detection method for liquid chromatography based on aerosol charging, Anal. Chem. 74 (2002) 2930–2937.

[22] P. Jandera, M. Holcapek, G. Theodoridis, Investigation of chromatographic behavior of ethoxylated alcohol surfactants in normal-phase and reversed-phase systems using high-performance liquid chromatography-mass spectrometry, J. Chromatogr. A 813 (1998) 299–311.

[23] ICH Guideline Q2(R1), Validation of Analytical Procedures: Text and Methodology, International Conference on Harmonisation of Technical Requirements for Registration of Pharmaceuticals for Human Use, Geneva, Switzerland, 2005.

[24] C. Crafts, B., Bailey, M., Plante, I. Acworth, Validating analytical methods withcharged aerosol detection, http://www.dionex.com/en-us/webdocs/110512-PO-HPLC-ValidateAnalyticalMethods-CAD-31Oct2011-LPN2949-01.pdf (Accessed: 10.07.2014).

[25] D. Ilko, C.-J. Nap, U. Holzgrabe, S. Almeling, Validation and application of an HPLC-CAD-TOF/MS method for identification and quantification of pharmaceutical counterions, Pharm. Bio Scientific Notes (2014) 81–91, sept.

[26] D. Ilko, A. Braun, O. Germershaus, L. Meinel, U. Holzgrabe, Fatty acid composition analysis in polysorbate 80 with high performance liquid chromatography coupled to charged aerosol detection, Eur. J. Pharm. Biopharm. (2014) (in press).

4.4 Protein release from electrospun nonwovens: Improving the release characteristics through rational combination of polyester blend matrices with polidocanol

Sebastian Puhl, David Ilko, Linhao Li, Ulrike Holzgrabe, Lorenz Meinel, Oliver Germershaus

Reprinted with permission Int J Pharm **2014**, 477(1-2), 273-281.

Abstract

Nonwoven scaffolds consisting of poly-ε-caprolactone (PCL), poly(lactic-*co*-glycolic acid) (PLGA) and polidocanol (PD), and loaded with lysozyme crystals were prepared by electrospinning. The composition of the matrix was varied and the effect of PD content in binary mixtures, and of PD and PLGA content in ternary mixtures regarding processability, fiber morphology, water sorption, swelling and drug release was investigated. Binary PCL/PD blend nonwovens showed a PD-dependent increase in swelling of up to 30% and of lysozyme burst release of up to 45% associated with changes of the fiber morphology. Furthermore, addition of free PD to the release medium resulted in a significant increase of lysozyme burst release from pure PCL nonwovens from approximately 2–35%. Using ternary PCL/PD/PLGA blends, matrix degradation could be significantly improved over PCL/PD blends, resulting in a biphasic release of lysozyme with constant release over 9 weeks, followed by constant release with a reduced rate over additional 4 weeks. Based on these results, protein release from PCL scaffolds is improved by blending with PD due to improved lysozyme desorption from the polymer surface and PD-dependent matrix swelling.

1. Introduction

Nonwovens prepared by electrospinning are extremely versatile scaffolds allowing the controlled and localized delivery of various drugs in a broad variety of applications ranging from tissue engineering to topical gene delivery. The large surface area of electrospun nonwovens, their versatility with regards to attainable structures as well as the large number of biocompatible polymers suitable for elecrospinning such as poly-ε-caprolactone (PCL), poly(lactic-*co*-glycolic acid) (PLGA), poly(ethylene glycol) (PEG) or poly(L-lysine) (PLL) constitute the exceptional suitability of nonwoven scaffolds for drug delivery (Meinel et al., 2012 and Wendorff et al., 2012). PCL is frequently used as a polymer matrix for various drug delivery applications, including the production of electrospun nonwovens, because of its biodegradability, biocompatibility, advantageous material characteristics such as low glass transition- and melting temperature, and broad solvent compatibility as well as its excellent mechanical properties (Cipitria et al., 2011, Dash and Konkimalla, 2012 and Qin and Wu, 2012). Moreover, PCL has been used in several FDA approved drug delivery systems and implants, as suture material and adhesion barrier (Gunatillake and Adhikari, 2003). Despite these advantages, release of hydrophilic, high molecular weight drugs was frequently found to be challenging because of PCLs semicrystalline nature, slow degradation and high hydrophobicity (Chen et al., 2000 and Wang et al., 2009), requiring copolymerization or blending with hydrophilic polymers or polymers possessing a higher degradation rate such as PLGA (Anderson and Shive, 1997, Briggs and Arinzeh, 2014, Liu et al., 2008 and Puhl et al., 2014).

In previous studies we observed that the combination of PCL nonwovens and protein crystals allows control of both, amount of burst release as well as long-term release rate through variation of protein crystal–fiber size ratio, degree of loading and polymer matrix composition (Puhl et al., 2014). However, despite the significant variability achieved through the novel combination of electrospun fibers and protein crystals, the low amount of total released protein and limited control over release rate required further optimization. Furthermore, blending of PCL with PEG and PLGA alone, while in part successful, still resulted in slow and incomplete protein release.

Within this study we explore the mode of protein release from pure and blended PCL matrices containing protein crystals. We hypothesize that besides polymer degradation and drug diffusion, wettability of the nonwoven, swelling of the polymer matrix

and desorption play an important role in protein release from nonwoven scaffolds. Therefore, we studied the effect of matrix composition on protein release using electrospun nonwovens consisting of a novel blend of PCL, polidocanol (PD) and PLGA. PD is used in pharmaceutical and cosmetic formulations as an O/W emulsifier and as an active pharmaceutical ingredient for topical therapy, as local anesthetic and antipruritic drug at concentrations between 3 and 8% m/m, and as sclerosant after injection into varicose veins at concentrations between 0.25 and 3% m/m. Because of its surface activity and well-established topical application, PD may represent a valuable excipient to improve the material characteristics of PCL nonwovens.

2. Materials and methods

PCL (Mw 70,000–90,000), chicken egg white lysozyme and trifluoroacetic acid (HPLC grade) were purchased from Sigma–Aldrich (Munich, Germany). Polidocanol (Macrogoli aether laurilicum 9, Ph. Eur. 6.0) was bought from Fagron (Barsbüttel, Germany). Poly(d,l-lactide-*co*-glycolide) 50:50 (Resomer RG 502H, Mw 7000–17,000) was a kind gift from Evonik Industries (Essen, Germany). Acetonitrile (gradient grade) was purchased from VWR Prolabo (Fontenay-sous-Bois, France). Poly(ethylene glycol) 6000 was obtained from MERCK Schuchardt (Hohenbrunn, Germany). Chloroform, ethanol, sodium phosphate, sodium hydroxide, sodium chloride, sodium azide and acetic acid were of analytical grade.

2.1. Lysozyme crystallization and crystal size determination

Lysozyme crystallization was performed according to the method of Falkner et al. (2005) with modifications as described before (Puhl et al., 2014). Lysozyme was dissolved in 100 mM sodium acetate buffer pH 3.5 at a concentration of 8.0 mg/ml. Precipitation buffer consisting of 20% sodium chloride, 10% PEG 6000 and 500 mM sodium acetate at pH 3.5 at 8 °C was poured quickly into the lysozyme solution and stirred at 500 rpm. Mixing ratio of precipitation buffer to lysozyme solution was 2:1. After centrifugation at 3500 × *g* for 5 min to separate crystals, they were washed twice with ethanol/chloroform (volume ratio 3:10). Finally, crystals were dried over night under mild vacuum. Average particle size of crystals was measured by laser diffraction analysis using ethanol as dispersion medium (LS 230, Beckman Coulter, Brea, CA).

2.2. PCL electrospinning

Electrospinning was performed using a custom-built apparatus consisting of a DC power supply HCP 140-350000 (FuG Elektronik, Rosenheim, Germany) and a syringe pump (Type 540200, TSE Systems, Bad Homburg, Germany). Nonwovens were produced by electrospinning onto a stationary copper plate using a similar setup as described before (Pham et al., 2006 and Puhl et al., 2014). Protein crystals were dispersed in ethanol at a concentration of 3.0 mg/ml and homogenized for 20 s using an ultrasonic bath (Branson 3200, Bransonic, Danbury, CT). Subsequently, chloroform and the particular polymers were added. Ethanol and chloroform were mixed in a volume ratio of 1:6. Ratios of polidocanol and PLGA were calculated as dry mass in relationship to PCL (m/m%) and compositions are summarized in Table 1. No sedimentation, dissolution or disintegration of the protein crystals was observed during processing in polymer solution. The resulting suspensions were filled into a syringe with an attached gauge 22 metal needle. The needle was centered within a copper ring of 20 cm diameter consisting of copper wire of 2 mm diameter placed in a vertical plane around it and both were connected to the DC power supply and charge was adjusted to 27 kV. The flow rate was set to 10 ml/h and the stationary copper plate was placed at a distance of 40 cm from the needle. The lysozyme crystal loading of the nonwovens was calculated individually. Average loading was 0.15 ± 0.04% m/m. All data is depicted as results from triplicated experiments and represents the average ± standard deviation (SD).

2.3. Morphology and fiber diameter

SEM images were recorded using a JSM-7500F field emission scanning electron microscope (Jeol, Tokyo, Japan) with an acceleration voltage of 2 kV. ImageJ (NIH, Bethesda, MD) was used to determine the fiber diameter. Sixty individual fiber diameters were manually measured vertically to the fiber surface for every preparation. Samples were cut out of the incubated nonwovens and washed with purified water, dried under mild vacuum overnight and studied by SEM using fresh nonwovens as reference.

Table 1. Compositions of the electrospun nonwovens. All ratios are expressed as % m/m.

Name	PCL [%]	PD [%]	PLGA [%]
PCL	100	--	--
PCL/PD2	98	2	--
PCL/PD10	90	10	--
PCL/PD20	80	20	--
PCL/PD50	50	50	--
PCL/PD20/PLGA2	78	20	2
PCL/PD20/PLGA10	70	20	10

2.4. Wettability and sorption rate of the nonwovens

Contact angle measurements were performed using casted films as substitutes for electrospun nonwovens using a drop shape analysis (DSA 10, Krüss GmbH, Hamburg, Germany). Films were used instead of nonwovens to avoid bias by variable capillarity and uneven surfaces, respectively. Polymer blends were coated on a glass microscope slide and allowed to dry under ambient conditions. A drop of release medium was placed on the polymer films and contact angle was measured over time.

Sorption of PBS release medium into capillaries of the nonwovens was determined similar as described before (Puhl et al., 2014). According to the Washburn theory the sorption rate is correlated to contact angle and wettability of a nonwoven (Washburn, 1921).

$$t = A \times m^2 \tag{1}$$

$$A = \frac{\eta}{c \times \rho^2 \times \sigma \times \cos\theta} \tag{2}$$

$$\frac{m^2}{t} = \frac{c \times \rho^2 \times \sigma \times \cos\theta}{\eta} \tag{3}$$

where m is the sorbed mass of water, η is the viscosity of the immersion liquid, c is the capillarity of the sample, ρ is the density of the immersion liquid, σ is the surface tension of the immersion liquid, and θ is the contact angle between immersion liquid and nonwoven. Briefly, for each nonwoven composition the short side of a sample with the size of 9 mm × 36 mm was dipped 0.1 mm deep into the release medium using a tensiometer (K12, Krüss GmbH, Hamburg, Germany). Mass increase per area nonwoven over time was recorded and depicted as the sorption rate expressed as (µg/s)/mm^2.

2.5. Swelling of polymer blends

Swelling of the polymer blends was investigated similar as described before (Sahoo et al., 2010). Films of the same compositions as those of nonwovens were used to avoid any bias from variability of the capillarity of nonwovens. Films of all the respective polymer-compositions were casted on a glass plate, dried at room temperature and weighed. Masses ranged from 150 to 350 mg and films were approximately 1 mm thick with a diameter of approximately 15 mm. The films were then immersed into 4 ml of PBS and incubated for 24 h at 37 °C. Subsequently, the polymer films were dried on the outside with a paper towel and weighed. Since PD was known to leach from the polymer films resulting in substantial mass loss, samples were dried at RT for 72 h and weighed again to determine the absolute amount of water absorbed. Swelling is expressed as the swelling ratio Q_m according to Eq. (4).

$$Q_m = \frac{W_s - W_d}{W_d} \qquad (4)$$

W_s and W_d represent the weight of the sample after swelling and the weight of the sample after drying for 72 h, respectively.

2.6. Differential scanning calorimetry

Differential scanning calorimetry (DSC) analysis was performed using a DSC 8000 (PerkinElmer, Waltham, MA). Electrospun samples of approximately 3 mg were accurately weighed into aluminum pans and heated twice in a cycle from −50 to 150 °C with a heating rate of 20 K/min. For analysis the second heating step was used.

2.7. In vitro release

Potential residual solvents in the nonwovens after preparation were removed by storage at reduced pressure over night. Afterwards, the nonwovens were weighed (approximately 150–300 mg) and cut into smaller pieces. For release studies they were placed into 4.0 ml PBS, pH 7.4 with 0.1% sodium azide at 37 °C. Sink conditions both for lysozyme and PD were guaranteed at all times. At defined time points, 250 µl of the release medium were sampled and replaced by the same volume of fresh buffer. In additional experiments, free PD at a concentration of 0.112 mg/ml, 15 mg/ml or 45 mg/ml was added to the release medium prior to incubation of pure PCL nonwovens and 0.112 mg/ml of free PD was added to the medium prior to incubation

of PCL/PD50 nonwovens. The concentrations were chosen as follows: 0.112 mg/ml equals twice the critical micelle concentration (CMC), a concentration of 15 mg/ml PD was found after incubating PCL/PD20 nonwovens, and a concentration of 45 mg/ml PD was found after incubation of PCL/PD50 nonwovens. These additional release experiments were performed to decipher the role of PD during lysozyme release. Lysozyme concentrations were determined using RP-HPLC as described before (Puhl et al., 2014).

Polidocanol concentration was measured using an Agilent 1100 LC system (Waldbronn, Germany) equipped with a binary pump, an online degasser and a thermostated column compartment. For detection a charged aerosol detector (Corona® CAD, Thermo Scientific, Idstein, Germany) was used because of the lack of chromophores in PD (Ilko et al., 2014). The gas inlet pressure (nitrogen) was 35 psi, the filter was set to “none” and the range to 100 pA. The optimized method used a Kinetex C18 (100 mm × 3.0 mm, 2.6 µm particle size) analytical column from Phenomenex (Aschaffenburg, Germany). The column compartment was maintained at 40 °C. The mobile phase consisted of water–acetonitrile (15:85, V/V) at a flow rate of 0.6 ml/min. The injection volume was 10 µl. Samples were diluted with mobile phase to give a PD concentration of about 10–100 µg/ml. Quantification was done by establishing a five point calibration curve over a range from 5 to 150 µg/ml and log–log transformation of concentration and peak area. Limit of quantification was determined at 0.86 µg/ml of PD.

2.8. Relative bioactivity of lysozyme

Relative bioactivity was determined using *Micrococcus lysodeiktikus* cell wall preparation as described before (Gorin et al., 1971 and Liao et al., 2001). Briefly, bacteria were suspended in 1.0 ml of a 0.1 M KH_2PO_4, pH 6.2 at a concentration of 200 mg/l. Then 33.3 µl of the sample solution was added and stirred for 5 s. The subsequent decline of absorbance at 570 nm was recorded for 3 min using a UV-spectrophotometer (Genesys 10S, Thermo Scientific, Rockford, IL). The slope of the decline was proportional to lysozyme bioactivity and the limit of quantification was found to be 0.96 µg/ml lysozyme. Bioactivity of the individual samples was determined using a calibration curve constructed using fresh lysozyme. Relative biological activity of lysozyme is expressed in reference to the lysozyme amount as determined by HPLC.

2.9. Statistical analysis

All data are reported as mean ± standard deviation of at least three independent experiments unless specified otherwise. Statistical significance was calculated by one-way ANOVA using multiple comparisons by the Holm–Sidak method for comparison of multiple groups with an overall significance level of 0.05 (Origin Pro Northampton, MA).

3. Results

3.1. Morphology of nonwovens

Nonwovens were generated from PCL or blends using electrospinning as established before (Puhl et al., 2014). Blending of PCL or PCL/PLGA with PD had no negative impact on processability within the investigated PD concentration range and required no adaption of the pre-established electrospinning parameters. As shown before, processing of lysozyme crystals in organic solvents during electrospinning did not negatively affect lysozyme bioactivity or crystal morphology and the high viscosities of polymer solutions prevented sedimentation of lysozyme crystals during processing (Puhl et al., 2014). Narrow fiber diameter distributions were obtained for all preparations except for PCL/PD20/PLGA10 nonwovens (Fig. 1F and G). Fiber diameters of the nonwovens were found to be reproducible between individual experiments. Overall, SEM micrographs revealed reduction of fiber surface roughness and separation between fibers with increasing PD ratio (Fig. 1A–D). Nonwovens prepared from ternary blends containing PCL, PLGA and PD had an average fiber diameter of 4.2 ± 2.7 µm (PCL/PD20/PLGA2) and 6.5 ± 11.1 µm (PCL/PD20/PLGA10). With both blends a less homogenous distribution of fiber diameters was observed with an apparently bimodal distribution in the case of PCL/PD20/PLGA2 and the presence of large beads in the case of PCL/PD20/PLGA10 (Fig. 1E and F).

After incubation of PCL/PD nonwovens in release medium, fiber diameters were virtually unchanged but the fiber surface roughness appeared to be increased with noticeable wrinkles and indentations (Fig. 1G and Fig. 2A–D). The surface roughness after incubation seemed to positively correlate with PD content as assessed by SEM. No further changes of fiber morphology were detected after the first 6 h of incubation (data not shown).

Similar patterns were found after incubation of nonwovens containing 20% PD and 2 or 10% PLGA (Fig. 2E and F). Surface morphology of both preparations was quite comparable to nonwovens consisting of PCL and 20% PD only, after incubation for 6 h. After an extended incubation of 9 weeks, PCL/PD20/PLGA10 nonwovens showed signs of fiber degradation in the form of cracks and fractures but fiber diameter remained virtually unchanged (Fig. 2G and H).

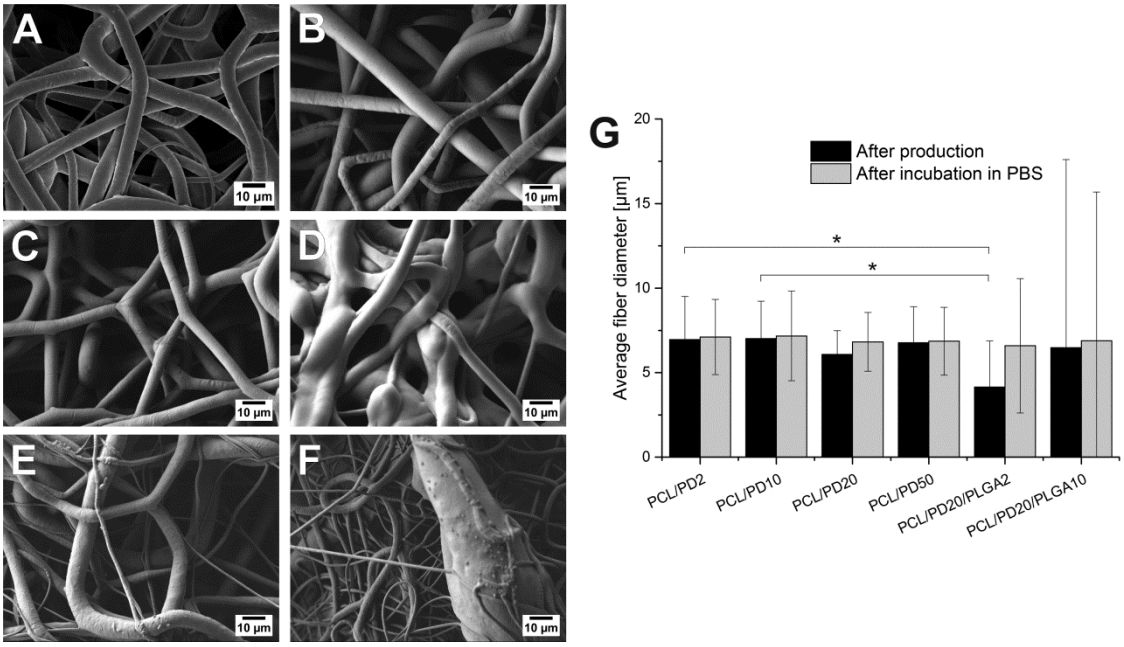

Fig. 1. Morphology and fiber diameter of electrospun nonwovens: PCL/PD2 (A), PCL/PD10 (B), PCL/PD20 (C), PCL/PD50 (D), PCL/PD20/PLGA2 (E), PCL/PD20/PLGA10 (F), and average fiber diameter of the dried electrospun nonwovens before and after incubation in release medium for 8 weeks (G).

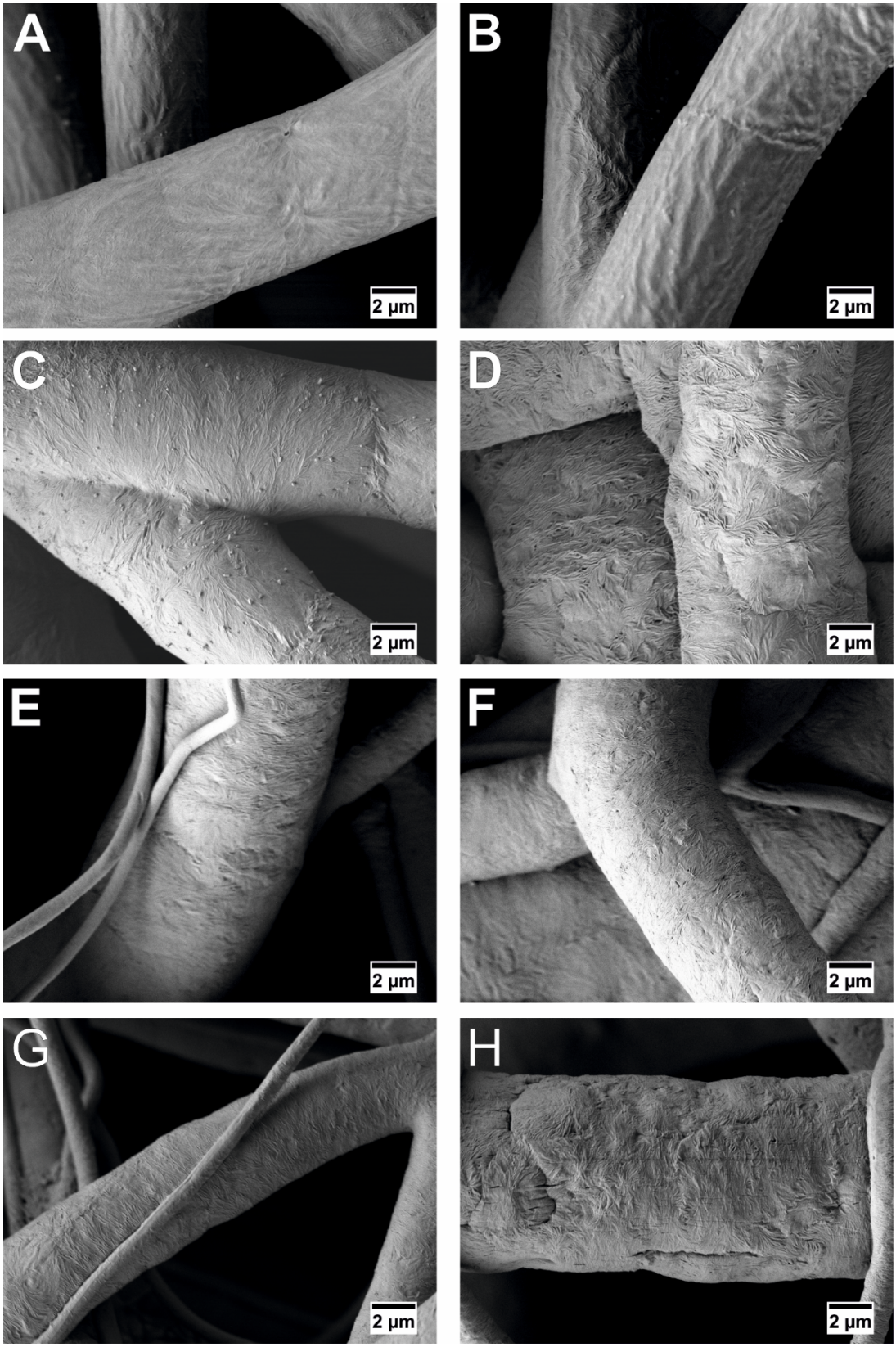

Fig. 2. Morphology of nonwovens after incubation in release medium for 1 day: PCL/PD2 (A), PCL/PD10 (B), PCL/PD20 (C), PCL/PD50 (D), PCL/PD20/PLGA2 (E), PCL/PD20/PLGA10 (F). Morphology of formulations containing PLGA after 8 weeks of incubation in release medium: PCL/PD20/PLGA2 (G), and PCL/PD20/PLGA10 (H).

3.2. Differential scanning calorimetry

Melting points of PCL and PD were determined by DSC with 59.6 and 23.8 °C, respectively, being in good agreement with previously reported results (Bittiger et al., 1970 and Eckmann, 2009). Glass transition point of PLGA was observed at 44.4 °C (Fig. 3A) (Friess and Schlapp, 2002). PCL/PD blends showed a decreasing melting temperature with increasing PD content (Fig. 3B). Below 10% PD, neither glass transition nor melting of PD was detected, while above 10% PD glass transition but no melting of PD was observed. At 50% PD both, glass transition and melting of PD were detected. Both ternary blend formulations additionally showed glass transition of PLGA between 50 and 60 °C, however not clearly separated from melting of PCL.

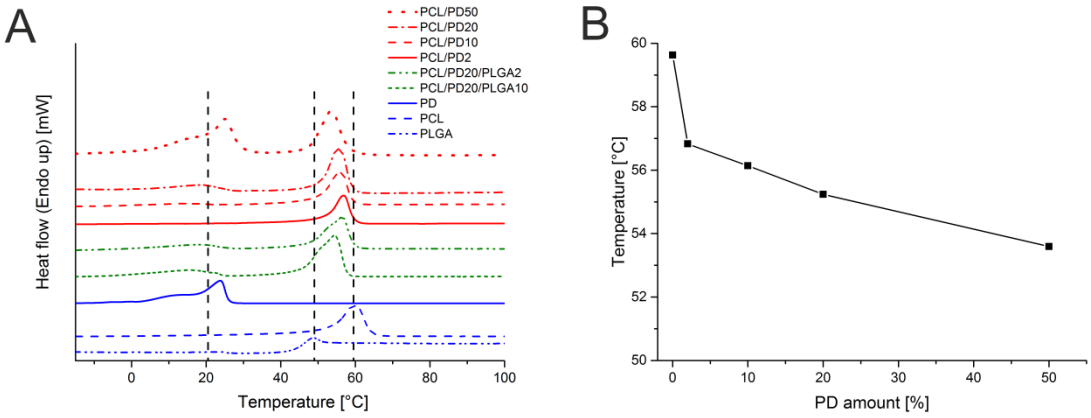

Fig. 3. DSC analysis of pure polymers and electrospun polymer blends (A). Vertical lines represent the melting respectively glass transition point of the pure polymers. Effect of PD content on melting temperature of PCL/PD nonwovens (B).

3.3. Contact angle, sorption rate and swelling behavior

The contact angle of PBS with pure PCL films was found to be 85.3 ± 4.9°. Because of the surface activity of PD, contact angles were considerably reduced for films containing PD and fast spreading of the drop complicated analysis. A significant reduction of the contact angle to 72.6 ± 4.9° was observed in the case of samples containing 2% PD. For samples containing higher percentages of PD, contact angles could not be determined because of fast spreading of the liquid on the surface and thus were considered to be 0°.

In addition, sorption of incubation medium to nonwovens was investigated (Fig. 4A). The sorption rate is influenced by the contact angle as well as the capillarity of the nonwovens and thus may describe the initial contact of release medium with nonwovens and the general wettability of nonwovens (Washburn, 1921). Interesting-

ly, sorption of PBS into the nonwovens was found to decrease with increasing PD concentration. With nonwovens containing 50% PD sorption was not completed within the time frame of wicking experiments, signified by PBS sorption only within the first 5 mm of the total 36 mm length of the sample. Addition of PLGA resulted in a significant increase of the sorption rate compared to nonwovens containing PCL and PD alone.

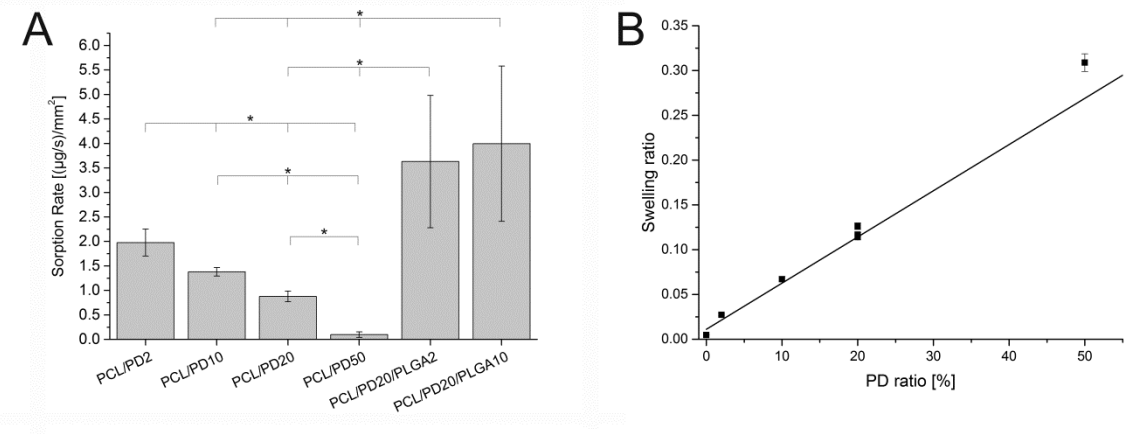

Fig. 4. Effect of nonwoven composition on sorption of PBS (A) and on swelling of PCL/PD and PCL/PD/PLGA films (B).

The swelling of pure PCL films was found to be negligible (Fig. 4B). However, with increasing PD content in the polymer films the swelling ratio increased linearly (R^2 = 0.995) and the correlation between PD content and swelling ratio was found to be statistically significant ($p < 0.0001$). Addition of PLGA had no statistically significant effect on swelling within the investigated time frame of 24 h, i.e., swelling was comparable to PCL/PD nonwovens with the same PD content. Incubation of pure PCL films with 15 mg/ml PD in the release medium resulted in a small but significant increase of swelling (0.73 ± 0.14%) compared to pure PCL films without addition of PD (0.46 ± 0.003%).

3.4. Polidocanol release

Maximum PD concentrations were reached after incubation for approximately 1 h in release medium for all nonwovens (Fig. 5). Relative PD release depended on the PD content of nonwovens, generally increasing with increasing PD content. However, at high PD content of 50% PD/PCL only 80.5 ± 5.7% of PD contained in the nonwovens was released.

Addition of free PD to the release medium prior to incubation of pure PCL nonwovens revealed that PD adsorbed to the nonwovens, resulting in a drop of free PD concentration in the medium from 112 µg/ml to 12.9 ± 3.1 µg/ml. However, at higher free PD concentration of 15 or 45 mg/ml in release medium no drop of the PD concentration after addition of the nonwovens was observed, most likely because of the limited amount of PD absorbed being not detectable at high total concentration.

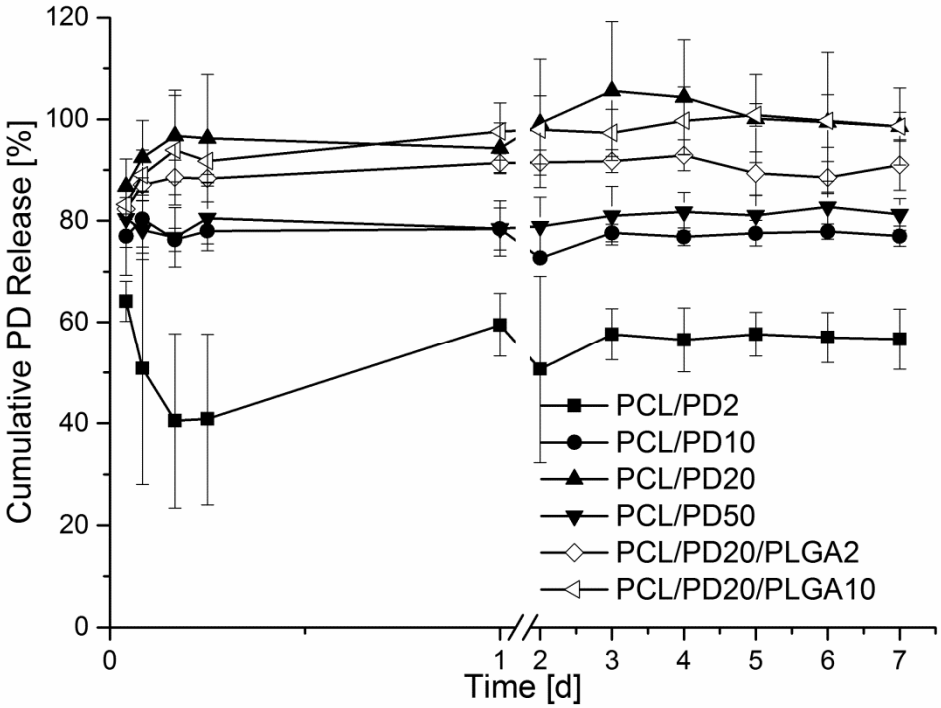

Fig. 5. Cumulative release of polidocanol from nonwovens prepared from PCL/PD or PCL/PD/PLGA blends.

3.5. Lysozyme release

Lysozyme release from pure PCL fibers was found to be low with 1.98 ± 0.5% and 8.5 ± 1.1% of total encapsulated protein released after 1 day and 3 weeks, respectively (Fig. 6A). Hence, under these conditions, very low burst release and a very low release rate was found. A PD concentration dependent increase of burst release was obtained using binary mixtures of PCL and PD, with higher PD content in the nonwoven resulting in higher burst release of up to 45.4 ± 1.5% at 50% PD after 1 day incubation (Fig. 6A). Similarly, lysozyme burst release from nonwovens consisting of PCL, 20% PD and 2 or 10% PLGA, respectively, was significantly increased compared to pure PCL nonwovens (Fig. 6B). However, compared to nonwovens consist-

ing of the binary blend PCL/PD20, burst release from ternary blend nonwovens was significantly lower (17.5% for PCL/PD20 versus approximately 10% for PCL, PCL/PD20/PLGA2 or PCL/PD20/PGLA10). The release rate from nonwovens produced from binary mixtures of PCL/PD was negligible after burst and comparable to the one from ternary mixtures (PCL/PD/PLGA) within the first week of release. Solely PCL/PD50 nonwovens showed a slow release up to 7 days. Subsequently, only nonwovens containing PLGA showed an accelerated release, which was more pronounced with higher PLGA content, achieving an almost constant release rate. With 10% PLGA (PCL/PD20/PLGA10) 42.8 ± 1.5% of encapsulated lysozyme was released after 4 weeks. Subsequently, lysozyme concentration decreased in the case of the PCL/PD20/PLGA10 nonwovens because of PLGA degradation products resulting in a pH drop in the release buffer from 7.4 to 3.3 and inducing protein degradation. This effect was a direct result of the setup chosen for release studies. The volume of release medium withdrawn for analysis and replaced by fresh release medium at each time point was small compared to the total volume of release medium, resulting in accumulation of both released lysozyme and PLGA degradation products in the release buffer. Nonwovens containing 2% PLGA showed an almost linear release of lysozyme from week 2 until week 9 resulting in cumulative release of 43.6 ± 2.7% after 9 weeks. Thereafter, lysozyme release rate dropped considerably and was almost constant during the following 4 weeks. The pH of the release buffer at the end of the incubation was 5.2.

The effect of the presence of PD in the release medium was investigated by adding free PD to the release medium before incubation of the nonwovens. Addition of 0.112 mg/ml PD (approximately twice the CMC of PD) to the release medium prior to incubation of pure PCL nonwovens led to a significant increase of lysozyme burst release after 1 day incubation from 1.98 ± 0.54% without PD in the release medium to 24.5 ± 2.52% (Fig. 6C). Addition of 15 mg/ml PD (equal to the PD concentration after release from PCL/PD20 nonwoven) and 45 mg/ml (equal to the PD concentration after release from PCL/PD50 nonwoven) resulted in further increased burst release, most prominently at the higher PD concentration (Fig. 6C). Addition of 0.112 mg/ml PD to the release medium prior of incubation of PCL/PD50 nonwovens resulted in increased burst release compared to the same nonwovens incubated without PD addition to the release medium (Fig. 6D).

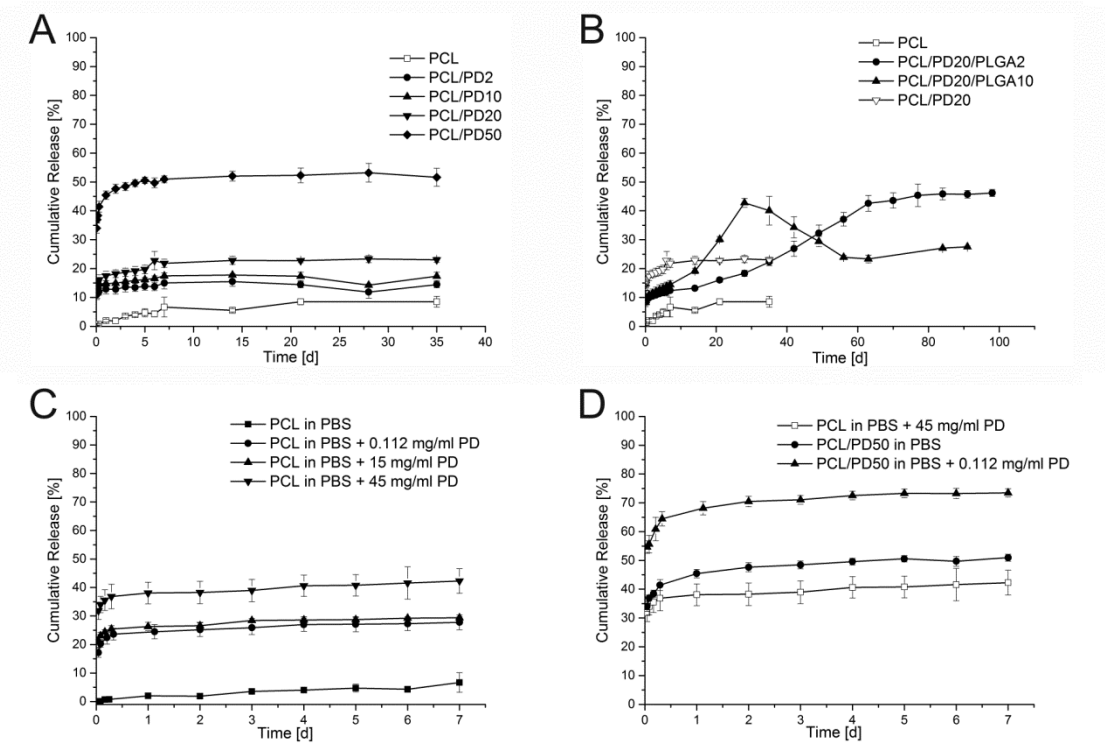

Fig. 6. Effect of nonwoven composition and addition of PD into release medium prior to incubation of the nonwovens on cumulative lysozyme release. The effect of PD content in PCL/PD blend nonwovens (A), PLGA content in PCL/PD/PLGA blend nonwovens (B), concentration of free PD in the release medium in combination with nonwovens of pure PCL (C), and concentration of free PD in combination with PCL/PD blend nonwoven (D) on lysozyme release is shown.

Table 2. Relative bioactivity of released lysozyme determined at selected time points during the release study.

Sample	Time	Bioactive Lysozyme [%]
2 % PD	5 weeks	102.4 ± 9.6
10 % PD	5 weeks	110.3 ± 14.7
20 % PD	5 weeks	106.1 ± 8.6
50 % PD	5 weeks	88.9 ± 18.0
20 % PD 2 % PLGA	5 weeks	112.9 ± 7.0
	9 weeks	105.1 ± 3.2
	13 weeks	108.9 ± 10.7
20 % PD 10 % PLGA	5 weeks	109.2 ± 10.9
	9 weeks	100.7 ± 46.6
	13 weeks	53.7 ± 18.9

3.6. Bioactivity

Lysozyme retained its biological activity after electrospinning including after suspending in the respective organic solvents (Puhl et al., 2014). Moreover, bioactivity was investigated throughout the release study. After 5 weeks incubation, bioactivity was mostly retained for all nonwoven compositions (average of all samples 104.9 ± 13.0%). Release from nonwovens containing PLGA was investigated for 13 weeks and biological activity was determined until the end of incubation. Relative bioactivity was strongly reduced to 53.7 ± 18.9% after 13 weeks release from nonwovens containing 10% PLGA. In contrast, relative bioactivity of lysozyme after release from nonwovens containing 2% PLGA activity was found to be 108.9 ± 10.7% (Table 2).

4. Discussion

With its broad solvent compatibility, high structural stability and optimal processability by electrospinning, PCL offers numerous advantages as a polymer matrix for electrospun drug delivery systems. PCL on the other hand is a semicrystalline, hydrophobic and slowly degrading polymer, resulting in significant challenges, most notably related to drug release, when applied as a polymer matrix for the delivery of large, hydrophilic drugs (Chen et al., 2000). Therefore, PCL based copolymers or blends are needed that maintain most of the advantageous properties of PCL, most importantly its superior processability, while improving the release of large, hydrophilic drugs from the scaffold (Jiang et al., 2005 and Lu and Lin, 2002). We have recently shown that the encapsulation of protein crystals into electrospun nonwovens is a promising new approach toward protein delivery from nonwovens in terms of processing, loading capacity and control over burst and long-term release (Puhl et al., 2014). We herein apply this novel strategy and investigate the physicochemical properties and release characteristics of nonwoven blends composed of PCL, PLGA and PD in an attempt to identify compositions that improve the release of lysozyme.

Electrospinning of PCL/PD blends was straightforward up to a PD content of 50%. Characterization of the morphology of nonwovens by SEM revealed that fiber surface roughness and the separation between fibers decreased with increasing PD content (Fig. 1A–D). Analysis of the melting points of PCL/PD blends by DSC on the one hand showed that homogeneous mixtures were obtained up to a PD content of ap-

proximately 20%. Above this point a separate melting peak of PD was observed, which may be attributed to partial phase separation of PCL and PD (Fig. 3). On the other hand, an increase of the PD content resulted in melting point depression of PCL, i.e., PD acted as a plasticizer in the PD/PCL blends. Therefore, the morphological changes observed by SEM with increasing PD content can be attributed to the melting point depression of PCL/PD blends and, above 20% PD, phase separation, potentially leading to coating of the fiber surface with PD. The fiber morphology was distinctly different prior and after incubation for 1 day in the release medium. After incubation, the fiber surface showed wrinkles and indentations, which appeared to increase with increasing PD content (Fig. 2A–F). These structural changes after incubation are interpreted as a result of matrix swelling during incubation in release medium (Fig. 4B) followed by shrinking during drying of the nonwovens prior to SEM imaging on the one hand and PD leaching from the fibers on the other hand.

The water sorption into capillaries of the nonwovens was investigated to estimate their overall wettability. Surprisingly, water sorption decreased with increasing PD ratios, which was in contrast to the significantly decreasing contact angles. Examination of the swelling behavior of the polymer compositions revealed a linear increase of swelling ratios with increasing PD concentrations. Swelling takes place inside each fiber while sorption takes place in capillaries between the fibers of the nonwovens. With increasing fiber diameters due to swelling, capillarity of the nonwovens is reduced. According to the Washburn theory the sorption rate is inversely proportional to the capillarity explaining the decrease of water sorption while wettability increases.

PD release from nonwovens occurred within the first hour of incubation in all cases (Fig. 5). Furthermore, relative PD release increased with increasing PD content up to PCL/PD20. The low molecular weight and hydrophilicity of PD leads to immediate dissolution of solvent-accessible PD. The fraction of solvent-accessible PD increases with increasing PD content because of (a) geometrical consideration similar to the release of lysozyme at increasing lysozyme loading (Puhl et al., 2014) and (b) increased swelling of the matrix (Fig. 4B), resulting in improved water penetration into the polymer matrix (Dordunoo et al., 1997 and Karami et al., 2013). However, at a higher PD content of 50% (PCL/PD50) relative release was reduced to $80.5 \pm 5.7\%$ compared to almost complete release observed with PCL/PD20. Considering the results of SEM and DSC analysis, where partial phase separation was identified above a PD content of 20% (Fig. 1A–D and Fig. 3), we conclude that with PCL/PD50 no

further increase of water penetration into the polymer matrix was achieved resulting in reduction of relative release of PD. Moreover, increased swelling may partly bind PD in a gel composed of PCL, PD and water.

Apart from its release from the nonwoven matrix, PD also adsorbs to the PCL surface, though a relatively low amount is required to saturate the latter. When incubating pure PCL nonwovens in release medium containing 0.112 mg/ml of free PD, the concentration of free PD decreased to about a tenth of initial concentrations. Incubating pure PCL nonwovens in release media with higher free PD concentrations did not lead to higher adsorption, or the adsorbed amount was not detectable in relation to the high concentration of free PD.

Lysozyme burst release from PCL/PD scaffolds increased with increasing PD content. In addition, close evaluation of the initial phase of lysozyme release revealed a gradual change of release profile with increasing PD content (Fig. 6A). To explain these observations a release model based on (a) PD-induced desorption of lysozyme from the polymer matrix and (b) increased matrix swelling with increasing PD content and thus a diffusion controlled mechanism is proposed (Karami et al., 2013 and Yang et al., 2001). Recently, Srikar et al. (2008) reported a model describing the release of hydrophilic drugs from electrospun, slowly degrading polymer matrices. Within this model it is assumed that drug release is primarily controlled by drug desorption from nanopores and from the polymer surface. Furthermore, the model assumes that only drug present at the surface can be released, whereas encapsulated drug is not or only very slowly released. Based on this model, both, increasing the solvent accessible fraction of lysozyme and improving desorption of lysozyme from the polymer surface would result in increased release (Crotts et al., 1997). The rapid release of PD from the nonwovens (Fig. 5) results in morphological changes of the fiber structure, signified by formation of wrinkles and indentations as observed by SEM (Fig. 2A–F). The observed structural changes are a consequence of swelling of the polymer matrix, as discussed above, resulting in an increased solvent accessible surface. Increasing the PD content therefore resulted in increased lysozyme burst release. Furthermore, PD efficiently adsorbs to the PCL surface (see above), displacing and releasing lysozyme from the scaffold. Addition of PD to the release medium during release of lysozyme from pure PCL nonwovens confirmed the assumed desorption-controlled release mechanism resulting in increased burst release while the subsequent release rate was unaffected (Fig. 6C).

On the other hand, swelling of the polymer matrix is assumed to increase diffusion distance and potentially tortuosity, resulting in slower lysozyme release (Bromberg and Ron, 1998). According to Higuchi's law, solubility within the polymer matrix is substantial for a diffusional release (Higuchi, 1963). In a study by Li et al. (2008), release of lysozyme from PCL nonwovens was successfully increased through formation of lysozyme–oleate complexes, improving the solubility of the drug in the polymer matrix, as well as blending with PEG to enhance the wettability of the polymer matrix (Li et al., 2008). Because of the poor solubility of lysozyme in the polymer matrix, pure PCL and PCL/PD blends with low PD content showed little diffusional release of the protein. With increasing PD ratios swelling and thus water uptake into the polymer matrix was increased, thus allowing diffusional release. Consequently, we observed increasing diffusional release characteristics with increasing PD content, most prominently in the case of PCL/PD50 nonwovens showing a release up to 7 days (Fig. 6A). When incubating the PCL/PD blend nonwovens in release medium supplemented with PD, burst release was increased significantly but release profile was almost unaffected (Fig. 6D). This observation is attributed to increased desorption of lysozyme prior to swelling of the matrix with PD present in the release medium.

Despite the achieved improvements of lysozyme desorption and solvent accessible surface through blending of PCL with PD, the low degradation rate of PCL limited drug release subsequent to the initial burst. Through generation of nonwovens consisting of PCL, PD and PLGA, degradability of the polymer matrix is significantly improved as shown before (Puhl et al., 2014). Matrix swelling and improved drug desorption induced by PD proved to be effective also with the ternary blend (Fig. 4B). Consequently, we identified three release mechanisms: desorption, diffusion and matrix degradation while the latter added a significant increase of overall protein release. Furthermore, sorption of release medium to nonwovens was improved compared to PCL/PD nonwovens, most likely because of increased capillarity of nonwovens resulting from broader fiber diameter distributions (Fig. 1E–G).

In summary, the rational combination of PCL, serving as slowly biodegradable, structurally stable component, PLGA, which improves polymer matrix degradability and PD inducing matrix swelling and drug desorption led to marked improvement of lysozyme release. The improved release of hydrophilic drugs from PCL or PCL/PLGA matrices achieved by using PD as matrix component and the identification of the re-

lease mechanism for such scaffolds may significantly improve the utilization of PCL nonwovens for topical drug delivery and tissue engineering. Furthermore, PD's ability to improve drug release from polymer matrices is according to our knowledge described for the first time herein.

Although the goal of incorporation of PD into fibers was to improve lysozyme release, pharmacological activity of PD is to be expected from all nonwoven preparations since minimum effective concentrations for topical application are reached. In the case of topical application of nonwoven scaffolds as wound dressings, pharmacologic activity of PD might be considered beneficial. However, potential side effects should be considered as well.

Future research might harness the concept of improved matrix swelling and improved desorption by addition of surfactants as a guiding principle for the design of polyester based drug delivery systems. PD proved to be an effective excipient with regards to this concept, however its pharmacological activity might limit its use. Therefore, future research might focus on finding alternative surfactants without pharmacologic activity that improve swelling and drug desorption from polyester matrices.

5. Conclusion

Novel PCL/PD and PCL/PD/PLGA blend nonwovens with encapsulated lysozyme crystals were characterized with regards to physical properties and lysozyme release. Blending of PCL and PD resulted in reduction of the contact angle and increased swelling depending on PD content. Ternary blends of PCL, PD and PLGA showed similar properties to PCL/PD nonwovens. The total fraction of lysozyme released from PCL/PD nonwovens increased with increasing PD content and addition of PLGA to PCL/PD blends resulted in controlled release over up to 13 weeks with cumulative release of up to approximately 50% of encapsulated lysozyme. Lysozyme release was shown to depend on both matrix swelling and desorption, which both is facilitated by PD. Addition of PLGA lead to a concentration dependent augmentation of matrix degradation resulting in controlled release of lysozyme.

References

Anderson, J.M., Shive, M.S., 1997. Biodegradation and biocompatibility of PLA and PLGA microspheres. Adv. Drug Deliv. Rev. 28, 5–24.

Bittiger , H., Marchess, R., Niegisch, W.D., 1970. Crystal structure of poly-eta-caprolact one. Acta Crystallogr. B 26, 1923.

Briggs, T., Arinzeh, T.L., 2014. Examining the formulation of emulsion electro-spinning for improving the release of bioactive proteins from electrospun fibers. J. Biomed. Mater. Res. A 102, 674–684.

Bromberg, L.E., Ron, E.S., 1998. Temperature-responsive gels and thermogelling polymer matrices for protein and peptide delivery. Adv. Drug Deliv. Rev. 31, 197–221.

Chen, D.R., Bei, J.Z., Wang, S.G., 2000. Polycaprolactone microparticles and their biodegradati on. Polym. Degrad. Stabil. 67, 455–459.

Cipitria, A., Skelton, A., Dargaville, T.R., Dalton, P.D., Hutmacher, D.W., 2011. Design, fabrication and characterization of PCL electrospun scaffolds–a review. J. Mater. Chem. 21, 9419–9453.

Crotts, G., Sah, H., Park, T.G., 1997. Adsorption determines in-vitro protein release 615 rat e from biodegradable microspheres: quantitative analysis of surface area during degradation. J. Control Release 47, 101–111.

Dash, T.K., Konkimalla, V.B., 2012. Poly-epsilon-caprolactone based formulations for drug delivery and tissue engineering: a review. J. Control Release 158, 15–33.

Dordunoo, S.K., Oktaba, A.M.C., Hunter, W., Min, W., Cruz, T., Burt, H.M.,1997. Release of taxol from poly(epsilon-caprolactone) pastes: effect of water-soluble additiv es. J. Control Release 44, 87–94.

Eckmann, D.M., 2009. Polidocanol for endovenous microfoam sclerosant therapy. Exp. Opin. Inv. Drug 18, 1919–1927.

Falkner, J.C., Al-Somali, A.M., Jamison, J.A., Zhang, J.Y., Adrianse, S.L., Simpson, R.L.,Calabretta, M.K., Radding, W., Phillips, G.N., Colvin, V.L., 2005. Generation of size-contr olled, submicrometer protein crystals. Chem. Mater. 17, 2679–2686.

Friess, W.F., Schlapp, M., 2002. Release mechanisms from gentamicin loaded poly(lactic-co-glycolic acid) (PLGA) microparticles. J. Pharm. Sci. 91, 845–855.

Gorin, G., Wang, S.F., Papapavl, L., 1971. Assay of lysozyme by its lytic action on *m*-lysodeikticus cells. Anal. Biochem. 39, 113.

Gunatillake, P.A., Adhikari, R., 2003. Biodegradable synthetic polymers for tissue engineering. Eur. Cells Mater. 5, 1–16 discussion 16.

Higuchi, T.,1963. Mechanism of sustained-action medication – theoretical analysis of 634 rate of release of solid drugs dispersed in solid matrices. J. Pharm. Sci. 52, 1145.

Ilko, D., Braun, A., Germershaus, O., Meinel, L., Holzgrabe, U., 2014. Fatty acid composition analysis in polysorbate 80 with high performance liquid chromatography coupled to charged aerosol detection. Eur. J. Pharm. Biopharm.

Jiang, H.L., Hu, Y.Q., Li, Y., Zhao, P.C., Zhu, K.J., Chen, W.L., 2005. A facile technique to prepare biodegradable coaxial electrospun nanofibers for controlled release of bioactive agents. J. Control Release 108, 237–243.

Karami, Z., Rezaeian, I., Zahedi, P., Abdollahi, M., 2013. Preparation and performance evaluations of electrospun poly(epsilon-caprolactone), poly(lactic acid), and their hybrid (50/50) nanofibrous mats containing thymol as an herbal drug for effective wound healing. J. Appl. Polym. Sci. 129, 756–766.

Li, Y., Jiang, H.L., Zhu, K.J., 2008. Encapsulation and controlled release of lysozyme from electrospun poly(epsilon-caprolactone)/poly(ethylene glycol) non-woven membranes by formation of lysozyme–oleate complexes. J. Mater. Sci. 19, 827–832.

Liao, Y.H., Brown, M.B., Martin, G.P., 2001. Turbidimetric and HPLC assays for the determination of formulated lysozyme activity. J. Pharm. Pharmacol. 53, 549–554.

Liu, Y.J., Jiang, H.L., Li, Y., Zhu, K.J., 2008. Control of dimensional stability and degradation rate in electrospun composite scaffolds composed of poly(D,L-lactide-*co*-glycolide) and poly(epsilon-caprolactone). Chin. J. Polym. Sci. 26, 63–71.

Lu, C.H., Lin, W.J., 2002. Permeation of protein from porous poly(epsilon-caprolactone) films. J. Biomed. Mater. Res. 63, 220–225.

Meinel, A.J., Germershaus, O., Luhmann, T., Merkle, H.P., Meinel, L., 2012. Electrospun matrices for localized drug delivery: current technologies and selected biomedical applications. Eur. J. Pharm. Biopharm. 81, 1–13.

Pham, Q.P., Sharma, U., Mikos, A.G., 2006. Electrospun poly(epsilon-caprolactone) microfiber and multilayer nanofiber/microfiber scaffolds: characterization of scaffolds and measurement of cellular infiltration. Biomacromolecules 7, 2796– 662 2805.

Puhl, S., Li, L., Meinel, L., Germershaus, O., 2014. Controlled protein delivery from electrospun non-wovens: novel combination of protein crystals and a biodegradable release matrix. Mol. Pharm. 11, 2372–2380.

Qin, X.H., Wu, D.Q., 2012. Effect of different solvents on poly(caprolactone) (PCL) electrospun nonwoven membranes. J. Therm. Anal. Calorim. 107, 1007–1013.

Sahoo, S., Sasmal, A., Nanda, R., Phani, A.R., Nayak, P.L., 2010. Synthesis of chitosan-polycaprolactone blend for control delivery of ofloxacin drug. Carbohydr. Polym. 670 79, 106–113.

Srikar , R., Yarin, A.L., Megaridis, C.M., Bazilevsky, A.V., Kelley, E., 2008. Desorption-limited mechanism of release from polymer nanofibers. Langmuir 24, 965–974.

Wang, X.D., Wang, Y.J., Wei, K., Zhao, N.R., Zhang, S.H., Chen, J.D., 2009. Drug distribution within poly(epsilon-caprolactone) microspheres and in vitro release. J. Mater. Process. Tech. 209, 348–354.

Washburn, E.W., 1921. The dynamics of capillary flow. Phys. Rev. 17, 273–283.

Wendorff, J.H., Agarwal, S., Greiner, A., 2012. Electrospinning: Materials, Processing, and Applications. Wiley-VCH, Weinheim, Germany.

Yang, Y.Y., Chung, T.S., Ng, N.P., 2001. Morphology, drug distribution, and in vitro release profiles of biodegradable polymeric microspheres containing protein fabricate d by double-emulsion solvent extraction/evaporation method. Biomaterials 22, 231–241.

4.5 Fatty acid composition analysis in polysorbate 80 with high performance liquid chromatography coupled to charged aerosol detection

David Ilko, Alexandra Braun, Oliver Germershaus, Lorenz Meinel, Ulrike Holzgrabe

Reprinted with permission from Eur J Pharm Biopharm **2014**.

Abstract

The fatty acid (FA) composition of polysorbate 80 (PS80), a sorbitan oleic acid ester copolymerized with about 20 mole of ethylene oxide, is typically characterized by gas chromatography. Here, an alternative method was developed. After saponification with potassium hydroxide the FA fraction was collected with liquid–liquid extraction using methyl-*tert.*-butyl ether. HPLC in combination with a Corona® charged aerosol detector (CAD) was applied for the separation and detection. The method was fully validated in terms of specificity, repeatability, limits of quantification, linearity, range, accuracy and robustness.

The characterization of 16 different PS80 batches demonstrated variability regarding their FA composition, with e.g. the amount of oleic acid ranging from 67.8 ± 0.7% to 96.6 ± 1.4%. Furthermore, we identified petroselinic acid, a double-bond positional isomer to oleic acid in all batches, an FA not known to pharmacopoeias at present. In addition, 11-hydroxy-9-octadecenoic acid, an oxidation product of oleic acid was identified. Structure elucidation was performed by means of HPLC-MS/MS. In addition, the method was expanded to the evaluation of the free FAs. Having determined the entire FA composition, the acid value according to EP and USP can be calculated.

1. Introduction

Polysorbate 80 (PS80) is a nonionic surfactant commonly used in pharmaceutical formulations as emulsifier and solubilizer for poorly soluble drug substances [1] or as stabilizing agent in protein formulations [2]. Moreover, it serves as coating material for drug delivering nanoparticles [3]. PS80 is an excipient frequently used in formulations of biologics, addressing aggregation challenges. This excipient and possible degradation products thereof warrant tight quality assurance and control. In spite of the fact that these are formulated at low concentrations, typically in a range of 0.01–0.1% (w/v), a possible impact of degradation products and impurities on protein stability has been reported [4,5].

Polysorbates are fatty acid esters of sorbitol anhydrides copolymerized with about 20 moles ethylene oxide for each mole sorbitol and sorbitol anhydrides. The number in PS80 indicates the type of fatty acid (FA) used in the manufacturing process. PS80 is esterified with oleic acid mainly, but may contain both saturated and unsaturated FAs with a chain length between 14 and 18 in considerable amounts with a minimum of 58% of oleic acid being required to meet the European Pharmacopoeia (EP) and United States Pharmacopoeia (USP) specifications, respectively [6,7].

Due to their complex and heterogeneous composition, a variety of analytical techniques are applied to characterize polysorbates. The distribution of polyoxyethylene chains [8] and the amount of non-esterified ethoxylates [9] are determined by means of nuclear magnetic resonance spectroscopy (NMR). The identification of the different polysorbate species was achieved with matrix-assisted laser desorption ionization time-of-flight mass spectrometry (MALDI-TOF-MS) [10,11] or with liquid chromatography and subsequent electrospray ionization-mass spectrometry (ESI-MS) [12–14]. To the best of our knowledge, no attempt was reported in the literature comparing different PS80 batches regarding their fatty acid composition.

The analysis of FAs is typically performed by gas chromatography (GC) following the transesterification to fatty acid methyl esters. However, thermally labile compounds such as hydroperoxylated or epoxylated FAs might not be detectable due to degradation [15]. Therefore, we decided to utilize liquid chromatography coupled with charged aerosol detection (CAD) for the identification and quantification of the FAs in PS80. CAD detects non-volatile and some semi-volatile compounds providing universal response regardless of their chemical structure without a need for pre-column

derivatization of the analyte [16]. The applicability of CAD to the analysis of polysorbates [17–20] as well as lipids [21–28] has previously been demonstrated, and here we report an extension of these studies for the analysis of other polysorbates, including PS40, 60, and 80 as well as limitations, as demonstrated for short fatty acids (PS20).

2. Experimental

2.1. Reagents and material

All chemicals were of analytical grade unless otherwise stated. Capric acid, caprylic acid, formic acid, lauric acid, linoleic acid, α-linolenic acid, myristic acid, palmitic acid, palmitoleic acid, petroselinic acid, potassium hydroxide, methyl-*tert.*-butyl ether (MTBE), oleic acid (>99%), oleic acid (meets Ph. Eur. specifications) and stearic acid were purchased from Sigma–Aldrich (Taufkirchen, Germany). Margaric acid, gradient grade acetonitrile and methanol (HiPerSolv Chromanorm_) were purchased from VWR International (Darmstadt, Germany). Ultra-pure water (>18.2 MΩ) was delivered by a Milli-Q Synthesis system (Merck Millipore, Schwalbach, Germany). The polysorbate samples were from Croda (East Yorkshire, UK), Kolb (Hedingen, Switzerland), Merck (Darmstadt, Germany) and NOF (Tokyo, Japan). The order of the supplier names does not necessarily coincide with the order of the codes used within the manuscript.

2.2. Preparation of sample and reference solutions for thedetermination of the fatty acid composition

The saponification process was modified from [29]. About 15 mg of the analyte was dissolved in 1 M potassium hydroxide solution containing 10% methanol and the volume was made up to 10.0 mL with the same solvent. The sample was then incubated at 40 °C for 6 h.

The protocol for the extraction of the fatty acids with MTBE was modified from [30]. 250 µL of this solution was acidified with 50 µL formic acid in a centrifuge tube (VWR International, Darmstadt, Germany) to a resulting pH value of about 3.2. Then, 500 µL MTBE was added and the tube was vortexed. After 5 min of incubation, the tube was centrifuged for 5 min at 2700g using a Centrifuge 5702 (Eppendorf, Hamburg, Germany). The organic phase was collected and dried under a gentle stream of

nitrogen. The residue was reconstituted in 1000 µL of a mixture of water/acetonitrile (25:75, v/v).

Stock solutions of fatty acids were prepared in methanol at a concentration of 1 mg/mL and stored at -20 °C. Reference solutions were prepared by diluting the stock solutions to the desired concentration with a mixture of water/acetonitrile (25:75, v/v).

2.3. Preparation of sample and reference solutions for the determination of the free fatty acids

An internal standard (IS) solution was prepared by dissolving margaric acid in methanol at a concentration of 0.5 mg/mL. About 100.0 mg of the analyte was dissolved in 1.0 mL of the IS solution. The volume was then made up to 10.0 mL with water. 1000 µL of this solution, 100 µL formic acid and 1000 µL MTBE were added to a glass centrifuge tube and vortexed. After 5 min of incubation, the tube was centrifuged for 45 min at 2700g using an EBA 20 centrifuge (Hettich, Tuttlingen, Germany). 500 µL of the organic phase was collected and dried under a gentle stream of nitrogen. The residue was reconstituted in 500 µL of a mixture of water/acetonitrile (25:75, v/v).

The reference solution contained oleic acid and margaric acid at concentrations of 50 µg/mL prepared by diluting the respective stock solutions with a mixture of water/acetonitrile (25:75, v/v).

2.4. HPLC-CAD

Measurements were carried out using an Agilent 1100 HPLC system (Waldbronn, Germany) equipped with a binary pump, an online degasser and a thermostated column compartment. The Kinetex C_{18} (100 x 3.0 mm, 2.6 µm particle size) analytical column (Phenomenex, Aschaffenburg, Germany) was used for the separation of the fatty acids at 25 °C. The injection volume was 10 µL. A gradient was applied using 0.05% (v/v) formic acid in water as mobile phase A and 0.05% (v/v) formic acid in acetonitrile as mobile phase B and starting with 75% mobile phase B for the initial 5 min followed by a linear increase to 85% mobile phase B within 10 min. Subsequently, the column was re-equilibrated for 3 min. The mobile phase flow rate was set to 0.6 mL/min. Detection was performed using a Corona® charged aerosol detector

(Thermo Scientific, Idstein, Germany). The settings for the CAD were as follows: gas inlet pressure (nitrogen) 35 psi; filter ‘‘none’’; and an electric current range of 100 pA.

2.5. HPLC-MS/MS

For the identification of unknown peaks, a 6300 Series Ion Trap from Agilent connected to an Agilent 1100 HPLC system (Waldbronn, Germany) was used. The chromatographic conditions were the same as described in Section 2.4. The ion trap was operated in both ESI-positive and negative modes. Nebulizer pressure was set to 50 psi; dry gas (nitrogen) flow and temperature were 10 L/min and 350 °C, respectively.

3. Results and discussion

3.1. Method development

The method included the release of the FAs from PS80 through basic hydrolysis, extraction and subsequent analysis via HPLC-CAD. The saponification of PS80 was carried out with 1 M KOH at 40 °C for 6 h as described before [29]. We studied the stability of some FAs (oleic, linoleic and α-linolenic acids) at these conditions by HPLC-CAD, monitoring the peak areas for 6 h. These FAs were selected based on their susceptibility to degradation as a result of their unsaturated character. Additionally, stability was investigated at 60 °C, in order to evaluate whether a higher temperature can be applied for a shorter reaction time. FAs turned out to be stable at a temperature of 40 °C for 6 h (98.1%, 102.3% and 99.3% of the initial peak area after incubation for linolenic, linoleic and oleic acids, respectively). However, substantial degradation occurred at 60 °C, indicated by the decreasing peak area over time (79.6%, 91.5% and 87.2% of the initial peak area after incubation for linolenic, linoleic and oleic acids, respectively).

The FAs were then extracted from the reaction medium in order to avoid the injection of the concentrated solution of potassium hydroxide and residues from the hydrolyzation of PS80 into the detector. First, we evaluated the use of solid phase extraction (SPE) [31]. After neutralization of the reaction medium with formic acid, the FAs were protonated and could thus be retained on a C_{18} cartridge and eluted with chloroform/methanol (50:50, v/v). The eluate was then evaporated under a stream of nitrogen; the residue was dissolved in water/acetonitrile (25:75, v/v) and injected into the

HPLC. However, the removal of residues from the solution, indicated by a large injection peak, was found to exceed the detector's range and thus, the application of SPE was not satisfactory.

Therefore, liquid–liquid extraction with methyl-*tert.*-butyl ether (MTBE) according to previous reports was applied [30]. For that, the reaction medium was acidified with a calculated amount of formic acid in a centrifuge tube to a resulting pH value of about 3.2 and MTBE was added. It was necessary to use glass centrifuge tubes instead of polypropylene tubes, because the organic solvent is capable of extracting substances from the plastic material, which can be detected by the CAD and may interfere with the analysis. For the complete separation of the two phases, the solution was centrifuged for 5 min. The organic phase was collected and dried under a stream of nitrogen. The residue was dissolved in water/acetonitrile (25:75, v/v). The liquid–liquid extraction was found to be superior to SPE in terms of the removal of residues from the solution. Additionally, it required less time as the evaporation of MTBE was much faster than that of chloroform/methanol.

As a first approach, we selected compendial fatty acids for our method complying with the monographs for polysorbate 80 in the European (EP, 8th edition) and the U.S. pharmacopoeias (USP 37 NF 32). In particular, specifications in both monographs are as follows: myristic acid (≤5.0%), palmitic acid (≤16.0%), palmitoleic acid (≤8.0%), stearic acid (≤6.0%), oleic acid (≥58%), linoleic acid (≤18.0%) and α-linolenic acid (≤4.0%). An artificial mixture of these fatty acids, mirroring the aforementioned FA composition could readily be separated by HPLC under isocratic conditions using water/acetonitrile/formic acid (20:80:0.05, v/v/v) as a mobile phase within about 10 min (data not shown). However, when it came to the analysis of the PS80 batches, the occurrence of additional peaks required a slight adaptation of the chromatographic conditions. In order to increase the retention of an early eluting but unknown peak, we decreased the amount of acetonitrile in the mobile phase to 75%. Additionally, a gradient starting at 5 min increasing the proportion of acetonitrile to 85% had to be applied to shorten the analysis time and provide narrow peaks for late eluting FAs, i.e. stearic acid.

Unknown peaks were detected at about 2 and 9 min and characterized by HPLC-MS/MS, accordingly. Since only volatile mobile phases can be used with the CAD, the method is mass-compatible without any modification. The early eluting peak at a

retention time of about 2 min (Fig. 1d and e) gave an m/z of 297 in ESI-negative mode. The facile in-source loss of 18 u giving an m/z of 279 pointed to a monounsaturated FA with chain length of 18 containing a hydroxyl group. Applying MS/MS, an ion at m/z of 169 was observed. Taking into account that α-cleavage is a common fragmentation for aliphatic alcohols, we concluded that the hydroxyl group is positioned at C11 (see Fig. 3). The peak was, therefore, assigned to 11-hydroxy-9-octadecenoic acid. The presence of this hydroxy-FA in thermally stressed PS80 has previously been reported by Hvattum et al. [13]. The primary oxidation products of unsaturated FAs are hydroperoxides formed after abstraction of one of the allylic hydrogens via a radical mechanism [32]. For oleic acid, the hydroperoxide group is introduced at C8 or C11. These primary oxidation products decompose to a variety of compounds, such as short chain FAs, aldehydes, epoxy-, keto- and hydroxy-FAs [33]. Even though we did not find any oxidation products different from 11-hydroxy-9-octadecenoic acid, the formation of the hydroxylated FA is likely to be reasoned by the autoxidation.

The peak eluting after oleic acid at about 9 min was found in every batch studied, showing an m/z of 283 in ESI-positive mode and thus indicating the presence of an additional monounsaturated FA with a chain length of 18. The substance was identified as petroselinic acid, a double bond positional isomer to oleic acid, via retention time and HPLC-MS analysis of an authentic standard.

For the quantification of the free FAs, we intended to extract them from a PS80 solution using the same extraction procedure analysis (*vide supra*). As the aqueous sample solution was vortexed with MTBE and intact surfactant was present, an emulsion was formed during the extraction. This required considerably higher centrifugation time with 45 min to achieve complete phase separation compared to 5 min as required for the compositional analysis.

Due to the amphiphilic character of PS80 it was impossible to extract the free FAs without carrying over surfactant into the organic phase. Having an HLB value of 14.4–15.6 [34], PS80 is a hydrophilic surfactant, hence most of PS80 remained in the aqueous phase. This residual PS80 species in the organic phase eluted as several peaks between about 2 and 8 min, rendering the detection of most of the FAs impossible due to peak overlap. However, the oleic acid peak eluted after these PS80 peaks (Fig. 2). Therefore, we decided to quantify the oleic acid peak via an internal

standard (IS). The total amount of the free FAs was calculated taking into account the FA composition determined as described above. Margaric acid, a saturated FA with a chain length of 17, was chosen as IS as it was not present in any of the batches, did not co-elute with any other peak (retention time of about 10 min) and provided comparable physico-chemical properties as our analyte. The IS was added to the sample solution before the extraction step at a concentration of 0.5% referred to the sample weight of PS80.

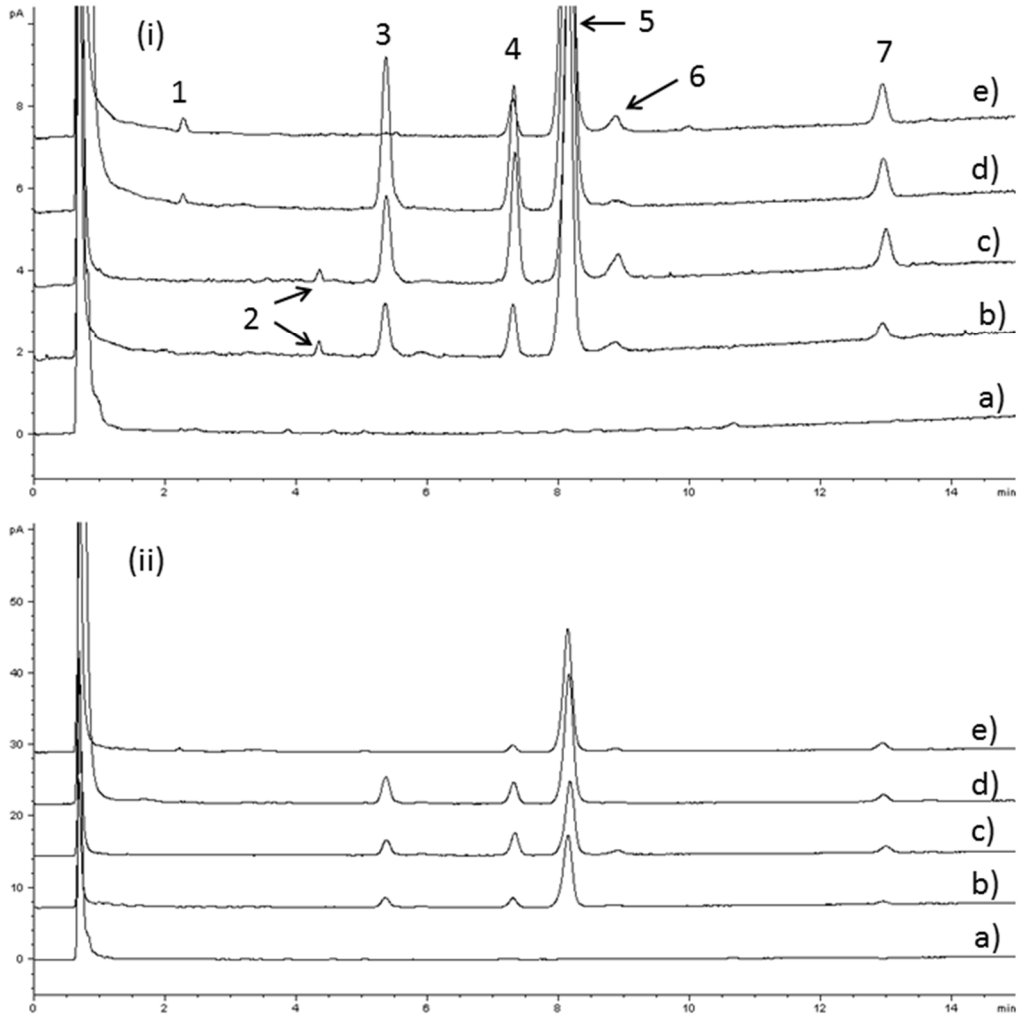

Fig. 1. Chromatograms of the studied batches are shown with a focus on the baseline (i) and in total (ii): a) blank extraction showing no interfering peaks from the sample preparation step; b) manufacturer A; c) manufacturer C; d) manufacturer D; e) manufacturer E (extra pure PS80). Elution order: 1-11-Hydroxy-9-decenoic acid; 2-palmitoleic acid; 3-linoleic acid; 4-palmitic acid; 5-oleic acid; 6-petroselinic acid; 7-stearic acid.

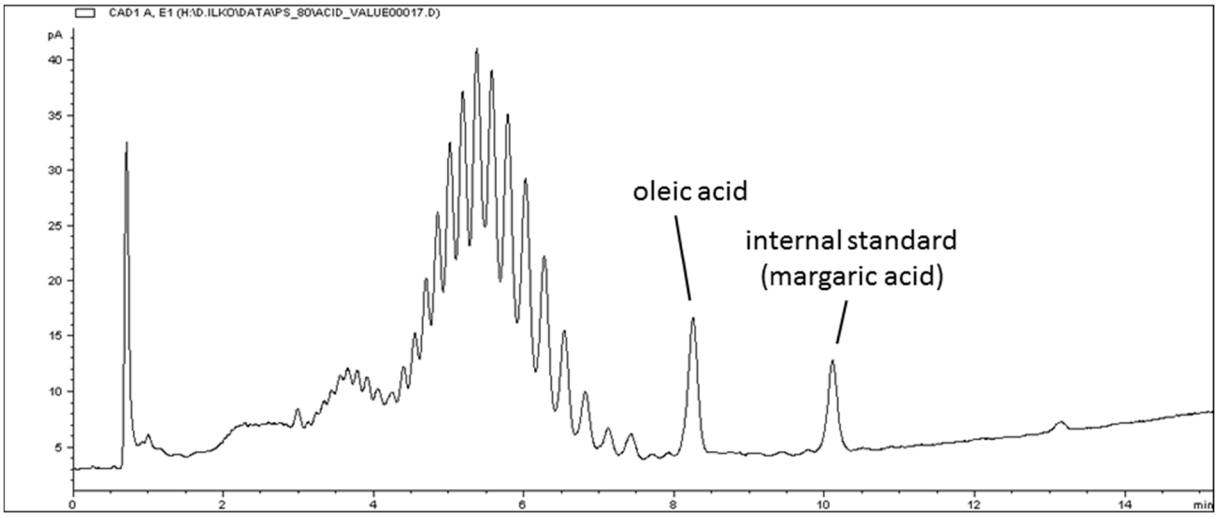

Fig. 2. Chromatogram of a solution of PS80 spiked with 0.5% of each oleic acid and the internal standard after extraction with MTBE. Chromatographic conditions and sample preparation are described in chapters 2.3 and 2.4.

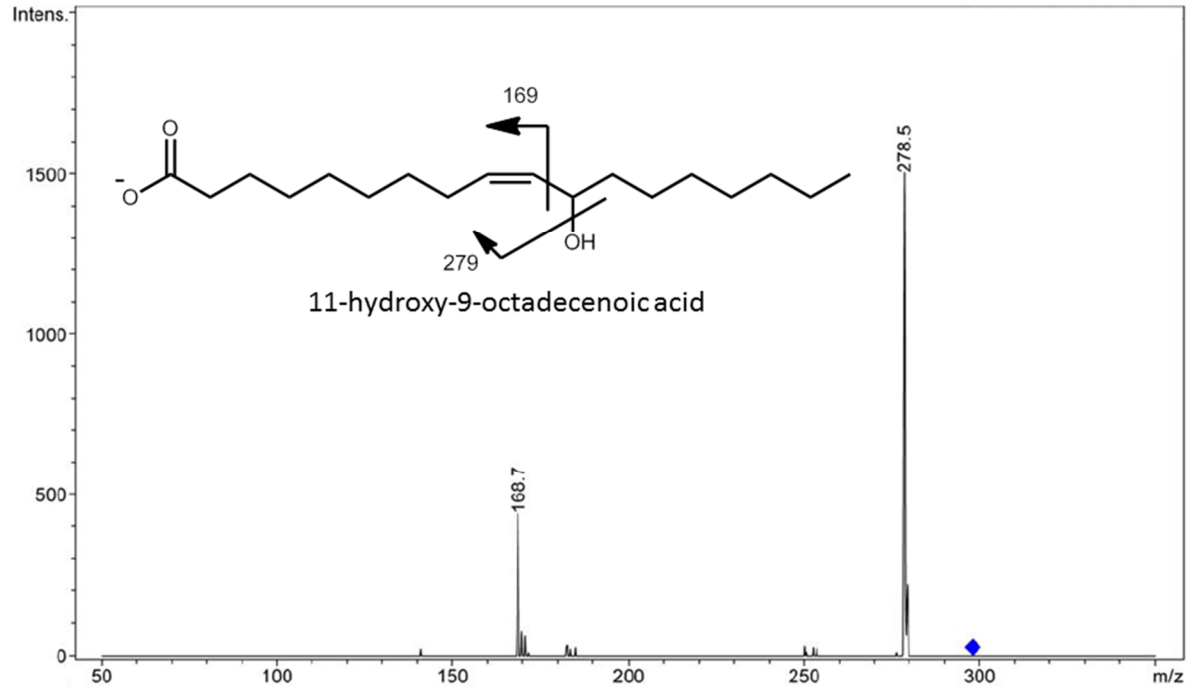

Fig. 3. Product ion spectrum (ESI-negative) of the peak at about 2 minutes with *m/z* 297 in batch 2 from manufacturer E and proposed fragmentation pattern. Chromatographic conditions and MS settings are described in chapters 2.4 and 2.5. The CID voltage was set to 2.50 V.

According to EP and USP, the amount of free FAs is determined by means of titration with potassium hydroxide and is expressed as the acid value, i.e. the quantity of potassium hydroxide in milligrams required to neutralize the free acids present in 1 g of the substance [35]. By converting the % (m/m) FA composition into mol-% and considering the amount of free FAs, the acid value can be calculated using our method.

3.2. Validation

The method was validated with regard to ICH guideline Q2(R1) [36]. Specificity, repeatability, limit of quantification (LOQ), linearity, range, accuracy and robustness were investigated.

Specificity was assessed by analyzing a solution containing all possible fatty acids. All substances were separated from each other. Furthermore, a blank extraction was performed in order to evaluate probable extraction from materials or residues from any solvents used. No interfering peaks were found. For the determination of the free FAs, it was demonstrated that oleic and margaric acids were separated from each other and from the residues of PS80 in the sample (Fig. 2).

For each fatty acid, *repeatability* was determined at three different concentration levels (1, 25 and 50 µg/mL) in triplicate. All values found for the relative standard deviation (% RSD) were in the range from 0.01% to 1.69% indicating a precise method.

The *limits of quantification* were determined with the signal-to-noise (S/N) approach and corresponded to the concentration introduced into the analysis and giving an S/N of 10. For fatty acids with a chain length of 14 or greater, we achieved satisfactory sensitivity with LOQs between 2.1 and 6.1 ng on column. With shorter chain length and thus higher volatility, the LOQs increased considerably. The quantification of lauric acid (C12) required an amount of at least 46 ng on column, and of capric (C10) and caprylic acids (C8) required 0.47 and 2.4 µg, respectively. This considerable decrease in sensitivity impeded the application of this method to surfactants containing FAs with a chain length of 12 or less, such as polysorbate 20. However, the shorter chain lengths are not present in PS80.

Linearity and range. A calibration curve including at least five concentration levels was established for each analyte, equally covering a range from 1 to 100 µg/mL. Analogous to other evaporation-based detectors, the CAD does not show a linear response curve over the whole dynamic range [16]. Therefore, the logarithm of the peak area was plotted against the logarithm of the concentration to obtain a linear calibration curve (Table 1). We found a satisfactory linearity for all investigated fatty acids. The correlation coefficients (R^2) were between 0.9933 and 0.9998.

For the determination of the free FAs, we investigated the linearity of oleic acid in the range of 0.1–1.5% referred to a 10 mg/mL solution of PS80 in the presence of the IS

at a concentration of 0.5%. Five solutions were prepared equally distributed among this concentration range. R^2 was 0.9963 without log–log transformation which allowed the quantification with one single reference solution.

Table 1. Correlation coefficient of the calibration curve (after log-log transformation), LOQ, correction factor and relative retention of investigated FAs.

	R^2	LOQ (ng on column)	correction factor	relative retention time to oleic acid
α-linolenic	0.9998	2.1	1.10	0.43
myristic	0.9933	6.1	1.15	0.48
palmitoleic	0.9985	5.4	0.89	0.53
linoleic	0.9993	3.0	0.98	0.66
palmitic	0.9974	4.0	1.00	0.90
oleic	0.9986	3.9	1.00	1.00
petroselinic	0.9995	3.2	0.88	1.09
stearic	0.9992	3.4	0.86	1.59

Accuracy. Quantification was performed by establishing a calibration curve with oleic acid as external standard. A stock solution of oleic acid was diluted with a mixture of water/acetonitrile to give the desired concentrations (1, 25, 50, 75 and 100 µg/mL). Linear regression was done after log–log-transformation of concentration and peak area. In order to take possible differences in response into account, correction factors (CFs) were determined for all analytes (see Table 1). Accuracy was determined at three different levels (1, 25 and 50 µg/mL) with mean recoveries ranging from 100.0% to 101.8% (n = 3, %RSD 1.94–5.30%).

For robustness testing, the HPLC parameters were varied as follows: column temperature (±2.5 °C), mobile phase flow rate (±0.06 mL/min), % mobile phase B at the begin of the gradient (±1%), % mobile phase B at the end of the gradient (±1%) and amount of formic acid in the mobile phase (±0.005%). No considerable changes in resolution of the critical peak pair (oleic acid–petroselinic acid) and recoveries were observed (see Table 2).

3.3. Batch investigation

16 PS80 samples of five qualities (A–E, qualities being different manufacturers or different grades provided by one manufacturer) were investigated (Table 3). Several of the batches were advertised by the supplier as being refined and manufactured with a higher purity of the oleic acid.

From these experiments, we observed considerable differences among batches. The amount of oleic acid varied from 67.8% to 96.6%, with the linoleic and palmitic acid contents showing the largest fluctuation (0.0–11.8% for linoleic and 0.8–14.6% for

palmitic acid). Lauric acid or a-linolenic was not found in any sample. Free FAs were not present in any of the batches from B and E, but could be detected in all other batches in concentrations between 0.2% and 1.2% (m/m). Despite these differences, all batches were found to be within specification limits for the parameters reported here given in EP and USP. For further information on statistical analysis of the data and correlations of the chemical composition to functionality related characteristics, e.g. critical micelle concentration, hydrophilic–lipophilic-balance, cloud point or micelle molecular weight see [34].

As described in Section 3.1 we found and identified two FAs which are not mentioned in the EP or USP. The monographs do not limit any compounds different from the specified FAs. Petroselinic acid, a double-bond positional isomer to oleic acid was found in every batch in contents of up to 2.6%. The stability investigation of oleic acid proved that petroselinic acid was not formed during sample preparation.

11-Hydroxy-9-octadecenoic acid was found in all batches from manufacturer B, D and E except from E1. This indicated oxidative degradation during storage, which has been shown to impact the stability of active pharmaceutical ingredient which is prone to oxidation [5].

In order to evaluate the applicability to other polysorbates, one batch each of PS20, 40 and 60 was investigated. The results are shown in Table 3. Both PS40 and 60 complied with the Ph.Eur specifications. The FA fraction of these polysorbates consists of palmitic and stearic acids in different amounts (PS40: ≥92.0% palmitic acid, PS60: 40.0–60.0% stearic acid, sum of palmitic and stearic acid ≥90.0%).

In PS20, the content of palmitic acid was found to be out of specification (16.41%, specification: 7.0–15.0%). This was likely to be caused by the lacking sensitivity for short chain FAs of our analytical method. The sum of the contents of caproic, caprylic and capric acids can make up a content of up to 21.0% of the total FAs in PS20 regarding the Ph. Eur. specifications. By disregarding the short chain FAs in the calculation of the overall composition, the contents of all other detectable FAs can be overestimated. Thus, this method was shown to be applicable to PS40, 60 and 80, but not PS20.

Table 2. Robustness of the HPLC method. The influence of major HPLC parameters on recovery and resolution of the critical peak pair (oleic and petroselinic acid) is shown.

		no variation	temperature (°C)		flow rate (mL/min)		% mobile phase B at start		% mobile phase B at end		% formic acid	
			22.5	27.5	0.54	0.66	74	76	84	86	0.045	0.055
% recovery	**α-linolenic**	100	100	100	103	99	96	107	100	98	107	103
	myristic	100	104	104	101	97	100	108	106	103	93	100
	palmitoleic	100	101	98	100	97	97	103	100	101	100	102
	linoleic	100	99	100	101	99	94	101	97	96	105	100
	palmitic	100	100	100	100	98	93	100	96	96	101	99
	oleic	100	100	100	102	100	97	99	97	97	103	100
	petroselinic	100	104	103	107	99	96	101	98	99	103	103
	stearic	100	102	100	104	99	98	98	97	98	106	105
resolution (oleic – petroselinic)		2.41	2.44	2.31	2.41	2.44	2.50	2.34	2.37	2.39	2.44	2.40

Table 3. FA composition of the investigated polysorbate batches. n = 2. [1]n.s. = not specified. [2]additional specification for PS60: sum of the contents of palmitic and stearic acid: minimum 90.0%.

		hydroxy-oleic [%]	α-linolenic [%]	myristic [%]	palmitoleic [%]	linoleic [%]	palmitic [%]	oleic [%]	petroselinic [%]	stearic [%]	% (m/m) free fatty acids	acid value
PS40	**Specifications Ph. Eur. (8th edition)**	n.s.[1]	n.s.	n.s.	n.s.	n.s.	≥92.0	n.s.	n.s.	n.s.	n.s.	≤ 2.0
		-	-	-	-	-	93.0	-	-	7.0	0.5	1.1
PS60	**Specifications Ph. Eur. (8th edition)[2]**	n.s.	n.s.	n.s.	n.s.	n.s.	n.s.	n.s.	n.s.	40.0-60.0	n.s.	≤ 2.0
		-	-	-	-	-	41.1	-	-	58.9	0.5	1.0
PS80	**Specifications Ph. Eur. (8th edition)**	n.s.	≤ 4.0	≤ 5.0	≤ 8.0	≤ 18.0	≤ 16.0	≥ 58.0	n.s.	≤ 6.0	n.s.	≤ 2.0
	A1	-	-	-	0.8	6.6	5.4	85.2	0.8	1.2	0.6	1.1
	A2	-	-	-	0.5	9.6	5.4	81.9	1.2	1.4	0.6	1.1
	A3	-	-	-	0.8	10.1	5.8	80.6	1.0	1.7	1.2	2.3
	A4	-	-	-	0.6	6.8	5.7	84.1	1.2	1.6	0.6	1.2
	B1	2.2	-	-	-	-	0.8	96.6	-	0.4	0.0	0.0
	B2	2.1	-	-	-	-	1.0	96.4	-	0.5	0.0	0.0
	B3	3.7	-	-	-	-	0.7	95.3	-	0.4	0.0	0.0
	C1	-	-	-	0.6	9.4	12.2	74.0	1.0	2.7	0.7	1.3
	C2	-	-	-	0.5	7.1	10.6	78.0	0.9	2.9	0.2	0.3
	C3	-	-	-	0.7	10.7	14.6	67.8	2.6	3.6	0.3	0.5
	D1	0.5	-	-	-	11.3	8.3	77.7	0.3	2.0	0.4	0.8
	D2	0.5	-	0.2	-	11.6	7.5	78.2	0.3	1.9	0.2	0.4
	D3	0.5	-	0.1	-	11.8	7.4	78.1	0.3	2.0	0.3	0.6
	E1	-	-	-	-	1.1	2.5	92.6	1.2	2.7	0.0	0.0
	E2	0.7	-	-	-	-	3.0	92.2	1.0	3.1	0.0	0.0
	E3	1.6	-	-	-	-	2.4	92.3	1.0	2.8	0.0	0.0

Table 3. *(Continued)*.

	batch	caproic [%]	caprylic [%]	capric [%]	lauric [%]	myristic [%]	palmitic [%]	stearic [%]	oleic [%]	linoleic [%]	% (m/m) free fatty acids	acid value
PS20	**Specifications Ph. Eur. (8th edition)**	-	-	-	46.1	14.9	16.4	6.2	13.9	2.5	n.s.	≤ 2.0
		≤ 1.0	≤ 10.0	≤ 10.0	40.0-60.0	14.0-25.0	7.0-15.0	≤ 7.0	≤ 11.0	≤ 3.0	not determined	

4. Conclusions

We developed and validated an alternative method for the determination of the FA composition in PS80 using HPLC-CAD after saponification and liquid–liquid extraction. Two FAs not known by current pharmacopoeias in the context of PS80 were identified as petroselinic acid, a double-bond positional isomer of oleic acid and 11-hydroxy-9-octadecenoic acid, an oxidation product of oleic acid. Although all studied batches fulfilled the specifications in the pharmacopoeias with respect to the analyses reported here within, their FA composition was quite heterogeneous. The content of oleic acid ranged from 67.8 ± 0.7% to 96.6 ± 1.4%. The method was successfully applied to other polysorbates (PS40 and 60). However, due to the lacking sensitivity for short chain FAs, PS20 was not reliably analyzed. Therefore, we report an alternative approach to GC method of the current pharmacopeias, with comparable effort in terms of sample pretreatment that can detect degradation products.

References

[1] A.H. Kibbe, Handbook of Pharmaceutical Excipients, third ed., American Pharmaceutical Association, Washington, DC, 2000.

[2] W. Wang, Y.J. Wang, D.Q. Wang, Dual effects of Tween 80 on protein stability, Int. J. Pharm. 347 (2008) 31–38.

[3] K. Gao, X. Jiang, Influence of particle size on transport of methotrexate across blood brain barrier by polysorbate 80-coated polybutylcyanoacrylate nanoparticles, Int. J. Pharm. 310 (2006) 213–219.

[4] R.S. Kishore, S. Kiese, S. Fischer, A. Pappenberger, U. Grauschopf, H.-C. Mahler, The degradation of polysorbates 20 and 80 and its potential impact on the stability of biotherapeutics, Pharm. Res. 28 (2011) 1194–1210.

[5] E. Ha, W. Wang, Y.J. Wang, Peroxide formation in polysorbate 80 and protein stability, J. Pharm. Sci. 91 (2002) 2252–2264.

[6] Polysorbate 80 Monograph 01/2011:0428, in: European Pharmacopoeia, eighth ed., European Directorate for the Quality of Medicines & HealthCare (EDQM), Strasbourg, France, 2014.

[7] Polysorbate 80 Monograph, in: United States Pharmacopoeia, USP 37 NF 32, The United States Pharmacopeial Convention, Rockville, MD, USA, 2014.

[8] H. Vu Dang, A.I. Gray, D. Watson, C.D. Bates, P. Scholes, G.M. Eccleston, Composition analysis of two batches of polysorbate 60 using MS and NMR techniques, J. Pharm. Biomed. Anal. 40 (2006) 1155–1165.

[9] M. Verbrugghe, E. Cocquyt, P. Saveyn, P. Sabatino, D. Sinnaeve, J.C. Martins, P. Van der Meeren, Quantification of hydrophilic ethoxylates in polysorbate surfactants using diffusion ^{1}H NMR spectroscopy, J. Pharm. Biomed. Anal. 51 (2010) 583–589.

[10] F.O. Ayorinde, S.V. Gelain, J.H. Johnson Jr., L.W. Wan, Analysis of some commercial polysorbate formulations using matrix-assisted laser desorption/ ionization time-of-flight mass spectrometry, Rapid Commun. Mass Spectrom. 14 (2000) 2116–2124.

[11] S. Abrar, B. Trathnigg, Separation of polysorbates by liquid chromatography on a HILIC column and identification of peaks by MALDI-TOF MS, Anal. Bioanal. Chem. 400 (2011) 2119–2130.

[12] R. Zhang, Y. Wang, L. Tan, H.Y. Zhang, M. Yang, Analysis of polysorbate 80 and its related compounds by RP-HPLC with ELSD and MS detection, J. Chromatogr. Sci. 50 (2012) 598–607.

[13] E. Hvattum, W.L. Yip, D. Grace, K. Dyrstad, Characterization of polysorbate 80 with liquid chromatography mass spectrometry and nuclear magnetic resonance spectroscopy: specific determination of oxidation products of thermally oxidized polysorbate 80, J. Pharm. Biomed. Anal. 62 (2012) 7–16.

[14] D. Hewitt, M. Alvarez, K. Robinson, J. Ji, Y.J. Wang, Y.H. Kao, T. Zhang, Mixedmode and reversed-phase liquid chromatography-tandem mass spectrometry methodologies to study composition and base hydrolysis of polysorbate 20 and 80, J. Chromatogr. A 1218 (2011) 2138–2145.

[15] A.N. Grechkin, L.S. Mukhtarova, M. Hamberg, Thermal conversions of trimethylsilyl peroxides of linoleic and linolenic acids, Chem. Phys. Lipids 138 (2005) 93–101.

[16] R.W. Dixon, D.S. Peterson, Development and testing of a detection method for liquid chromatography based on aerosol charging, Anal. Chem. 74 (2002) 2930–2937.

[17] A. Christiansen, T. Backensfeld, S. Kuhn, W. Weitschies, Stability of the nonionic surfactant polysorbate 80 investigated by HPLC-MS and charged aerosol detector, Pharmazie 66 (2011) 666–671.

[18] S. Almeling, D. Ilko, U. Holzgrabe, Charged aerosol detection in pharmaceutical analysis, J. Pharm. Biomed. Anal. 69 (2012) 50–63.

[19] Y. Li, D. Hewitt, Y.K. Lentz, J.A. Ji, T.Y. Zhang, K. Zhang, Characterization and stability study of polysorbate 20 in therapeutic monoclonal antibody formulation by multidimensional UHPLC-CAD-MS, Anal. Chem. (2014).

[20] S. Fekete, K. Ganzler, J. Fekete, Simultaneous determination of polysorbate 20 and unbound polyethylene-glycol in protein solutions using new core-shell reversed phase column and condensation nucleation light scattering detection, J. Chromatogr. A 1217 (2010) 6258–6266.

[21] S. Khoomrung, P. Chumnanpuen, S. Jansa-Ard, M. Stahlman, I. Nookaew, J. Boren, J. Nielsen, Rapid quantification of yeast lipid using microwave-assisted total lipid extraction and HPLC-CAD, Anal. Chem. 85 (2013) 4912–4919.

[22] I. Acworth, M. Plante, B. Bailey, C. Crafts, Quantitation of Underivatized Omega-3 and Omega-6 Fatty Acids in Foods by HPLC and Charged Aerosol Detection, Thermo Fisher Scientific, Inc. Publication Number LPN, 2931, 2011, pp. 01–12.

[23] M. Plante, B. Bailey, I. Acworth, The use of charged aerosol detection with HPLC for the measurement of lipids, in: Lipidomics, Humana Press, 2009, pp. 469–482.

[24] R.A. Moreau, Lipid analysis via HPLC with a charged aerosol detector, Lipid Technol. 21 (2009) 191–194.

[25] R.A. Moreau, The analysis of lipids via HPLC with a charged aerosol detector, Lipids 41 (2006) 727–734.

[26] M. Plante, B. Bailey, I. Acworth, An Improved Global Method for the Quantitation and Characterization of Lipids by High Performance Liquid Chromatography and Corona Charged Aerosol Detection. <http://www.dionex.com/en-us/webdocs/87439-PO-HPLC-Global-Lipids-PN70533_E.pdf> (accessed 29.10.14).

[27] Lipid Analysis by Reversed Phase HPLC and Corona CAD: Free Fatty Acids. <http://www.coronaultra.com/Applications/Notes/70-8332-Lipid-Analysisby-Reverse-Phase-HPLC-and-CoronaCAD-Free-Fatty-Acids.pdf> (accessed 29.10.14).

[28] Unsaturated Fatty Acids: Arachidonic, Linoleic, Linolenic and Oleic Acid. <http://www.coronaultra.com/Applications/Notes/70-6808-Unsaturated-Fatty-Acids-Arachidonic-Linoleic-Linolenic-and-Oleic-Acids.pdf,> (accessed 29.10.14).

[29] M. Hu, M. Niculescu, X.M. Zhang, A. Hui, High-performance liquid chromatographic determination of polysorbate 80 in pharmaceutical suspensions, J. Chromatogr. A 984 (2003) 233–236.

[30] V. Matyash, G. Liebisch, T.V. Kurzchalia, A. Shevchenko, D. Schwudke, Lipid extraction by methyl-tert-butyl ether for high-throughput lipidomics, J. Lipid Res. 49 (2008) 1137–1146.

[31] <http://www.mn-net.com/DesktopModules/TabID/8854/defauld.aspx> (accessed 28.10.13).

[32] M.K. Logani, R.E. Davies, Lipid oxidation: biologic effects and antioxidants—a review, Lipids 15 (1980) 485–495.

[33] J. Velasco, S. Marmesat, G. Márquez-Ruiz, M.C. Dobarganes, Formation of short-chain glycerol-bound oxidation products and oxidised monomeric triacylglycerols during deep-frying and occurrence in used frying fats, Eur. J. Lipid Sci. Technol. 106 (2004) 728–735.

[34] A. Braun, D. Ilko, B. Merget, H. Gieseler, O. Germershaus, U. Holzgrabe, L. Meinel, Predicting critical micelle concentration and micelle molecular weight of polysorbate 80 using compendial methods, Eur. J. Pharm. Biopharm. (2014) (accepted).

[35] European Pharmacopoeia, eighth ed., European Directorate for the Quality of Medicines & HealthCare (EDQM), Strasbourg, France, 2014.

[36] ICH Guideline Q2(R1), Validation of analytical procedures: text and methodology, in: International Conference on Harmonisation of Technical Requirements for Registration of Pharmaceuticals for Human Use, Geneva, Switzerland, 2005.

4.6 Predicting critical micelle concentration and micelle molecular weight of polysorbate 80 using compendial methods

Alexandra C. Braun, David Ilko, Benjamin Merget, Henning Gieseler, Oliver Germershaus, Ulrike Holzgrabe, Lorenz Meinel

Reprinted with permission from Eur J Pharm Biopharm **2014**.

Abstract

This manuscript addresses the capability of compendial methods in controlling polysorbate 80 (PS80) functionality. Based on the analysis of sixteen batches, functionality related characteristics (FRC) including critical micelle concentration (CMC), cloud point, hydrophilic–lipophilic balance (HLB) value and micelle molecular weight were correlated to chemical composition including fatty acids before and after hydrolysis, content of non-esterified polyethylene glycols and sorbitan polyethoxylates, sorbitan- and isosorbide polyethoxylate fatty acid mono- and diesters, polyoxyethylene diesters, and peroxide values. Batches from some suppliers had a high variability in functionality related characteristic (FRC), questioning the ability of the current monograph in controlling these. Interestingly, the combined use of the input parameters oleic acid content and peroxide value – both of which being monographed methods – resulted in a model adequately predicting CMC. Confining the batches to those complying with specifications for peroxide value proved oleic acid content alone as being predictive for CMC. Similarly, a four parameter model based on chemical analyses alone was instrumental in predicting the molecular weight of PS80 micelles. Improved models based on analytical outcome from fingerprint analyses are also presented. A road map controlling PS80 batches with respect to FRC and based on chemical analyses alone is provided for the formulator.

1. Introduction

Polysorbate 80 (PS80) is a frequently used surfactant for biopharmaceutical product formulation. This non-ionic emulsifier is typically formulated at concentrations of 0.01–0.1% (v/v) for active pharmaceutical ingredient (API) stabilization, reduction of surface adsorption, or to avoid stress-induced aggregation (e.g., freezing, storage, transport, reconstitution of lyophilized products) [1-3]. Compendial grade PS80 is composed of polyoxyethylene sorbitan esters with fatty acids, at least 58% of which being specified as oleic acid along with myristic, palmitic, palmitoleic, stearic, linoleic, and α-linolenic acid esters, respectively [4,5]. Critical PS80 material attributes were derived from a focus on its impact on API or excipient stability, as e.g., residual peroxides within PS80 batches may drive oxidation. However, PS80 attributes were to a lesser extent selected based on galenical considerations/functionality related characteristics (FRC), an aspect which is thoroughly addressed here within. The batch-to-batch variability e.g., in residual peroxides was linked to the supplier's manufacturing and purification processes, packaging, or storage [6]. Polysorbates are inherently prone to radical autoxidation, leading to hydrolysis [2,7-9], and placing formulated proteins at risk of oxidative damage [10-12]. Apart from peroxides, variability is introduced by the type and amount of esterified and free fatty acids, unbound ethoxylates as well as the level of impurities [13-16]. Consequently, the United States Pharmacopeia (USP) and the European Pharmacopeia (Ph. Eur.) specify the entire (free and esterified) fatty acid composition, the peroxide value as well as the acid, saponification, and hydroxyl value, respectively. In addition, ethylene oxide, dioxin and heavy metal content are specified [4,5]. In more recent efforts, both pharmacopoeias allude to functionality related characteristics (FRCs; Ph. Eur. 5.15) or excipient performance (USP <1059>) in non-mandatory sections, detailing an approach for reliable excipient performance through additional specifications designed on top of compendial requirements. Several studies within the context of PS80 suggest a need for such additional specifications. For example, the stability of biologic formulations during processing or storage has been linked to the surface activity of polysorbates [17]. Other reports detailed the impact of polydispersed oxyethylenes on colloidal properties [18,19]. However, neither surface activity nor colloidal properties are monographed at present. It is for these exemplary selected reports on PS80 that compliance with compendial specifications alone has been questioned before yielding stable formulation outcome [20,21].

Consequently, we are addressing the need to set additional PS80 specification. We are also addressing the hypothesis, that monographed methods are sufficient in specifying PS80 batches for stable outcome with respect to FRC, when these are released based on adequate models. In order to identify possible input parameters for model building, PS80 batches were broadly characterized by numerous methods. For that, we correlated galenical functionality from sixteen PS80 batches (CMC, cloud point, hydrophilic–lipophilic balance (HLB) value and micelle molecular weight) with batch composition from thorough analytical studies (PS80 fatty acid composition before and after hydrolysis [22], unbound PEGs, sorbitan polyethoxylates, and mono- and diesters) as well as with peroxide value.

2. Experimental details

2.1. Materials

Sixteen PS80 batches of 5 different qualities (qualities being different suppliers or different supplier grades being distributed from one supplier) were used for the study. The polysorbate samples were from Croda (East Yorkshire, UK), Kolb (Hedingen, Switzerland), Merck (Darmstadt, Germany) and NOF (Tokyo, Japan). The order of the supplier names does not necessarily coincide with the order of the codes used within the manuscript. Grade, supplier and date of manufacture from each sample were detailed (Table 1). All samples were stored at room temperature, under nitrogen and protected from light and the experiments were conducted after storage times as indicated. Sorbitan monooleate 80 (Span 80), methylene blue, paraffin oil were from Sigma–Aldrich (Taufkirchen, Germany). Type 2 water (ASTM D1193, ISO 3696) was used (Millipore, Billerica, MA). All other chemicals or solvents were of at least analytical or pharmaceutical grade and obtained from Sigma–Aldrich or VWR (Darmstadt, Germany).

2.2. Sample preparation

For the cloud point determination, the polysorbate 80 samples were dissolved at 3% (w/v) in freshly prepared 1 M sodium chloride in water on a roller mixer to minimize foaming (SRT1, Sigma–Aldrich, Germany) until the solution was visibly clear and free from foam before further processing. Samples for surface tension measurement were dissolved in water.

Table 1. Overview of the PS80 batches.

Quality	Batch	Months of storage	Peroxide value at time of release*	Peroxide value after storage
A	1	26	0.6	8.2
A	2	18	1.3	8.2
A	3	21	0.2	9.2
A	4	21	0.5	16.5
B	1	17	0.4	21.2
B	2	20	0.0	19.7
B	3	31	0.6	16.1
C	1	27	1.0	4.8
C	2	27	1.0	3.7
C	3	16	0.0	4.4
D	1	10	0.1	4.9
D	2	20	0.1	4.4
D	3	18	0.8	2.9
E	1	6	0.2	11.6
E	2	18	1.3	3.9
E	3	14	1.7	8.7

* taken from CoA

2.3. Critical micelle concentration (CMC) by surface tension measurement

The CMC was determined by surface tension measurements using the Wilhelmy plate method with a Krüss K12 (Hamburg, Germany). Temperature was controlled at 20 ± 0.5 °C (Fryka, G. Heinemann, Schwäbisch-Gmünd, Germany) and experiments were conducted at atmospheric pressure. The surface tension of water was determined prior to measurements of the surfactant samples and to ensure agreement (±5 mN/m) with the reference value of 72.75 mN/m [23]. Freshly prepared, serial dilutions of the surfactants each in about 75–80 mL of water were equilibrated at 20 ± 0.5 °C for at least 30 min and then stirred for 60 s [24], and again equilibrated for 5 min before measurement (n = 3). The surface tension was recorded from ten different dilutions per sample and the CMC was fitted from the intersection of the straight lines for the linear concentration-dependent section and the concentration-independent section using Krüss tensiometer software (version 5.05) [25-27].

2.4. Cloud point

The cloud point was turbidimetrically determined from a 3% (w/v) PS80 sample solution in 1 M sodium chloride, measured in a water bath at increasing temperature. Vials with 8 mL of the surfactant solution were placed in the water bath with heating at a rate of 1.2 °C/min. from room temperature to 45 °C and then at a rate of 0.3 °C/min. until the cloud point, controlled with a thermometer accuracy of 0.2 °C. The cloud point was visually assessed by phase separation. Furthermore, the cloud point was

confirmed by microcalorimetry. For that, 3 mL of identically prepared samples as used for the turbidimetric method were heated at a rate of 0.5 K/min from 35 to 90 °C in the small volume sample vessel of a C80 calorimeter (Setaram, Caluire, France) and recorded against 3 mL of the identical solution without PS80 in the reference cell. Cells were equilibrated at 35 °C until heat flow between the cells was constant.

2.5. Hydrophilic–lipophilic balance (HLB) value

Determination of HLB values was performed using the “Blender-Centrifuge Method” [28], combining polysorbate 80 sample (HLB ~ 15), sorbitan oleate (Span 80; HLB ~ 4.3), paraffin (required HLB (RHLB) ~ 10.5) and water. In brief, stock emulsions of 25 mg emulsifier per gram emulsion were prepared by diluting the polysorbate sample with water and diluting Span 80 with the paraffin oil and mixing them in varying proportions, with stock A yielding a HLB of 12.33 and stock B yielding a HLB of 6.98, respectively. Stocks were homogenized for 2 min after addition of a small amount of methylene blue. A series of emulsions were prepared from stocks, bracketing the RHLB by weighing each stock emulsion into a 15 mL centrifuge tube to yield a total amount of 10 g emulsion. Tubes were shaken to ensure mixing, centrifuged at 4000 r.p.m. for 20 min and stored at room temperature. After 15 days, the heights of the aqueous phase were measured and the HLB value of the emulsion showing the least phase separation was recorded as the RHLB value, from which the PS80 HLB value was calculated.

2.6. Static light scattering

All static light scattering experiments were conducted at 23 °C using a CGS-3 MD Goniometer (ALV, Langen, Germany). The laser light source was a He–Ne laser operating at λ = 632.8 nm. All measurements were collected at scattering angles in the range of 30–150° using 8 separate detectors. Serial dilutions of the PS80 samples in the concentration range between 1 and 5 g/L were freshly prepared and filtered through a 0.22 µm PVDF syringe filter (Carl Roth, Karlsruhe, Germany) prior to use. The refractive index increment of the sample dilutions was measured using a SEC-3010 refractometer (WGE Dr. Bures, Dallgow-Doeberitz, Germany). The micelle molecular weight and the second virial coefficient were calculated by means of the multiangular Zimm-Plot using ALV-Fit & Plot software.

2.7. HPLC-CAD

Fatty acid composition and free fatty acid content were determined by high performance liquid chromatography with charged aerosol detection as described by Ilko et al. [22]. In brief, following hydrolysis with 1 M potassium hydroxide solution, the fatty acids were extracted with methyl-*tert.*-butylether (MTBE) modified from a previous protocol [29]. For the determination of free fatty acids, heptadecanoic acid was used as internal standard and mixed with the samples and MTBE followed by centrifugation and collection of the organic phase. Measurements were performed with a 1100 HPLC system (Agilent, Waldbronn, Germany) and a Kinetex C18 (100 × 3.0 mm, 2.6 µm particle size) analytical column (Phenomenex, Aschaffenburg, Germany). A gradient was applied (mobile phase A being 0.05% formic acid in water, and mobile phase B being 0.05% formic acid in acetonitrile) starting with 75% mobile phase B for 5 min followed by a linear increase to 85% within 10 min at a flow rate of 0.6 mL/min. Detection was performed with a Corona charged aerosol detector (Thermo Scientific, Idstein, Germany) using a gas inlet pressure (nitrogen) of 35 psi and settings set to no filter at an electric current range of 100 pA.

2.8. Fingerprint analyses

Fingerprinting was performed as described before with modification [30]. The separation was carried out on an LC1100 (Agilent) using a Kinetex C18 (100 × 3.0 mm, 2.6 µm particle size) analytical column. Mobile phase A consisted of 0.1% (v/v) formic acid in water and mobile phase B of 0.1% (v/v) formic acid and 5% water in acetonitrile. A gradient was used increasing the portion of mobile phase B from 10–100% within 12 min and holding this for further 12 min. The flow rate was 0.6 mL/min. and the injection volume 10 µL. A CAD was used for detection with following settings: range: 100 pA, filter: “none”.

2.9. Peroxide value

Peroxide content was determined using a peroxide quantification kit (Pierce Quantitative Peroxide Assay Kit, Thermo Scientific, Rockford, USA). Samples were diluted with water to 2% (w/v). 20 µL of the diluted samples were mixed with 200 µL of the reagent (250 µM ammonium ferrous(II) sulfate, 125 µM xylenol orange, 100 µM sorbitol in 25 mM sulfuric acid), incubated for 20 min at room temperature prior to read-

ing at λ = 595 nm on a SPECTRAmax 250 automated microtiter plate reader (Molecular Devices, Sunnyvale, USA). Hydrogen peroxide was used to prepare standard curves and peroxide levels in polysorbate 80 were obtained as peroxide equivalent to the hydrogen peroxide concentration.

2.10. Statistics

Comparisons were performed using one way ANOVA and normality was tested according to Shapiro–Wilk. *Post hoc* test was performed according to Tukey (pairwise comparison). The statistical software Minitab® 16 (Minitab, Coventry, UK) was used for analysis. Statistically significant results were concluded for $p < 0.05$ (the use of the term “significant” is exclusively used in a statistical way within the manuscript). Results are displayed as mean with standard deviation (SD) and measurements were in triplicate, unless otherwise noted. Linear models were derived, analyzed and plotted using the statistical framework R and associated packages.

3. Results

3.1. Critical micelle concentration, cloud point, and hydrophilic–lipophilic balance values

Sixteen PS80 samples from 4 suppliers (including two different qualities of one supplier, which are for simplicity categorized as if from two suppliers) were assigned A–E and numbers indicate the different batches from the respective supplier (e.g., E1–E3 are three different batches from E). Structural formulas are provided for polysorbate 80 and relevant molecules referred to within this manuscript (Fig. 1). The batches were sorted according to CMC outcome, covering a range from 13.4 ± 0.6 mg/L to 24.7 ± 1.4 mg/L (Fig. 2A). Batches E1–E3 clustered at a low CMC range and were significantly lower as compared to all other samples apart from A1. Batches B1–B3 were significantly different as compared to batches E1–E3, or A4. C3 was significantly higher as compared to C1 and C2 and D1 was significantly lower as compared to D2 and D3. Therefore, significant within-quality differences were observed for A, C, and D but not for B and E.

A similar distribution was observed for the results of the cloud point measurements (Fig. 2B) covering a range from 56.0 ± 0.2 °C to 65.3 ± 0.4 °C with the majority of samples ranging from 59.8 °C to 61.4 °C. Quality E was significantly higher as com-

pared to all other qualities other than sample A1. Quality A had a high variability ranging from 56.0 ± 0.2 °C to 64.3 ± 0.1 °C, whereas qualities B and C had a narrow distribution in the range of 60.7 ± 0.2 °C to 61.2 ± 0.2 °C and 60.4 ± 0.2 °C to 61.1 ± 0.1 °C, respectively. Within-batch variability was observed for qualities D and E (one batch being significantly different compared to the other two) and A (all batches differed significantly from each other) but no differences among samples as observed within B and C.

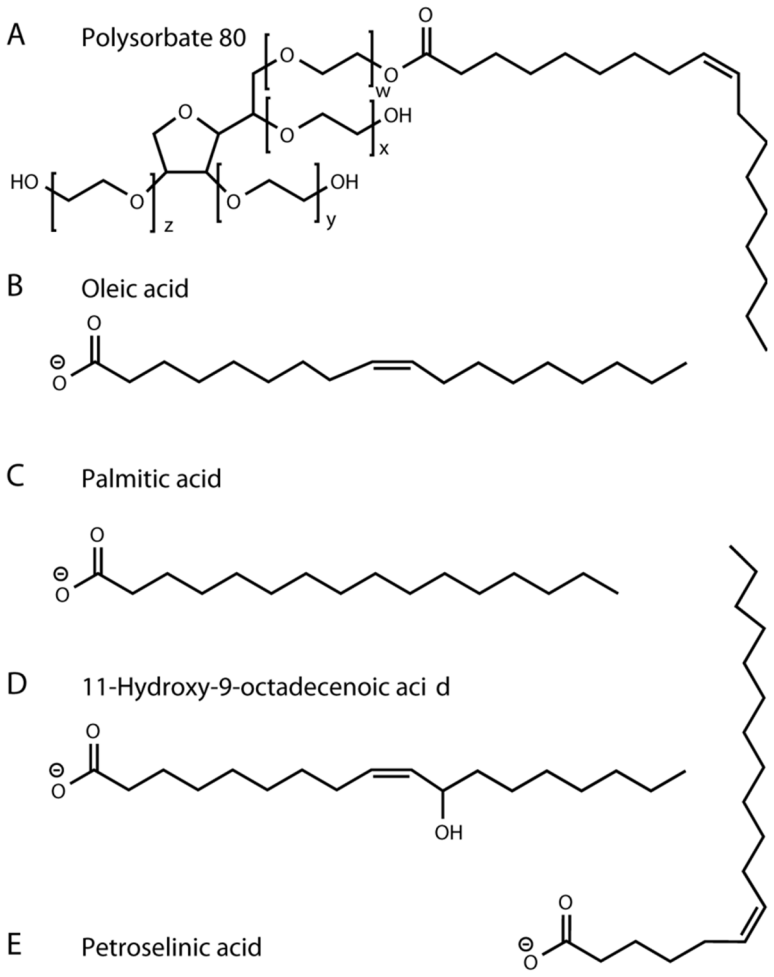

Fig. 1. Selected structures contained in polysorbate 80: (A) main structure of polysorbate 80, (B) structure of oleic acid, (C) structure of palmitic acid, (D) structure of 11-hydroxy-9-octadecenoic acid, and (E) structure of petroselinic acid.

Cloud points determined by the turbidimetric method (Fig. 2B) correlated strongly with cloud point assessment by calorimetric measurements

$$Tc_{turbidimetric}[°C] = 0.89 \times Tc_{calorimetric}[°C] - 4.4$$

(r^2 = 0.97, Supplementary Fig. 1A and B)

and were consistently found 2 °C above those measured by the turbidimetric method, likely due to pressure differences (turbidimetric method was performed under isobaric while the calorimetric method was performed under isochoric conditions, respectively).

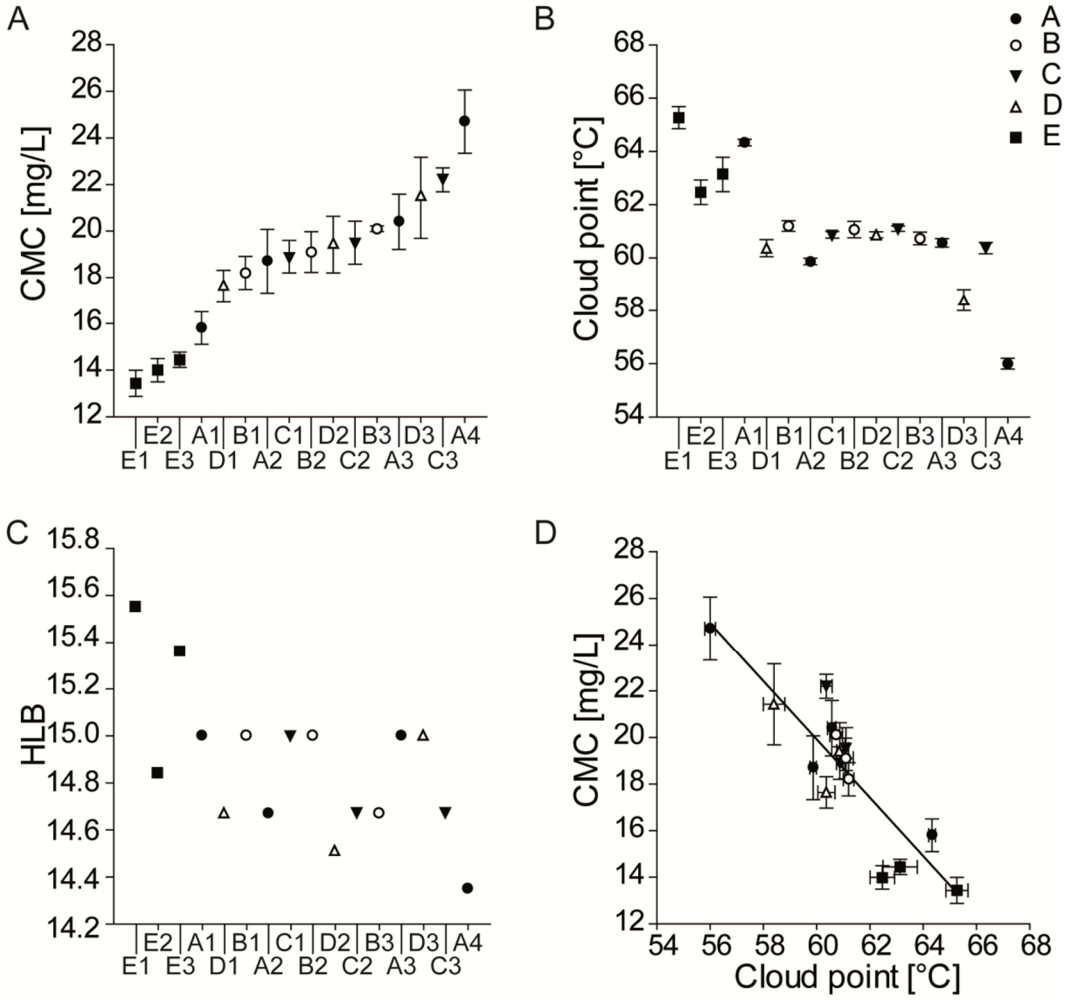

Fig. 2. (A) Critical micelle concentration (CMC) [mg/L] and (B) cloud point [turbidimetric; °C] of the different batches. (C) Hydrophilic–lipophilic balance (HLB) of the different batches (n = 1). (D) Correlation of CMC and cloud point. Please note that axes do not start at zero.

HLB values scattered within 14.4–15.6 with the majority of the batches scattering within a range from 14.5 to 15.1 (*n* = 1; Fig. 2C). Outcome from E suggested clustering of HLB values exceeding 15.0, in contrast to the other qualities which clustered below that threshold. A linear correlation following

$$CMC[mg/L] = -1.25 \times Tc_{turbidimetric}[°C] - 95;$$

(r^2 = 0.79);

was observed between CMC and cloud point (Fig. 2D). We correlated HLB with CMC and cloud point for the reason that these physicochemical parameters reflect the amphiphilic structure of the surfactant and the variability in the hydrophilic or lipophilic moieties may impact both parameters [31-34]. Linear regression of CMC over HLB and cloud point over HLB demonstrated a poor correlation when fitted linearly (r^2 = 0.47; Supplementary Fig. 1C and r^2 = 0.51; Supplementary Fig. 1D), however, demonstrating a relationship among these parameters.

3.2. Impact of supplier/quality and storage on critical micelle concentration and peroxide value

The CMC of batches from A scattered widely (Fig. 3A) in contrast to qualities B and more strongly E. The CMC of E was significantly lower as compared to all other qualities. Generally, no trend (increase or decrease) in CMC was recorded with storage time (Fig. 3B). For example, E1–E3 (covering storage of 6–18 months) were not significantly different in CMC whereas – in spite of identical storage times – batches A3 and A4 differed significantly.

Peroxide values of the polysorbate batches were determined at the same time when all experiments were conducted (and do not reflect values as provided from manufacturers at the time of release at which all batches complied with specifications of the monograph at ≤10 ppm according to the certificates of analyses [4]; Fig. 3C; Table 1). 5 Batches exceeded 10 ppm (Fig. 3C). Generally, the peroxide values of the different batches covered a range from 2.9 to 21.2 ppm with storage times of 6–31 months. The highest peroxide values were observed for batches B1–B3 (16.1–21.2 ppm) and A4 (16.5 ppm). Interestingly, no impact of storage time on peroxide value was detected (Fig. 3D), with e.g., low-peroxide batches C1 and C2 being stored for 27 months in contrast to high-peroxide-batches B1 and B2 being stored within 17–20 months. Peroxide value variability was strikingly different among suppliers, with C, and D, displaying low, A, and E intermediate and B high variability, respectively (Fig. 3E). A correlation between oleic acid content and CMC was apparent (Fig. 3F). However, 4 batches clearly deviated from the linearity and all these did not comply with the compendial specifications for peroxide value (≤10 ppm) and the relationship is further analyzed in more detail (*vide infra*). A potential trend of increasing peroxide value with elevated amount of polyethoxylate diesters may be postulated (Supple-

mentary Fig. 3E). At this point we concluded that oleic acid and peroxide value may be instrumental input parameters for model building of a predicted CMC.

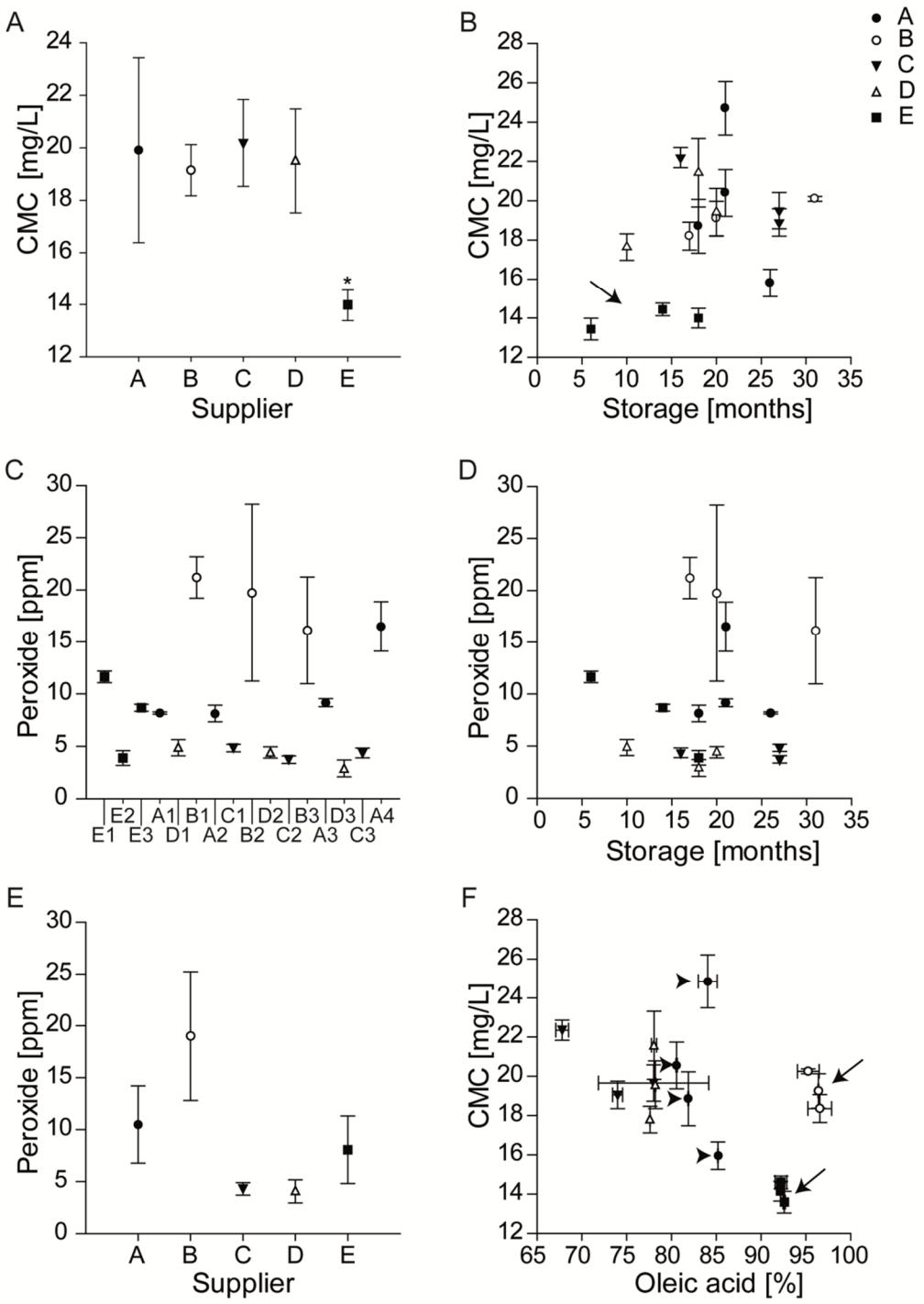

Fig. 3. (A) Critical micelle concentration [mg/L] as a function of the supplier/quality. (B) CMC as a function of months of storage. (C) Peroxide value [ppm] of the different batches. (D) Peroxide value [ppm] as a function of months of storage. (E) Peroxide value [ppm] as a function of the supplier/quality. (F) Correlation of CMC with the content of oleic acid [%; after hydrolysis]. Arrows in (B) and (F) highlight the low outcome variability of batches E1–E3 in spite of different storage times (B) or oleic acid content (F). Arrowheads in (F) indicate supplier A which in spite of a narrow distribution of oleic acid content displays large variability in CMC.

3.3. Impact of the PS80 chemical batch composition on CMC

Following hydrolysis, the fatty acid composition of all batches was analyzed by HPLC-CAD (Table 2). The monographs request oleic acid contents of at least 58% upon hydrolysis [4]. The content of oleic acid complied with compendial specifications for all batches and ranged from 67.8 ± 0.7% to 96.6 ± 1.3% (Fig. 3F), representing differences of up to 30% among batches. HPLC-CAD analyses were also conducted on non-hydrolyzed (i.e., crude) PS80 samples, referred to as “free acid” in this manuscript ([15,22,35], Supplementary Fig. 2A). A general trend of increasing CMC with increasing free fatty acid content was observed (Supplementary Fig. 2B). Batches from B and E had a significantly lower free fatty acid content as compared to the other qualities, and variability was strikingly low for B, D, and E and in contrast to A and C (Supplementary Fig. 2C). Storage did not impact the amount of free fatty acids (Supplementary Fig. 2D; [22]).

Table 2. Fatty acid composition of the PS80 batches after hydrolysis and liquid-liquid extraction (n=3).

Supplier/quality	Batch	Petroselinic acid [%]	Linoleic acid [%]	Palmitoleic acid [%]	Stearic acid [%]	Palmitic acid [%]	Oleic acid [%]	Hydroxy-oleic acid [%]
A	1	0.82	6.58	0.76	1.24	5.40	85.22	0.00
A	2	1.20	9.59	0.52	1.40	5.38	81.92	0.00
A	3	1.00	10.13	0.79	1.65	5.83	80.61	0.00
A	4*	1.20	6.80	0.60	1.62	5.74	84.08	0.00
B	1	0.00	0.00	0.00	0.38	0.82	96.58	2.24
B	2	0.00	0.00	0.00	0.48	1.01	96.44	2.08
B	3	0.00	0.00	0.00	0.35	0.67	95.29	3.69
C	1	1.03	9.44	0.64	2.72	12.16	74.05	0.00
C	2	0.87	7.10	0.49	2.94	10.56	78.04	0.00
C	3*	2.65	10.74	0.66	3.55	14.58	67.84	0.00
D	1	0.28	11.34	0.00	2.04	8.25	77.65	0.45
D	2*	0.33	11.55	0.00	1.86	7.52	78.24	0.50
D	3	0.25	11.79	0.00	2.01	7.38	78.09	0.54
E	1*	1.16	1.06	0.00	2.66	2.53	92.62	0.00
E	2	1.03	0.00	0.00	3.08	2.99	92.21	0.70
E	3	0.96	0.00	0.00	2.80	2.41	92.25	1.60
Specification Ph.Eur (8th Edition)		Not specified	≤ 18.0%	≤ 8.0%	≤ 6.0%	≤ 16.0%	≥ 58%	Not specified
Specification USP 37 NF 32								

* Data was previously reported and is summarized again for completeness [22]

Besides free fatty acid composition and fatty acid composition upon hydrolysis, the content of unesterified PEG/sorbitan polyethoxylates (peaks are reported together), sorbitan- and isosorbide polyethoxylate mono- and diesters, as well as polyoxyethylene diesters, was followed by “fingerprinting” analyses (Supplementary Fig. 3A–D). Among qualities, some differences were observed especially in content of free PEGs and sorbitan polyethoxylates. For example, batches of E were low in terms of free PEGs and sorbitan polyethoxylates (Supplementary Fig. 3A). Polyethoxylate-fatty acid diesters were found in batches of qualities A and B but only in selected batches of the other qualities (Supplementary Fig. 3D). None of these parameters alone (unesterified PEG/sorbitan polyethoxylates, sorbitan-, isosorbide polyethoxylate mono- and diesters, polyoxyethylene diesters) correlated with CMC or peroxide value.

3.4. Impact of supplier, critical micelle concentration, or fatty acid composition on micelle molecular weight (MM_w)

MM_w was characterized for selected batches (Fig. 4A), covering a range from 111.2 to 126.8 kDa ($n = 1$) and the highest MM_w was observed for batches C1, and B2. Substantial differences for MM_w were observed within all qualities apart from supplier/quality E.

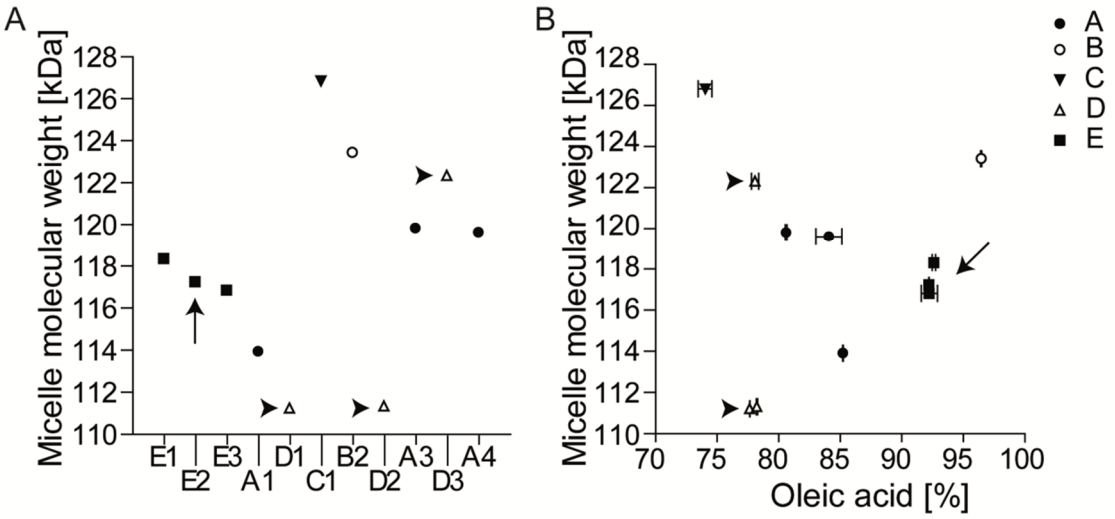

Fig. 4. (A) Micelle molecular weight [kDa] as a function of different batches. (B) Correlation of micelle molecular weight with oleic acid content [%; after hydrolysis]. Arrows highlight the low outcome variability in (A) within quality E and for the correlation of micelle molecular weight with (B) oleic acids, respectively. Arrowheads (A and B) indicate supplier D which in spite of a narrow distribution of unsaturated fatty acid content displayed large variability in micelle molecular weight.

MM_w was correlated with oleic acid content (Fig. 4B). In spite of a low variability in the oleic acid composition within qualities, substantial differences in MM_w were found other than for E. In summary, oleic acid content alone is not adequately predicting MM_w outcome (Fig. 4B). However, the pattern of variability as identified by the CMC (Fig. 3A) was also reflected by the MM_w (Supplementary Fig. 4A and B). The static light scattering experiments with which the MM_w was determined were also used to calculate the second virial coefficient (B_2) of the batches (Supplementary Fig. 4C) and no correlation was found to any of the parameters mentioned above (data not shown).

3.5. Model building for the prediction of CMC and MM_w by the input parameters fatty acids, fingerprint data and peroxide value

Our general inability to reliably predict CMC and MM_w as galenical parameters for PS80 performance by individual values (*vide supra*) prompted us to combine all input parameters for model building (Fig. 5; Table 3). On the basis of outcome from all batches, a valuable prognostic model was built for CMC by use of oleic acid content and peroxide value (Fig. 5A). Both of these input parameters are specified in the compendial monographs. These results demonstrated that once both parameters were used in combination, a prediction of CMC is possible. They also demonstrated that independent use of these parameters – as currently done – did not necessarily control CMC. A second model using data obtained from all batches proved valuable deploying the amount of polyoxyethylene diesters as additional input parameter (Fig. 5B) thus refining the model based on peroxide value and oleic acid content alone (Fig. 5A). Complicated models using more than four factors are not presented here due to their complexity likely rendering them useless in daily practice but are reported (Supplementary Fig. 5A). In a second set of model building for the prediction of CMC, we restricted the analysis to batches which complied with the release specifications of the pharmacopeias for peroxide values. Thereby, we excluded data from batches E1, B1–B3 and A4 due to the peroxide values exceeding 10 ppm (as specified by the monographs). Interestingly, the 10 ppm value specification for peroxide content was sufficient to allow building of a valuable model with a single input parameter – oleic acid content – yielding a precise prediction of CMC (Fig. 5C). In more detail, the first model (Fig. 5A) was

$$CMC[mg/L] = 48.2 - 0.4 \times c(oleic\ acid[\%]) + 0.5 \times c(peroxides[ppm])$$

n = 16; r^2 = 0.66; F = 12.4; model built with data from all batches; these and the following factors were rounded. In this model, all parameters were significant (p < 0.01).

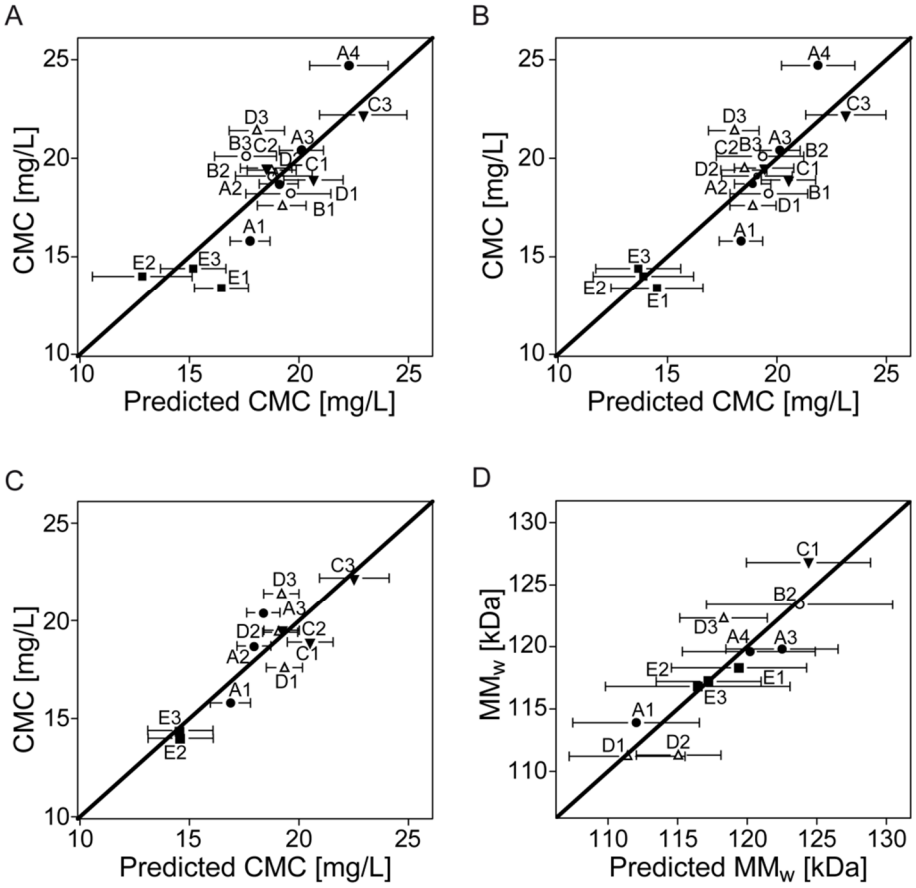

Fig. 5. (A) Measured CMC [mg/L] versus predicted CMC [mg/L] including 90% confidence intervals calculated by oleic acid content and peroxide value for the complete data set from all batches (r^2 = 0.66) and (B) with oleic acid content, peroxide value and amount of polyoxyethylene diesters for the complete data set from all batches (r^2 = 0.74) and (C) with oleic acid content alone for reduced data (excluding batches not complying with compendial specifications for peroxide value; r^2 = 0.77). (D) Measured MMw [kDa] versus predicted MMw [kDa] calculated by CMC, hydroxy-oleic acid content, amount of sorbitan- and isosorbide-polyethoxylate monoesters and sorbitan- and isosorbide-polyethoxylate diesters (r^2 = 0.80). Please note that axes do not start at zero.

The second model was built from the same batches/samples and included 3 parameters as of

$$CMC[mg/L] = 52.1 + 0.8 \times c(polyoxyethylene\ diesters[\%]) - 0.4 \times c(oleic\ acid[\%]) + 0.3 \times c(peroxides[ppm]);$$

n = 16; r^2 = 0.74; F = 11.3; (Fig. 5B). By involving polyoxyethylene diester content as additional parameter, the correlation resulted in increased accuracy (r^2 = 0.74 as compared to r^2 = 0.66) with comparable F value, indicating that the additional parameter and the associated increase in r^2 did not negatively impact the F value, as the

evidence that the extended model did not result in overfitting (F = 11.3 compared to F = 12.4 for the first model with 2 parameters). The level of significance for polyoxyethylene diester content ($p < 0.1$) was lower as compared to the two parameters, peroxide value and oleic acid content ($p < 0.05$).

For model building using readouts from batches complying with compendial specifications for the peroxide value (≤10 ppm), a (surprisingly) simple model was adequate as of

$$CMC[mg/L] = 44.6 - 0.3 \times c(oleic\ acid[\%]);$$

n = 11; r^2 = 0.77; F = 29.6; (Fig. 5C).

Oleic acid was a highly significant input parameter for the model ($p < 0.001$). Therefore, the specification by the monograph for the peroxide value at 10 ppm was sufficient to render the model independent of peroxide content (Supplementary Fig. 5B).

The CMC as measured input parameter also proved suitable for the prediction of the micelle molecular weight of PS80. For the prediction of MM_w, building of a valuable prognostic model required 4 parameters (Fig. 5D). By using the experimental CMC in combination with hydroxy-oleic acid content, amount of sorbitan- and isosorbide-polyethoxylate monoesters and sorbitan- and isosorbide-polyethoxylate diesters, MM_w was predicted by

$$MM_W[kDa] = 91.4 + 1.4 \times CMC[mg/L] - 0.7 \times c(Monoester[\%]) + 1.7 \times c(Diester[\%]) + 5.4 \times c(hydroxy - oleic\ acid[\%]);$$

n = 11; r^2 = 0.80; F = 5.9; (Fig. 5D). In this model, all parameters were significant ($p < 0.05$). Again, even more complicated models were not reported in detail here but are provided (Supplementary Fig. 5C).

Table 3. Glossary (Input or output parameters for models are highlighted in bold)

Parameter	Method of measurement	Impact on a model
Critical micelle concentration (CMC, [mg/L])	Surface tension measurement	Output parameter for models 1-3 (**Fig. 5A-C**), Input parameter for model 4
Cloud point [°C]	Turbidimetric / calorimetric	[d]
Hydrophilic-lipophilic balance (HLB)	Stability evaluation on emulsion series	[e]
Micelle molecular weight (MM_W; [kDa])	Static light scattering	Output parameter for model 4 (**Fig. 5D)**
Second virial coefficient (B_2,[mol*L/g^2])	Static light scattering	[e]
Peroxide value [ppm]	FOX Assay (colourimetric)	Input parameter for models 1 and 2 (**Fig. 5A** and **B**)
Oleic acid content [%]	Fatty acid composition determined after hydrolysis (according to monograph) using HPLC-CAD [22]	Input parameter for models 1-3 (**Fig. 5A-C**)
Hydroxy-oleic acid [%][a]		Input parameter for models 4 (**Fig. 5D**)
Palmitic acid content [%]		[c]
Stearic acid content [%]		[c]
Palmitoleic acid content [%]		[c]
Linoleic acid content [%]		[c]
Petroselinic acid content [%][b]		[c]
Free fatty acids [%]	HPLC-CAD analysis on crude (non-esterified) material	[c]
Free PEGs and sorbitan-polyethoxylates [%]	Fingerprint analyses using HPLC-CAD [30]	[c]
Sorbitan- and isosorbide-polyethoxylate monoesters [%]		Input parameter for models 4 (**Fig. 5D**)
Sorbitan- and isosorbide-polyethoxylate diesters [%]		Input parameter for models 4 (**Fig. 5D**)
Diester-polyethoxylates [%]		Input parameter for model 2 (**Fig. 5B**)

[a] Oxidation product of Oleic acid (**Fig. 1D**).

[b] Double bond positional isomer to oleic acid (**Fig. 1E**).

[c] Had no significant impact on model (**Supplementary Fig. 5**).

[d] Was not used as an output parameter due tot he correlation with CMC.

[e] Could not be predicted by a model based on the input parameters addressed here within.

4. Discussion

Striking physical, geometrical and chemical differences were observed among batches (in spite of complying with specifications), with some qualities (e.g., E) demonstrating significantly lower variability in outcome than others (e.g., Fig. 3A). The supplier variability in CMC was neither a function of storage time nor predicted by one chemical parameter in isolation such as free fatty acid content (Supplementary Fig. 2). As a result, one may conclude that a careful selection of the supplier is perhaps the most important parameter impacting the quality of PS80 containing formulations, and presumably at least as important as storage conditions or storage time at the supplier or the end user. The demonstrated homogeneity in chemical and physical properties e.g., observed for E suggested that refined manufacturing and purification processes lead to controlled physicochemical properties and overall low variability among all parameters tested. However, a pharmaceutical manufacturer likely resists relying on the supplier alone; instead one requires reliable and standardized methods to internally control/predict PS80 quality. The challenge in the previous sentence is the term “standardized methods”. For example, batches of quality A – demonstrating significant variability in chemical and physicochemical features – can be adequately controlled if additional release specifications are set on outcome from cloud point or CMC measurements, respectively. However, neither CMC, nor cloud point, nor static light scattering are compendial methods (Ph. Eur.; light scattering is mentioned in method < 851 > of the United States Pharmacopeia (USP) [5]). It is easier for the manufacturer and supplier alike if specifications are set on methods known by the pharmacopeias. We studied the possibility to use compendial methods for the control over the CMC (with CMC serving as the surrogate to address functionality related characteristics (FRC) as it correlated with other physical parameters including cloud point (Fig. 2D), HLB (Supplementary Fig. 1C) but not readily detectable to MM_w (Supplementary Fig. 4A).

Surprisingly simple models were built, allowing easy implementation in manufacturers’ and suppliers’ laboratories. One of the models suggested, that if the peroxide value does not exceed 10 ppm (the specified threshold in the monographs), oleic acid content alone is sufficient and appropriate in predicting CMC outcome (Fig. 5C). Hence, for those batches matching peroxide value specifications, precise determination of oleic acid content correlates with sufficient prediction of the CMC. An illustra-

tion is provided to demonstrate the potential use of the models outlined here within. For example, batches E2 and C3 complied with compendial specifications regarding the peroxide value (3.9 versus 4.4 ppm, respectively; Table 1). Consequently, the model described as of

$$CMC[mg/L] = 44.6 - 0.3 \times c(oleic\ acid[\%])$$

(Fig. 5C) would be selected for the prediction of the CMC and resulted in 17 mg/L and 24.5 mg/L for E2 and C3, respectively, with a difference of 7.5 mg/L among batches. Experimental data indicated a mean CMC of 14 mg/L and 22 mg/L for E2 and C3, respectively (Fig. 2A), hence a difference of 8 mg/L. The intercept with the ordinate as of 44.6 mg/L indicated, that extrapolation of the model outside the design space assessed here within might be misleading whereas prediction within the range used for model building was robust (67.8–96.6%, Table 2). Possibly, the model can be extended to the specification limit of 58% provided by the current monograph but more data are required to substantiate this extrapolation. This also corroborated the excellent compendial choice of 10 ppm for the peroxide value, not only from the perspective of oxidative stress on API/excipients, but also from a galenical perspective. Another conclusion is that the oleic acid content was linked to the respective CMC by a factor of 0.3. Therefore, batches complying with compendial specifications (range as of 58% to perhaps practically less than 98% leading to a difference as of maximally 40%) have predicted differences in CMC up to 12 mg/L (and accepting the extrapolation of the model to 58% as outlined above). The model built on outcome from all batches (including those with peroxide values ≥10 ppm), required the peroxide value as input parameter along with oleic acid content (Fig. 5A). Therefore, we conclude that CMC (as a surrogate for FRCs) can indeed be adequately predicted by current compendial methods. We also conclude, that once peroxide values comply with compendial specifications (≤10 ppm), oleic acid content alone (for which a compendial method is described) is sufficient to control FRCs of polysorbate 80 with respect to micelle related processes/CMC.

In each model, oleic acid concentration in batches was negatively correlated with CMC. Thermodynamic considerations may help to approach the fundamentals of this observation. To assess the effectiveness of a surfactant, the free enthalpy balance between two processes may be discussed (i) of micelle formation and (ii) the migration of surfactant molecules from the bulk into interfaces [31-34]. One potential model

is that during the process of micelle formation, the polar head groups of the surfactant remain in the polar environment of the aqueous environment (changes before and after micelle formation are negligible), whereas the hydrophobic chains get in close contact with each other (driving the change). Therefore, the change in Gibb's free enthalpy – as a result of micelle formation – is mainly from the new hydrophobic environment and due to the arrangement of the hydrophobic tails within the spherical micelles. A possible entropy change due to arrangement of these tails within the micelles is ignored in this consideration as is any effect of changes of solvent molecule arrangements as a result of micelle formation. The adsorption at the interface/surface follows similar considerations as for micelles, but the hydrophobic element of the surfactant in the interface is between two phases and not within a micelle. Therefore, the packaging of the hydrophobic tail is different (like staked palisades) and likely more arranged as compared to the spherical micelles. The higher the degree of order the lower is the respective Gibb's free enthalpy. In addition, the difference of the free enthalpies of the micelle formation process and the adsorption at the interfaces, respectively, directly correlates to the logarithm of the quotient of the CMC and C_{20} [36]. C_{20} is the concentration of the surfactant yielding a reduction of the surface tension by 20 mJ/m² starting off the pure solvent (C_{20}; ≪CMC for polysorbate 80). C_{20} – a measure for the efficiency of a surfactant – is presumably less impacted by structural changes as a result of oleic acid content differences among batches, as C_{20} relevant events are at concentrations by far lower than the CMC (but typically in the area in which the maximal surface excess Γ_{max} has already been reached in all experiments). To this point we assume, that enthalpic terms can be neglected (as suggested before [2]), that C_{20} as a characteristic for surfactant efficiency is equivalent among batches and, that entropy changes to the surrounding solvent molecules can be ignored. Based on these assumptions, one may speculate that the impact of "kinked" oleic acid (Fig. 1) on the molecular order can be higher in the more ordered interface as compared to the less ordered micelles. In other words, the potential of the "kinked" structure to more effectively induce disorder in the relatively more ordered surface of the interface as compared to the (generally less ordered) micelle would explain a difference in entropy among batches with high versus low oleic acid content and as detailed (Table 2). Under these assumptions (*vide supra*), the indirect correlation of oleic acid content and CMC would be partially explained. Obviously, the assumptions above reflect the simplicity of this explanation and the lack of required experiments to

substantiate our explanation. With peroxide value being a parameter impacting many possible events within polysorbate 80 batches, we refrain from linking this to basic considerations based on the data set reported here within and leave this observation at an empirical level. Previous attempts have linked autoxidation to degradation products (generation of short chain ethoxylates), and linking the surface activity of these impurities/degradation products to differences in CMC [37].

The model was further refined by integrating the next parameter, the amount of polyoxyethylene diesters (Supplementary Fig. 5). The more complex model corroborated the negative correlation for oleic acid with CMC and positive correlation of peroxide value with CMC while in addition suggesting a positive correlation for polyoxyethylene diesters. Manufacturers are also confirmed by these models in their strong effort to control peroxide values until use, as the strong impact of this input parameter was again demonstrated in this multifactorial model. Lastly, a model was postulated for the prediction of the micelle molecular weight (MM_w). The correlation of MM_w with CMC alone was weak, with the model indicating that higher CMC may result in an increase in MM_w (Supplementary Figs. 5C and 4A). Notably, this model indirectly confirmed the predictive value of peroxide value and oleic acid content for the CMC. Similarly, the model suggested that fatty acid monoesters correlate negatively, while fatty acid diesters and hydroxyl-oleic acid correlated positively.

5. Conclusion

Our data demonstrated that PS80 batches in spite of complying with compendial specifications demonstrated high variability in physical characteristics, as described by CMC, cloud point, HLB, and micelle molecular weight, respectively. The pharmaceutical manufacturer should translate this insight in that complying with compendial specifications alone may not necessarily yield reliable galenical outcome in instances in which a high reproducibility e.g., of CMC is desired. Homogenous outcome among batches is important in controlling PS80 quality, as demonstrated. Surprisingly, functionality related characteristics (FRC) – as demonstrated for CMC as a surrogate for micelle related processes – were excellently predicted by oleic acid content alone, when the analysis was restricted to batches complying with compendial specifications for the peroxide values (≤10 ppm). Another conclusion from our data is that compendial specifications are elegantly set for peroxide value and oleic acid content and no

changes in the current specifications are needed based on the data reported here within.

Supplementary data

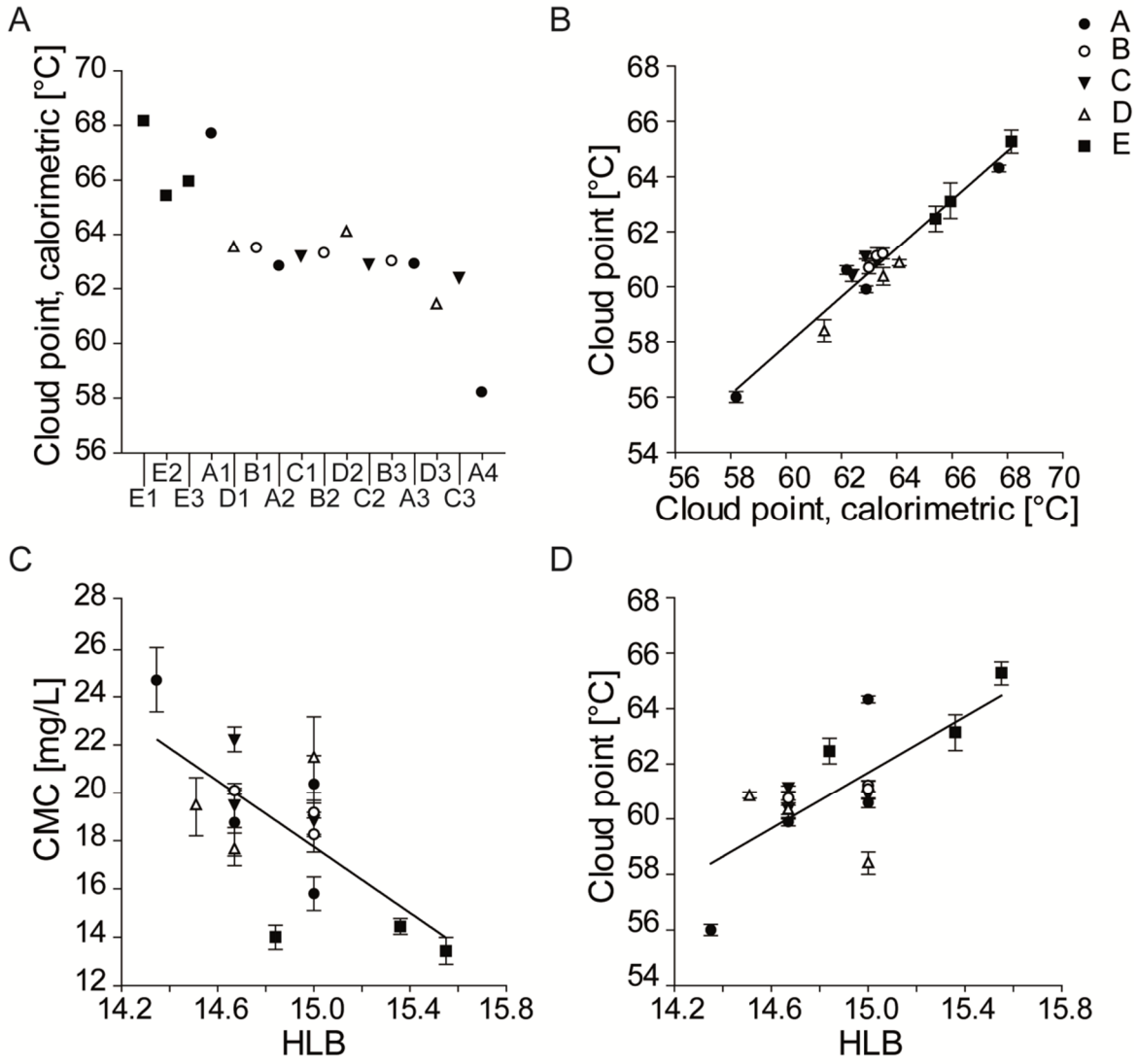

Supplementary Fig. 1. (A) Cloud point [calorimetric; °C] as a function of different batches. (B) Correlation of cloud point measured by the turbidimetric method [°C] and cloud point determined by calorimetric measurement [°C]. (C) Correlation of CMC and HLB. (D) Correlation of cloud point [turbidimetric; °C] and HLB.

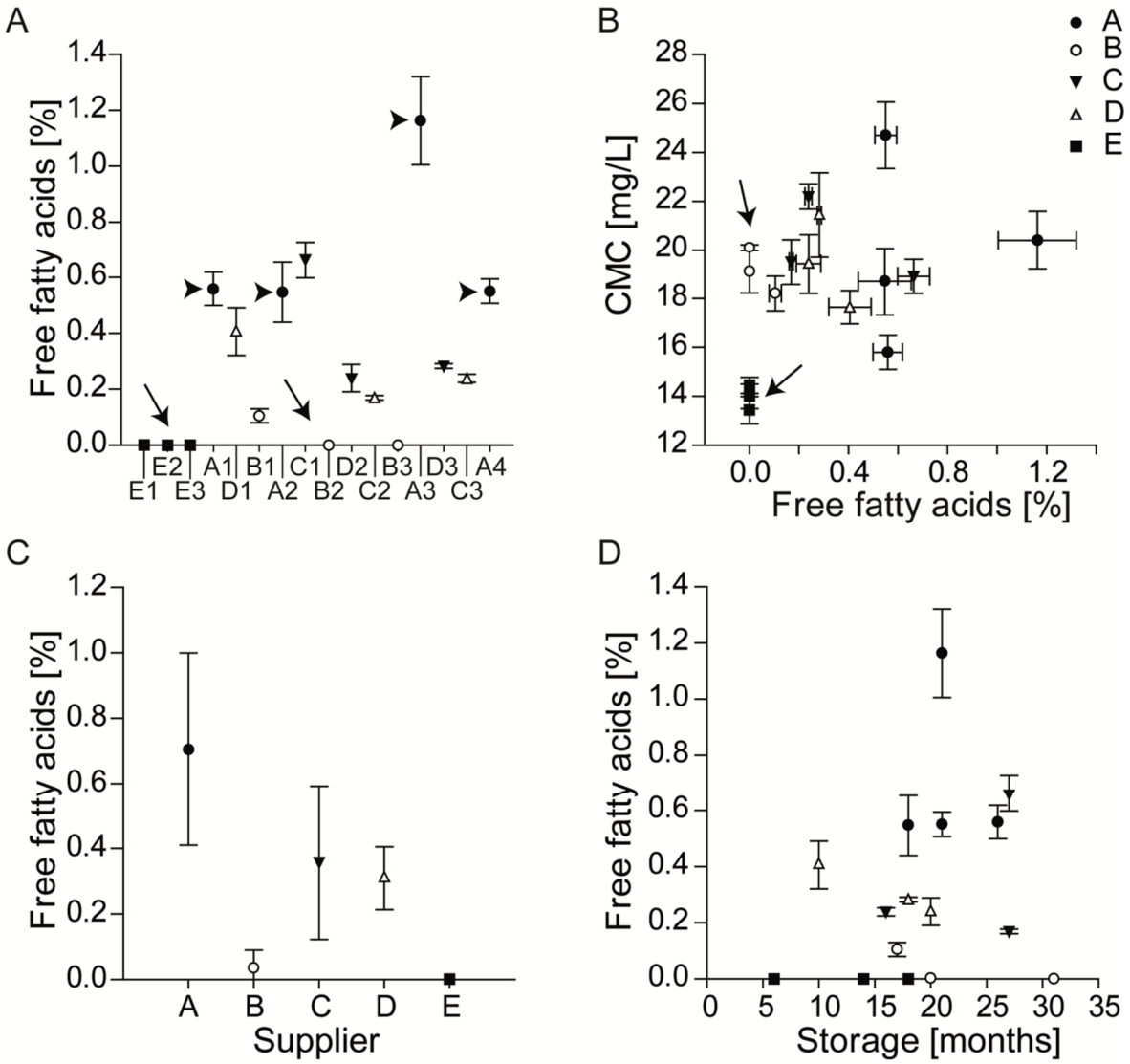

Supplementary Fig. 2. (A) Free fatty acid content [%; no hydrolysis] as a function of batches. (B) Correlation of CMC [mg/L] with free fatty acid content [%; no hydrolysis]. (C) Free fatty acid content [%] as a function of supplier or (D) storage [months]. Arrows indicate batches with low, arrowheads batches with high variability.

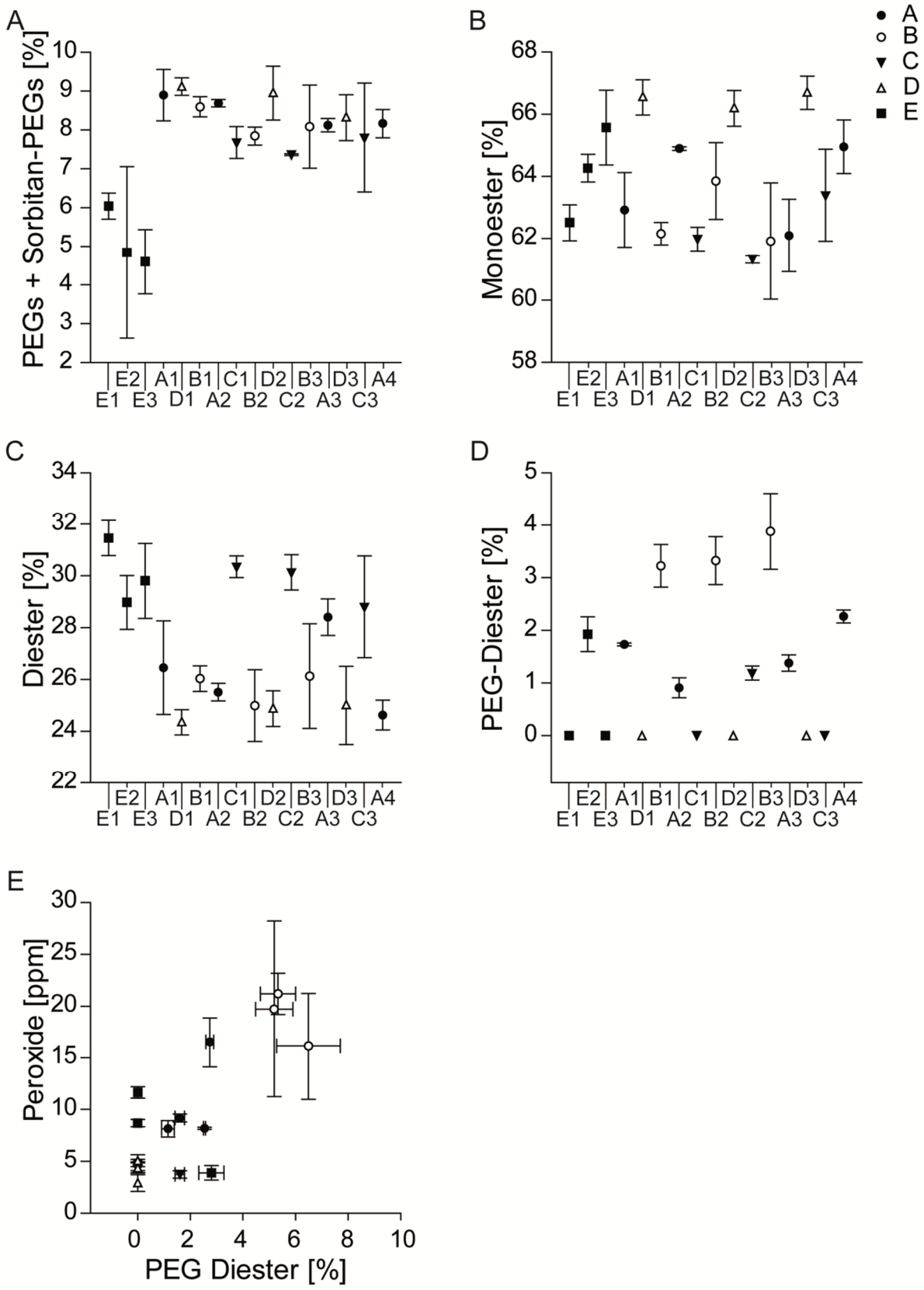

Supplementary Fig. 3. (A) Content of non-esterified polyethylene glycols and sorbitan polyethoxylates [%]; and (B) sorbitan- and isosorbide-polyethoxylate monoesters [%]; and (C) sorbitan- and isosorbide-polyethoxylate diesters [%]; and (D) diester-polyethoxylates [%] of the different batches. (E) Correlation of diester-polyethoxylates [%] and peroxides [ppm].

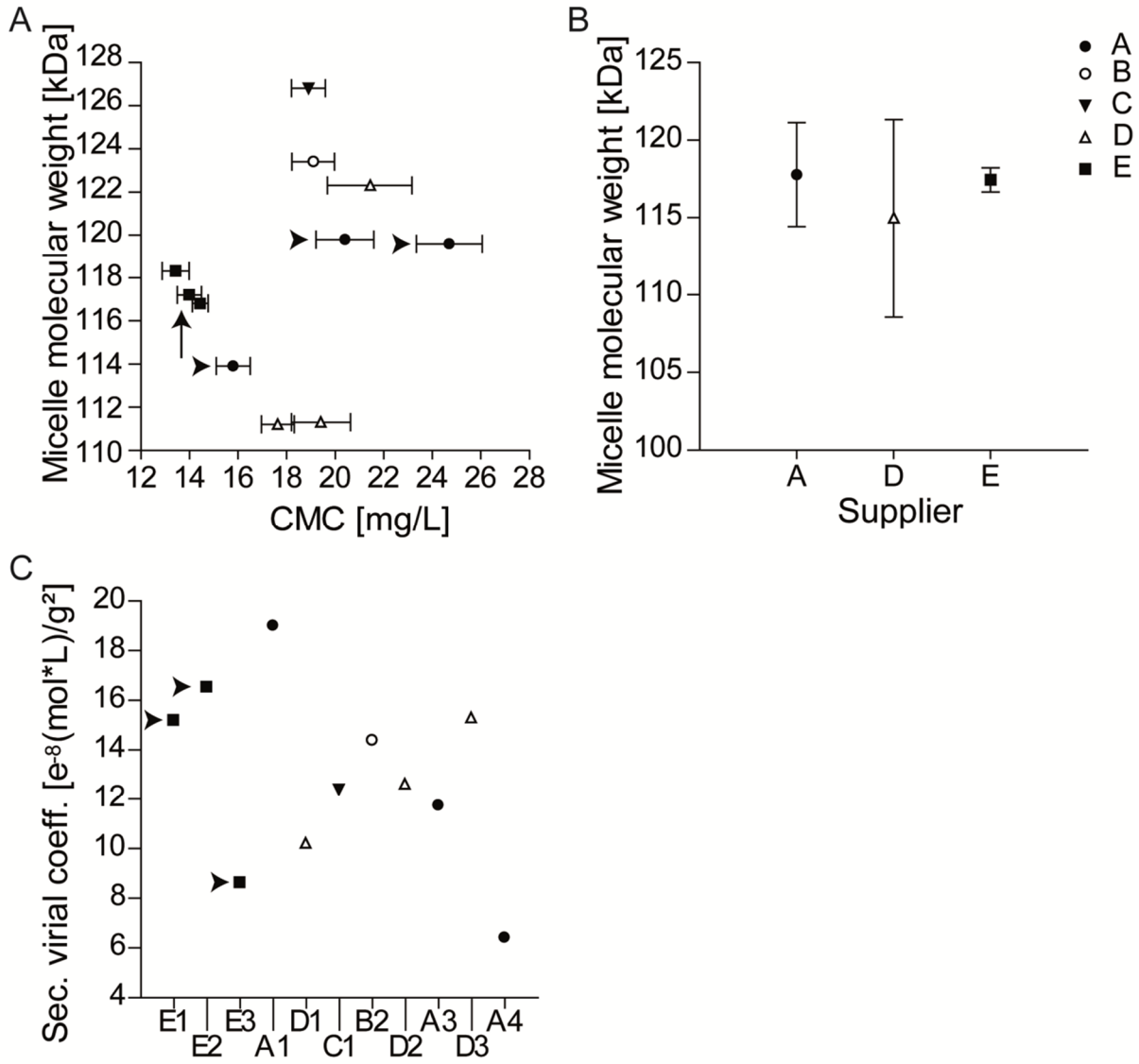

Supplementary Fig. 4. (A) Correlation of micelle molecular weight [kDa] and CMC [mg/L]. (B) Micelle molecular weight [kDa] as a function of supplier. (C) Second virial coefficient [e^{-8} (mol ∗ L)/g^2] as a function of different batches (n = 1). Arrows indicate batches with low, arrowheads batches with high variability.

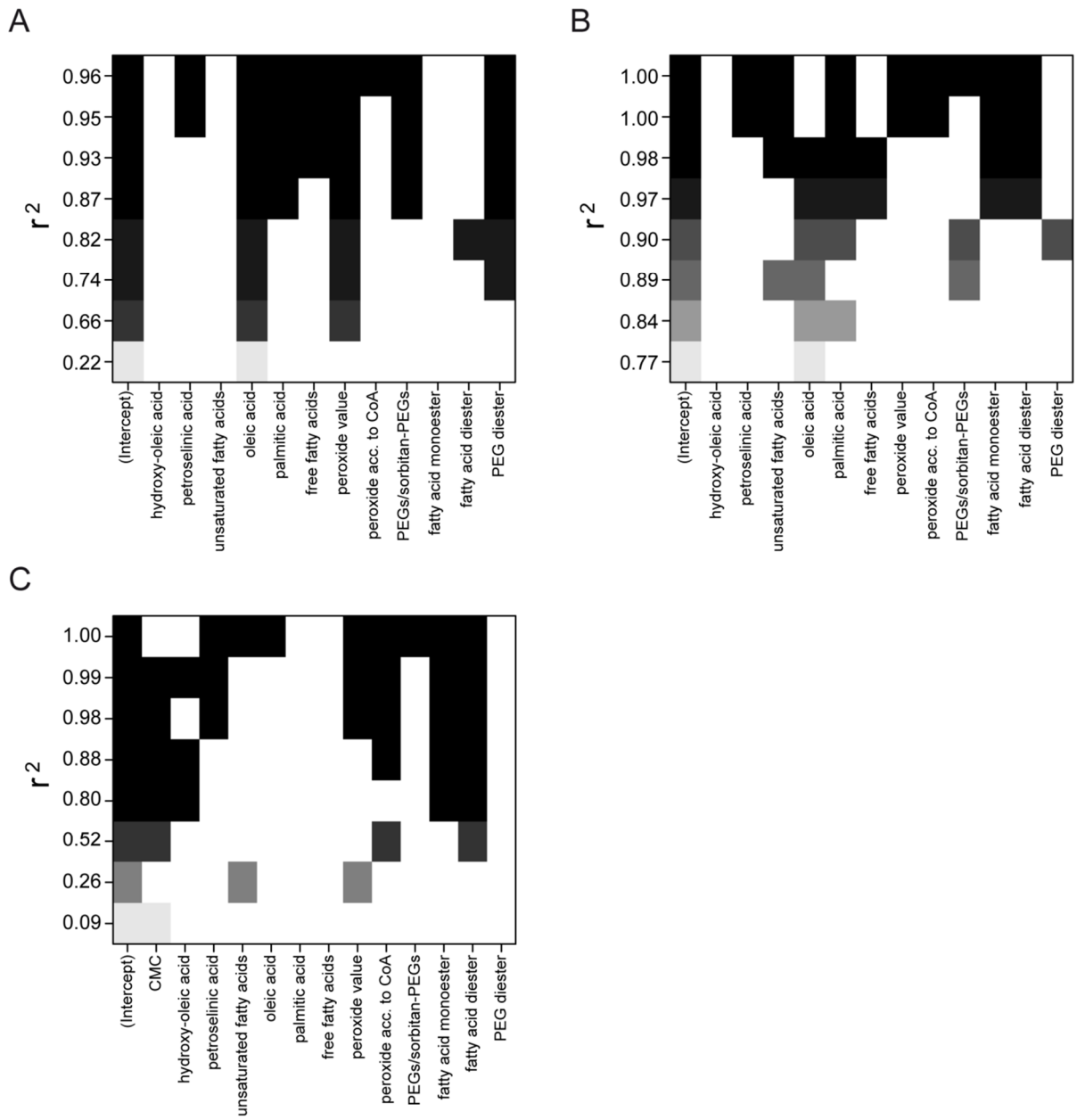

Supplementary Fig. 5. Parameter selection for model building with calculated r^2 as a function of considered parameters for (A) CMC prediction for the complete data set from all batches and (B) from the data set excluding batches not complying with compendial specifications for peroxide value, and (C) for MM_w prediction based on the complete data set from all batches. For example, using oleic acid content alone in panel (A) yielded an r^2 of 0.22, using the peroxide value in addition increased r^2 to 0.66, including PEG diesters on top resulted in a model with a r^2 of 0.74, etc. Thereby, the reader can see the impact of the various outcomes reported here within on model building. One should not be misled by the improvement of the correlation when oleic acid and palmitic acid are used together, as both parameters are confounded. Nevertheless, we mention both parameters here as they were independently determined. However, model building using both parameters would be useless. For each output parameter, the best possible model was identified (Fig. 5**)**.

References

[1] B.S. Chang, B.S. Kendrick, J.F. Carpenter, Surface-induced denaturation of proteins during freezing and its inhibition by surfactants, J. Pharm. Sci. 85 (1996) 1325–1330.

[2] B.A. Kerwin, Polysorbates 20 and 80 used in the formulation of protein biotherapeutics: structure and degradation pathways, J. Pharm. Sci. 97 (2008) 2924–2935.

[3] T.M. Göppert, R.H. Müller, Polysorbate-stabilized solid lipid nanoparticles as colloidal carriers for intravenous targeting of drugs to the brain: comparison of plasma protein adsorption patterns, J. Drug Target. 13 (2005) 179–187.

[4] Polysorbate 80 Monograph, in: European Pharmacopoeia, European Directorate for the Quality of Medicines & HealthCare (EDQM), Strasbourg, France, 2014.

[5] Polysorbate 80 Monograph, in: United States Pharmacopoeia, The United States Pharmacopeial Convention, Rockville, MD, USA, 2014.

[6] S.R. Singh, J. Zhang, C. O'Dell, M.-C. Hsieh, J. Goldstein, J. Liu, A. Srivastava, Effect of Polysorbate 80 quality on photostability of a monoclonal antibody, Aaps Pharmscitech 13 (2012) 422–430.

[7] M. Donbrow, E. Azaz, A. Pillersdorf, Autoxidation of polysorbates, J. Pharm. Sci. 67 (1978) 1676–1681.

[8] R.S.K. Kishore, A. Pappenberger, I.B. Dauphin, A. Ross, B. Buergi, A. Staempfli, H.-C. Mahler, Degradation of Polysorbates 20 and 80: studies on thermal autoxidation and hydrolysis, J. Pharm. Sci. 100 (2011) 721–731.

[9] J. Yao, D.K. Dokuru, M. Noestheden, S.S. Park, B.A. Kerwin, J. Jona, D. Ostovic, D.L. Reid, A quantitative kinetic study of polysorbate autoxidation: the role of unsaturated fatty acid ester substituents, Pharmaceut. Res. 26 (2009) 2303–2313.

[10] E. Ha, W. Wang, Y.J. Wang, Peroxide formation in polysorbate 80 and protein stability, J. Pharm. Sci. 91 (2002) 2252–2264.

[11] W. Wang, Y.J. Wang, D.Q. Wang, Dual effects of Tween 80 on protein stability, Int. J. Pharm. 347 (2008) 31–38.

[12] V.M. Knepp, J.L. Whatley, A. Muchnik, T.S. Calderwood, Identification of antioxidants for prevention of peroxide-mediated oxidation of recombinant human ciliary neurotrophic factor and recombinant human nerve growth factor, PDA J. Pharmaceut. Sci. Technol./PDA 50 (1996) 163–171.

[13] S. Frison-Norrie, P. Sporns, Investigating the molecular heterogeneity of polysorbate emulsifiers by MALDI-TOF MS, J. Agric. Food Chem. 49 (2001) 3335–3340.

[14] M. Verbrugghe, E. Cocquyt, P. Saveyn, P. Sabatino, D. Sinnaeve, J.C. Martins, P. Van der Meeren, Quantification of hydrophilic ethoxylates in polysorbate surfactants using diffusion H-1 NMR spectroscopy, J. Pharmaceut. Biomed. 51 (2010) 583–589.

[15] A. Christiansen, T. Backensfeld, S. Kuehn, W. Weitschies, Stability of the nonionic surfactant polysorbate 80 investigated by HPLC-MS and charged aerosol detector, Pharmazie 66 (2011) 666–671.

[16] R.S.K. Kishore, S. Kiese, S. Fischer, A. Pappenberger, U. Grauschopf, H.-C. Mahler, The degradation of Polysorbates 20 and 80 and its potential impact on the stability of biotherapeutics, Pharmaceut. Res. 28 (2011) 1194–1210.

[17] H.L. Kim, A. McAuley, J. McGuire, Protein effects on surfactant adsorption suggest the dominant mode of surfactant-mediated stabilization of protein, J. Pharm. Sci. 103 (2014) 1337–1345.

[18] T. Chakraborty, S. Ghosh, S.P. Moulik, Micellization and related behavior of binary and ternary surfactant mixtures in aqueous medium: cetyl pyridinium chloride (CPC), cetyl trimethyl ammonium bromide (CTAB), and polyoxyethylene (10) cetyl ether (Brij-56) derived system, J. Phys. Chem. B 109 (2005) 14813–14823.

[19] M. Donbrow, R. Hamburger, E. Azaz, A. Pillersdorf, Development of acidity in nonionic surfactants – formic and acetic-acid, Analyst 103 (1978) 400–402.

[20] H. Kristensen, Functionality-related characteristics of excipients, Pharm. Technol. 31 (2007) 134–138.

[21] N.A. Armstrong, Functionality related tests for excipients, Int. J. Pharm. 155 (1997) 1–5.

[22] D. Ilko, A. Braun, O. Germershaus, L. Meinel, U. Holzgrabe, Fatty acid composition analysis in polysorbate 80 with high performance liquid chromatography coupled to charged aerosol detection, Eur. J. Pharm. Bio-pharm., accepted for publication, http://dx.doi.org/10.1016/j.ejpb.2014.11.018.

[23] N.B. Vargaftik, B.N. Volkov, L.D. Voljak, International tables of the surfacetension of water, J. Phys. Chem. Ref. Data 12 (1983) 817–820.

[24] E. Mohajeri, G.D. Noudeh, Effect of temperature on the critical micelle concentration and micellization thermodynamic of nonionic surfactants: polyoxyethylene sorbitan fatty acid esters, E-J. Chem. 9 (2012) 2268–2274.

[25] K.L. Mittal, Determination of CMC of polysorbate 20 in aqueous-solution by surface-tension method, J. Pharm. Sci. 61 (1972) 1334.

[26] L.S.C. Wan, P.F.S. Lee, CMC of polysorbates, J. Pharm. Sci. 63 (1974) 136–137.

[27] A. Patist, S.S. Bhagwat, K.W. Penfield, P. Aikens, D.O. Shah, On the measurement of critical micelle concentrations of pure and technical-grade nonionic surfactants, J. Surfactants Deterg. 3 (2000) 53–58.

[28] J.E. Robbers, V.N. Bhatia, Technique for rapid determination of HLB and required-HLB values, J. Pharm. Sci. 50 (1961) 708–709.

[29] V. Matyash, G. Liebisch, T.V. Kurzchalia, A. Shevchenko, D. Schwudke, Lipid extraction by methyl-tert-butyl ether for high-throughput lipidomics, J. Lipid Res. 49 (2008) 1137–1146.

[30] E. Hvattum, W.L. Yip, D. Grace, K. Dyrstad, Characterization of polysorbate 80 with liquid chromatography mass spectrometry and nuclear magnetic resonance spectroscopy: specific determination of oxidation products of thermally oxidized polysorbate 80, J. Pharm. Biomed. Anal. 62 (2012) 7–16. [31] N.T. Southall, K.A. Dill, A.D.J. Haymet, A view of the hydrophobic effect, J. Phys. Chem. B 106 (2002) 521–533.

[32] M. Dahanayake, A.W. Cohen, M.J. Rosen, Relationship of structure to properties of surfactants. 13. Surface and thermodynamic properties of some oxyethylenated sulfates and sulfonates, J. Phys. Chem. 90 (1986) 2413–2418.

[33] P. Atkins, P. de Julio, Physical Chemistry, Oxford University Press, Oxford, 2010.

[34] P.C. Hiemenz, Principles of Colloid and Surface Chemistry, Marcel Dekker, Inc., New York, 1986. pp. 127, 133, 147.

[35] F.O. Ayorinde, S.V. Gelain, J.H. Johnson Jr., L.W. Wan, Analysis of some commercial polysorbate formulations using matrix-assisted laser desorption/ionization time-of-flight mass spectrometry, Rapid Commun. Mass Spectrom. 14 (2000) 2116–2124.

[36] M.J. Rosen, Solubilization by solutions of surfactants: micelle related catalysis, in: Surfactants and Interfacial Phenomena, John Wiley Sons, Inc., New York, 1989, pp. 170–206.

[37] A. Patist, S.S. Bhagwat, K.W. Penfield, P. Aikens, D.O. Shah, On the measurement of critical micelle concentrations of pure and technical-grade nonionic surfactants, J. Surfactants Deterg. 3 (2000) 53–58.

5 Final Discussion

The aim of the studies performed here was to evaluate the suitability of the CAD in pharmaceutical analysis. Therefore, substances from different compound classes were investigated. Depending on the type of analytical procedure, i.e. content determination or impurity control, requirements for performance characteristics differ. While high precision and accuracy is demanded for the content determination of pharmaceutical bulk ware, the method sensitivity is an important factor when impurities have to be quantified down to a concentration of 0.03% of the drug substance [1]. The following sections give an overall evaluation of the performance of the CAD.

5.1 Sensitivity

The charged aerosol detector is reported to provide universal response independent from physico-chemical properties of the respective analyte. The only prerequisite is that the analyte is non-volatile, as semi-volatile substances are partly evaporated during the detection process and the response is therefore diminished [2]. For the CAD's user, it would be helpful to predict whether a compound is detectable with sufficient sensitivity or not.

The sensitivity needed is depending on the type of analytical test. For a content determination in bulk drug substance, the main peak in the chromatogram is of interest. It is evident that sufficient sensitivity is provided as long as the substance is giving a detector signal and is not completely evaporated in the detector – assuming that all validation characteristics, such as repeatability, linearity or signal-to-noise ratio are fulfilled. For impurity control however, higher requirements are demanded. To comply with current ICH guidelines, impurities must be reported down to a content of 0.05% or even 0.03%, depending weather the daily intake of the drug substance is less or more than 2 g [1].

An LOQ of 100 ng on column or less is postulated as sufficient to achieve proper impurity control. Assuming an injection volume of 25 µL, a concentration of 13.3 mg/mL would then be necessary for the test solution so that an impurity can be quantified at 0.03%. The use of such highly concentrated solutions is common practice in pharmaceutical analysis.

Volatility is determined by a compound's vapor pressure. Table 4-1 and Figure 4-1 show the LOQs and the vapor pressures of the analytes investigated in this thesis (if the analyte possesses an ionizable group, the vapor pressure of the uncharged species is given). No linear correlation was found between vapor pressure and LOQ (R^2 = 0.0457). Nevertheless, a trend can be observed. For all analytes with a vapor pressure of less than 10^{-5} Torr the CAD was sufficiently sensitive (B in Figure 4-1). No analyte with a vapor pressure of less than 10^{-5} Torr had an LOQ of more than 100 ng on column (A in Figure 4-1).

Analytes with a higher vapor pressure had an LOQ of more than 100 ng on column and sensitive detection was not possible (C in Figure 4-1). However, there were some exceptions to this observation. Laurate, sulfate, mesylate, besylate, phosphate, chloride, bromide, and nitrate (D in Figure 4-1) have a vapor pressure of more than 10^{-5} Torr LOQ but can be detected with sufficient sensitivity (LOQ of less than 100 ng on column). All these analytes are acids and therefore capable of forming a salt. Volatility of a compound is considerably decreased through salt formation [3]. It was shown that volatile analytes can be detected presumed that they are charged at the respective pH value of the mobile phase and a buffer additive is present that can serve as counterion [4]. Then, the molecular species causing the detector signal is the salt of the analyte with the buffer additive [5].

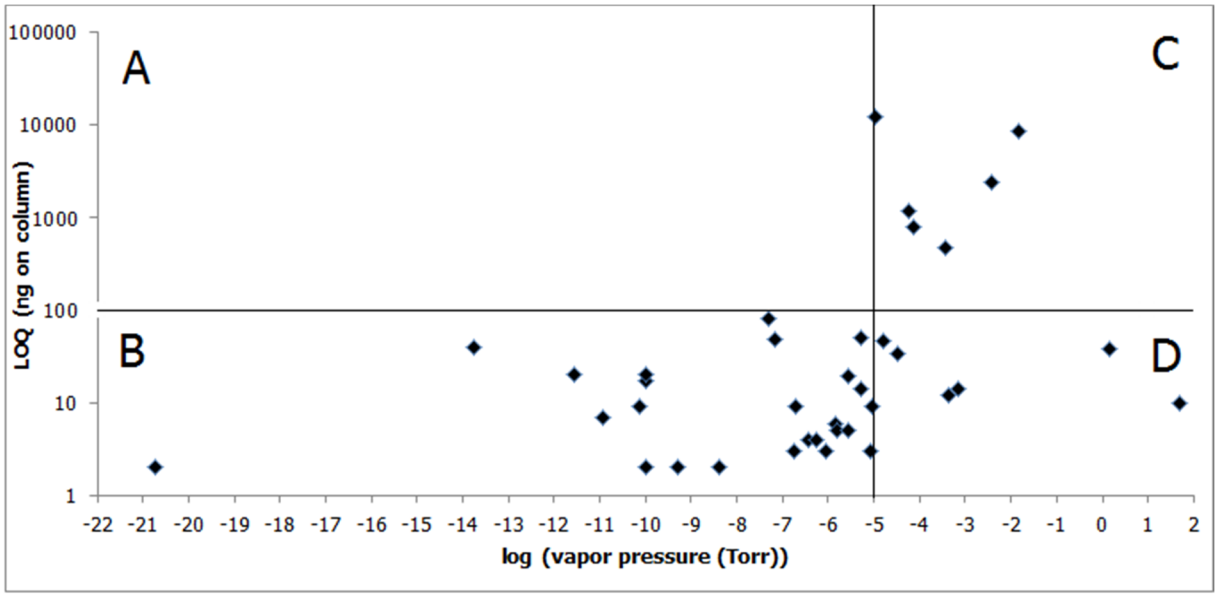

Figure 4-1. LOQs from the analytes given in Table 4-1 plotted against the logarithm of their vapor pressure (Torr) at 25 °C. CAD is considered sufficiently sensitive for the detection of compounds as impurities when the LOQ is below 100 ng on column presented by the horizontal line.

The pK_a values of the corresponding acids of sulfate, mesylate, besylate, chloride, bromide, and nitrate are all less than 0, and phosphoric acid has a pK_a of about 2.1 [6]. Since the pH value of the respective mobile phase was 4.0 (cf. chapter 3.2), they are deprotonated and, thus, sensitively detectable.

Lauric acid has a pK_a of 4.5 [7] and the calculated pH of the mobile phase (0.05% formic acid in water) is 2.8. Hence about 98% of lauric acid is present in its protonated and thus in a more volatile form. As expected, its LOQ is higher compared to other analytes detected with the same method with a vapor pressure below the limit of 10^{-5} Torr, e.g. myristic acid (cf. Table 4-1). Still, lauric acid can be detected with satisfactory sensitivity.

Table 4-1. LOQs and vapor pressure of the analytes studied within this thesis.

Analyte	LOQ (ng on column)	Vapor pressure at 25 °C (Torr)	Reference
Besylate	14	$7.00*10^{-4}$[a]	(2)
Bromide	11	gaseous[a]	(1)
Calcium	17	0[a]	(2)
Capric acid	$4.7*10^{2}$	$3.66*10^{-4}$	(2)
Caprylic acid	$2.4*10^{3}$	$3.71*10^{-3}$	(1)
Chloride	8	gaseous[a]	(1)
Choline	2	$4.93*10^{-10}$	(4)
Citrate	$1.2*10^{3}$	$5.73*10^{-5}$	(1)
Fumaric acid	51	$5.19*10^{-6}$	(1)
Lactate	$8.6*10^{3}$	0.0150	(1)
Lauric acid	46	$1.60*10^{-5}$	(2)
Linoleic acid	3	$8.68*10^{-7}$	(2)
α-Linolenic acid	2	$4.24*10^{-9}$	(1)
Magnesium	2	0[a]	(2)
Malate	$8.0*10^{2}$	$7.19*10^{-5}$	(1)
Maleate	14	$5.19*10^{-6}$	(1)
Meglumine	7	$1.12*10^{-11}$	(1)
Mesylate	12	$4.28*10^{-4}$[a]	(2)
Myristic acid	6	$1.39*10^{-6}$	(2)
Nitrate	10	49.8[a]	(1)
Oleic acid	4	$5.46*10^{-7}$	(2)
Palmitic acid	4	$3.80*10^{-7}$	(2)
Palmitoleic acid	5	$2.82*10^{-6}$	(1)
Petroselinic acid	3	$1.76*10^{-7}$	(1)
Phosphate	38	1.41[a]	(1)
Polidocanol	9	$7.50*10^{-11}$	(2)
Potassium	2	1 (at 714 °C)[a]	(2)
Procaine	9	$8.84*10^{-6}$	(1)
Sodium	2	$1.82*10^{-21}$	(2)
Stearic acid	3	$8.58*10^{-6}$	(1)
Succinate	9	$1.91*10^{-7}$	(2)
Sulfate	34	$3.35*10^{-5}$[a]	(2)
Tartaric acid	82	$4.93*10^{-8}$	(1)

Analyte	LOQ (ng on column)	Vapor pressure at 25 °C (Torr)	Reference
Topiramate	48	$6.76*10^{-8}$	(1)
Topiramate impurity A	$3.8*10^{4}$	$1.04*10^{-5}$	(1)
Topiramate impurity B	29	no value reported	-
Topiramate impurity C	20	$2.69*10^{-12}$	(1)
Topiramate impurity D	22	no value reported	-
Topiramate impurity E	40	$1.79*10^{-14}$	(1)
Tosylate	19	$2.70*10^{-6}$[a]	(3)
TRIS	5	$1.57*10^{-6}$	(1)
Zinc	20	0[a]	(2)

[a] vapor pressure of the corresponding acid or base; (1): https://scifinder.cas.org/ (calculated values using Advanced Chemistry Development (ACD/Labs) Software V11.02 (© 1994-2015 ACD/Labs); (2): http://pubchem.ncbi.nlm.nih.gov; (3): http://toxnet.nlm.nih.gov/cgi-bin/sis/search/a?dbs+hsdb:@term+@DOCNO+2026; (4): http://www.inchem.org/documents/sids/sids/67481.pdf.

Topiramate impurity A (diacetonide) has the highest LOQ among all analytes tested in this thesis while its vapor pressure is only slightly above the limit of 10^{-5} Torr ($1.04*10^{-5}$ Torr). Topiramate impurity A has no ionizable group that could lower its volatility through salt formation. Sensitivity could be enhanced by means of post-column addition of acetonitrile and lowering of the nebulizer temperature of the CAD ultra RS. LOQ was lowered by a factor of nine (cf. chapter 3.3). However, it was still about 1000-fold higher than Topiramate impurities B, C, D and E.

The LOQ of a substance in the CAD cannot be predicted. However, in a first approach it can be estimated if a compound might show reduced response. The dataset given here suggests that there is a limit for the analyte's vapor pressure of 10^{-5} Torr above which the CAD's sensitivity is diminished. In contrast, if an analyte possesses an ionizable functional group, its volatility can be considerably lowered at a pH of the mobile phase that enables salt formation.

5.2 Linearity

It is reported that the CAD provides a linear signal when the measuring range does not exceed two orders of magnitude [8-11]. Table 4-2 shows the results of the linearity studies for the analytes investigated in this thesis. The coefficient of determination (R^2) of the linear regression and the measuring range is presented. In case R^2 was less than 0.995, a log-log transformation was applied for R^2 calculation.

The linearity of besylate, citrate, fumaric acid, malate, maleate, mesylate, nitrate, phosphate, polidocanol, tartaric acid, topiramate, topiramate impurities B, C, D, and E, and tosylate was investigated in a range of less than two orders of magnitude. Thus, it was expected that sufficient linearity will be achieved without log-log-

transformation. However, R^2 of citrate, malate, and topiramate impurity E was less than 0.99. Applying the logarithm to concentration and peak area, R^2 of malate and topiramate impurity E was satisfactory, while that for citrate was considerably diminished (from 0.9835 to 0.8992).

It can be seen from the linearity plot of citrate (Figure 4-2) that the low R^2 value might be due to an outlier in the calibration curve. The diminished linearity of malate might be due to partly evaporation of the analyte during the detection process. Malate has a relatively high vapor pressure (cf. chapter 4.1.1 and Table 4-1). The theory of particle forming in the CAD claims that the diameter of the particles increases with increasing analyte concentration. The relative surface area of a particle is indirectly proportional to its diameter. Assuming that an analyte molecule can only vaporize from the surface of the particle, it can be concluded that a larger portion of the analyte is lost due to evaporation when the particle diameter is small. From the linearity plot of malate, it can be seen that the correlation of concentration and peak area is best described by a power function ($y = a\,x^b$, dotted line in Figure 4-3). The curvature is concave upward (increasing slope, exponent > 1) indicating a better detector efficiency at higher concentrations which is opposing to the usual observations for the CAD [12]. The linearity of the detector signal is therefore negatively affected.

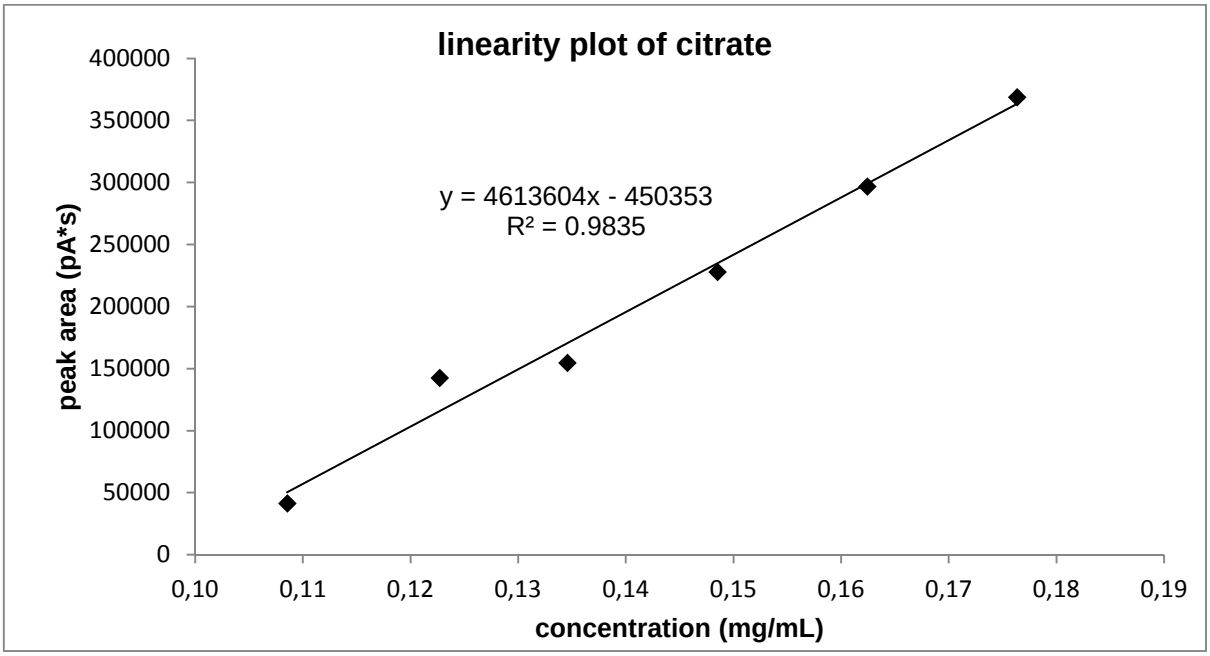

Figure 4-2. Linearity plot of citric acid.

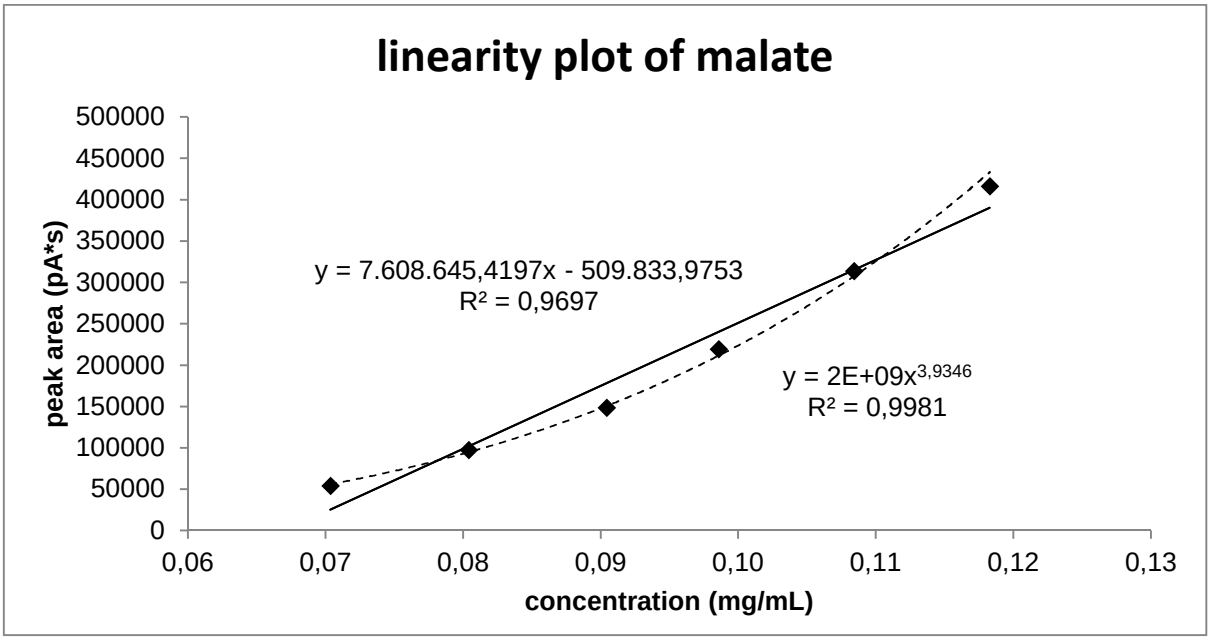

Figure 4-3. Linearity plot of malate with linear (solid) and quadratic (dotted) regression line.

In the topiramate study, topiramate impurity E was the only analyte showing an R^2 of less than 0.99. Compared to the other analytes in this study, it had the widest measuring range. However, compounds with similar range from other studies, e.g. nitrate gave better results for linearity. Thus, it seems to be depending on the actual method setup and the analyte itself in addition to the range, if satisfactory linearity is achieved without log-log transformation, or not.

For bromide, chloride, potassium, sodium, sulfate, linoleic, α-linolenic, oleic, palmitic, palmitoleic, petroselinic, and stearic acid the measuring range was more than or equal to two orders of magnitude. Despite the large range, all analytes except for sodium showed satisfactory linearity with an R^2 of more than 0.995. R^2 of the log-log-linear calibration curve of sodium was 0.9960. It should be expected that the CAD provides similarly linear response curves for sodium and potassium as both are inorganic cations and the same range was investigated. As concluded above, it is depending on the analyte if a good linearity without log-log-transformation is reached.

5.3 Precision

Table 4-2 displays the repeatability expressed as % RSD for the analytes investigated in this thesis. For all compounds % RSD was not more than 3%, for 32 of the 37 substances this value was not more than 2%. In the topiramate study (cf. chapter 3.3), the performance of the CAD was compared to that of an ELSD. The CAD was

much more precise than the ELSD (% RSD between 0.2 and 2.4% for the CAD and 1.2 and 18% for the ELSD).

The CAD is reported to provide the highest precision among all aerosol-based detectors [13] with typical values of less than 2% [14]. The results found here are in full accordance with the reported precision.

Table 4-2. Repeatability of the analytes investigated in this thesis. *In case one value is reported, n = 6. Where three values are given, n = 3 for each of these values.

Analyte	% RSD*	R^2 (linear)	R^2 (log-log-linear)	Range (ng on column)
Besylate	1.4	0.9979	-	7.5 – 500
Bromide	1.7	0.9970	-	5 – 500
Calcium	2.0		not determined	
Chloride	0.6	0.9996	-	10 – 500
Choline	0.6		not determined	
Citrate	2.9	0.9835	0.8992	475 – 880
Fumaric acid	0.5	0.9953	-	30 – 2000
Linoleic acid	0.2 – 0.0 – 0.2	0.9993	-	10 – 1000
α-Linolenic acid	0.4 – 0.1 – 0.1	0.9998	-	10 – 1000
Magnesium	0.5		not determined	
Malate	2.3	0.9697	0.9981	350 – 600
Maleate	1.2	0.9979	-	7.5 – 500
Meglumine	0.8		not determined	
Mesylate	0.7	0.9973	-	7.5 – 500
Myristic acid	0.9 – 1.1 – 0.8		not determined	
Nitrate	1.0	0.9971	-	7.5 – 450
Oleic acid	1.1 – 0.9 – 0.4	0.9986	-	10 – 1000
Palmitic acid	1.2 – 0.5 – 1.3	0.9974	-	10 – 1000
Palmitoleic acid	1.1 – 1.1 – 1.0	0.9985	-	10 – 1000
Petroselinic acid	0.2 – 0.7 – 1.2	0.9995	-	10 – 1000
Phosphate	1.7	0.9969	-	40 – 500
Polidocanol (assay)	0.9	0.9973	-	400 – 600
Polidocanol (release)	0.9	-	0.9969	50 – 1500
Potassium	1.4	0.9986	-	1 - 500
Procaine	1.9		not determined	
Sodium	0.8	0.9871	0.9960	1 – 500
Stearic acid	0.7 – 1.7 – 1.7	0.9992	-	10 – 1000
Succinate	2.3		not determined	
Sulfate	1.0	0.9978	-	20 – 2000
Tartaric acid	1.2	0.9950	-	300 – 1000
Topiramate	0.2 – 0.5 – 0.2	0.9983	-	400 – 600
Topiramate impurity B	2.4 – 1.3 – 0.8	0.9991	-	25 – 75
Topiramate impurity C	1.1 – 0.4 – 0.8	0.9956	-	25 – 75
Topiramate impurity D	0.3 – 0.5 – 0.7	0.9924	-	25 – 75
Topiramate impurity E	0.6 – 0.4 – 0.7	0.9880	0.9966	25 – 250
Tosylate	2.2	0.9984	-	13 – 830
TRIS	1.1		not determined	
Zinc	1.2		not determined	

5.4 Quantification

An important characteristic of a method is that the analyte can be accurately quantified. Table 4-3 summarizes the accuracy values express as % recovery of the analytes investigated here. For some analytes, there seems to be a trend in accuracy. Linoleic and α-linoleic acid show an increasing recovery with increasing concentration, while the recoveries of myristic, palmitic, palmitoleic, and petroselinic acid, polidocanol (assay), topiramate, topiramate impurity C, and topiramate impurity E decrease with higher concentration. No trend was observed for oleic acid, polidocanol (release), topiramate impurity B, and topiramate impurity D. Thus, no general conclusion can be given.

The highest accuracy was reached for the content determination of topiramate and polidocanol (assay) with recoveries ranging from 98.3 to 101.1% and 99.2 to 101.3%, respectively. Here, the measuring range was rather small, i.e. ± 20% of the concentration of the test solution. This allowed for the utilization of single-point-calibration with an external standard. Generally, the CAD is reported to provide a precision of less than 2% RSD [14]. Therefore, the results obtained here indicate a high accuracy for an aerosol-based detector.

Table 4-3. Accuracy of analytes investigated in this thesis expressed as % recovery at the lower (low) and upper (high) limits and in the middle (mid) of the measuring range, and corresponding measuring range (ng on column).

Analyte	Recovery (%) (n=3)			Type of calibration	Range (ng on column)
	low	mid	high		
Linoleic acid	94.9	100.5	105.1	LLL[1] + CF[2]	50 – 500
α-Linolenic acid	98.1	99.0	103.1	LLL + CF	50 – 500
Myristic acid	114.3	100.7	88.4	LLL + CF	50 – 150
Oleic acid	104.1	95.8	100.5	LLL	50 – 1000
Palmitic acid	105.5	100.2	94.9	LLL + CF	50 – 150
Palmitoleic acid	104.4	97.9	97.9	LLL + CF	50 – 500
Petroselinic acid	101.4	98.7	-	LLL + CF	50 – 250
Polidocanol (assay)	101.1	98.4	98.3	SP[3]	400 – 600
Polidocanol (release)	95.3	102.7	92.7	LLL	50 – 1500
Stearic acid	-	100.0	-	LLL + CF	50
Topiramate	101.3	100.3	99.2	SP	400 – 600
Topiramate impurity B	99.3	104.9	101.1	SP + CF	50 – 150
Topiramate impurity C	112.6	108.5	104.4	SP + CF	50 – 150
Topiramate impurity D	99.8	101.6	99.1	SP + CF	50 – 150
Topiramate impurity E	104.8	101.5	94.5	SP + CF	50 – 300

[1] LLL: quantification with a log-log-linear calibration curve consisting of at least five concentration levels was performed; [2] CF: the external standard was different from the analyte and a correction factor was applied in order to compensate unequal response; [3] SP: quantification using single-point-calibration with an external standard was performed.

Topiramate impurities B, C, D and E were quantified with single-point-calibration using topiramate as external standard. Correction factors were applied. The measuring range was ± 50% (- 50%/+ 200% for topiramate impurity E) corresponding to the concentration of the test solution. The recoveries ranged from 94.5 to 112.6%. Although much higher recovery values were found compared to the determination of polidocanol (assay) and topiramate, these are still satisfactory results for the quantification of impurities. The higher deviation from the true value may be attributed to the larger relative measuring range.

All other analytes were quantified over a larger concentration range. Therefore, a log-log-linear calibration curve was established. Furthermore, correction factors were applied in case that the external standard was a different substance than the analyte. Recoveries found were higher compared to the analyte determined via single-point-calibration, i.e. between 88.4 and 114.3%. This is in accordance with the highest measuring ranges among all analytes.

5.5 Conclusion

Compared to routinely employed HPLC detectors, such as UV/Vis or MS detectors, the CAD is less sensitive (UV/Vis: LOD of 10 pg on column, MS: LOD of less than 1 pg on column, [15]). Also, UV and MS detectors provide a perfectly linear signal over the entire measuring range which makes quantification less troublesome. Hence, if an analyte possesses a suitable chromophor, UV detection would be preferred over CAD. If a decision should be made between MS and CAD, it has to be considered individually for the respective analytical problem.

The purchase and maintenance costs of an MS detector are considerably higher than for the CAD. Therefore, many laboratories for routine pharmaceutical analysis do not run an MS system due to economic reasons. Here, the CAD presents a cost efficient alternative to mass detection. This applies only to analyses where no structural elucidation is intended, i.e. assay and impurity determination. For structure elucidation or quantification of low quantities of analytes and/or in the presence of a matrix, MS detection should be chosen.

The CAD is best suited for analyses where at least one compound of interest has a poor or no UV/Vis chromophore. Among all alternatives to UV/Vis and MS, i.e. ELSD, NQAD or RI detection, CAD provides the best sensitivity, linearity and precision.

A promising field of research might be the characterization of excipients using the CAD. Many of these substances do not provide a suitable UV/Vis chromophore and many of the current analysis methods are no longer considered state of the art. Here, the added value of this universal detection technique for the analysis of polysorbate 80 and polidocanol was well demonstrated.

Table 4-4. Compilation of advantages and disadvantages of the Corona® CAD.

	Advantages	**Disadvantages**
Response	independent of physico-chemical properties, e.g. no UV/Vis chromophore	diminished for semi-volatile and volatile substances
	independent of compound class	dependent on mobile phase composition
		not linear
Mobile phase	compatible with MS detectors	only volatile buffer additives
Sensitivity	sufficient sensitivity for pharmaceutical applications especially excipients	less sensitive than UV and MS

5.6 References

[1] *ICH Guideline Q3A(R2), Impurities in New Drug Substances,* International Conference on Harmonisation of Technical Requirements for Registration of Pharmaceuticals for Human Use, 2005, Geneva, Switzerland.

[2] Dixon, R.W., Peterson, D.S., *Development and testing of a detection method for liquid chromatography based on aerosol charging.* Anal. Chem., 2002. **74**(13): p. 2930-2937.

[3] Petritis, K., Dessans, H., Elfakir, C., Dreux, M., *Volatility evaluation of mobil phase/electrolyte additives for mass spectrometry.* LC-GC Eur., 2002. **15**(2): p. 98, 100, 102.

[4] Cohen, R.D., Liu, Y., Gong, X., *Analysis of volatile bases by high performance liquid chromatography with aerosol-based detection.* J. Chromatogr. A, 2012. **1229**: p. 172-9.

[5] Lantz, M.D., Risley, D.S., Peterson, J.A., *Simultaneous Resolution and Detection of a Drug Substance, Impurities, and Counter Ion Using A Mixed-Mode HPLC Column with Evaporative Light Scattering Detection.* Journal of Liquid Chromatography & Related Technologies, 1997. **20**(9): p. 1409-1422.

[6] Hall, J., *Lab Manual for Zumdahl*. 6th Edition. 2002, New York: Brooks Cole Pub Co.

[7] Wojciechowski, K., Buffle, J., *The interaction of azacrown ether with fatty acid in nonpolar solvents and at the organic–aqueous interface.* Biosens. Bioelectron., 2004. **20**(6): p. 1051-1059.

[8] Holzgrabe, U., Nap, C.-J., Almeling, S., *Control of impurities in l-aspartic acid and l-alanine by high-performance liquid chromatography coupled with a corona charged aerosol detector.* J. Chromatogr. A, 2010. **1217**(3): p. 294-301.

[9] Holzgrabe, U., Nap, C.J., Kunz, N., Almeling, S., *Identification and control of impurities in streptomycin sulfate by high-performance liquid chromatography coupled with mass detection and corona charged-aerosol detection.* J. Pharm. Biomed. Anal., 2011. **56**(2): p. 271-9.

[10] Nováková, L., Solichová, D., Solich, P., *Hydrophilic interaction liquid chromatography – charged aerosol detection as a straightforward solution for simultaneous analysis of ascorbic acid and dehydroascorbic acid.* J. Chromatogr. A, 2009. **1216**(21): p. 4574-4581.

[11] Forsatz, B., Snow, N.H., *HPLC with charged aerosol detection for pharmaceutical cleaning validation.* LCGC North Am., 2007. **25**(9): p. 960, 962, 964, 966, 968.

[12] *Thermo Scientific/Dionex Corona CAD Manual*.

[13] Holzgrabe, U., Nap, C.-J., Beyer, T., Almeling, S., *Alternatives to amino acid analysis for the purity control of pharmaceutical grade L-alanine.* J. Sep. Sci., 2010. **33**(16): p. 2402-2410.

[14] *Dionex Corona CAD Brochure*. http://www.dionex.com/en-us/webdocs/88700-Bro-Corona-CAD-Brochure-21Oct10-LPN2633.pdf *(Accessed: April 2015)*

[15] Skoog, D.A., Holler, F.J., Crouch, S.R., *Instrumentelle Analytik: Grundlagen - Geräte - Anwendungen*. 6. Auflage. 2013, Heidelberg: Springer-Verlag.

6 Summary

The Corona® charged aerosol detector (CAD) is an aerosol-based detector first described by *Dixon* and *Peterson* in 2002. It is capable of detecting compounds independent from their physico-chemical properties presumed the analyte is sufficiently non-volatile. Consequently, the CAD is often applied to the analysis of substances that do not possess a suitable UV chromophore. Major drawbacks are however, the detector signal is non-linear and depending on the content of organic solvent in the mobile phase.

This thesis tried to explore possible applications of the CAD for pharmaceutical analysis. Therefore, several substances from different compound classes were investigated. Newly developed or existing methods were validated. Thus the performance of the CAD could be examined. Both assay and impurity determination were evaluated for their compliance with ICH Q2(R1) “Validation of Analytical Procedures” and the “Technical Guide for the Elaboration of Monographs”.

In the course of the establishment of reference substances at the EDQM, a generic screening method for the identification of organic and inorganic pharmaceutical counterions was needed. An HPLC-CAD method developed by *Zhang et al.* was therefore investigated for its suitability for pharmacopoeial purpose. Method validation was performed. It was found that 23 ions could be separated and detected. Identification was achieved via retention time of an authentic standard of the corresponding ions. Alternatively, peak assignment was performed by determination of the exact mass using TOF-MS. Ions could be quantified as impurities or for stoichiometric purpose.

For the impurity control in topiramate, the performance characterstics of the CAD were compared to that of an ELSD. CAD was superior to ELSD in terms of repeatability, sensitivity and linearity. However, impurities could be quantified with satisfactory accuracy with both detectors. The application of the ELSD was not feasible due to non-reproducible spike peaks eluting after the principle peak in the chromatogram of the test solution. One of the impurities, topiramate impurity A (diacetonide), gave no or a vastly diminished signal in the ELSD and the CAD, respectively. It is evaporated during the detection process due to its relatively high vapor pressure. The response could be enhanced by a factor of nine via post-column addition of acetonitrile and a lower nebulizer temperature. As the response of topiramate impurity A was still about thousand-fold lower than the response of all other impurities, its quantification was

not feasible. Additionally, the HPLC-CAD was successfully validated as an assay procedure for topiramate.

There seems to be a great potential in the application of the CAD to the analysis of excipients as most compounds do not possess a suitable UV chromophore. Here, a simple and rapid HPLC-CAD method for the determination of polidocanol (PD) was developed. The method was successfully validated as a potential assay procedure for the Ph. Eur. as none is described in either of the two PD monographs. The same method was applied to the determination of the PD release from a pharmaceutical polymer matrix.

A method for the determination of the fatty acid (FA) composition of polysorbate 80 (PS80) was developed and validated. Using the CAD and mass spectrometry, we were able to identify two new FAs in 16 batches from four manufacturers. All batches complied with pharmacopoeial specification. Furthermore, the overall composition of the different PS80 species (“fingerprinting”) and the peroxide content were determined. In addition to the chemical characterization, functionality related characteristics (FRCs) were determined. Correlations between chemical composition and FRCs were found.

The validation data of the above mentioned methods suggests that the CAD represents a viable detection technique for pharmaceutical analysis. The CAD was sufficiently sensitive for non-volatile analytes. Impurity control down to concentrations of 0.05 or 0.03%, as demanded by ICH Q3A (R2), is achievable. However, the response of semi-volatile compounds may be drastically diminished. It could be confirmed that the response of the CAD is linear when the range does not exceed two orders of magnitude. Exceptions may be observed depending on the actual method setup. When the measuring range is sufficiently narrow, quantification can be done using single-point calibration which is common practice in pharmaceutical anlysis. Impurities may also be quantified against a single calibration solution. However, correction factors may be needed and the accuracy is considerably lower compared to an assay method. If a compound is to be quantified over a large concentration range, log-log transformation of the calibration curve is needed and a decreased accuracy has to be accepted.

7 Zusammenfassung

Der “Corona® charged aerosol detector” (CAD) ist ein aerosol-basierter Detektor, welcher 2002 von *Dixon* und *Peterson* vorgestellt wurde. Damit lassen sich nichtflüchtige Substanzen unabhängig von ihren physiko-chemischen Eigenschaften detektieren. Daraus folgt, dass der CAD oft zur Analyse von Substanzen ohne UV-Chromophor angewandt wird. Großes Manko ist jedoch, dass das Signal nicht linear und abhängig vom Anteil organischen Lösemittels in der mobilen Phase ist.

Ziel dieser Arbeit war es, mögliche Anwendungen des CAD in der pharmazeutischen Analytik zu erschließen. Dies wurde anhand von Beispielen aus unterschiedlichen Substanzklassen untersucht. Dabei wurden neu entwickelte oder bestehende Methoden validiert um die Leistung des CAD beurteilen zu können. Sowohl Gehaltsbestimmungen als auch Methoden zur Erfassung von Verunreinigungen wurden hinsichtlich ihrer Konformität mit dem Europäischen Arzneibuch (Ph. Eur.) geprüft.

Im Zuge der Charakterisierung von Referenzsubstanzen beim EDQM wurde eine Methode zur Identifikation von pharmazeutischen Gegenionen benötigt. Zu diesem Zweck wurde eine HPLC-CAD-Methode von *Zhang et al.* hinsichtlich ihrer Eignung für das Ph. Eur. überprüft. Mit dieser Methode ließen sich 23 pharmazeutisch relevante Ionen trennen und detektieren. Die Ionen wurden durch Vergleich der Retentionszeiten eines Standards erreicht. Zusätzlich wurde die Peakzuordnung mittels der Bestimmung der Präzisionsmasse des Gegenions oder des Arzneistoffes durch ein TOF-MS durchgeführt. Die Methode ließ die Quantifizierung von Ionen als Verunreinigung oder zur Bestimmung der Stöchiometrie eines Salzes zu.

Bei der Bestimmung von Verunreinigungen von Topiramat wurde ein Vergleich zwischen CAD und ELSD angestellt. Es zeigte sich, dass der CAD in den Punkten Wiederholbarkeit, Empfindlichkeit und Linearität überlegen war. Mit beiden Detektoren wurde eine ähnlich gute Richtigkeit erzielt. Durch das Auftreten von nicht reproduzierbaren Peaks, welche nach dem Hauptpeak im Chromatogramm der Testlösung auftraten, war die Anwendung des ELSD hier auszuschließen. Eine der Verunreinigungen, Topiramat Verunreinigung A (Diacetonid) lieferte kein bzw. ein verringertes Signal in ELSD und CAD. Aufgrund des relativ hohen Dampfdrucks der Substanz wurde sie während des Detektionsvorgangs verdampft. Das Signal konnte durch Zugabe von Acetonitril nach der Säule und durch eine Verringerung der Temperatur des Vernebler um das neunfache vergrößert werden. Da aber die Empfindlichkeit für

alle anderen Verunreinigungen dennoch um das tausendfache höher war, war eine Quantifizierung von Topiramat Verunreinigung A nicht möglich. Die HPLC-CAD Methode wurde zusätzlich als Gehaltsbestimmungsmethode für Topiramat validiert.

Die Anwendung des CAD zur Analyse von Hilfsstoffen birgt großes Potenzial, da viele Substanzen nicht über ein Chromophor verfügen. Im Zuge dieser Arbeit wurde eine einfache und schnelle Methode zur Gehaltsbestimmung von Polidocanol (PD) entwickelt. Diese wurde als mögliche Methode für das Ph. Eur. validiert. Zusätzlich wurde die Methode zur Bestimmung der Freisetzung von PD aus einer pharmazeutischen Matrix verwendet.

Es wurde eine Methode zur Bestimmung der Fettsäurezusammensetzung von Polysorbat 80 (PS80) entwickelt und validiert. Mittels CAD und Massenspektrometrie war es möglich zwei neue Fettsäuren in 16 Chargen von vier verschiedenen Herstellern zu identifizieren. Alle Chargen entsprachen den Anforderungen des Ph. Eur. Weiterhin wurde die Zusammensetzung der einzelnen PS80-Spezies („fingerprinting“) sowie der Peroxidgehalt untersucht. Neben dieser chemischen Charakterisierung wurden auch funktionalitätsbezogene Eigenschaften (FRCs) bestimmt. Korrelationen zwischen chemischen Zusammensetzung und FRCs wurden gefunden.

Die Validierungsdaten der genannten Methoden legen nahe, dass der CAD sinnvoll zur pharmazeutischen Analytik angewendet werden kann. Für nicht-flüchtige Substanzen wurde stets eine ausreichende Empfindlichkeit erreicht. Somit können Verunreinigungen bis zu einer Konzentration von 0.05 bzw. 0.03%, wie von der ICH Richtlinie Q3A (R2) gefordert, quantifiziert werden. Jedoch kann das Detektorsignal bei halb-flüchtigen Substanzen stark erniedrigt sein. Es konnte bestätigt werden, dass sich das Detektorsignal über zwei Größenordnungen linear verhält. Abweichungen davon sind in Abhängigkeit der jeweiligen Methode möglich. Ist der Messbereich genügen klein, so kann ein Stoff mittels Einpunkt-Kalibrierung quantifiziert werden. Dieses Vorgehen sollte bei Gehaltsbestimmungen angewandt werden. Ebenfalls mittels Einpunkt-Kalibrierung können Verunreinigungen erfasst werden. Jedoch kann es notwendig sein, Korrekturfaktoren zu bestimmen. Die Richtigkeit ist hier deutlich niedriger als bei einer Gehaltsbestimmungsmethode. Über einen großen Konzentrationsbereich muss eine Ausgleichskurve mit log-log-Transformation verwendet werden. Die Richtigkeit ist hierbei ebenfalls geringer als bei einer Gehaltsbestimmung.

8 Appendix

8.1 List of Publications

Review article

Almeling, S.; Ilko, D.; Holzgrabe, U. *Charged aerosol detection in pharmaceutical analysis,* J Pharm Biomed Anal **2012**, 69, 50-63.

Research papers

- Ilko, D.; Nap, C.-J.; Holzgrabe, U.; Almeling, S. *Validation and application of an HPLC-CAD-TOF/MS method for identification and quantification of pharmaceutical counterions,* Pharmeuropa Bio & SN **2014**, 2014, 81-91.

- Ilko, D.; Neugebauer, R. C.; Brossard, S.; Almeling, S.; Türck, M.; Holzgrabe, U. *Impurity control in Topiramate with high performance liquid chromatography: Validation and comparison of the performance of evaporative light scattering detection and charged aerosol detection [manuscript in preparation].*

- Ilko, D.; Puhl, S.; Meinel, L.; Germershaus, O.; Holzgrabe, U. *Simple and rapid high performance liquid chromatography method for the determination of polidocanol as bulk product and in pharmaceutical polymer matrices using charged aerosol detection,* J Pharm Biomed Anal **2015**, 104, 17-20.

- Puhl, S.; Ilko, D.; Li, L.; Holzgrabe, U.; Meinel, L.; Germershaus, O. *Protein release from electrospun nonwovens: Improving the release behavior through rational combination of polyester blend matrices with polidocanol,* Int J Pharm **2014**, 477(1-2), 273-281.

- Ilko, D.; Braun, A.; Germershaus, O.; Meinel, L.; Holzgrabe, U. *Fatty acid composition analysis in polysorbate 80 with high performance liquid chromatography coupled to charged aerosol detection,* Eur J Pharm Biopharm **2014**, *[in press, corrected proof].*

- Braun, A. C.; Ilko, D.; Merget, B; Gieseler, H.; Germershaus, O.; Holzgrabe, U.; Meinel, L. *Predicting critical micelle concentration and micelle molecular weight of polysorbate 80 using compendial methods,* Eur J Pharm Biopharm **2014**, *[in press, corrected proof].*

Other publications

- Ilko, D.; Holzgrabe, U. *Influence of the capillary diameter on the separation efficiency and sensitivity: A systematic approach,* Electrophoresis **2012**, 33(11), 1494-1498.
- Ilko, D.; Steiger, C.; Keller, R.; Holzgrabe, U.; Meinel, L.; *Coding of tablet coatings with polyethylene glycols as anti-counterfeiting strategy*, Pharm Res **2015**, *[submitted].*

8.2 Documentation of authorship

This section contains a list of the individual contribution for each author to the publications reprinted in this thesis. Unpublished manuscripts are handled, accordingly.

P1	**Almeling S, Ilko D, Holzgrabe U** (2012) Charged aerosol detection in pharmaceutical analysis. Journal of Pharmaceutical and Biomedical Analysis **69:** 50-63			
Author		**1**	**2**	**3**
Study design/concept development		x		x
Literature analysis and interpretation		x	x	
Manuscript planning		x		
Manuscript writing		x	x	
Correction of manuscript		x		x
Supervision of David Ilko				x

P2	**Ilko D, Nap C-J, Holzgrabe U, Almeling S** (2014) Validation and application of an HPLC-CAD-TOF/MS method for identification and quantification of pharmaceutical counterions. Pharmeuropa Bio & Scientific Notes **2014:** 81-91				
Author		**1**	**2**	**3**	**4**
Method validation		x			
Application of the method		x			
Study design/concept development		x			x
Data analysis and interpretation		x	x		x
Manuscript planning		x			x
Manuscript writing		x			
Correction of manuscript			x	x	x
Supervision of David Ilko			x		x

M1	**Ilko D, Neugebauer R C, Brossard S, Almeling S, Türck M, Holzgrabe U** Impurity control in Topiramate with high performance liquid chromatography: Validation and comparison of the performance of evaporative light scattering detection and charged aerosol detection. (unpublished manuscript)						
Author		**1**	**2**	**3**	**4**	**5**	**6**
Method validation: impurity control		x					
Method validation: assay		x					
TLC and HPTLC limit test for impurity A				x			
Study design/concept development		x	x				x
Data analysis and interpretation		x	x	x			
Manuscript planning		x					
Manuscript writing		x					
Correction of manuscript			x		x	x	x
Supervision of David Ilko					x		x

P3	**Ilko D, Puhl S, Meinel L, Germershaus O, Holzgrabe U** (2015) Simple and rapid high performance liquid chromatography method for the determination of polidocanol as bulk product and in pharmaceutical polymer matrices using charged aerosol detection. Journal of Pharmaceutical and Biomedical Analysis **104:** 17-20					
Author		**1**	**2**	**3**	**4**	**5**
Method development		x				
Method validation		x				
Preparation of the fibres			x			
Incubation of the fibres for release study			x			
Sample preparation and conduction of the analysis		x				
Study design/concept development		x	x		x	x
Data analysis and interpretation		x	x			
Manuscript planning		x				x
Manuscript writing		x				
Correction of manuscript			x	x	x	x
Supervision of David Ilko						x

P4	**Puhl S, Ilko D, Li L, Holzgrabe U, Meinel L, Germershaus O** (2015) Protein release from electrospun nonwovens: Improving the release behavior through rational combination of polyester blend matrices with polidocanol. International Journal of Pharmaceutics **477:** 273-281						
Author		**1**	**2**	**3**	**4**	**5**	**6**
Lysozyme crystallization and crystal size determination		x					
PCL electrospinning		x		x			
Morphology and fiber diameter		x		x			
Wettability and sorption rate of the nonwovens		x					
Differential scanning calorimetry		x					
Relative bioactivity of lysozyme		x					
Statistical analysis		x					
Contact angle, sorption rate and swelling behavior		x					
Polidocanol release		x	x				
Lysozyme release		x					
Study design/concept development		x			x	x	x
Data analysis and interpretation		x	x	x			x
Manuscript planning		x				x	x
Manuscript writing		x	x				x
Correction of manuscript			x		x	x	x
Supervision of David Ilko					x		

P5	**Ilko D, Braun A, Germershaus O, Meinel L, Holzgrabe U** (2014) Fatty acid composition analysis in polysorbate 80 with high performance liquid chromatography coupled to charged aerosol detection. European Journal of Pharmaceutics and Biopharmaceutics [in press, corrected proof]					
Author		**1**	**2**	**3**	**4**	**5**
Method development		x				
Method validation		x				
Sample analysis		x				
Study design/concept development		x		x		x
Data analysis and interpretation		x	x		x	x
Manuscript planning		x				
Manuscript writing		x				
Correction of manuscript			x	x	x	x
Supervision of David Ilko						x

P6	**Braun A C, Ilko D, Merget B, Gieseler H, Germershaus O, Holzgrabe U, Meinel L** (2014) Predicting critical micelle concentration and micelle molecular weight of polysorbate 80 using compendial methods. European Journal of Pharmaceutics and Biopharmaceutics [in press, corrected proof]

Author	**1**	**2**	**3**	**4**	**5**	**6**	**7**
Sample preparation	x						
Critical micelle concentration (CMC) by surface tension measurement	x						
Cloud point	x				x		
Hydrophilic–lipophilic balance (HLB) value	x						
Static light scattering	x						
HPLC-CAD		x					
Fingerprint analyses		x					
Peroxide value	x						
Study design/concept development	x				x	x	x
Data analysis and interpretation	x	x	x			x	x
Manuscript planning	x						x
Manuscript writing	x						x
Correction of manuscript		x	x	x	x	x	x
Supervision of David Ilko						x	

Erklärung zu den Eigenanteilen des Doktoranden sowie der weiteren Doktoranden als Koautoren an Publikationen und Zweitpublikationsrechten bei einer kumulativen Dissertation.

Für alle in dieser kumulativen Dissertation verwendeten Manuskripte liegen die notwendigen Genehmigungen der Verlage (‚reprint permission') für die Zweitpublikation vor, außer das betreffende Kapitel ist noch gar nicht publiziert. Dieser Umstand wird einerseits durch die genaue Angabe der Literaturstelle der Erstpublikation auf der ersten Seite des betreffenden Kapitels deutlich gemacht oder die bisherige Nichtveröffentlichung durch den Vermerk „unpublished" oder „nicht veröffentlicht" gekennzeichnet.

Die Mitautoren der in dieser kumulativen Dissertation verwendeten Manuskripte sind sowohl über die Nutzung als auch über die oben angegebenen Eigenanteile informiert.

Die Beiträge der Mitautoren an den Publikationen sind in den vorausgehenden Tabellen aufgeführt.

Prof. Dr. Ulrike Holzgrabe	11. Juni 2015	Unterschrift
David Ilko	11. Juni 2015	Unterschrift

8.3 Conference Contributions

- Ilko, D.; Holzgrabe, U.

Influence of injection parameters on detection and quantification limit in capillary zone electrophoresis.

Joint Meeting ÖPhG-DPhG, **2011**, Innsbruck.

- Ilko, D.; Wiest, J.; Türck, M.; Holzgrabe, U.

Impurity control in topiramate by HPLC with charged aerosol detection and quantitative NMR.

International Symposium on Pharmaceutical and Biomedical Analysis (PBA), **2013**, Bologna.

- Ilko, D.; Nap, C.-J.; Holzgrabe, U.; Almeling, S.

Counterion screening and quantification in pharmaceutical substances with charged aerosol detection and TOF-MS.

International Symposium on Pharmaceutical and Biomedical Analysis (PBA), **2013**, Bologna.

- Ilko, D.; Braun, A.; Germershaus, O.; Meinel, L.; Holzgrabe, U.

Fatty acid composition analysis in polysorbate 80 with high performance liquid chromatography coupled to charged aerosol detection.

Joint Meeting DPhG, **2014**, Frankfurt.